

Noncovalently Associated Cell Penetrating Peptides for Nonviral Gene Delivery

By

Nabil Abdulhafiz A. Alhakamy

Submitted to the graduate degree program in Pharmaceutical Chemistry and the Graduate Faculty of the University of Kansas in partial fulfillment of the requirements for the degree of Doctor of Philosophy.

Committee members:

Cory J. Berkland, Chairperson

Prajnaparamita Dhar

David Volkin

Michael Wang

Susan M. Lunte

Arghya Paul

Date Defended: April 26, 2016

The Dissertation Committee for Nabil Abdulhafiz A. Alhakamy
certifies that this is the approved version of the following dissertation:

Noncovalently Associated Cell Penetrating Peptides for Nonviral Gene Delivery

Cory J. Berkland, Chairperson

Prajnaparamita Dhar, Co-advisor

Date Approved: April 26, 2016

Abstract

Gene therapy has become a promising strategy for treatment of numerous diseases such as cancer, hemophilia, and neurodegenerative diseases. Glybera® (alipogene tiparvovec) became the first gene therapy approved in the European Union, for the treatment of lipoprotein lipase deficiency (LPLD). Promising late-stage clinical trials of this drug may herald the first gene therapy to be approved in the United States. The advancement of vectors (viral and nonviral) for efficient and safe gene delivery has garnered significant attention recently. Although viral vectors (e.g., retroviruses and adenoviruses) are the most effective vectors, applied in 70% of gene therapy clinical trials, they present several notable challenges including safety concerns (e.g., immunogenicity and pathogenicity), production difficulties, and rapid clearance from circulation. In contrast, nonviral vectors could be promising gene carriers due to their low cost, ease of synthesis, and decreased immunogenicity relative to viral vectors.

Key progress has been made in the development of several nonviral gene delivery vectors. The use of cell penetrating peptides (CPPs) to deliver genetic materials for gene therapy has been a topic of interest for more than 20 years. One strategy is through covalent conjugation of CPPs with genetic materials, which requires complex synthesis procedures. In contrast, electrostatic complexation of CPPs with genetic materials is relatively simple and has been demonstrated to improve gene delivery both *in vitro* and *in vivo*. Reported herein, a simple method to generate small CPP complexes (100-200 nm) capable of high transfection efficiency was explored. Positively charged CPPs (e.g., polyarginine 9 [R9] and polylysine 9 [K9]) were complexed with plasmid DNA (pDNA), which resulted in unstable large particles (~1 micron). These were then condensed into small nanoparticles using Ca^{2+} . CPPs also displayed negligible cytotoxicity. These CPP-pDNA- Ca^{2+} complexes showed high transfection efficiency and low cytotoxicity *in vitro*

(human and mouse cell lines) and *in vivo* (syngeneic mice). Thus, Ca²⁺-condensed CPP complexes emerged as simple, attractive candidates for future studies on nonviral gene delivery.

Furthermore, the relationships between transfection efficiency and polyarginine molecular weight, polyarginine-pDNA charge ratios, and calcium concentrations were studied. Polyarginine 7 was significantly more effective than other polyarginines under most formulation conditions, suggesting a link between molecular weight and transfection efficiency. Furthermore, Polylysine 9 was complexed with angiotensin II type 2 receptor (AT2R) plasmid DNA (pAT2R). The polylysine 9 complex (K9-pAT2R-Ca²⁺) showed high transfection efficiency and negligible *in vitro* cytotoxicity towards human and mouse cell lines. This complex demonstrated cancer-targeted gene delivery *in vivo* when administered *via* intravenous injection or intratracheal spray. A single administration of this complex markedly attenuated lung cancer growth.

Mechanistic understanding of CPP-mediated membrane insertion and intracellular translocation of nonviral gene complexes would allow rational design of next-generation CPPs for gene delivery. To this aim, we employed zwitterionic and anionic phospholipid monolayers as models to mimic the membrane composition of the outer leaflet of cell plasma and intracellular vesicular membranes at relevant intracellular pH. Subsequently, we investigated the membrane insertion potential of CPPs and gene complexes (CPP-pDNA-Ca²⁺ complexes) into model membranes. The insertion potential of CPPs and complexes were recorded using a Langmuir monolayer approach that records peptides and complexes adsorption to model membranes. Results showed that small changes to amino acids and peptide sequences resulted in dramatically different insertion potentials and membrane reorganization.

Lastly, the effect of CPP charge type, charge spacing, and hydrophobicity on transfection efficiency was investigated by replacing three residues of the polyarginine 9 with a hydrophilic

residue (histidine) or hydrophobic residues (alanine, leucine, and tryptophan) at positions 3, 4, and 7. R9 and RW9 complexes appeared especially effective compared to other CPP complexes, whereas RH9, RA9, and RL9 complexes seemed to have moderate- to low-gene expression. Initially, this suggested CPPs with better membrane penetration yielded higher gene expression. After further exploration, we discovered the charge spacing of CPPs affected the ability of CPPs to complex with nucleic acids and this property correlated to gene expression levels. In conclusion, our complexes emerged as simple, attractive candidates for further *in vivo* studies on nonviral gene delivery.

Acknowledgement

First and foremost, I have to thank my parents, Abdulhafiz and Howida, and my family for their love and support throughout my life. Thank you for giving me strength to reach for the stars and chase my dreams. Their faith and confidence in my abilities and in me is what has shaped me to be the person I am today. My experience at the University of Kansas has been nothing short of amazing. I would like to express my honest appreciation to my Ph.D advisor, Professor Cory Berkland, for all of his support, care, leadership, endurance, understanding, and most importantly, his friendship during my graduate studies at The University of Kansas. Cory is someone you will instantly love and never forget once you meet him. He is one of the smartest people I have ever met and the funniest advisor I know. I hope that I could be as active, eager, and energetic as Cory. He has been supportive and has given me the freedom to pursue various projects without any objections. Cory is a good advisor who encouraged and expected us to think more independently about our experiments and results. The extensive knowledge, vision, and creative thinking of Cory have been the source of inspiration for me throughout this work. He encouraged me to not only grow as a researcher but as an independent thinker to use scientific approaches to face the challenges in my future research career. For everything you have done for me, Dr. Berkland, I sincerely appreciate.

I will forever be thankful to my Ph.D co-advisor, Professor Prajnaparamita Dhar for her guidance, inspiration and continuous support through the course of my work. Prajna has been helpful in providing advice countless times during my graduate school career. She was and remains my best role model for a scientist and mentor. Her enthusiasm and love for researching is contagious. She has also provided insightful discussions about my research and life. I have been fortunately blessed to have an advisor who gave me a great opportunity to develop my own

individuality by being allowed to work with such independence and at the same time have her guidance. I think of her as a big sister. I express my heartfelt gratefulness for her guidance and support that I believed I learned from the best. For everything you have done for me, Professor Prajna Dhar, I greatly appreciate.

I would like to thank the members of my oral prelims and dissertation committee: Professor Jennifer Laurence, Professor David Volkin, Professor Susan M. Lunte, Professor Michael Wang, Professor Arghya Paul, and Professor Stevin Gehrke for their commitment to my dissertation and for their helpful suggestions and corrections. I would like to sincerely thank Dr. Abdulgader Baoum for his guidance and support during my first year here. I learned from his insight a lot. I was grateful for the discussion and interpretation of some results presented in this work. I would like to express my sincere appreciation to Professor Masaaki Tamura for his guidance and encouragement. He has been helpful in providing advice many times during my graduate school career.

I am deeply grateful for all the generous help and support from Dr. Berkland's lab group members, past to present: Dr. Amir Fahkari, Dr. Joshua Sestak, Dr. Supang Khondee, Dr. Chuda Chittasupho, Dr. Jian Qian, Dr. Nashwa El-Gendy, Dr. Chris Kuehl, Dr. Shara Thati, Dr. Warangkana Pornputtapitak, Dr. Connor Dennis, Dr. Bradley Sullivan, Adel Alghaith, Brittany Hartwell, Chad Pickens, Lorena Antunez, Laura Northrup, Matthew Christopher, Singkome Tima, Jimmy Song, Danny Griffin, and Martin Leon. Also, I would like to sincerely thank Dr. Dhar's lab group members, past to present: Dr. Yan Gao, Dr. Anubhav Kaviratna, Aishik Chakraborty, Ibrahim Elandalousi, Patrick Sedarous, Aditya Tata, Rachel Hattaway, Nicolas Mucci, Saba Ghazvini, and Oindrila Gupta. I would like to thank all of our colleagues and collaborators at Kansas State University especially, Dr. Susumu Ishiguro and Deepthi Uppalapati. Also, I would

like to thank all of our colleagues and collaborators at Oklahoma State University especially, Dr. Joshua Ramsey and Dr. Adane Nigatu for their valuable help. Also, I would like to gratefully thank all of our colleagues and collaborators at the University of Kansas Medical Center especially, Dr. Nikki Cheng, Dr. Wei Fang, Dr. Shahid Umar, and Dr. Ishfaq Ahmed.

I would like to take the opportunity to thank Dr. Adrian Goodey, Dr. Li Ying, and Dr. Carlos Santos for providing me with an invaluable learning experience during my time at Merck & Co. It has been a pleasure to work with the staff, and I have gained much practical knowledge. I appreciate the fact that you afforded me the opportunity to take on significant responsibility, which provided me with a depth of knowledge.

Also, I would like to sincerely thank my three best friends, Aishik Chakraborty, Khalid Abudawood, and Khalid Alhazmy for their providing support and friendship throughout my time here. I think of them as brothers. I also thank my friends (too many to list here but you know who you are!) for providing support and friendship that I needed. I would like to thank Abdullah Al-Hossaini, Mohammad Alsalman, Dr. Ahmed Alaofi, Khalid Al-Kinani, Adel Alhowyan, Adel Alghaith, Abdullah Alabdulkarim, Dr. Mohammad Alsenaidy and Qi Zheng for being supportive throughout my time here. I also want to extend my special gratitude to Niveen Samman for all help and support. I would like to thank all faculty members in The Pharmaceutical Chemistry Department as well as in other departments for numerous discussions and lectures that helped me to improve my knowledge in this area. I would like to acknowledge all staff in the department of Pharmaceutical Chemistry especially, Nancy Helm and Nicole Brooks for all of their assistance and support. I also thank the Macromolecule and Vaccine Stabilization Center (University of Kansas) for the use of laboratory equipment. I would like to thank the KU Writing Center for their help. I am also grateful to Saudi Arabian Government scholarship and King Abdulaziz University,

Jeddah, for the financial support to live, learn and experience beyond education here in such a great country, the United States.

Finally, people here are genuinely nice and want to help you out and I'm glad to have interacted with many. If I have forgotten anyone, I apologize and you have always being so helpful and friendly. Additionally, the years spent in Lawrence would not have been as wonderful without my friends. I greatly value their friendship and I deeply appreciate their belief in me.

Nabil A. Alhakamy

April, 2016

I dedicate this thesis to the supreme God, my family, my mentors (Cory Berkland, Prajna Dhar, Jim Rohn, Muhammad Ali, Arnold Schwarzenegger, Tony Robbins, and Les Brown) and my friends for their constant support and unconditional love. Without your help, kindness, and support I would never have arrived at this destination.

Table of Contents

Chapter 1: Introduction	1
1.1. Introduction to Noncovalently Associated Cell Penetrating Peptides for Nonviral Gene Delivery Applications.....	2
1.2. Overview of Current Classifications	4
1.3. Formulation Strategies.....	6
1.4. Motivation for Using Noncovalently Associated CPPs.....	8
1.5. Current Applications Using the Noncovalent Strategy for Nonviral Gene Delivery.....	12
1.5.1. CPP-Enhanced Nonviral Gene Delivery.....	12
1.5.2. Genetic Material Condensation with CPPs.....	13
1.5.3. Endosomolytic and Fusogenic CPPs.....	18
1.5.4. Nuclear Localization CPPs.....	20
1.5.5. Noncovalently Associated CPPs for Targeted Delivery.....	21
1.6. Thesis Overview.....	22
1.7. References.....	26
Chapter 2: Polyarginine Molecular Weight Determines Transfection Efficiency of Calcium Condensed Complexes	40
2.1. Introduction.....	41
2.2. Materials and Methods.....	44
2.2.1. Materials.....	44
2.2.2. Preparation of Polyarginine-pDNA-Ca ²⁺ Complexes.....	45
2.2.3. Preparation of PEI-pDNA Complexes.....	45
2.2.4. Agarose Gel Electrophoresis.....	45
2.2.5. Size and Zeta Potential.....	45
2.2.6. Cell Culture.....	46
2.2.7. Transfection Studies	46
2.2.8. Cytotoxicity Assay of Polyarginine.....	46
2.2.9. Optical Microscopy.....	47
2.2.10. Statistical Analysis.....	47

2.3. Results and Discussion	48
2.4. Conclusions	57
2.5. References	58

Chapter 3: AT2R Gene Delivered by Condensed Polylysine Complexes Attenuates Lewis Lung Carcinoma after Intravenous Injection or Intratracheal Spray.....66

3.1. Introduction.....	67
3.2. Materials and Methods.....	69
3.2.1. Materials.....	69
3.2.2. Preparation of the K9-pDNA-Ca ²⁺ complex.....	70
3.2.3. Preparation of the PEI-pLUC complex.....	70
3.2.4. Agarose Gel Electrophoresis.....	70
3.2.5. Size and Zeta Potential.....	71
3.2.6. Cell Culture.....	71
3.2.7. Transfection Efficiency of the K9-pDNA-Ca ²⁺ Complexes to Cultured Cells.....	71
3.2.8. Cytotoxicity of K9 peptide, PEI, and Calcium Chloride <i>in vitro</i>	72
3.2.9. Assessment of DNA Accessibility to the K9-pLUC Complex by SYBR Green Assa.....	72
3.2.10. Animals.....	73
3.2.11. Lung Cancer Graft in Syngeneic Mouse and Treatment with the K9-pAT2R-Ca ²⁺ Complex.....	73
3.2.12. Immunohistochemical Analysis for AT2R, Cell Proliferation and Apoptosis in LLC Allografts.....	73
3.2.13. Statistical Analysis.....	74
3.3. Results	75
3.3.1. Formation of the K9-pLUC-Ca ²⁺ Complex.	75
3.3.2. Physical Characterization of the K9-pLUC-Ca ²⁺ and the PEI-pLUC Complexes.....	76
3.3.3. The K9-pLUC-Ca ²⁺ Complex Caused Efficient Gene Transfection with Low Cytotoxicity <i>In Vitro</i>	78
3.3.4. Treatment with the K9-pAT2R-Ca ²⁺ Complex <i>via</i> Intravenous Injection or Intratracheal Spray Caused Significant Growth Attenuation of Lung Tumors.....	81

3.3.5. Immunohistochemical Analysis of AT2R Expression, Cell Proliferation and Apoptosis in LLC Grafts.....	83
3.4. Discussion.....	85
3.5. Conclusions.....	90
3.6. References.....	91
Chapter 4: Dynamic Measurements of Membrane Insertion Potential of Synthetic Cell Penetrating Peptides.....	97
4.1. Introduction.....	98
4.2. Materials and Methods.....	103
4.2.1. Materials.....	103
4.2.2. Methods.....	103
4.2.2.1. Langmuir Trough Experiments.....	104
4.2.2.2. Fluorescence Microscopy.....	105
4.2.2.3. Statistical Analysis.....	106
4.3. Results and Discussion.....	106
4.3.1. Penetration of CPPs into POPG Phospholipid Monolayers.....	107
4.3.2. Penetration of the CPPs in DPPC and POPC Phospholipid Monolayers.....	112
4.3.3. Penetration of the CPPs in Mixed (POPG:DPPC) Phospholipid Monolayers.....	115
4.3.4. Fluorescence Microscopy.....	120
4.4. Conclusions.....	124
4.5. References.....	115
Chapter 5: Effect of Lipid Headgroup Charge and pH on the Stability and Membrane Penetration Potential of Calcium Condensed Gene Complexes.....	133
5.1. Introduction.....	134
5.2. Materials and Methods.....	139
5.2.1. Materials.....	139
5.2.2. Methods.....	140
5.2.2.1. Preparation of CPP-pDNA-Ca ²⁺ Complexes.....	140
5.2.2.2. Agarose Gel Electrophoresis.....	140

5.2.2.3. Particle Size.....	141
5.2.2.4. Zeta Potential	141
5.2.2.5. Langmuir Trough Experiments.....	141
5.2.2.6. Statistical Analysis.....	142
5.3. Results and discussion.....	143
5.3.1. Physical Characterization of the CPP-pDNA-Ca ²⁺ Complexes.....	143
5.3.2. Insertion of the CPP-pDNA-Ca ²⁺ Complexes into Model Membranes.....	145
5.3.3. Insertion of the CPP-pDNA-Ca ²⁺ Complexes into POPC, POPS, and POPG PMs at Acidic pH.....	152
5.4. Conclusions.....	163
5.5. References.....	165
Chapter 6: Charge Type, Charge Spacing, and Hydrophobicity Dictate Delivery Properties of Nanoparticles Containing Arginine-Rich Cell Penetrating Peptide.....	173
6.1. Introduction.....	174
6.2. Materials and Methods.....	177
6.2.1. Materials.....	177
6.2.2. Methods.....	178
6.2.2.1. Nanoparticle Formation.....	178
6.2.2.2. Agarose Gel Electrophoresis.....	179
6.2.2.3. Size and Zeta Potential.....	179
6.2.2.4. Cell Culture.....	179
6.2.2.5. Transfection Studies.....	179
6.2.2.6. Cytotoxicity Assay.....	180
6.2.2.7. SYBR Green Assay.....	181
6.2.2.8. The Effect of Dextran Sulfate on the Stability of CPPs and PEI Nanoparticles.....	181
6.2.2.9. Langmuir Trough Experiments.....	182
6.2.2.10. Statistical Analysis.....	182
6.3. Results and Discussion.....	183

6.4. Conclusions.....	199
6.5. References.....	200
 Chapter 7: Conclusion and Future Directions	
7.1.	
Conclusion.....	206
7.2. Future Directions	209
Appendices	211

Chapter 1

Introduction

Noncovalently associated cell-penetrating peptides for gene delivery applications

Published as:

Alhakamy, N. A.; Nigatu, A. S.; Berkland, C. J.; Ramsey, J. D. Noncovalently associated cell-penetrating peptides for gene delivery applications. *Therapeutic delivery* 2013, 4, (6), 741-757.
(2013)

1.1. Introduction to Noncovalently Associated Cell Penetrating Peptides for Nonviral Gene Delivery Applications

The past decade has witnessed a dramatic acceleration in the production of new therapeutic macromolecules, such as proteins, peptides, and nucleic acids, with the interest of overcoming limitations of small-molecule drugs such as specificity, poor potency and rapid elimination. Gene therapy, which involves the delivery of large macromolecules of nucleic acids, has emerged as a popular topic among researchers because of its potential to treat severe and challenging-to-cure diseases, such as inherited genetic diseases, viral infections and various cancers ¹. Genetic treatment of these diseases has garnered significant attention over the past 20 years ² and is nearly a reality, as supported by the hundreds of clinical trials ³.

Gene therapy utilizes the delivery of genetic material into target cells to replace a gene that is missing, mutated or poorly expressed. Gene therapy also used to silence gene expression and production of proteins using siRNA ⁴. Clinical applications, however, have been hindered by formulation issues, poor *in vivo* stability, problems with delivery to target cells, and inefficient cellular uptake ⁵. One of the main hindrances for administering genetic material is the inability of DNA or RNA to reach cellular and intracellular target sites such as nuclei and mitochondria ^{6,7}. The cellular plasma membrane is an impermeable barrier for most hydrophilic macromolecules ⁸. Transporting nucleic acids across the plasma membrane, however, is necessary since these therapeutic agents must be internalized for biological activity ⁹.

Notable effort is being made to develop viral and nonviral vectors that can cross the plasma membrane and deliver therapeutic agents into target cells ¹⁰. Viral vectors (e.g., adenoviruses, adeno-associated viruses, and retroviruses) can be highly efficient and are currently used in the majority of ongoing clinical trials. Viral vectors have the natural ability to attach and enter target

cells while protecting genetic material and providing long-term gene expression. In some cases, however, dependency of the virus on certain cellular receptors compromises the efficiency of the viral vector. In addition, viral vectors introduce safety concerns such as the risk of oncogenesis and immunogenicity ¹¹. Consequently, nonviral vectors are being pursued as flexible, easy, and potentially safer alternatives ^{12, 13}, yet, they continue to lack the necessary efficiency required for clinical application ¹⁴.

Since their discovery two decades ago, cell penetrating peptides (CPPs) have been used for a diverse number of applications in numerous types of cells ¹. CPPs are generally defined as cationic or amphipathic peptides consisting of 30 or fewer amino acids with a structure that can mediate movement across a plasma membrane into the cell cytoplasm ¹⁵⁻¹⁷. CPPs translocate into cells without cytotoxic effects, are efficiently internalized across cell membranes and aid in carrying cargo into live cells ¹⁸. Although the internalization mechanisms are debatable, the application of CPPs is growing rapidly ¹⁹. Some studies suggest that CPPs directly penetrate (e.g., carpet, inverted micelle, and toroidal) through the lipid bilayer of the cell membrane, and others suggest that CPPs employ diverse endocytic pathways (e.g., macropinocytosis, clathrin-dependent, caveolae-mediated, and clathrin-/caveolae-independent) (**Figure 1**) ^{16, 20, 21}. Additionally, some CPPs are capable of using both direct penetration and endocytosis for cellular internalization. One study indicated that the internalization mechanism of arginine-containing CPPs is dominated by direct membrane penetration, while the internalization mechanism of arginine-containing CPPs mediating delivery of DNA is dominated by endocytosis ²². Another study found that direct membrane penetration occurs at low extracellular CPP concentrations, while endocytosis is activated at higher peptide concentrations ²³. This review focuses mainly on current classifications,

formulation approaches, and applications relating to strategies that use noncovalent association of CPPs and gene vectors (viral and nonviral) to improve delivery of genetic material.

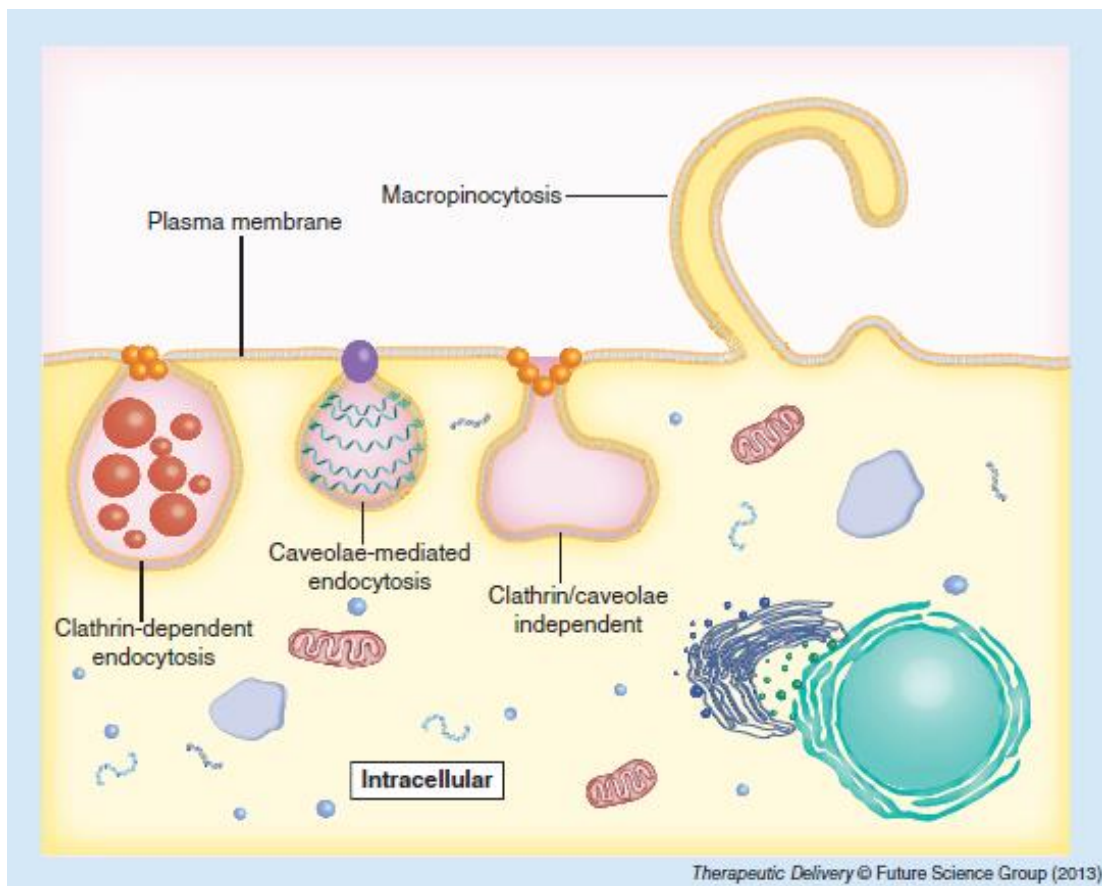


Figure 1. Three proposed endocytic pathways for cell penetrating peptide entry. Cell penetrating peptides may enter target cells through macropinocytosis, clathrin-dependent endocytosis, caveolae-mediated endocytosis, or clathrin-/caveolae-independent endocytosis.

1.2. Overview of Current Classifications

CPPs are used to enhance cellular internalization of different biomolecules or vectors (e.g., pDNA, siRNA, oligonucleotides, liposomes, peptides, proteins and viruses) ⁴. The existence of diverse internalization mechanisms is of great importance when considering the use of CPPs as drug transporters. The exact mechanism, however, is not well understood. Some researchers

indicated that uptake pathways of CPPs do not involve cellular receptors ²⁴. Other studies have reported that the electrostatic interaction of cationic CPP with negatively charged heparan sulfate proteoglycans that are found abundantly on the cell membrane triggers endocytotic internalization ²⁵. The exact mechanism of internalization is governed by cell type, cargo type and CPP properties, such as sequence, molecule length, and secondary structure ²⁶. The nature of the CPPs (e.g., size, surface charge, or hydrophilicity) ²⁷ and whether the CPPs are covalently or noncovalently attached (**Figure 2**) influence the internalization mechanism ²⁸. The origin of a CPP also provides some insight into the mechanism of internalization.

Over the past two decades, more than 100 diverse peptide sequences (5–40 peptide residues), isolated from various sources, have been identified as being capable of mediating the transport of diverse biological molecules, such as pDNA, siRNA, and large molecules, such as viruses ²⁹. The TAT of HIV, which was discovered in 1988, was found to efficiently enter mammalian cells ³⁰. In 1991 Joliot et al. discovered that *Drosophila* Antennapedia homeodomain could translocate into neuronal cells ³¹. A short while later in 1996, Derossi and colleagues demonstrated that the peptide Antennapedia, commonly called penetratin (RQIKIYFQNRRMKWKK), could be covalently bound to cargo and translocate into cells ³². The minimum peptide sequence of TAT (YGRK-KRRQRRR) thought to be necessary for cellular uptake was identified by Vives et al. in 1997 ³³.

CPPs can be classified in different ways, and one manner of classification is on the basis of their origin. This classification sort CPPs into three major classes:

- Protein derived peptides (e.g., TAT and penetratin);
- Chimeric peptides (e.g., transportan);
- Synthetic peptides (e.g., polylysine [PLL]) ³⁴.

CPPs can also be divided into two groups based on the internalization mechanism: energy-dependent (endocytosis) and energy-independent (direct translocation) transport through the cell membrane³⁵. Another way of classifying CPPs is based on their physicochemical properties. Here, CPPs are divided into three classes:

- Cationic CPPs, which are short peptide residue sequences that mostly consist of arginine, lysine, and/or histidine (e.g., TAT and PLL);
- Amphipathic CPPs, which have a lipophilic (non-polar) domain and a hydrophilic (polar) domain (e.g., MPG);
- Hydrophobic CPPs, which consist of hydrophobic residues, such as valine, leucine and tryptophan (e.g., Bip and FGF12)³⁶.

1.3. Formulation Strategies

Two main strategies have explored the use of CPPs to deliver cargo (**Figure 2**). The first strategy uses chemical linkers to covalently attach CPPs to their cargo, and the second strategy relies on electrostatic, self-assembly to form noncovalent complexes between CPPs and their cargo. Various CPPs including peptides derived from TAT³⁷, penetratin,³⁸ transportan³⁹ and polyarginine peptides⁴⁰ have been covalently attached to viral and nonviral gene and⁴¹⁻⁴³ shown to increase transfection and biological effects⁴⁴.

Approaches for forming conjugates include mainly thioester or disulfide bonds⁴⁵. Muratovska and Eccles investigated the transfection efficiency of different CPPs (e.g., penetratin) conjugated to siRNA *via* disulfide bonds and reported that these CPP–siRNAs efficiently reduced transient and stable expression of reporter transgenes in different cell types equivalent or better than cationic liposomes. Disulfide bonds were said to increase CPP affinity for genetic material (e.g., DNA or RNA) by the ‘chelate effect’, which increases the complex stability and reduces

cytotoxicity by rapid degradation in the cytoplasmic space^{46, 47}. Other studies have observed that cysteine residues added onto CPPs can have a significant impact on delivery. One study, for example, demonstrated that the introduction of a single cysteine residue on the C-terminal of various CPPs (e.g., TAT and transportan) resulted in formation of peptide dimers that greatly enhanced the transfection efficiency of DNA in HEK293T cells⁴⁸.

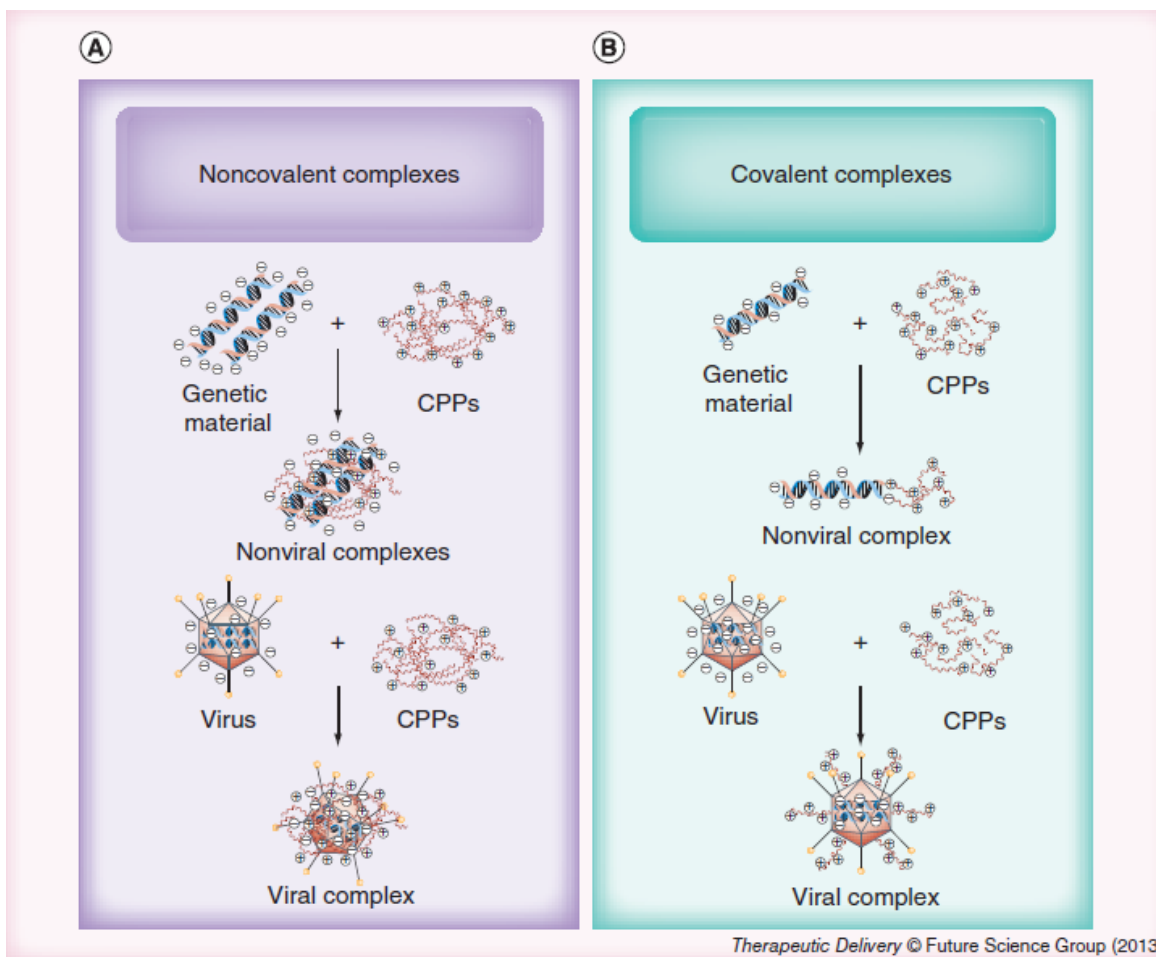


Figure 2. Approaches to forming viral and nonviral vector complexes. Formation of (A) covalently and (B) noncovalently formed CPP–genetic material and CPP–virus complexes. CPPs: Cell penetrating peptides.

Cargos without thiol groups or disulfide bonds can be altered by chemical synthesis and/or recombinant techniques. One example is a study where two types of CPP–oligonucleotide conjugates were prepared in order to improve the transfection efficiency. Unexpectedly, the CPP–oligonucleotide conjugates were more effective in the presence of serum than when used with serum-free medium, which is in notable contrast to most other approaches to gene delivery⁴⁹. The development of CPP-conjugated cargo necessitates careful assessment to determine if there is a therapeutic benefit gained by conjugation²⁴.

The second strategy of using CPPs foregoes the formation of chemical bonds and simply complexes CPPs or CPP-containing molecules with cargo *via* electrostatic interactions. MPG⁵⁰,⁵¹, Pep-1⁵² and TAT⁵³ were among the first CPPs used following this method for complex formation and gene delivery⁵⁴. This strategy has recently been extended to other CPPs, such as polyarginine⁵⁵. CPP complexation with genetic material originally devised to facilitate exploration of numerous peptides that may condense nucleic acids or favor endosomal escape²⁴.

1.4. Motivation for Using Noncovalently Associated CPPs

Both viral and nonviral vectors suffer from drawbacks that hinder the advancement of gene therapy beyond the clinical trial stages, and there is much emphasis on design of improved vectors⁵⁶. CPPs provide an additional strategy for improving existing vectors. Such improvements include enhanced transfection efficiency, increased cargo capacity, low cytotoxicity and reduced immunogenicity². While there is the potential for significant enhancement of existing vectors, there are also some drawbacks associated with CPPs and the methods by which they are associated with the genetic cargo. For example, one shortcoming of CPPs is their general lack of specificity^{57, 58}. A second drawback is associated with the covalent attachment of CPPs. While covalently bound CPPs form well-defined chemical entities that are more likely to be approved for clinical

use than less defined nanoparticles formed through electrostatics, the chemical linking of CPPs to the cargo has been reported to lead to loss of biological activity in some cases. For example, one study found that chemical conjugation of CPPs to methotrexate improved the intracellular concentration of the drug but reduced its potency by 20-fold compared with the unconjugated drug⁵⁹.

Covalent conjugation of cationic CPPs has been observed to enhance cellular uptake by engaging the cell surface⁶⁰, but many have asserted that the covalent bond between CPP and vector must be reversible inside the cellular environment for desired cytoplasmic and nuclear localization⁶¹. Since conjugation of cargo with CPPs may affect nuclear localization and lead to loss of biological activity, an attractive approach is to develop linker strategies that will enable genetic material to be cleaved from CPPs as soon as the vector reaches the cytoplasm²⁴. The linker chemistry, however, becomes more difficult and complicated when dealing with CPPs and nucleic acids or viruses, since several functional components are represented. In addition, the CPP-conjugated vector should be easy to produce and cost-effective to manufacture in order to develop this strategy at an industrial scale for clinical applications⁵⁶. Furthermore, as mentioned earlier, the risk of diminishing the biological activity of the cargo may limit the benefit of this strategy. Although chemical conjugation of CPPs appears promising, several concerns and questions are still under investigation⁶².

Strategies that do not rely on chemical conjugation of CPPs also offer promise for developing gene vectors¹. This method is advantageous because it usually employs simple mixing of the two components, thus eliminating the need to imbue reactive sites or optimize synthetic schemes. The dense positive charge of CPPs assists with electrostatic packaging of the negatively charged genetic material and often yields a positively charged particle⁶³⁻⁶⁵. This strategy is often

avored over chemical reactions when exploring gene therapy in preclinical studies ¹. In addition, the use of cationic or amphipathic CPPs to form complexes with nucleic acids was found to improve the transfection efficiency and nuclear uptake of siRNA within non-dividing cells ^{64, 65}. The following sections review some current applications of noncovalently associated CPPs for improving viral and nonviral gene delivery. **Table 1** contains a list of classical CPPs that have been investigated for their ability to penetrate the cell membrane.

Table 1. Current applications of noncovalent strategies of classical cell penetrating peptides.

Strategy	Function	Peptide	Sequence
Nonviral	Genetic material Condensation	Polylysine	$K_{(n)}$
		Lysine-rich CPPs	K_{rich}
		Polyarginine	$R_{(n)}$
		Arginine-rich CPPs	R_{rich}
		TAT	RKKRRQRRR
	Endosomolytic CPPs	Histidine-rich CPPs	H_{rich}
		MPG	GALFLGFLGAAGSTMGAWSQPKKKRKV
		Penetratin	RQIKIWFQNRRMKWKK
	Fusogenic CPPs	Transportan	GWTLNSAGYLLGKINLKALAALAKKIL
		Melittin	GIGAVLKVLTTGLPALISWIKRKRQQ
		GALA	WEAALAEALAEALAEHLAEALAEALEALAA
		KALA	WEAKLAKALAKALAKHLAKALAKALKACEA
	Nuclear Localization CPPs	SV40 T antigen	CGPGDDEAAADAQHAAPPKKKRKVGY
		M9	NQSSNFGPMKGGNFGGRSSGPYGGGGQYFAKPRNQGGY
		TAT	RKKRRQRRR
	Noncovalently Associated CPPs for Cellular Targeting	RVG	YTIWMPENPRPGTPCDIFTNSRGKRASNG
Viral	Noncovalent CPP/virus	Penetratin	RQIKIWFQNRRMKWKK
		TAT	RKKRRQRRR
		Polyarginine	$R_{(n)}$
		HP4	RRRRPRRRTTRRRR
		Hph-1	YARVRRRGPRR

1.5. Current Applications Using the Noncovalent Strategy for Nonviral Gene Delivery

1.5.1. CPP-Enhanced Nonviral Gene Delivery

The inefficiency of nonviral vectors is due mainly to difficulty overcoming barriers between the administration site and the nucleus of the target cells. Examples of barriers include the physico-chemical stability of the genetic material and its delivery vehicle in the extracellular space; efficient cellular uptake, which may depend on the size of the complex; escape from the endosomal network before degradation within lysosomes; and genetic material unpackaging and entry into the nucleus (**Figure 3**). Overcoming these barriers is one of the greatest challenge for efficacious nonviral gene delivery³. Because of the ability of CPPs to transport cargo across the cell membrane, these peptides are an attractive option for helping nonviral particle overcome some of the barriers to gene delivery. A common approach for complexing CPPs to the nonviral vector is simple electrostatic formation of a complex between cationic CPPs and anionic nucleic acids. One example of how useful CPPs can be is the incorporation of CPPs in a PLL–siRNA polyplex⁴⁴. The investigators in this study used a PLL, modified to bind to CPPs, to first form an electrostatic complex with siRNA. The resulting polyplex was subsequently bound by CPPs to produce a CPP–PLL–siRNA polyplex. The investigators reported high transfection efficiency, but also emphasized the importance of the siRNA being released from the polyplex in order to function. While activity is not adversely affected as it may be when CPPs are chemically conjugated directly to the genetic material⁶⁶, unpackaging remains a concern with vectors formed through noncovalently bound CPPs. Additional studies have established various applications of electrostatic complexes by using diverse CPPs and conditions. The following section discusses CPPs that are able to perform several functions to carry out various gene delivery applications.

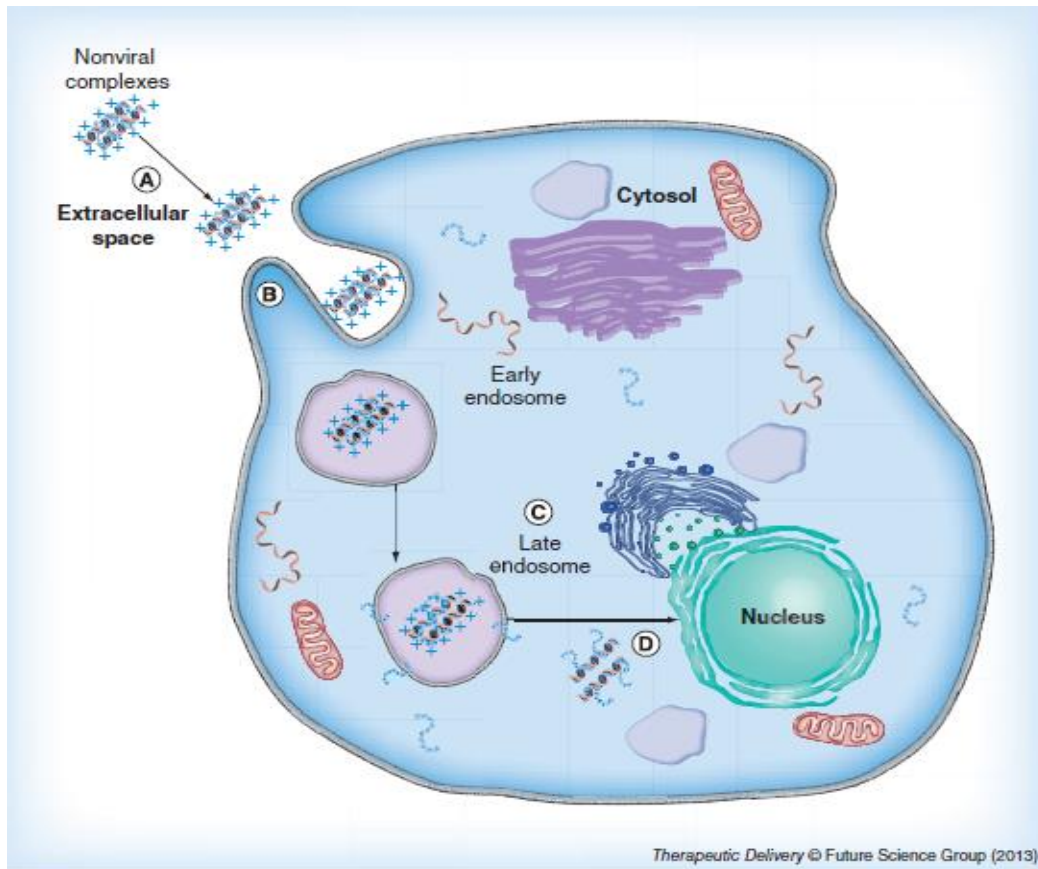


Figure 3. Barriers to nonviral gene delivery. **(A)** The physiochemical stability of nonviral complexes in the extracellular space. **(B)** Cellular uptake. **(C)** Escape from the endosome. **(D)** Genetic material unpackaging and entry into the nucleus.

1.5.2. Genetic Material Condensation with CPPs

Cationic CPPs interact with the negatively charged phosphate backbone of genetic material (e.g., pDNA and siRNA) through electrostatic interaction^{63,67}. This process can result in genetic material condensation and protection from nuclease enzyme digestion⁶⁸. If carried out properly, this approach leads to small nano-particles with a net positive charge that are capable of interaction with moieties such as heparan sulfate proteoglycans on cell surfaces^{69,70}.

PLL, a well-known nonviral DNA condensing agent used to mediate gene delivery, was one of the first cationic peptides studied. There is some toxicity associated with PLL, however,

and as with many polycations, the cytotoxicity increases as the molecular weight of the PLL increases. One group investigating the structure property relationships of PLL describe the *in vitro* cytotoxicity of PLL-based cations and demonstrated that both molecular weight and architecture were important factors ⁷¹. Another group studied a library of 13 PLL-graft-imidazoleacetic acid conjugates to examine the collective effects of polymer molecular weight, DNA:polymer ratio, and side chain change on DNA/polycation interaction, transfection efficiency, and cytotoxicity. They found that the *in vitro* cytotoxicity of the polymers increased while total protein expression decreased, with increasing molecular weight ⁷².

While higher molecular-weight PLL possesses greater toxicity, it is able to bind DNA tighter and form more stable complexes than low-molecular-weight PLL due to the greater abundance and density of positive charges ⁷³. Numerous scientists have turned to the development of homogenous PLL-containing peptides due to the lack of chemical control and poly-dispersity of PLL ^{74, 75}. In order to determine the optimal lysine chain length for DNA condensation and transfection efficiency, a group of researchers systematically studied different lengths of the cationic peptide Cys-Trp-Lys_n three to 36 lysine residues. Shorter peptides of eight or fewer lysine residues formed large particles due to weakly bound DNA, while peptides containing 13 or more lysine residues were able to strongly bind DNA and form small particles (from 50 to 200 nm) ⁷⁶. Another study reported that peptides containing 18 lysine residues could condense and protect DNA from degradation, while a short peptide containing less than eight residues could not prevent DNA degradation ⁷⁷.

The chemical nature of cationic residues has been found to influence cellular uptake ⁷⁸⁻⁸⁰. Arginine tends to mediate cell uptake better than ornithine or lysine and at least six to eight cationic residues were reported to be the minimum number required for DNA condensation ⁸⁰. Studies

demonstrated that when lysine residues were replaced with arginine residues in a penetratin variant, the modified penetratin had better cellular uptake than itself^{81,82}. Arginine-rich CPPs have also been reported to be more efficient than lysine-rich CPPs^{82,83}. In fact, polyarginine peptides have been demonstrated to play an important role in cytosol-to-nucleus transport and nuclear localization of plasmid DNA (**Figure 4**)^{84,85}.

The polyarginine peptides used by Kim *et al.* demonstrated significant co-localization of CPP and DNA near the nucleus, with some material located within the nucleus. Although, the majority of the complexes appears to have remained outside the nucleus in a perinuclear compartment. Location of the complexes near the nucleus will undoubtedly improve gene delivery to the nucleus, but the limited nuclear entry indicates the additional need for some type of active transport into the nucleus, such as an addition of a nuclear localization signal (NLS).

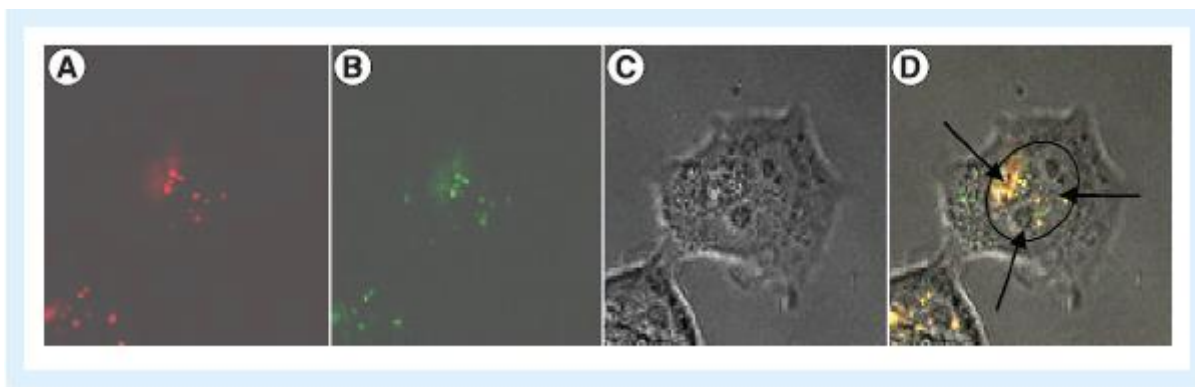


Figure 4. Arginine peptide-improved transportation of DNA around and into the nucleus in live cells. The cells were treated with FITC-labeled arginine peptide/rhodamine-labeled DNA complexes and imaged using confocal microscopy. (**A**) Rhodamine-labeled DNA (red); (**B**) FITC-labeled arginine peptide (green); (**C**) differential interference contrast; and (**D**) a merge of **A**, **B**, and **C**. Panel **D** illustrates the nucleus circled and the presence of both peptide-bound DNA and free DNA.

Polyarginine peptides have a strong tendency to electrostatically interact with both siRNA^{86, 87} and with DNA⁶⁷. One study indicated that as with PLL and other polycations, the length of polyarginine may affect transfection efficiency and cytotoxicity. A minimum chain length of six to ten amino acids is needed for delivery of genetic material, which is enough to condense DNA into stable complexes. With polyarginine 9, only four to five arginine residues were thought to be involved in forming the complexes with genetic material, while the extra arginine residues were available for interaction with the cell membrane. Furthermore, they have considered the possibility that genetic material may not be released from the complexes when the cationic CPPs bind too strongly with the negatively charged genetic material⁴⁷.

The size of polyarginines has been explored by several groups. One group studied the transfection efficiency of different polyarginine peptides (arginine 9, 12 and 16), which was found to increase when the molecular weight increased⁶⁷. Another group examined the transfection efficiency of different polyarginine molecular weights complexed with pDNA. They found that the high-molecular-weight polyarginines (41 and 83 kDa) demonstrated 100-times higher transfection efficiency (RLU/ug protein) than the lower molecular-weight polyarginine approximately (10 kDa)⁸⁸.

In addition to molecular weight and residue charge, peptide hydrophobicity has also been studied. One study examined the effects of introducing a hydrophobic group onto CPPs such as TAT and polyarginine. They found that N-terminal stearylolation of these CPPs increased the transfection efficiency by approximately 100-fold to reach the same order of magnitude as that of Lipofectamine 2000™ (Invitrogen, Paisley, UK). They suggested that the hydrophobic moieties contributed to absorption of the complexes on the surface of cell membrane thereby destabilizing the membrane. This explanation provides a possible understanding for the high transfection

efficiency of these complexes ⁸⁹. Another study tested the hypothesis that hydrophobically modified CPPs, cholesteryl polyarginine 9, may stabilize and improve tumor regression efficacy of the VEGF targeting siRNA. They indicated that this nonconjugate complexation of the siRNA with cholesteryl polyarginine 9 efficiently transfected siRNA into cells *in vitro*. Polyarginine peptide offers efficient siRNA packaging and cell membrane interaction. The cholesterol moiety was able to engage the hydrophobic residues of the extracellular cell surface, which enhanced the transfection efficiency of the complexes ⁸⁷.

Furthermore, calcium chloride was used as a condensing agent for large CPP complexes with DNA or RNA. The transfection of different CPPs (e.g., arginine 7 and TAT) complexed with siRNA or pDNA was practically nil; however, the addition of calcium chloride decreased the large size of these complexes through 'soft' cross-links. Adding calcium chloride to the CPP complexes led to an increase in transfection efficiency ^{62, 90}. In another report, arginine-rich CPPs (PR9, SR9 and HR9) were used to deliver genetic material into target cells. The researchers proposed that calcium condensed CPPs/DNA complexes into small particles and that including calcium chloride caused a significant increase in cellular internalization and gene expression (**Figure 5**) ⁴⁶.

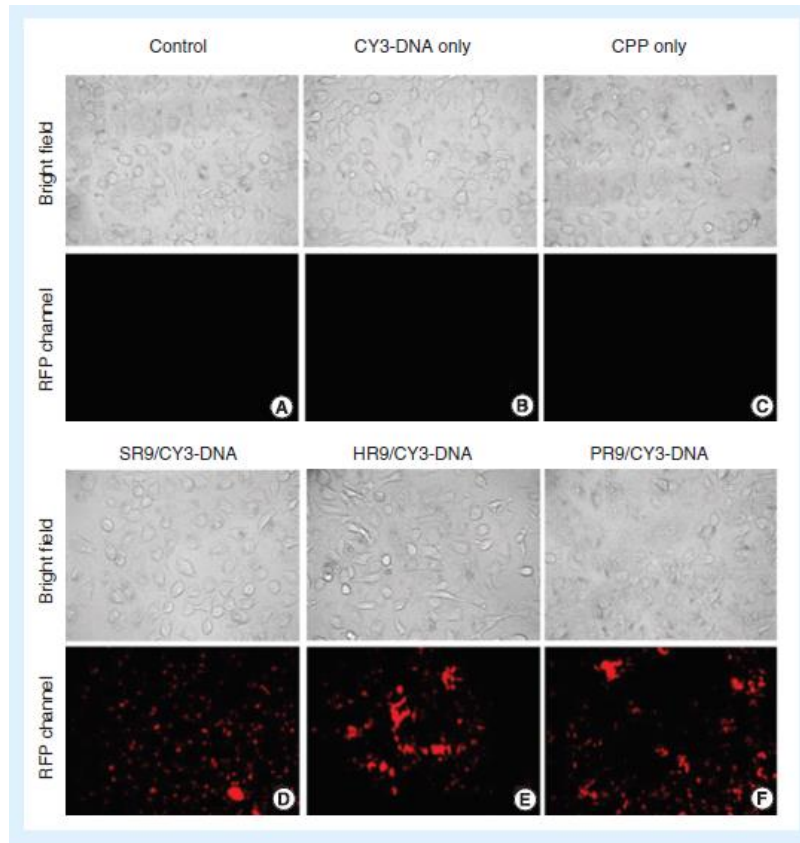


Figure 5. Cell penetrating peptide-mediated delivery of Cy3-labeled DNA into cells. Cells were treated with: (A) phosphate-buffered saline as a negative control; (B) Cy3-labeled DNA only; (C) peptide HR9 only; (D) SR9/Cy3-labeled DNA; (E) HR9/Cy3-labeled DNA; or (F) PR9/Cy3-labeled DNA. The fluorescent microscopy indicates the location of Cy3-labeled DNA inside cells. CPP: Cell penetrating peptide.

1.5.3. Endosomolytic and Fusogenic CPPs

One of the major limitations in the delivery of genetic material using CPPs complexes is the entrapment of the complexes within endosomal vesicles. In order to avoid this problem and enhance the transfection efficiency, an endosomolytic agent, such as chloroquine, may be used, but, unfortunately, this is not feasible for *in vivo* gene delivery⁶². Endosomolytic CPPs can be used to overcome this obstacle as they are able to enhance gene delivery by inducing release from endosomes. Several peptides with high charge density were surmised to act as a ‘proton sponge’ and become endosomolytic at the acidic environment of the endosome. These peptides can either

fuse with the endosomal membrane leading to pore formation or act as a ‘proton sponge’ causing lysis^{68, 91-93}. In order to apply the lysis activity to CPPs, histidine residues were added to CPP sequences. The imidazole group of histidine (pKa approximately 6.0) can remain neutrally charged at physiological pH. Then, it can become protonated in the acidic environment of the endosome, thus, imparting selective membrane disruption⁶⁸. Histidine residues have been inserted into PLL in order to enhance the transfection efficiency of noncovalent complexes⁹⁴. A published study offered a comparative analysis of the ability of various CPPs (e.g., MPG and penetratin) to complex siRNA molecules and induces efficient cellular internalization⁹⁵. Other investigators studied the gene expression of three arginine-rich CPPs (SR9, PR9 and HR9). Researchers indicated that HR9 was superior, possibly because of the histidine facilitated DNA endosomal escape⁴⁶. Another group indicated that efficient endosomolytic peptides, such as EB1, can be applied to enhance the ability of CPP/siRNA complexes to effectively deliver siRNA across the endosomal membrane⁹⁵.

Fusogenic CPPs are short peptides with the potential to promote membrane destabilization, endosomal escape and delivery of genetic material to the cytosol and/or nucleus. Numerous fusogenic CPPs are derived from different proteins that interact with cell membranes such as TAT, transportan, and melittin. Fusogenic CPPs have hydrophilic and hydrophobic domains resulting in helical structures of the CPPs at endosomal pH, which can interact with the endosomal membrane to cause pore formation⁹⁶. A group of researchers used short peptides derived from the influenza virus hemagglutinin HA-2 and found that DNA polyplexes containing the influenza peptide as a fusogenic peptide conjugated to PLL could mediate significant gene expression when compared with complexes without the fusogenic peptide⁹³. Melittin has been developed into gene delivery CPPs that can condense DNA⁹⁷. GALA is the synthetic fusogenic CPP that has a repeating unit of

glutamic acid-alanine-leucine-alanine that gives melittin an amphipathic character. GALA can bind to bilayer membranes and induce leakage. Although GALA has fusogenic activity, it cannot bind and condense DNA for effective transfection due to the negative charge of this peptide. In order to increase the DNA condensation and transfection efficiency of GALA, some alanine residues have been substituted with lysine residues and glutamic acid was reduced, yielding the cationic KALA peptide. DNA complexes prepared with KALA were able to effectively transfect different cell lines⁹⁸.

1.5.4. Nuclear Localization CPPs

The passage of pDNA from the cytoplasm into the nucleus is one of the main barriers to nonviral gene delivery. The nuclear membrane of human cells is permeable to particles of up to approximately 9 nm. Transfer of large molecules such as pDNA through nuclear pore complexes is signal-mediated and energy dependent⁹⁹. NLS peptides mediate the transport of pDNA or RNA from the cytoplasm into the nucleus through nuclear pore complexes¹⁰⁰. The highly positively charged NLS peptides can efficiently interact with the negatively charged pDNA. There is a possibility that the NLS peptides dissociate from the pDNA before reaching the nucleus. In order to enhance the nuclear targeting of complexes, another condensation agent or CPPs may be added⁹⁶. NLS of SV40 large T-antigen is the most common nuclear localization peptide that has been used¹⁰¹ for efficiently transferring pDNA from cytoplasm to nucleus by forming noncovalent complexes with pDNA¹⁰². Another NLS peptide noncovalently complexed with pDNA is the M9 peptide, which was also complexed with SV40 large T-antigen to enhance ionic interaction with pDNA and increase gene expression¹⁰³. TAT, another NLS peptide, has been demonstrated to mediate the import of diverse cargos into the cell nucleus, including dye-labeled streptavidin protein and quantum dots for kinetic measurement. One study reported that TAT peptide could

import 90 nm beads into the cell nucleus, suggesting that its interaction with the nuclear envelope follows a mechanism different from that of other NLS ¹⁰⁴.

1.5.5. Noncovalently Associated CPPs for Targeted Delivery

Targeted gene delivery seeks to differentiate between healthy cells and diseased cells. The specificity for a target site is one of the main challenges that belie the efficiency of noncovalent gene complexes ¹⁰⁵. The first example of this approach was done by a group of scientists who fused a short peptide derived from RVG to RVG-9R, and then complexed RVG-9R with siRNA to specifically target neuronal cells ⁵⁵. Additionally, gene vectors that bind integrin with the help of peptide ligands have been used in the improvement of targeted vectors. Integrins are cell receptors, which have many roles such as cell migration, signal transduction, and cell to cell interactions. Integrin-binding peptides commonly have short sequences of amino acids and can bind a widespread variety of the receptors or be specific for a single peptide ¹⁰⁶. A group used the lectin-like oxidized LDL receptor as a target receptor. They sequenced and identified 60 innovative peptides, which will be beneficial for the selective target of gene transfer vectors to endothelial cells expressing the lectinlike oxidized LDL receptor and in particular dysfunctional endothelial cells associated with atherosclerosis and hypertension ¹⁰⁷. Lastly, a study observed differential transfection of cells overexpressing ICAM-1 when treated with a TAT-PEG-LABL peptide complexed with pDNA and condensed with calcium chloride. The results demonstrated the possibility of targeting gene transfection to inflammation sites¹⁰⁸.

1.6. Thesis Overview

This thesis work aimed to identify safe, and effective nonviral gene vectors. Short cationic cell penetrating peptides (CPPs) have been explored as carriers for gene delivery. **In chapter 2**, complexes of low-molecular-weight polyarginine and pDNA were condensed with calcium. These complexes showed high transfection efficiency and low cytotoxicity in A549 carcinomic human alveolar basal epithelial cells. The relationships between transfection efficiency and polyarginine size (5, 7, 9, or 11 amino acids), polyarginine/pDNA charge ratios, and calcium concentrations were studied. Polyarginine 7 was significantly more effective than other polyarginines under most formulation conditions, suggesting a link between cell penetration ability and transfection efficiency.

In chapter 3, a synthetic CPP (polylysine, K9 peptide) was complexed with angiotensin II type 2 receptor (AT2R) plasmid DNA (pAT2R) and complexes were condensed using calcium chloride. The resulting complexes were small (~150 nm) and showed high levels of gene expression *in vitro* and *in vivo*. This simple nonviral formulation approach showed negligible cytotoxicity in four different human cell lines (cervix, breast, kidney, and lung cell lines) and one mouse cell line (a lung cancer cell line). In addition, this K9-pDNA-Ca²⁺ complex demonstrated cancer-targeted gene delivery when administered *via* intravenous injection or intratracheal spray. The transfection efficiency was evaluated in Lewis lung carcinoma (LLC) cell lines cultured *in vitro* and in orthotopic cancer grafts in syngeneic mice. Immunohistochemical analysis confirmed that the complex effectively delivered pAT2R to the cancer cells, where it was expressed mainly in cancer cells along with bronchial epithelial cells. A single administration of these complexes markedly attenuated lung cancer growth, offering preclinical proof-of-concept for a novel nonviral

gene delivery method exhibiting effective lung tumor gene therapy *via* either intravenous or intratracheal administration.

In chapter 4, when designing synthetic CPPs for drug delivery applications, it is important to understand their ability to penetrate the cell membrane. Anionic or zwitterionic phospholipid monolayers at the air–water interface are used as model cell membranes to monitor the membrane insertion potential of synthetic CPPs. The insertion potential of CPPs (five hydrophilic CPPs [dTAT, R9, L9, H9, and RH9] and three amphiphilic CPPs [RA9, RL9, and RW9]) having different cationic and hydrophobic amino acids were recorded using a Langmuir monolayer approach that records peptide adsorption to model membranes. Fluorescence microscopy was used to visualize alterations in phospholipid packing due to peptide insertion. All CPPs had the highest penetration potential in the presence of anionic phospholipids. In addition, two of three amphiphilic CPPs penetrated into zwitterionic phospholipids, but none of the hydrophilic CPPs did. All the CPPs studied induced disruptions in phospholipid packing and domain morphology, which were most pronounced for amphiphilic CPPs. Overall, small changes to amino acids and peptide sequences resulted in dramatically different insertion potentials and membrane reorganization. Designers of synthetic CPPs for efficient intracellular drug delivery should consider small nuances in CPP electrostatic and hydrophobic properties.

In chapter 5, we show that calcium condensed gene complexes containing different hydrophilic (i.e., dTAT, K9, R9, and RH9) and amphiphilic (i.e., RA9, RL9, and RW9) CPPs formed stable cationic complexes of hydrodynamic radii 100 nm at neutral pH. However, increasing the acidity caused the complexes to become neutral or anionic and increase in size. Using zwitterionic and anionic phospholipid monolayers as models that mimic the membrane composition of the outer leaflet of cell membranes and intracellular vesicles, and pHs that mimic

the intracellular environment, we study the membrane insertion potential of these seven gene complexes (CPP-pDNA-Ca²⁺ complexes) into model membranes. At neutral pH, all gene complexes demonstrated the highest insertion potential into anionic phospholipid membranes, with complexes containing amphiphilic peptides showing the maximum insertion. However, at acidic pH, the gene complexes demonstrated maximum monolayer insertion into zwitterionic lipids, irrespective of the chemical composition of the CPP in the complexes. Our results suggest that in the neutral environment, the complexes are unable to penetrate the zwitterionic lipid membranes, but can penetrate through the anionic lipid membranes. However, the acidic pH mimicking the local environment in the late endosomes leads to a significant increase in adsorption of the complexes to zwitterionic lipid headgroups, and decreases for anionic headgroups. These membrane-gene complex interactions may be responsible for the ability of the complexes to efficiently enter the intracellular environment through endocytosis and escape from the endosomes to effectively deliver their genetic payload.

Finally, **in chapter 6**, small changes in CPP charge type, charge spacing, and hydrophobicity were studied by using five arginine-rich CPPs: the well-known hydrophilic polyarginine R9 peptide, a hydrophilic RH9 peptide, and three amphiphilic peptides (RA9, RL9, and RW9) with charge distributions that favor membrane penetration. Condensing these CPP-pDNA complexes *via* addition of calcium chloride produces small and stable nanoparticles with high levels of gene expression. This simple formulation offered high transfection efficiency and negligible cytotoxicity in HEK-293 (a virus-immortalized kidney cell) and A549 (a human lung cancer cell line). R9 and RW9 complexes were significantly more effective than the other CPPs under most formulation conditions. However, these CPPs exhibit large differences in membrane

penetration potential. Maximum transfection resulted from an appropriate balance of complexing with pDNA, releasing DNA, and membrane penetration potential.

1.7. References

1. Heitz, F.; Morris, M. C.; Divita, G. Twenty years of cell-penetrating peptides: from molecular mechanisms to therapeutics. *Br J Pharmacol* **2009**, *157*, (2), 195-206.
2. Hoyer, J.; Neundorff, I. Peptide vectors for the nonviral delivery of nucleic acids. *Accounts of Chemical Research* **2012**, *45*, (7), 1048-1056.
3. Wiethoff, C. M.; Middaugh, C. R. Barriers to nonviral gene delivery. *Journal of pharmaceutical sciences* **2003**, *92*, (2), 203-217.
4. Munyendo, W. L. L.; Lv, H.; Benza-Ingoula, H.; Baraza, L. D.; Zhou, J. Cell penetrating peptides in the delivery of biopharmaceuticals. *Biomolecules* **2012**, *2*, (2), 187-202.
5. Ilina, P.; Hyvonen, Z.; Saura, M.; Sandvig, K.; Yliperttula, M.; Ruponen, M. Genetic block of endocytic pathways reveals differences in the intracellular processing of non-viral gene delivery systems. *Journal of Controlled Release* **2012**, *163*, (3), 385-395.
6. Torchilin, V. P. Recent approaches to intracellular delivery of drugs and DNA and organelle targeting. *Annu. Rev. Biomed. Eng.* **2006**, *8*, (24), 343-375.
7. Medina-Kauwe, L.; Xie, J.; Hamm-Alvarez, S. Intracellular trafficking of nonviral vectors. *Gene therapy* **2005**, *12*, (24), 1734-1751.
8. Mäe, M.; Myrberg, H.; El-Andaloussi, S.; Langel, Ü. Design of a tumor homing cell-penetrating peptide for drug delivery. *International Journal of Peptide Research and Therapeutics* **2009**, *15*, (1), 11-15.
9. Wender, P. A.; Galliher, W. C.; Goun, E. A.; Jones, L. R.; Pillow, T. H. The design of guanidinium-rich transporters and their internalization mechanisms. *Advanced drug delivery reviews* **2008**, *60*, (4), 452-472.

10. Deshayes, S.; Morris, M.; Divita, G.; Heitz, F. Cell-penetrating peptides: tools for intracellular delivery of therapeutics. *Cellular and Molecular Life Sciences CMLS* **2005**, *62*, (16), 1839-1849.
11. Kay, M. A.; Glorioso, J. C.; Naldini, L. Viral vectors for gene therapy: the art of turning infectious agents into vehicles of therapeutics. *Nature medicine* **2001**, *7*, (1), 33-40.
12. De Jong, G.; Telenius, A.; Vanderbyl, S.; Meitz, A.; Drayer, J. Efficient in-vitro transfer of a 60-Mb mammalian artificial chromosome into murine and hamster cells using cationic lipids and dendrimers. *Chromosome research* **2001**, *9*, (6), 475-485.
13. Kreiss, P.; Mailhe, P.; Scherman, D.; Pitard, B.; Cameron, B.; Rangara, R.; Aguerre-Charriol, O.; Airiau, M.; Crouzet, J. Plasmid DNA size does not affect the physicochemical properties of lipoplexes but modulates gene transfer efficiency. *Nucleic acids research* **1999**, *27*, (19), 3792-3798.
14. Hassane, F. S.; Saleh, A.; Abes, R.; Gait, M.; Lebleu, B. Cell penetrating peptides: overview and applications to the delivery of oligonucleotides. *Cellular and molecular life sciences* **2010**, *67*, (5), 715-726.
15. Lundberg, M.; Wikström, S.; Johansson, M. Cell surface adherence and endocytosis of protein transduction domains. *Molecular therapy* **2003**, *8*, (1), 143-150.
16. Nakase, I.; Niwa, M.; Takeuchi, T.; Sonomura, K.; Kawabata, N.; Koike, Y.; Takehashi, M.; Tanaka, S.; Ueda, K.; Simpson, J. C. Cellular uptake of arginine-rich peptides: roles for macropinocytosis and actin rearrangement. *Molecular therapy* **2004**, *10*, (6), 1011-1022.
17. Foerg, C.; Ziegler, U.; Fernandez-Carneado, J.; Giralt, E.; Rennert, R.; Beck-Sickinger, A. G.; Merkle, H. P. Decoding the entry of two novel cell-penetrating peptides in HeLa cells: lipid raft-mediated endocytosis and endosomal escape. *Biochemistry* **2005**, *44*, (1), 72-81.

18. Järver, P.; Langel, Ü. Cell-penetrating peptides—a brief introduction. *Biochimica et Biophysica Acta (BBA)-Biomembranes* **2006**, *1758*, (3), 260-263.
19. Lorents, A.; Kodavali, P. K.; Oskolkov, N.; Langel, Ü.; Hällbrink, M.; Pooga, M. Cell-penetrating peptides split into two groups based on modulation of intracellular calcium concentration. *Journal of Biological Chemistry* **2012**, *287*, (20), 16880-16889.
20. Richard, J. P.; Melikov, K.; Brooks, H.; Prevot, P.; Lebleu, B.; Chernomordik, L. V. Cellular uptake of unconjugated TAT peptide involves clathrin-dependent endocytosis and heparan sulfate receptors. *Journal of Biological Chemistry* **2005**, *280*, (15), 15300-15306.
21. Fittipaldi, A.; Ferrari, A.; Zoppé, M.; Arcangeli, C.; Pellegrini, V.; Beltram, F.; Giacca, M. Cell membrane lipid rafts mediate caveolar endocytosis of HIV-1 Tat fusion proteins. *Journal of Biological Chemistry* **2003**, *278*, (36), 34141-34149.
22. Guterstam, P.; Madani, F.; Hirose, H.; Takeuchi, T.; Futaki, S.; Andaloussi, S. E.; Gräslund, A.; Langel, Ü. Elucidating cell-penetrating peptide mechanisms of action for membrane interaction, cellular uptake, and translocation utilizing the hydrophobic counter-anion pyrenebutyrate. *Biochimica et Biophysica Acta (BBA)-Biomembranes* **2009**, *1788*, (12), 2509-2517.
23. Jiao, C.-Y.; Delaroche, D.; Burlina, F.; Alves, I. D.; Chassaing, G.; Sagan, S. Translocation and endocytosis for cell-penetrating peptide internalization. *Journal of Biological Chemistry* **2009**, *284*, (49), 33957-33965.
24. Bolhassani, A. Potential efficacy of cell-penetrating peptides for nucleic acid and drug delivery in cancer. *Biochimica et Biophysica Acta (BBA)-Reviews on Cancer* **2011**, *1816*, (2), 232-246.

25. Fuchs, S. M.; Raines, R. T. Pathway for polyarginine entry into mammalian cell. *Biochemistry* **2004**, *43*, (9), 2438-2444.
26. Patel, L. N.; Zaro, J. L.; Shen, W. C. Cell penetrating peptides: intracellular pathways and pharmaceutical perspectives. *Pharmaceutical research* **2007**, *24*, (11), 1977-1992.
27. Nakase, I.; Akita, H.; Kogure, K.; Gräslund, A.; Langel, U.; Harashima, H.; Futaki, S. Efficient intracellular delivery of nucleic acid pharmaceuticals using cell-penetrating peptides. *Accounts of Chemical Research* **2012**, *45*, (7), 1132-1139.
28. Silhol, M.; Tyagi, M.; Giacca, M.; Lebleu, B.; Vives, E. Different mechanisms for cellular internalization of the HIV-1 Tat-derived cell penetrating peptide and recombinant proteins fused to Tat. *Eur J Biochem* **2002**, *269*, (2), 494-501.
29. Koren, E.; Torchilin, V. P. Cell-penetrating peptides: breaking through to the other side. *Trends in molecular medicine* **2012**, *18*, (7), 385-393.
30. Frankel, A. D.; Pabo, C. O. Cellular uptake of the tat protein from human immunodeficiency virus. *Cell* **1988**, *55*, (6), 1189-1193.
31. Joliot, A.; Pernelle, C.; Deagostini-Bazin, H.; Prochiantz, A. Antennapedia homeobox peptide regulates neural morphogenesis. *Proceedings of the National Academy of Sciences* **1991**, *88*, (5), 1864-1868.
32. Derossi, D.; Calvet, S.; Trembleau, A.; Brunissen, A.; Chassaing, G.; Prochiantz, A. Cell internalization of the third helix of the antennapedia homeodomain is receptor-independent. *Journal of Biological Chemistry* **1996**, *271*, (30), 18188-18193.
33. Vives, E.; Brodin, P.; Lebleu, B. A truncated HIV-1 Tat protein basic domain rapidly translocates through the plasma membrane and accumulates in the cell nucleus. *Journal of Biological Chemistry* **1997**, *272*, (25), 16010-16017.

34. Lindgren, M.; Langel, Ü., Classes and prediction of cell-penetrating peptides. In *Cell-Penetrating Peptides*, Springer: 2011; pp 3-19.
35. Wang, H.; Zhong, C. Y.; Wu, J. F.; Huang, Y. B.; Liu, C. B. Enhancement of TAT cell membrane penetration efficiency by dimethyl sulphoxide. *Journal of Controlled Release* **2010**, *143*, (1), 64-70.
36. Milletti, F. Cell-penetrating peptides: classes, origin, and current landscape. *Drug Discovery Today* **2012**, *15-16*, 850-860.
37. Fawell, S.; Seery, J.; Daikh, Y.; Moore, C.; Chen, L. L.; Pepinsky, B.; Barsoum, J. Tat-mediated delivery of heterologous proteins into cells. *Proceedings of the National Academy of Sciences* **1994**, *91*, (2), 664-668.
38. Derossi, D.; Joliot, A. H.; Chassaing, G.; Prochiantz, A. The third helix of the Antennapedia homeodomain translocates through biological membranes. *Journal of Biological Chemistry* **1994**, *269*, (14), 10444-10450.
39. Pooga, M.; Soomets, U.; Hällbrink, M.; Valkna, A.; Saar, K.; Rezaei, K.; Kahl, U.; Hao, J. X.; Xu, X. J.; Wiesenfeld-Hallin, Z. Cell penetrating PNA constructs regulate galanin receptor levels and modify pain transmission in vivo. *Nature biotechnology* **1998**, *16*, (9), 857-861.
40. Wender, P. A.; Rothbard, J. B.; Jessop, T. C.; Kreider, E. L.; Wylie, B. L. Oligocarbamate molecular transporters: design, synthesis, and biological evaluation of a new class of transporters for drug delivery. *Journal of the American Chemical Society* **2002**, *124*, (45), 13382-13383.
41. Pujals, S.; Fernández-Carneado, J.; López-Iglesias, C.; Kogan, M. J.; Giralt, E. Mechanistic aspects of CPP-mediated intracellular drug delivery: relevance of CPP self-assembly. *Biochimica et Biophysica Acta (BBA)-Biomembranes* **2006**, *1758*, (3), 264-279.

42. Schwarze, S. R.; Hruska, K. A.; Dowdy, S. F. Protein transduction: unrestricted delivery into all cells? *Trends in cell biology* **2000**, *10*, (7), 290-295.
43. Gratton, J. P.; Yu, J.; Griffith, J. W.; Babbitt, R. W.; Scotland, R. S.; Hickey, R.; Giordano, F. J.; Sessa, W. C. Cell-permeable peptides improve cellular uptake and therapeutic gene delivery of replication-deficient viruses in cells and in vivo. *Nature medicine* **2003**, *9*, (3), 357-362.
44. Mo, R. H.; Zaro, J. L.; Shen, W. C. Comparison of Cationic and Amphipathic Cell Penetrating Peptides for siRNA Delivery and Efficacy. *Molecular Pharmaceutics* **2011**, *9*, (2), 299-309.
45. Muratovska, A.; Eccles, M. R. Conjugate for efficient delivery of short interfering RNA (siRNA) into mammalian cells. *FEBS letters* **2004**, *558*, (1), 63-68.
46. Liu, B. R.; Lin, M. D.; Chiang, H. J.; Lee, H. J. Arginine-rich cell-penetrating peptides deliver gene into living human cells. *Gene* **2012**.
47. Won, Y. W.; Kim, H. A.; Lee, M.; Kim, Y. H. Reducible poly (oligo-D-arginine) for enhanced gene expression in mouse lung by intratracheal injection. *Molecular Therapy* **2009**, *18*, (4), 734-742.
48. Åmand, H. L.; Nordén, B.; Fant, K. Functionalization with C-terminal cysteine enhances transfection efficiency of cell-penetrating peptides through dimer formation. *Biochem Biophys Res Commun* **2012**, *505*, (1), 37-45.
49. Astriab-Fisher, A.; Sergueev, D. S.; Fisher, M.; Shaw, B. R.; Juliano, R. L. Antisense inhibition of P-glycoprotein expression using peptide–oligonucleotide conjugates. *Biochemical pharmacology* **2000**, *60*, (1), 83-90.

50. Morris, M.; Vidal, P.; Chaloin, L.; Heitz, F.; Divita, G. A new peptide vector for efficient delivery of oligonucleotides into mammalian cells. *Nucleic acids research* **1997**, *25*, (14), 2730-2736.
51. Morris, M. C.; Chaloin, L.; Méry, J.; Heitz, F.; Divita, G. A novel potent strategy for gene delivery using a single peptide vector as a carrier. *Nucleic acids research* **1999**, *27*, (17), 3510-3517.
52. Morris, M. C.; Depollier, J.; Mery, J.; Heitz, F.; Divita, G. A peptide carrier for the delivery of biologically active proteins into mammalian cells. *Nature biotechnology* **2001**, *19*, (12), 1173-1176.
53. Tung, C.-H.; Mueller, S.; Weissleder, R. Novel branching membrane translocational peptide as gene delivery vector. *Bioorganic & medicinal chemistry* **2002**, *10*, (11), 3609-3614.
54. Vivès, E.; Brodin, P.; Lebleu, B. A truncated HIV-1 Tat protein basic domain rapidly translocates through the plasma membrane and accumulates in the cell nucleus. *Journal of Biological Chemistry* **1997**, *272*, (25), 16010-16017.
55. Kumar, P.; Wu, H.; McBride, J. L.; Jung, K.-E.; Kim, M. H.; Davidson, B. L.; Lee, S. K.; Shankar, P.; Manjunath, N. Transvascular delivery of small interfering RNA to the central nervous system. *Nature* **2007**, *448*, (7149), 39-43.
56. Temsamani, J.; Vidal, P. The use of cell-penetrating peptides for drug delivery. *Drug discovery today* **2004**, *9*, (23), 1012-1019.
57. Nakase, I.; Hirose, H.; Tanaka, G.; Tadokoro, A.; Kobayashi, S.; Takeuchi, T.; Futaki, S. Cell-surface accumulation of flock house virus-derived peptide leads to efficient internalization via macropinocytosis. *Molecular Therapy* **2009**, *17*, (11), 1868-1876.

58. Andreu, D.; Merrifield, R.; Steiner, H.; Boman, H. G. N-terminal analogs of cecropin A: synthesis, antibacterial activity, and conformational properties. *Biochemistry* **1985**, *24*, (7), 1683-1688.
59. Lindgren, M.; Rosenthal-Aizman, K.; Saar, K.; Eiríksdóttir, E.; Jiang, Y.; Sassian, M.; Östlund, P.; Hällbrink, M.; Langel, Ü. Overcoming methotrexate resistance in breast cancer tumour cells by the use of a new cell-penetrating peptide. *Biochemical pharmacology* **2006**, *71*, (4), 416-425.
60. Wadia, J. S.; Dowdy, S. F. Transmembrane delivery of protein and peptide drugs by TAT-mediated transduction in the treatment of cancer. *Advanced drug delivery reviews* **2005**, *57*, (4), 579-596.
61. Meade, B. R.; Dowdy, S. F. Exogenous siRNA delivery using peptide transduction domains/cell penetrating peptides. *Advanced drug delivery reviews* **2007**, *59*, (2), 134-140.
62. Männistö, M.; Vanderkerken, S.; Toncheva, V.; Elomaa, M.; Ruponen, M.; Schacht, E.; Urtti, A. Structure–activity relationships of poly (l-lysines): effects of pegylation and molecular shape on physicochemical and biological properties in gene delivery. *Journal of Controlled Release* **2002**, *83*, (1), 169-182.
63. McKenzie, D. L.; Collard, W. T.; Rice, K. G. Comparative gene transfer efficiency of low molecular weight polylysine DNA-condensing peptides. *The Journal of peptide research* **1999**, *54*, (4), 311-318.
64. Gottschalk, S.; Sparrow, J.; Hauer, J.; Mims, M.; Leland, F.; Woo, S.; Smith, L. A novel DNA-peptide complex for efficient gene transfer and expression in mammalian cells. *Gene therapy* **1996**, *3*, (5), 448.

65. Wadhwa, M. S.; Collard, W. T.; Adami, R. C.; McKenzie, D. L.; Rice, K. G. Peptide-mediated gene delivery: influence of peptide structure on gene expression. *Bioconjugate chemistry* **1997**, *8*, (1), 81-88.
66. Adami, R. C.; Collard, W. T.; Gupta, S. A.; Kwok, K. Y.; Bonadio, J.; Rice, K. G. Stability of peptide-condensed plasmid DNA formulations. *Journal of pharmaceutical sciences* **1998**, *87*, (6), 678-683.
67. Rydberg, H. A.; Matson, M.; Åmand, H. L.; Esbjörner, E. K.; Nordén, B. Effects of Tryptophan Content and Backbone Spacing on the Uptake Efficiency of Cell-Penetrating Peptides. *Biochemistry* **2012**, *51*, (27), 5531-5539.
68. Walrant, A.; Correia, I.; Jiao, C. Y.; Lequin, O.; Bent, E. H.; Goasdoué, N.; Lacombe, C.; Chassaing, G.; Sagan, S.; Alves, I. D. Different membrane behaviour and cellular uptake of three basic arginine-rich peptides. *Biochimica et Biophysica Acta (BBA)-Biomembranes* **2011**, *1808*, (1), 382-393.
69. Plank, C.; Tang, M. X.; Wolfe, A. R.; Szoka, F. C. Branched cationic peptides for gene delivery: role of type and number of cationic residues in formation and in vitro activity of DNA polyplexes. *Human gene therapy* **1999**, *10*, (2), 319-332.
70. Åmand, H. L.; Boström, C. L.; Lincoln, P.; Nordén, B.; Esbjörner, E. K. Binding of cell-penetrating penetratin peptides to plasma membrane vesicles correlates directly with cellular uptake. *Biochimica et Biophysica Acta (BBA)-Biomembranes* **2011**, *1808*, (7), 1860-1867.
71. Åmand, H. L.; Fant, K.; Nordén, B.; Esbjörner, E. K. Stimulated endocytosis in penetratin uptake: effect of arginine and lysine. *Biochemical and biophysical research communications* **2008**, *371*, (4), 621-625.

72. Mitchell, D.; Steinman, L.; Kim, D.; Fathman, C.; Rothbard, J. Polyarginine enters cells more efficiently than other polycationic homopolymers. *The Journal of Peptide Research* **2000**, *56*, (5), 318-325.
73. Kim, H. H.; Choi, H. S.; Yang, J. M.; Shin, S. Characterization of gene delivery in vitro and in vivo by the arginine peptide system. *International Journal of Pharmaceutics* **2007**, *335*, (1-2), 70-78.
74. Lundberg, M.; Johansson, M. Positively charged DNA-binding proteins cause apparent cell membrane translocation. *Biochemical and biophysical research communications* **2002**, *291*, (2), 367-371.
75. Meade, B. R.; Dowdy, S. F. Enhancing the cellular uptake of siRNA duplexes following noncovalent packaging with protein transduction domain peptides. *Advanced drug delivery reviews* **2008**, *60*, (4), 530-536.
76. Kim, W. J.; Christensen, L. V.; Jo, S.; Yockman, J. W.; Jeong, J. H.; Kim, Y.-H.; Kim, S. W. Cholesteryl oligoarginine delivering vascular endothelial growth factor siRNA effectively inhibits tumor growth in colon adenocarcinoma. *Molecular Therapy* **2006**, *14*, (3), 343-350.
77. Koo, H.; Kang, H.; Lee, Y. Analysis of the relationship between the molecular weight and transfection efficiency/cytotoxicity of Poly-L-arginine on a mammalian cell line. *Notes* **2009**, *30*, (4), 927.
78. Futaki, S.; Ohashi, W.; Suzuki, T.; Niwa, M.; Tanaka, S.; Ueda, K.; Harashima, H.; Sugiura, Y. Stearylated arginine-rich peptides: a new class of transfection systems. *Bioconjugate chemistry* **2001**, *12*, (6), 1005-1011.

79. Baoum, A.; Ovcharenko, D.; Berkland, C. Calcium condensed cell penetrating peptide complexes offer highly efficient, low toxicity gene silencing. *International journal of pharmaceutics* **2012**, *427*, (1), 134-142.
80. Midoux, P.; LeCam, E.; Coulaud, D.; Delain, E.; Pichon, C. Histidine containing peptides and polypeptides as nucleic acid vectors. *Somatic cell and molecular genetics* **2002**, *27*, (1-6), 27-47.
81. Midoux, P.; Kichler, A.; Boutin, V.; Maurizot, J.-C.; Monsigny, M. Membrane permeabilization and efficient gene transfer by a peptide containing several histidines. *Bioconjugate chemistry* **1998**, *9*, (2), 260-267.
82. Wagner, E.; Plank, C.; Zatloukal, K.; Cotten, M.; Birnstiel, M. L. Influenza virus hemagglutinin HA-2 N-terminal fusogenic peptides augment gene transfer by transferrin-polylysine-DNA complexes: toward a synthetic virus-like gene-transfer vehicle. *Proceedings of the National Academy of Sciences* **1992**, *89*, (17), 7934-7938.
83. Midoux, P.; Monsigny, M. Efficient gene transfer by histidylated polylysine/pDNA complexes. *Bioconjugate chemistry* **1999**, *10*, (3), 406-411.
84. Lundberg, P.; El-Andaloussi, S.; Sütli, T.; Johansson, H.; Langel, Ü. Delivery of short interfering RNA using endosomolytic cell-penetrating peptides. *The FASEB Journal* **2007**, *21*, (11), 2664-2671.
85. Martin, M. E.; Rice, K. G. Peptide-guided gene delivery. *The AAPS journal* **2007**, *9*, (1), 18-29.
86. Chen, C. P.; Kim, J.; Steenblock, E.; Liu, D.; Rice, K. G. Gene transfer with poly-melittin peptides. *Bioconjugate chemistry* **2006**, *17*, (4), 1057-1062.

87. Wyman, T. B.; Nicol, F.; Zelphati, O.; Scaria, P.; Plank, C.; Szoka, F. C. Design, synthesis, and characterization of a cationic peptide that binds to nucleic acids and permeabilizes bilayers. *Biochemistry* **1997**, *36*, (10), 3008-3017.
88. Zanta, M. A.; Belguise-Valladier, P.; Behr, J. P. Gene delivery: a single nuclear localization signal peptide is sufficient to carry DNA to the cell nucleus. *Proceedings of the National Academy of Sciences* **1999**, *96*, (1), 91-96.
89. Escriou, V.; Carrière, M.; Scherman, D.; Wils, P. NLS bioconjugates for targeting therapeutic genes to the nucleus. *Advanced drug delivery reviews* **2003**, *55*, (2), 295-306.
90. Lanford, R. E.; Butel, J. S. Construction and characterization of an SV40 mutant defective in nuclear transport of T antigen. *Cell* **1984**, *37*, (3), 801.
91. Collas, P.; Husebye, H.; Aleström, P. The nuclear localization sequence of the SV40 T antigen promotes transgene uptake and expression in zebrafish embryo nuclei. *Transgenic research* **1996**, *5*, (6), 451-458.
92. Subramanian, A.; Ranganathan, P.; Diamond, S. L. Nuclear targeting peptide scaffolds for lipofection of nondividing mammalian cells. *Nature biotechnology* **1999**, *17*, (9), 873-877.
93. Nitin, N.; LaConte, L.; Rhee, W. J.; Bao, G. Tat peptide is capable of importing large nanoparticles across nuclear membrane in digitonin permeabilized cells. *Annals of biomedical engineering* **2009**, *37*, (10), 2018-2027.
94. Schätzlein, A. G. Targeting of synthetic gene delivery systems. *Journal of Biomedicine and Biotechnology* **2003**, *2003*, (2), 149-158.
95. Hart, S. Integrin-mediated vectors for gene transfer and therapy. *Current opinion in molecular therapeutics* **1999**, *1*, (2), 197.

96. White, S. J.; Nicklin, S. A.; Sawamura, T.; Baker, A. H. Identification of peptides that target the endothelial cell-specific LOX-1 receptor. *Hypertension* **2001**, *37*, (2), 449-455.
97. Khondee, S.; Baoum, A.; Siahaan, T. J.; Berkland, C. Calcium condensed LABL-TAT complexes effectively target gene delivery to ICAM-1 expressing cells. *Molecular pharmaceuticals* **2011**, *8*, (3), 788-798.
98. Ginn, S. L.; Alexander, I. E.; Edelstein, M. L.; Abedi, M. R.; Wixon, J. Gene therapy clinical trials worldwide to 2012—an update. *The journal of gene medicine* **2013**, *15*, (2), 65-77.
99. Thomas, C. E.; Ehrhardt, A.; Kay, M. A. Progress and problems with the use of viral vectors for gene therapy. *Nature Reviews Genetics* **2003**, *4*, (5), 346-358.
100. Robbins, P. D.; Tahara, H.; Ghivizzani, S. C. Viral vectors for gene therapy. *Trends in Biotechnology* **1998**, *16*, (1), 35-40.
101. Warnes, A.; Fooks, A. R. Live viral vectors : construction of a replication-deficient recombinant adenovirus. *Methods Mol Med* **1996**, *4*, 33-45.
102. Bergelson, J. M.; Cunningham, J. A.; Droguett, G.; Kurt-Jones, E. A.; Krithivas, A.; Hong, J. S.; Horwitz, M. S.; Crowell, R. L.; Finberg, R. W. Isolation of a common receptor for Coxsackie B viruses and adenoviruses 2 and 5. *Science* **1997**, *275*, (5304), 1320-3.
103. Walther, W.; Stein, U. Viral vectors for gene transfer: a review of their use in the treatment of human diseases. *Drugs* **2000**, *60*, (2), 249-71.
104. Mizuguchi, H.; Hayakawa, T. Targeted adenovirus vectors. *Hum Gene Ther* **2004**, *15*, (11), 1034-44.
105. Schnierle, B.; Groner, B. Retroviral targeted delivery. *Gene therapy* **1996**, *3*, (12), 1069-1073.

106. Howitt, J.; Anderson, C. W.; Freimuth, P. Adenovirus interaction with its cellular receptor CAR. *Curr Top Microbiol Immunol* **2003**, *272*, 331-64.
107. Al-Jamal, W. T.; Kostarelos, K. Liposomes: from a clinically established drug delivery system to a nanoparticle platform for theranostic nanomedicine. *Acc Chem Res* **2011**, *44*, (10), 1094-104.
108. Arcasoy, S. M.; Latoche, J. D.; Gondor, M.; Pitt, B. R.; Pilewski, J. M. Polycations increase the efficiency of adenovirus-mediated gene transfer to epithelial and endothelial cells in vitro. *Gene Ther* **1997**, *4*, (1), 32-8.

Chapter 2

Polyarginine Molecular Weight Determines Transfection Efficiency of Calcium Condensed Complexes

Published as:

Alhakamy, N. A.; Berkland, C. J. Polyarginine molecular weight determines transfection efficiency of calcium condensed complexes. *Molecular pharmaceutics* 2013, 10, 1940-1948
(2013)

2.1. Introduction

Many studies have shown that nucleic acids complex electrostatically with polycations to form polyplexes. Unfortunately, the most effective polycations are often the most toxic. Polyethylenimine (PEI), polylysine and similar polycations can mediate high levels of gene expression, but high-molecular-weight polycations are often required to effectively condense the DNA to small particles¹⁻¹⁰. The needed increase in molecular weight; however, often increases cytotoxicity^{2, 11-13}. Cytotoxicity of polycations may be minimized by different approaches such as conjugation with hydrophilic or degradable polymers (e.g. hydroxypropyl methacrylamide (HPMA) or polyethylene glycol (PEG))^{11, 14-16}. A simple alternative is to identify ways to form small polyplexes using less cytotoxic polycations such as cell penetrating peptides (CPPs)^{1, 17-19}.

CPPs are short sequences of amino acids characterized by their cationic or amphipathic nature that aid cellular uptake of different molecular cargo^{1, 20-23}. Two general methods have been examined for CPP-mediated gene delivery, which are chemical conjugation of CPPs with nucleic acids or complexation^{11, 24-27}. The negative charge of genetic material (e.g. DNA or siRNA) and the positive charge of CPPs can impede direct conjugation. On the other hand, genetic material can be electrostatically bound and neutralized when complexed with CPPs^{1, 11, 28}.

The most commonly known CPPs are human immunodeficiency virus-1 (HIV-1) transcriptional activator (TAT) protein, and the herpes simplex virus structural protein VP22. Sequence similarities between TAT, and VP22 indicate the importance of basic amino acids, such as arginine or lysine. Short peptides containing only arginine have the ability to translocate through cell membranes^{1, 9, 24, 29-33}. Furthermore, polymers or CPPs with some of their residues altered with arginine or the guanidine group displayed highly enhanced transfection efficiency^{32, 34}.

The size, charge, and molecular weight of CPPs (e.g. polyarginine) play important roles in condensing DNA for delivering genetic material to target cells³⁵. CPPs containing cationic amino acids such as lysine or arginine were found to complex genetic material efficiently³⁶⁻³⁸. CPPs rich with arginine also tended to possess high transfection efficiency³⁹⁻⁴². Often, polyarginine peptides delivered genetic material into cells more efficiently than other homopolymer peptides (e.g. polylysine and polyhistidine) of equal length. A study also determined the uptake of different polyarginine lengths (e.g. R3, R6, R9, R15 and R30) and found that simply increasing the length of polyarginine did not necessarily increase the uptake. Polyarginines between R7 and R20 maximized uptake by cells^{41,43,44}. Other groups studied the translocation of different polyarginine lengths (R4, R6, R8, R10, R12 and R16) and found that the R8 peptide maximized cellular uptake, while others found R6 to R9 translocated optimally through the cell membrane. An analogous result occurred using polyarginines to mediate protein delivery^{30,41,44}. Thus, polyarginine size is essential for membrane permeability.

Some reports have suggested that low molecular-weight polyarginine peptides are able to form complexes with DNA and promote transfection in different mammalian cell types^{32, 45-47}. Although reports suggest low-molecular-weight polyarginine-pDNA complexes may achieve modest transfection with negligible cytotoxicity, the large particle size (microparticles) is a limitation³². Indeed, high-molecular-weight polycations often have the ability to condense DNA into small and stable complexes while low-molecular-weight polycations often yield large and unstable complexes^{32, 47-49}. A major shortcoming with high-molecular-weight polyarginines is cytotoxicity; however, low-molecular-weight polyarginines (< 10 kDa) typically exhibit poor transfection efficiency.

Calcium phosphate precipitation is a well-established approach to DNA condensation and gene delivery. Numerous *in vitro* studies demonstrated that the transfection efficiency of DNA increased when formulated as a calcium phosphate-DNA co-precipitate. Other studies found that calcium chloride has a positive effect on the transfection efficiency of plasmid DNA (pDNA)-cationic liposome complexes^{1, 50-53}. Still other studies showed that calcium might increase the endocytosis rate or accelerate endosomal release before degradation by lysosomes^{54, 55}. While the effect of calcium on transfection is unclear, these studies encouraged exploration of calcium with complexes formed using CPPs, such as polyarginine. Consequently, calcium was found to condense these large complexes and increase the positive charge, which dramatically enhanced transfection^{1, 11, 56}. In fact, titrating calcium can directly affect complex size and stability. Also, released polyarginines may maintain CPP properties since they are not chemically conjugated using this approach.

Thus, the delivery of polyarginine-pDNA complexes condensed with calcium chloride may offer a safe nonviral gene delivery technique with potential for clinical application.¹ This simple formulation (polyarginine-pDNA-Ca²⁺) maintained the viability of A549 lung cancer epithelial cells while achieving high transfection efficiency. This method also yields a small and stable particle size and is suitable for delivering large amounts of genetic material. In order to determine the importance of polyarginine molecular weight, *in vitro* transfection efficiency studies were conducted using different polyarginines (R5, R7, R9, and R11) (**Table 1**), and different calcium chloride concentrations (0, 50, 100, 150, 300, and 600 mM).

Table 1: Sequence and size of polyarginine 5, 7, 9 and 11.

Polyarginine	Sequence	Molecular Weight (Da)
5	RRRRR	797.97
7	RRRRRRR	1110.35
9	RRRRRRRRR	1422.73
11	RRRRRRRRRRR	1735.11

2.2. Materials and Methods

2.2.1. Materials

Plasmid DNA (pDNA) encoding firefly luciferase (pGL3, 4818 bp) was obtained from Promega (Madison, Wisconsin). The pDNA purity level was determined by UV-Spectroscopy and agarose gel electrophoresis. Polyarginine (polyarginine 5, 7, 9 and 11) were purchased from Biomatik (Cambridge, Ontario, Canada). Branched polyethylenimine (PEI, 25 kDa) was obtained from Sigma-Aldrich (Milwaukee, Wisconsin). A549 carcinomic human alveolar basal epithelial cell line was obtained from American Type Culture Collection (ATCC; Rockville, Maryland). The cell culture medium (F-12K Nutrient Mixture, Kaighn's modified with L-glutamine) was purchased through Cellgro (Mediatech, Inc., Manassas, VA). Fetal bovine serum (FBS) was purchased from Hyclone (Logan, UT). Penicillin-streptomycin was purchased from MB Biomedical, LLC (Solon, OH). Trypsin-EDTA was purchased from Invitrogen (Carlsbad, CA). Luciferase Assay System Freezer Pack and CellTiter 96® Aqueous one solution cell proliferation assay (MTS) were obtained from Promega (Madison, Wisconsin). BCA Protein Assay Reagent (bicinchoninic acid) was purchased from Thermo Fisher Scientific Inc. Tris-acetate-EDTA (TAE) Buffer (10 x) was purchased from Promega (Madison, Wisconsin). Sterile water (DNase, RNase free) was purchased from Fisher Scientific. Calcium chloride dihydrate (CaCl₂ · 2H₂O) was purchased from Fisher

Scientific. Agarose (Medium-EEO/Protein Electrophoresis Grade) was purchased from Fisher Scientific. Bench Top DNA Ladder was purchased from Promega (Madison, WI). SYBR Green I Nucleic Acid Gel Stain was obtained from Invitrogen (Carlsbad, CA).

2.2.2. Preparation of Polyarginine-pDNA-Ca²⁺ Complexes

Polyarginine-pDNA complexes were prepared by adding 15 μ L of polyarginine solution (different polymer nitrogen to pDNA phosphate (N/P) ratios) to 10 μ L (0.1 μ g/ μ L) of pDNA (TAE Buffer (1 x) was used as a solution for DNA storage), followed by fast pipetting for 20 seconds. At that point, 15 μ L of identified molarity (e.g., 50, 300, and 600 mM) CaCl₂ was added and mixed by fast pipetting. After preparing the complexes, they were stored at 4°C for 20-25 minutes.

2.2.3. Preparation of PEI-pDNA Complexes

PEI-pDNA complexes were prepared by adding 15 μ L of PEI solution (N/P ratio 10) to 10 μ L (0.1 μ g/ μ L) of pDNA followed by fast pipetting for 20 seconds. After preparing the complexes, they were stored at 4°C for 20-25 minutes. Complexes were prepared immediately before each experiment.

2.2.4. Agarose Gel Electrophoresis

Complexes were prepared as defined previously and subsequently 4 μ L of Tris-acetate-EDTA (TAE) buffer was added. Then, 4 μ L of SYBR Green 1 was mixed with the complexes. Afterwards, the mixture was stored at 4°C for 20 to 25 minutes. After the storage, 7 μ L of 6X DNA Loading Dye was added. A one kb DNA ladder was used. The mixture solutions were loaded onto a 1 % agarose gel and electrophoresed for 30 minutes at 110 V.

2.2.5. Size and Zeta Potential

The particle size (effective diameter (nm)) of polyarginine-pDNA complexes with or without calcium chloride was determined by dynamic light scattering (Brookhaven Instruments, Holtsville, NY). The zeta potentials of the complexes were measured by Zeta PALS dynamic light scattering (Brookhaven Instrument, Holtsville, NY). All samples intended for particle size and zeta potential measurements were prepared using 10 mM Tris buffer, pH 7.4.

2.2.6. Cell Culture

A549 carcinomic human alveolar basal epithelial cells were grown in F-12K Nutrient Mixture media (Kaighn's modified with L-glutamine) with 1% (v/v) Penicillin-streptomycin and 10% (v/v) fetal bovine serum (FBS) at 37°C in 5% CO₂ humidified air.

2.2.7. Transfection Studies

A549 cells were cultured in 96-well plates for 24 hours prior to transfection. The concentration of the cells in every well was approximately 80,000 cells/mL. The wells were washed once with serum-free media (SFM) and afterwards a 100 µL sample (which consisted of 20 µL of complex and 80 µL of SFM) was added to each well. Subsequently, a 96-well plate was incubated for 5 hours in an incubator. After 5 hours incubation, the sample was replaced with 100 µL of fresh serum medium and then incubated again for approximately 48 hours. In order to determine the gene expression of the complexes, the Luciferase Reporter Assay from Promega was used. The results of the transfections were expressed as Relative Light Units (RLU) per milligram (mg) of cellular protein, and PEI-pDNA was used as a control. BCA Protein Assay Reagent (bicinchoninic acid) was used to measure total cellular protein concentration in the cell extracts. The Luciferase Assay and BCA were measured by a microplate reader (SpectraMax; Molecular Devices Crophe, CA).

2.2.8. Cytotoxicity Assay of Polyarginine

Cytotoxicity of polyarginines was determined using a CellTiter 96® AQueous Non-Radioactive Cell Proliferation Assay (MTS) obtained from Promega (Madison, Wisconsin). A549 cells were cultured in a 96-well plate as described previously. After 24 hours of incubation, the media were replaced with a sample consisting of 100 μ L of fresh serum medium and 20 μ L of MTS. Then, the plate was incubated for 3 hours. In order to determine cell viability, the absorbance of each well was measured by a microplate reader (SpectraMax; Molecular Devices Crophe, CA) at 490 nm and normalized to untreated control cells.

2.2.9. Optical Microscopy

Cells were cultured, grown and incubated as mentioned above. Then, the complexes were added and cells were incubated again for 5 hours and 48 hours. Data were obtained using a Zeiss Axiovert 100 Microscope (AxioCam HRM).

2.2.10. Statistical Analysis

Data were analyzed by using GraphPad software. Statistical evaluation comparing the significance of the difference in gene expression (RLUs/mg protein) between the means of two data sets was performed using an unpaired *t* test. One-way ANOVA, Tukey post-test was used to analyze the differences when more than two data sets were compared.

2.3. Results and Discussion

Agarose gel electrophoresis studies indicated that the complexes without calcium were robust enough to immobilize DNA when complexed with polyarginine 7, 9 and 11. DNA complexes with polyarginine 5 were less stable without calcium than with calcium (**Figure 1**). The ability of the four distinct molecular weights of polyarginine to form complexes with pDNA was also studied using agarose gel electrophoresis at N/P ratios of 5, 10, 20, 30, 40, and 60. Polyarginines 5, 7, 9 and 11 were complexed with pDNA at these different N/P ratios and then condensed with calcium chloride (300 mM) (**Figure 2**). The immobilization of pDNA indicated that different polyarginine peptides could form complexes with pDNA even with the lowest N/P ratio of 5.

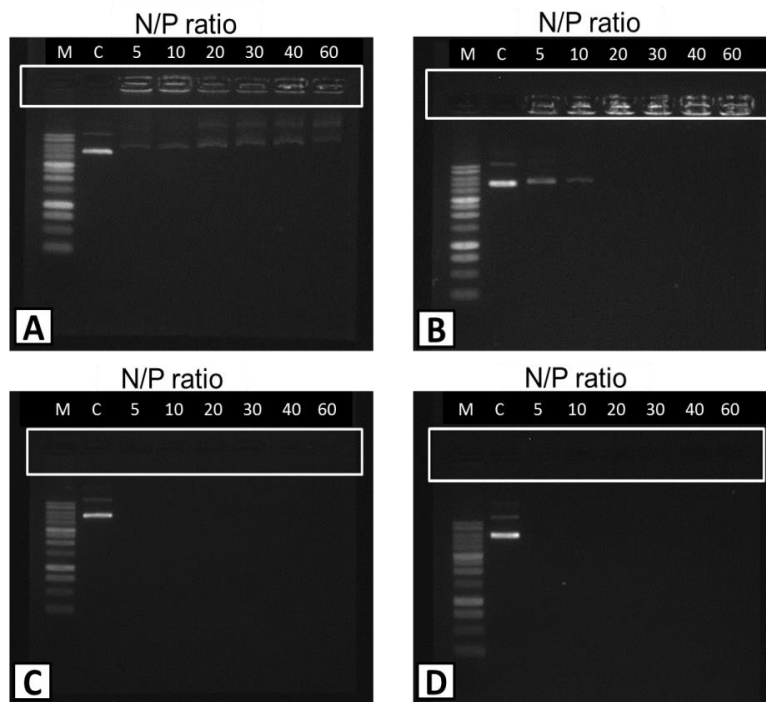


Figure 1. Agarose gels of polyarginine-pDNA complexes with and without CaCl₂ (300 mM) at N/P ratios of 5, 10, 20, 30, 40, and 60. (A) Polyarginine 5-pDNA complexes without CaCl₂ and (B) with CaCl₂. (C) Polyarginine 7-pDNA complexes without CaCl₂ and (D) with CaCl₂. “C” refers to control (pDNA). “M” Refers to the size marker.

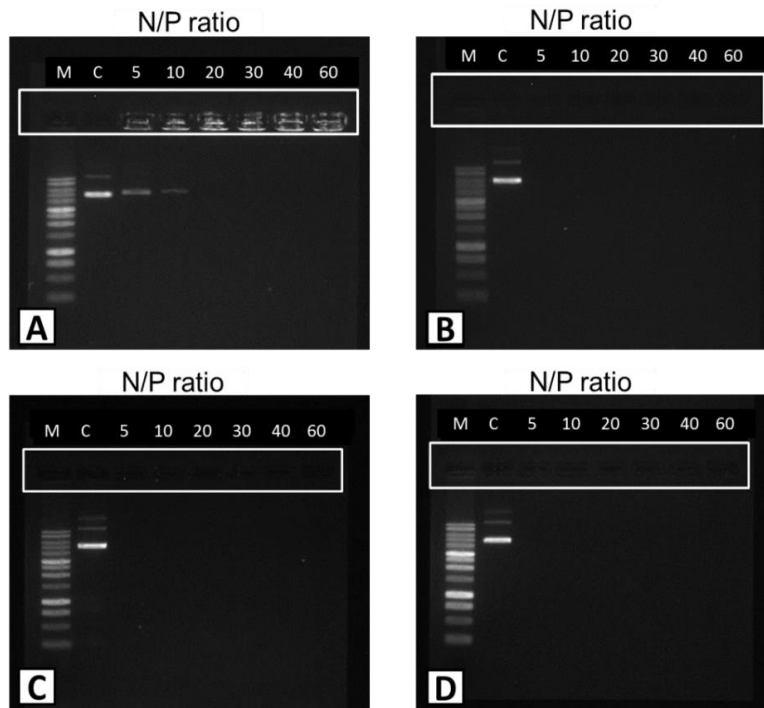


Figure 2. Agarose gels of polyarginine-pDNA complexes condensed with CaCl_2 (300 mM) at N/P ratios of 5, 10, 20, 30, 40, and 60. (A) Polyarginine 5-pDNA- Ca^{2+} complexes, (B) polyarginine 7-pDNA- Ca^{2+} complexes, (C) polyarginine 9-pDNA- Ca^{2+} complexes, and (D) polyarginine 11-pDNA- Ca^{2+} complexes. “C” refers to control (pDNA). “M” Refers to the size marker.

An important characteristic of the polyarginine-pDNA- Ca^{2+} complex is the size. A broad study of the relationship between the calcium concentration (150, 300, and 600 mM) and the particle size was conducted. The particle sizes of polyarginine 5, 7, 9 and 11 complexed with pDNA as a function of calcium chloride concentration (**Figure 3A and B**). The polyarginine-pDNA complexes generally showed a decrease in particle size as calcium concentration increased, whereas the complexes without calcium showed a large particle size. The total positive charge of complexes also plays an important role in transfection efficiency and can increase the attractive force to the negative charge of the cell surface. Overall, the zeta potential of polyarginine of 5, 7, 9 and 11-pDNA complexes increased considerably with increasing concentrations of calcium chloride. For example, the zeta potential of polyarginine 7-pDNA complexes increased

significantly from less than 5 to more than 20 mV with increasing concentration of calcium chloride (**Figure 3C**). Clearly, PEI-pDNA complexes had the highest positive zeta potential. The lowest values were associated with polyarginine 5-pDNA complexes.

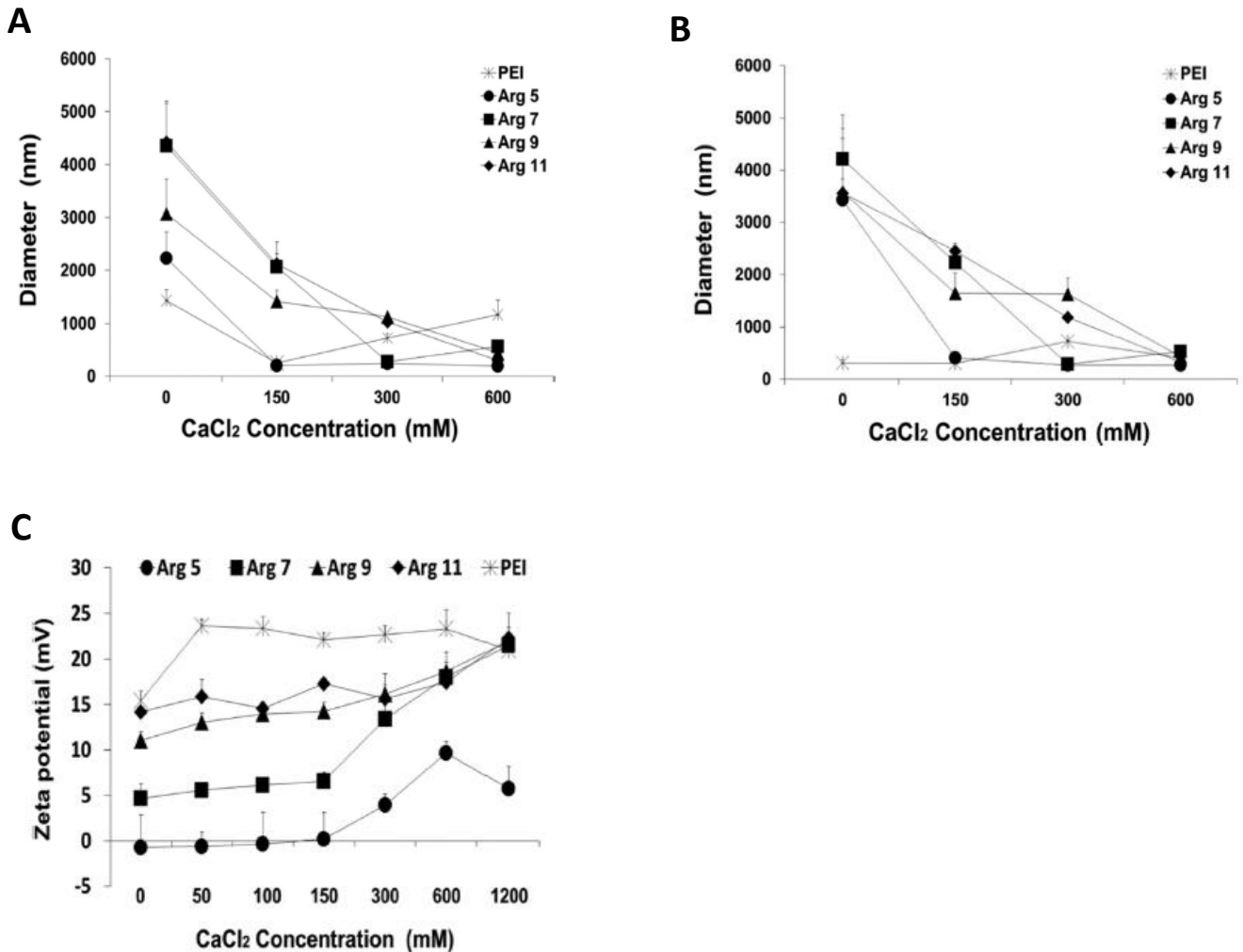


Figure 3. The effect of different calcium chloride concentrations on the particle size at (A) N/P ratio 5 and (B) N/P ratio 10 and zeta potential at (C) N/P ratio 10 of PEI-pDNA complexes and polyarginine 5, 7, 9 and 11-pDNA complexes. Results are presented as mean \pm SD (n = 3).

The cellular uptake of free polyarginine was previously reported to be proportional to the guanidine content ^{43, 57-60}. Here, different polyarginines were complexed with pDNA and the transfection of A549 cells was studied as a function of polyarginine molecular weight, calcium

concentration, and N/P ratio. Polyarginine-pDNA-Ca²⁺ complexes generally achieved high gene expression. Interestingly, there was no notable gene expression observed for the polyarginine complexes without calcium. Polyarginine 5 complexes had low gene expression with or without calcium. On the other hand, polyarginine 7, 9 and 11 complexes yielded high gene expression only when adding calcium chloride. Additionally, the transfection efficiency of the best polyarginine-pDNA-Ca²⁺ complexes (polyarginine 7 complex) was superior to PEI-pDNA complexes. Polyarginine 7 appeared significantly effective compared to the other polyarginines (**Figure 4**). **Figure 5** compares the same data to illustrate the difference in transfection efficiency between the polyarginine peptides at difference N/P ratios, (CaCl₂ concentration 100 and 150 mM).

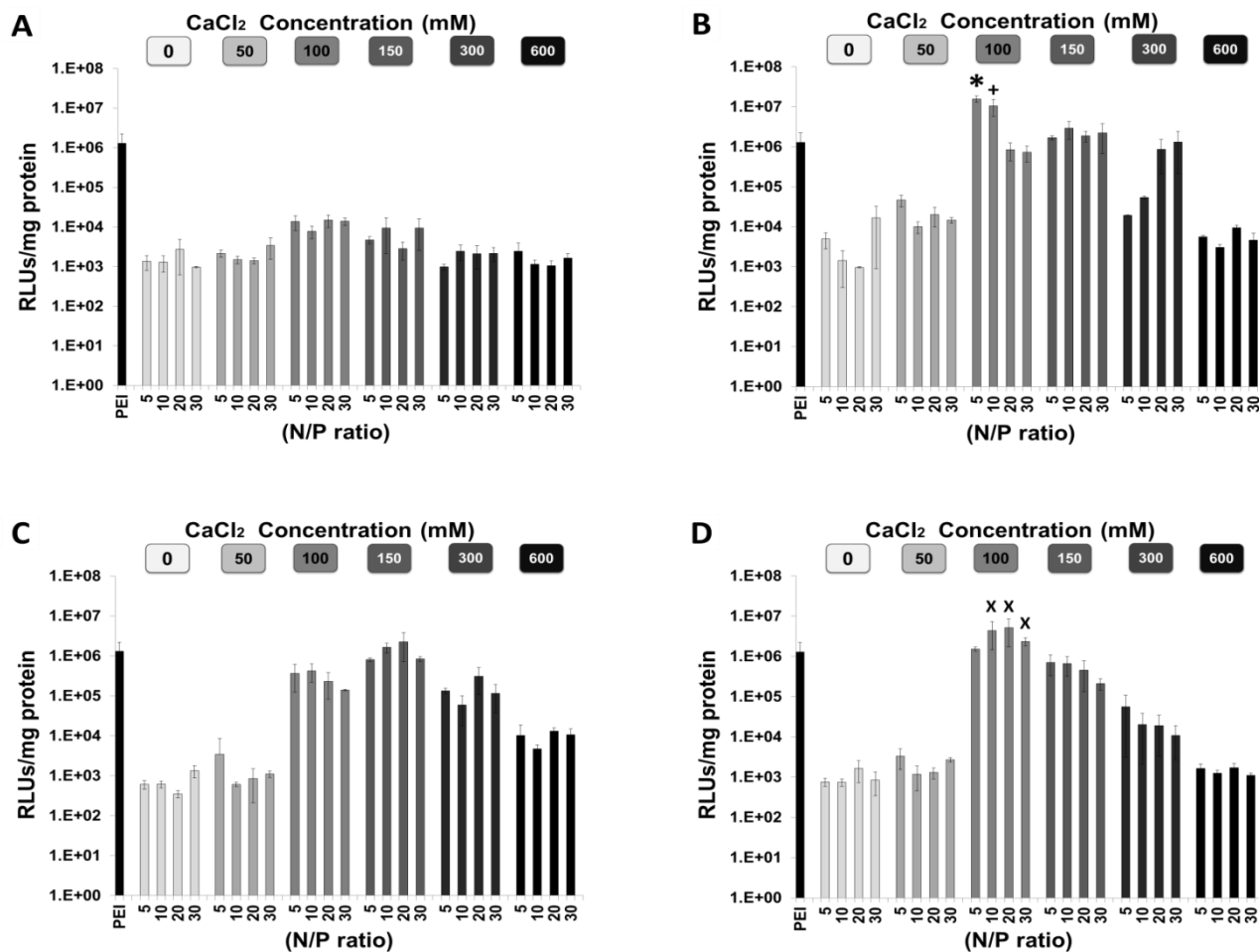


Figure 4. The transfection efficiency was determined for polyarginine-pDNA complexes at N/P ratios of 5, 10, 20, and 30 with different concentrations of added CaCl₂ (50, 100, 150, 300, and 600 mM). (A) Polyarginine 5-pDNA-Ca²⁺ complexes, (B) polyarginine 7-pDNA-Ca²⁺ complexes, (C) polyarginine 9-pDNA-Ca²⁺ complexes, (D) polyarginine 11-pDNA-Ca²⁺ complexes. PEI (N/P ratio 10) was used as a standard. RLUs refers to relative light units. Results are presented as mean ± SD (n = 4). The p of different polyarginine complexes were compared with PEI complexes (* = p < 0.0001, + = p < 0.008, and x = p < 0.09, *t* test).

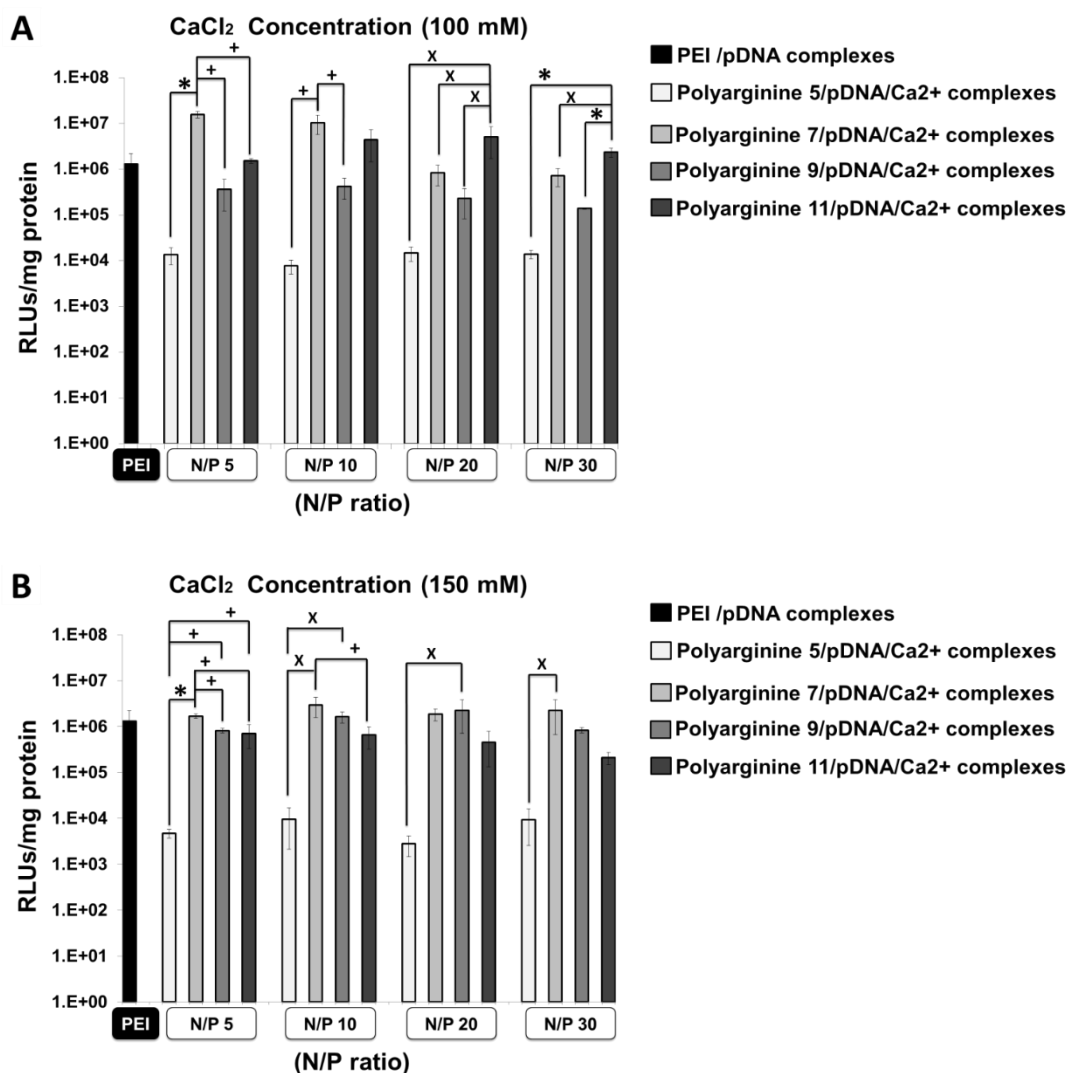


Figure 5. The transfection efficiency was determined for polyarginine-pDNA complexes at N/P ratios of 5, 10, 20, and 30 with different concentrations of added CaCl₂ (100 and 150 mM) for (A) polyarginine 5-pDNA-Ca²⁺ complexes and (B) polyarginine 7-pDNA-Ca²⁺ complexes. PEI (N/P ratio 10) was used as a standard. RLU refers to relative light units. Results are presented as mean ± SD (n = 4), (* = p < 0.0001, + = p < 0.005, and x = p < 0.05, one-way ANOVA, Tukey post-test).

Calcium is an important component to condense the complexes, yielding small complexes with optimized DNA release.⁴⁸ Consequently, only the combination of calcium and polyarginine effectively boosted gene transfection. In addition, others found that the cellular uptake of free polyarginine 16 was considerably higher than polyarginine 8, but the translocation of polyarginine

16 into the cytosol was less efficient than polyarginine 8. In light of this, it is possible that the polyarginines near 8 amino acids may mediate uptake of the complexes and optimize cytosolic release³⁰. This may help explain why polyarginine 7 had the highest gene expression (RLUs/mg protein) compared to other polyarginines. Moreover, **Figure 6** indicates that the transfection efficiency of pDNA-Ca²⁺ complexes without polyarginine peptides was significantly lower than the complexes with polyarginine when comparing the same calcium concentration.

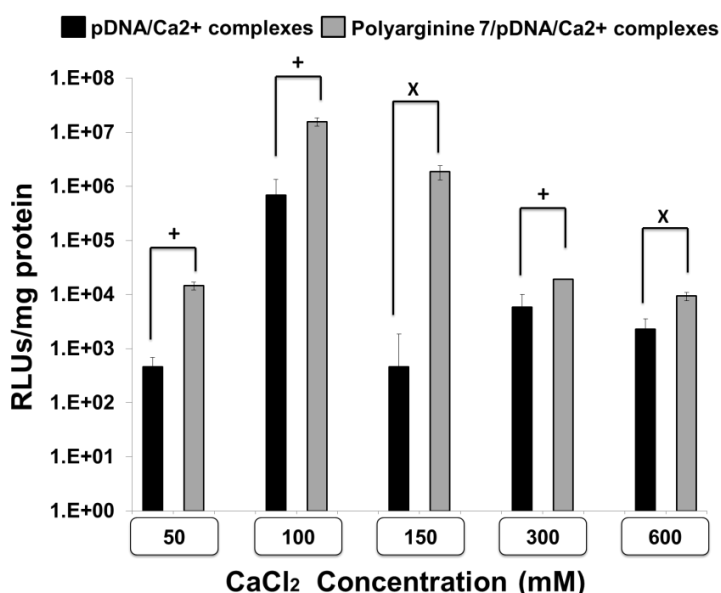


Figure 6. The transfection efficiency was determined for pDNA-Ca²⁺ complexes and compared to polyarginine 7-pDNA-Ca²⁺ complexes with different concentrations of added CaCl₂ (50, 100, 150, 300, and 600 mM), (+ = $p < 0.005$, and x = $p < 0.05$, one-way ANOVA, Tukey post-test).

Finally, an effective gene delivery vector must be able to deliver genetic material safely to target cells without cytotoxicity. Arginine is converted to ornithine by an enzyme called arginase. Ornithine is the precursor of numerous polyamines, which are essential for cell proliferation³¹. However, high-molecular-weight CPPs (e.g. polyarginine) can precipitate serum proteins and exhibit cytotoxicity at high concentration²⁷. Decreasing the molecular weight of polyarginine

tends to decrease cytotoxicity. Here, a cytotoxicity assay was used to measure the cytotoxicity of free PEI and polyarginines (**Figure 7**). Polyarginine 5, 7, 9 and 11 showed little evidence of cytotoxicity against A549 cells even at very high concentrations (1 mg/mL). These results supported the promise that polyarginine-pDNA-Ca²⁺ complexes had high transfection efficiency while maintaining low cytotoxicity.

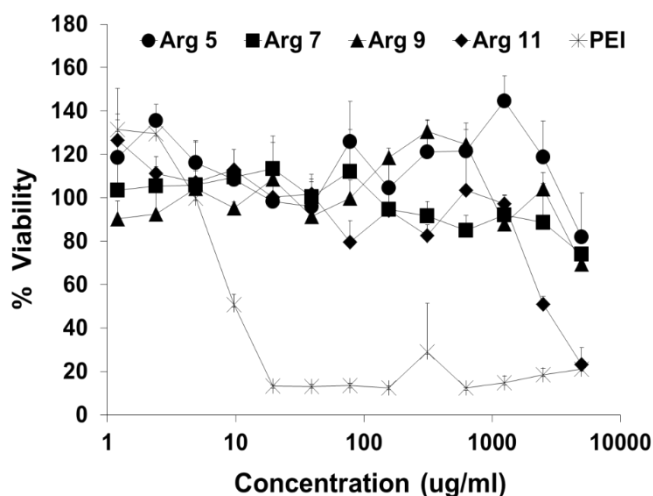


Figure 7. Polyarginine peptide 5, 7, 9 and 11 showed negligible cytotoxicity in comparison to PEI. Viability is expressed as a function of peptide concentration. Results are presented as mean \pm SD (n = 3).

Micrographs of A549 cells showed that PEI-pDNA complexes had a negative effect on cell growth compared to polyarginine-pDNA-Ca²⁺ complexes (**Figure 8**). Images of the cells after 5 hours and 48 hours were similar when incubated with PEI-pDNA complexes suggesting inhibition of cell growth. On the other hand, the cells proliferated as expected when incubated with polyarginine 7-pDNA-Ca²⁺ complexes. Other reports suggest that PEI inhibits cell proliferation and alternatively, arginine may even have a slight enhancing effect ^{48, 61, 62}. Additionally, we noticed that there was no precipitation when we used the low concentrations of CaCl₂ (\leq 300 mM), but there was precipitation with the high concentrations of CaCl₂ ($>$ 300 mM). Micrographs were

also supported by plots of total protein after 48 hours of incubation (**Figure 9**). In general, polyarginine 5, 7, 9 and 11 had higher protein levels than PEI and were similar to control cell cultures. This finding suggests that PEI transfection was artificially amplified due to inhibition of cell proliferation.

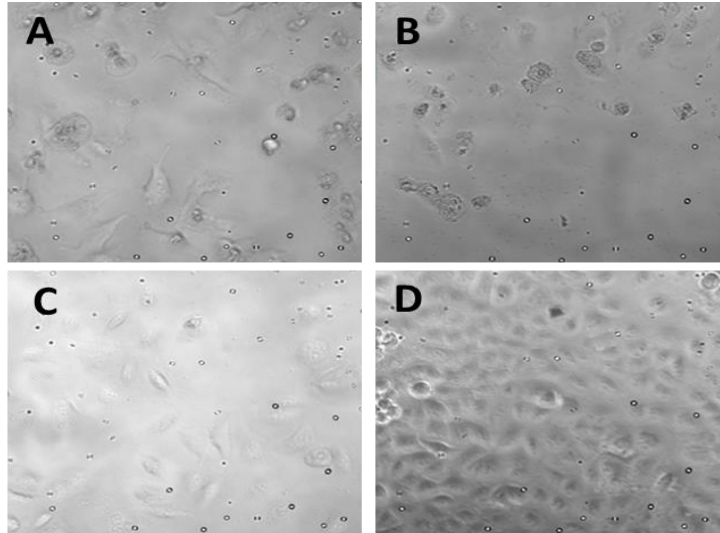


Figure 8. Representative images of A549 cells after incubation of PEI-pDNA complexes and polyarginine 7-pDNA- Ca^{2+} complexes. **(A)** PEI-pDNA complexes without calcium after 5 hours. **(B)** PEI-pDNA complexes without calcium after 48 hours. **(C)** Polyarginine 7-pDNA complexes with 50 mM calcium chloride after 5 hours. **(D)** Polyarginine 7-pDNA complexes with 50 mM calcium chloride after 48 hours.

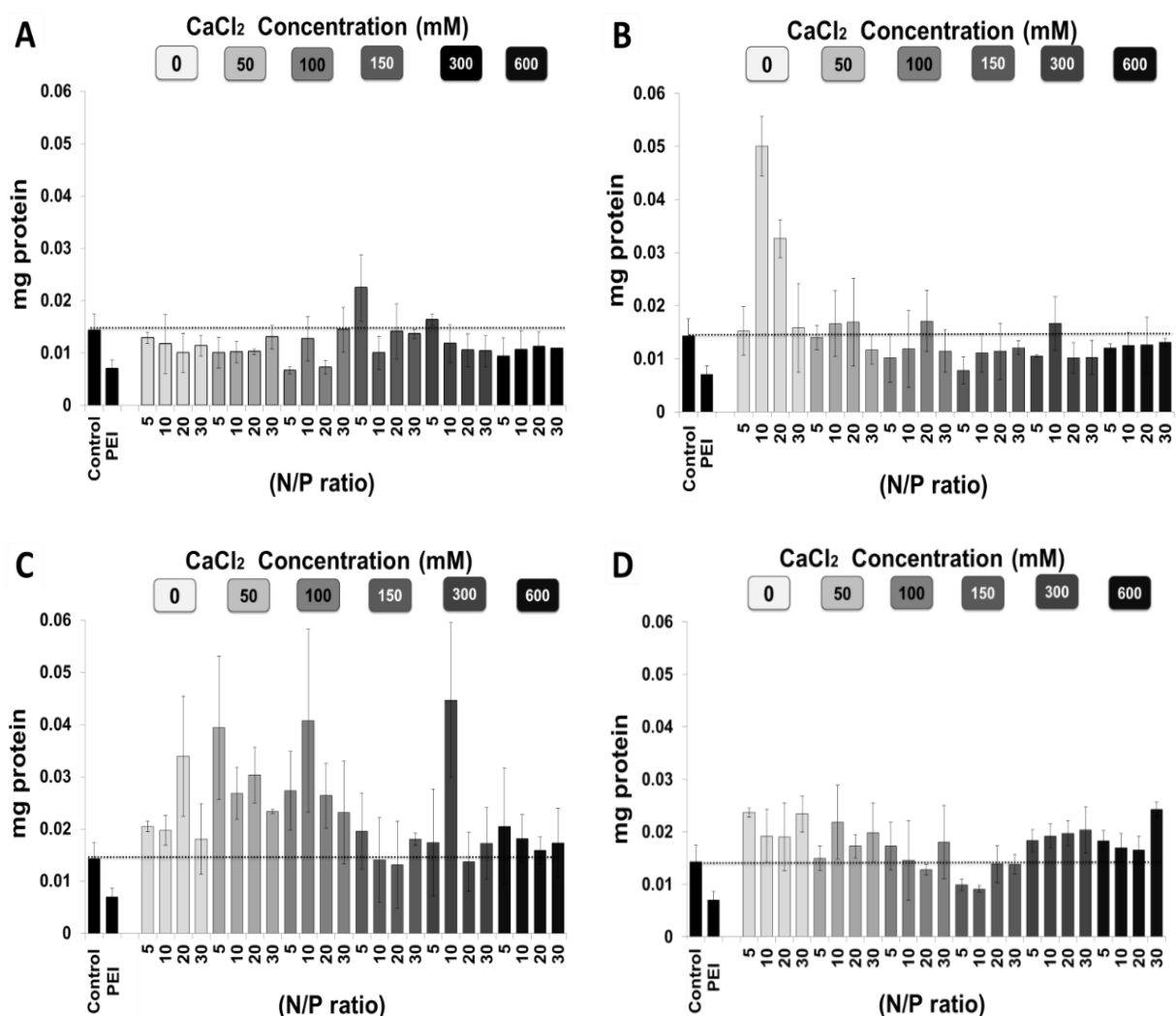


Figure 9. The mass of protein after 48 hours in cell cultures treated with polyarginine-pDNA complexes at N/P ratios of 5, 10, 20, and 30 with different concentrations of added CaCl₂ (50, 100, 150, 300, and 600 mM). The protein level of different polyarginine-pDNA complexes was typically higher than PEI-pDNA complexes. (A) Polyarginine 5-pDNA-Ca²⁺ complexes, (B) polyarginine 7-pDNA-Ca²⁺ complexes, (C) polyarginine 9-pDNA-Ca²⁺ complexes, (D) polyarginine 11-pDNA-Ca²⁺ complexes.

2.4. Conclusions

Polyarginines have been successfully used as cell penetrating peptides for delivering large cargos such as genetic material. Polyarginine-pDNA complexes condensed with calcium chloride possessed excellent transfection efficiency compared to PEI complexes in A549 lung epithelial cells. Calcium chloride concentration played a significant role in controlling the complex size and charge which were important for cell transfection. Moreover, calcium condensation of complexes allows the incorporation and release of low-molecular-weight polyarginine CPPs in the range of 7 to 11 amino acids, which may locally increase cell membrane permeability (e.g. within intracellular vesicles). Polyarginine 7 appeared especially effective compared to the other polyarginines. Polyarginine 5 was ineffective compared to the other polyarginines suggesting the minimum size should be > 5 amino acids. Furthermore, the low-molecular-weight polyarginine peptides (5, 7, 9 and 11) showed negligible cytotoxicity up to 5 mg/mL and maintained the expected cell proliferation rates. The incorporation of CPPs into polyelectrolyte complexes using this strategy potentially offers a safe and effective approach to gene delivery.

2.5. References

1. Baoum, A. A.; Berkland, C. Calcium condensation of DNA complexed with cell-penetrating peptides offers efficient, noncytotoxic gene delivery. *Journal of pharmaceutical sciences* **2011**, *100*, (5), 1637-1642.
2. Wang, C. F.; Lin, Y. X.; Jiang, T.; He, F.; Zhuo, R. X. Polyethylenimine-grafted polycarbonates as biodegradable polycations for gene delivery. *Biomaterials* **2009**, *30*, (27), 4824-4832.
3. Midoux, P.; Monsigny, M. Efficient gene transfer by histidylated polylysine/pDNA complexes. *Bioconjugate chemistry* **1999**, *10*, (3), 406-411.
4. Mady, M.; Mohammed, W.; El-guendy, N. M.; Elsayed, A. Effect of the polymer molecular weight on the DNA/PEI polyplexes properties. *Rom. J. Biophys* **2011**, *21*, (2), 151-165.
5. Godbey, W.; Mikos, A. Recent progress in gene delivery using non-viral transfer complexes. *Journal of controlled release* **2001**, *72*, (1), 115-125.
6. Wiethoff, C. M.; Middaugh, C. R. Barriers to nonviral gene delivery. *Journal of pharmaceutical sciences* **2002**, *92*, (2), 203-217.
7. Felgner, P.; Barenholz, Y.; Behr, J.; Cheng, S.; Cullis, P.; Huang, L.; Jessee, J.; Seymour, L.; Szoka, F.; Thierry, A. Nomenclature for synthetic gene delivery systems. *Human gene therapy* **1997**, *8*, (5), 511-512.
8. Duchardt, F.; Fotin-Mleczek, M.; Schwarz, H.; Fischer, R.; Brock, R. A Comprehensive Model for the Cellular Uptake of Cationic Cell-penetrating Peptides. *Traffic* **2007**, *8*, (7), 848-866.
9. Mann, A.; Thakur, G.; Shukla, V.; Singh, A. K.; Khanduri, R.; Naik, R.; Jiang, Y.; Kalra, N.; Dwarakanath, B.; Langel, U. Differences in DNA condensation and release by lysine and

arginine homopeptides govern their DNA delivery efficiencies. *Molecular Pharmaceutics* **2011**, 8, (5), 1729-1741.

10. Kircheis, R.; Kichler, A.; Wallner, G.; Kursa, M.; Ogris, M.; Felzmann, T.; Buchberger, M.; Wagner, E. Coupling of cell-binding ligands to polyethylenimine for targeted gene delivery. *Gene therapy* **1997**, 4, (5), 409.

11. Baoum, A.; Ovcharenko, D.; Berkland, C. Calcium condensed cell penetrating peptide complexes offer highly efficient, low toxicity gene silencing. *International journal of pharmaceutics* **2012**, 427, (1), 134-142.

12. Mayhew, E.; Harlos, J.; Juliano, R. The effect of polycations on cell membrane stability and transport processes. *Journal of Membrane Biology* **1973**, 14, (1), 213-228.

13. Kadlecova, Z.; Baldi, L.; Hacker, D.; Wurm, F. M.; Klok, H. A. A Comparative Study on the in-vitro Cytotoxicity of Linear, Dendritic and Hyperbranched Polylysine Analogues. *Biomacromolecules* **2012**, 13, (2), 3127-3137.

14. Greenwald, R. PEG drugs: an overview. *Journal of controlled release* **2001**, 74, (1), 159-171.

15. Qi, R.; Gao, Y.; Tang, Y.; He, R. R.; Liu, T. L.; He, Y.; Sun, S.; Li, B. Y.; Li, Y. B.; Liu, G. PEG-conjugated PAMAM dendrimers mediate efficient intramuscular gene expression. *The AAPS journal* **2009**, 11, (3), 395-405.

16. Putnam, D.; Zelikin, A. N.; Izumrudov, V. A.; Langer, R. Polyhistidine-PEG: DNA nanocomposites for gene delivery. *Biomaterials* **2003**, 24, (24), 4425-4433.

17. Vicent, M. J.; Duncan, R. Polymer conjugates: nanosized medicines for treating cancer. *Trends in biotechnology* **2006**, 24, (1), 39-47.

18. Soundara Manickam, D.; Bisht, H. S.; Wan, L.; Mao, G.; Oupicky, D. Influence of TAT-peptide polymerization on properties and transfection activity of TAT/DNA polyplexes. *Journal of controlled release* **2005**, *102*, (1), 293-306.
19. Davidson, T. J.; Harel, S.; Arboleda, V. A.; Prunell, G. F.; Shelanski, M. L.; Greene, L. A.; Troy, C. M. Highly efficient small interfering RNA delivery to primary mammalian neurons induces MicroRNA-like effects before mRNA degradation. *The Journal of neuroscience* **2004**, *24*, (45), 10040-10046.
20. Mo, R. H.; Zaro, J. L.; Shen, W. C. Comparison of Cationic and Amphipathic Cell Penetrating Peptides for siRNA Delivery and Efficacy. *Molecular Pharmaceutics* **2011**, *9*, (2), 299-309.
21. Gautam, A.; Singh, H.; Tyagi, A.; Chaudhary, K.; Kumar, R.; Kapoor, P.; Raghava, G. CPPsite: a curated database of cell penetrating peptides. *Database: The Journal of Biological Databases and Curation* **2012**, DOI: 10.1093/database/bas015.
22. Chiu, Y. L.; Ali, A.; Chu, C.; Cao, H.; Rana, T. M. Visualizing a correlation between siRNA localization, cellular uptake, and RNAi in living cells. *Chemistry & biology* **2004**, *11*, (8), 1165-1175.
23. Crombez, L.; Aldrian-Herrada, G.; Konate, K.; Nguyen, Q. N.; McMaster, G. K.; Brasseur, R.; Heitz, F.; Divita, G. A new potent secondary amphipathic cell-penetrating peptide for siRNA delivery into mammalian cells. *Molecular Therapy* **2008**, *17*, (1), 95-103.
24. Gupta, B.; Levchenko, T. S.; Torchilin, V. P. Intracellular delivery of large molecules and small particles by cell-penetrating proteins and peptides. *Advanced drug delivery reviews* **2005**, *57*, (4), 637-651.

25. Futaki, S. Oligoarginine vectors for intracellular delivery: Design and cellular-uptake mechanisms. *Peptide Science* **2005**, *84*, (3), 241-249.
26. Munyendo, W. L. L.; Lv, H.; Benza-Ingoula, H.; Baraza, L. D.; Zhou, J. Cell penetrating peptides in the delivery of biopharmaceuticals. *Biomolecules* **2012**, *2*, (2), 187-202.
27. Howl, J.; Nicholl, I.; Jones, S. The many futures for cell-penetrating peptides: how soon is now? *Biochemical Society Transactions* **2007**, *35*, 767-769.
28. Stevenson, M.; Ramos-Perez, V.; Singh, S.; Soliman, M.; Preece, J. A.; Briggs, S. S.; Read, M. L.; Seymour, L. W. Delivery of siRNA mediated by histidine-containing reducible polycations. *Journal of Controlled Release* **2008**, *130*, (1), 46-56.
29. Meyer, M.; Wagner, E. Recent developments in the application of plasmid DNA-based vectors and small interfering RNA therapeutics for cancer. *Human gene therapy* **2006**, *17*, (11), 1062-1076.
30. Futaki, S.; Suzuki, T.; Ohashi, W.; Yagami, T.; Tanaka, S.; Ueda, K.; Sugiura, Y. Arginine-rich peptides. *Journal of Biological Chemistry* **2001**, *276*, (8), 5836-5840.
31. Kim, H. H.; Choi, H. S.; Yang, J. M.; Shin, S. Characterization of gene delivery in vitro and in vivo by the arginine peptide system. *International journal of pharmaceutics* **2007**, *335*, (1), 70-78.
32. Koo, H.; Kang, H.; Lee, Y. Analysis of the relationship between the molecular weight and transfection efficiency/cytotoxicity of Poly-L-arginine on a mammalian cell line. *Notes* **2009**, *30*, (4), 927.
33. Saleh, A. F. A.; Aojula, H. S.; Pluen, A. Enhancement of gene transfer using YIGSR analog of Tat-derived peptide. *Biopolymers* **2008**, *89*, (1), 62-71.

34. El-Sayed, A.; Futaki, S.; Harashima, H. Delivery of macromolecules using arginine-rich cell-penetrating peptides: ways to overcome endosomal entrapment. *The AAPS journal* **2009**, *11*, (1), 13-22.
35. Emi, N.; Kidoaki, S.; Yoshikawa, K.; Saito, H. Gene transfer mediated by polyarginine requires a formation of big carrier-complex of DNA aggregate. *Biochemical and biophysical research communications* **1997**, *231*, (2), 421-424.
36. Brooks, H.; Lebleu, B.; Vivès, E. Tat peptide-mediated cellular delivery: back to basics. *Advanced drug delivery reviews* **2005**, *57*, (4), 559-577.
37. Zhao, M.; Weissleder, R. Intracellular cargo delivery using tat peptide and derivatives. *Medicinal research reviews* **2003**, *24*, (1), 1-12.
38. Rudolph, C.; Plank, C.; Lausier, J.; Schillinger, U.; Müller, R. H.; Rosenecker, J. Oligomers of the arginine-rich motif of the HIV-1 TAT protein are capable of transferring plasmid DNA into cells. *Journal of Biological Chemistry* **2003**, *278*, (13), 11411-11418.
39. Tung, C. H.; Weissleder, R. Arginine containing peptides as delivery vectors. *Advanced drug delivery reviews* **2003**, *55*, (2), 281-294.
40. Liu, B. R.; Lin, M. D.; Chiang, H. J.; Lee, H. J. Arginine-rich cell-penetrating peptides deliver gene into living human cells. *Gene* **2012**.
41. Bolhassani, A. Potential efficacy of cell-penetrating peptides for nucleic acid and drug delivery in cancer. *Biochimica et Biophysica Acta (BBA)-Reviews on Cancer* **2011**, *1816*, (2), 232-246.
42. Melikov, K.; Chernomordik, L. Arginine-rich cell penetrating peptides: from endosomal uptake to nuclear delivery. *Cellular and molecular life sciences* **2005**, *62*, (23), 2739-2749.

43. Mitchell, D.; Steinman, L.; Kim, D.; Fathman, C.; Rothbard, J. Polyarginine enters cells more efficiently than other polycationic homopolymers. *The Journal of Peptide Research* **2002**, *56*, (5), 318-325.
44. Won, Y. W.; Kim, H. A.; Lee, M.; Kim, Y. H. Reducible poly (oligo-D-arginine) for enhanced gene expression in mouse lung by intratracheal injection. *Molecular Therapy* **2009**, *18*, (4), 734-742.
45. McKenzie, D. L.; Collard, W. T.; Rice, K. G. Comparative gene transfer efficiency of low molecular weight polylysine DNA-condensing peptides. *The Journal of peptide research* **2003**, *54*, (4), 311-318.
46. Kim, H. H.; Lee, W. S.; Yang, J. M.; Shin, S. Basic peptide system for efficient delivery of foreign genes. *BBA-Rev. Cancer* **2003**, *1640*, (2), 129-136.
47. de Raad, M.; Teunissen, E. A.; Lelieveld, D.; Egan, D. A.; Mastrobattista, E. High-content screening of peptide-based non-viral gene delivery systems. *Journal of Controlled Release* **2012**, *158*, (3), 433-442.
48. Khondee, S.; Baoum, A.; Siahaan, T. J.; Berkland, C. Calcium Condensed LABL-TAT Complexes Effectively Target Gene Delivery to ICAM-1 Expressing Cells. *Molecular pharmaceutics* **2011**, *8*, (3), 788-798.
49. Reschel, T.; Koňák, Č.; Oupický, D.; Seymour, L. W.; Ulbrich, K. Physical properties and in vitro transfection efficiency of gene delivery vectors based on complexes of DNA with synthetic polycations. *Journal of controlled release* **2002**, *81*, (1), 201-217.
50. Loyter, A.; Scangos, G. A.; Ruddle, F. H. Mechanisms of DNA uptake by mammalian cells: fate of exogenously added DNA monitored by the use of fluorescent dyes. *Proceedings of the National Academy of Sciences* **1982**, *79*, (2), 422-426.

51. Roy, I.; Mitra, S.; Maitra, A.; Mozumdar, S. Calcium phosphate nanoparticles as novel non-viral vectors for targeted gene delivery. *International journal of pharmaceutics* **2003**, *250*, (1), 25-33.
52. Lam, A. M. I.; Cullis, P. R. Calcium enhances the transfection potency of plasmid DNA-cationic liposome complexes. *Biochim. Biophys. Acta* **2000**, *1463*, (2), 279-290.
53. Haberland, A.; Knaus, T.; Zaitsev, S. V.; Stahn, R.; Mistry, A. R.; Coutelle, C.; Haller, H.; Böttger, M. Calcium ions as efficient cofactor of polycation-mediated gene transfer. *Biochim. Biophys. Acta* **1999**, *1445*, (1), 21-30.
54. Zaitsev, S.; Haberland, A.; Otto, A.; Vorob'ev, V.; Haller, H.; Böttger, M. H1 and HMG17 extracted from calf thymus nuclei are efficient DNA carriers in gene transfer. *Gene therapy* **1997**, *4*, (6), 586.
55. Mozafari, M. R. Calcium Based Non-viral Gene Delivery: An Overview of Methodology and Applications. *Acta Medica Iranica* **2010**, *48*, (3).
56. Zaitsev, S.; Buchwalow, I.; Haberland, A.; Tkachuk, S.; Zaitseva, I.; Haller, H.; Böttger, M. Histone H1-mediated transfection: role of calcium in the cellular uptake and intracellular fate of H1-DNA complexes. *Acta histochemica* **2002**, *104*, (1), 85-92.
57. Wender, P. A.; Mitchell, D. J.; Pattabiraman, K.; Pelkey, E. T.; Steinman, L.; Rothbard, J. B. The design, synthesis, and evaluation of molecules that enable or enhance cellular uptake: peptoid molecular transporters. *Proceedings of the National Academy of Sciences* **2000**, *97*, (24), 13003-13008.
58. Schmidt, N.; Mishra, A.; Lai, G. H.; Wong, G. C. L. Arginine-rich cell-penetrating peptides. *FEBS letters* **2010**, *584*, (9), 1806-1813.

59. Åmand, H. L.; Rydberg, H. A.; Fornander, L. H.; Lincoln, P.; Nordén, B.; Esbjörner, E. K. Cell surface binding and uptake of arginine-and lysine-rich penetratin peptides in absence and presence of proteoglycans. *BBA-Rev. Cancer* **2012**.
60. Ye, S.; Tian, M.; Wang, T.; Ren, L.; Wang, D.; Shen, L.; Shang, T. Synergistic Effects of Cell Penetrating Peptide Tat and Fusogenic Peptide HA2 Enhance Cellular Internalization and Gene Transduction of Organosilica Nanoparticles. *Nanomedicine: Nanotechnology, Biology and Medicine* **2011**.
61. Singh, R.; Pervin, S.; Karimi, A.; Cederbaum, S.; Chaudhuri, G. Arginase activity in human breast cancer cell lines: N ω -hydroxy-L-arginine selectively inhibits cell proliferation and induces apoptosis in MDA-MB-468 cells. *Cancer research* **2000**, *60*, (12), 3305-3312.
62. Lind, D. S. Arginine and cancer. *J. Neurosci.* **2004**, *134*, (10), 2837S-2841S.

Chapter 3

AT2R Gene Delivered by Condensed Polylysine Complexes Attenuates Lewis Lung Carcinoma after Intravenous Injection or Intratracheal Spray

Published as:

Alhakamy, N. A.; Ishiguro, S.; Uppalapati, D.; Berkland, C. J.; Tamura, M. AT2R Gene Delivered by Condensed Polylysine Complexes Attenuates Lewis Lung Carcinoma after Intravenous Injection or Intratracheal Spray. *Molecular cancer therapeutics* 2016, 15, (1), 209-218. (2015)

3.1. Introduction

Lung cancer is the third most prevalent form of cancer behind prostate and breast cancer; however, treatment options are lagging^{1,2}. Even though progress has been made in early detection and prevention, mortality and morbidity associated with lung cancer is still unacceptably high³. In 2015, the American Cancer Society reported more than 430,000 people in the U.S. are living with lung cancer yielding the largest annual financial burden of any cancer type¹. Although incremental improvements have been made in the palliative care, currently available therapies have had minimal impact in reducing deaths³. In particular, the need for completely new therapeutics to treat the most aggressive lung cancers is especially great.

Gene therapy is experiencing a renaissance in the U.S. and around the globe. The European Union has recently approved the first gene therapy drug, Glybera®, for the treatment of Lipoprotein Lipase Deficiency (LPLD). Promising late stage clinical trials suggest the first gene therapy may be approved in the U.S. in 2016. Most gene therapy clinical trials (64.4%) have aimed at treating cancer, and yet cancer gene therapies have been slow to advance^{4,5}. Theoretical, and practical limitations still exist for gene therapy application to lung cancer. Biological barriers and toxicity continue to confound lung cancer treatment, even though the lungs may be accessed *via* inhalation or intravenous administration.

Gene vectors (viral and nonviral vectors) have steadily improved over the past 20 years. Viral vectors (*e.g.*, adenoviral) are highly efficient, and facilitate strong transgene expression in different tumor tissues^{6,7}. While these vectors are the most effective vectors applied in 70% of clinical trials, they continue to suffer from safety concerns (*e.g.*, immunogenicity and pathogenicity)⁸⁻¹¹, rapid clearance from circulation, and production problems¹¹⁻¹⁴. For these reasons, nonviral vectors could be more promising gene carriers due to easy synthesis, low cost,

and decreased immunogenicity compared to viral vectors^{10, 14-18}. These attributes suggest nonviral vectors could offer a safer approach for repeated dosing regimens when treating primary as well as recurrent cancers.

Nucleic acids complexed with cationic polymers (polyplexes) or cationic lipids (lipoplexes) are the most commonly used nonviral synthetic gene carriers^{16, 19-21}. Cationic polymers interact with cell membranes or extracellular components (e.g. glycosaminoglycans) *via* the positive charge of the amino acid residues (e.g. lysine and arginine)²². The molecular weight and charge of polycations play important roles in complexing nucleic acids for delivering genetic materials¹⁸. High-molecular-weight polycations often condense the genetic material (*e.g.*, plasmid DNA (pDNA)) into small and stable complexes. On the other hand, low-molecular-weight polycations often produce large and unstable complexes^{18, 23, 24}. Unfortunately, low-molecular-weight polycations have historically exhibited poor transfection efficiency while high-molecular-weight polycations have been plagued with cytotoxicity¹⁸.

Polylysine was one of the first polycations used for gene delivery²⁵. Polylysine-pDNA complexes have traditionally required polylysine chains with more than 20 residues to efficiently complex DNA, but yielding modest transfection efficiency and concerns about cytotoxicity¹⁴. Many attempts were made to increase transfection efficiency or reduce cytotoxicity by either chemically modifying polylysine (*e.g.*, PEGylation) or by adding excipients²⁶. Most research efforts focused on improving tolerability of high-molecular-weight polylysine^{10, 27, 28}, but we show that short polylysines with much lower cytotoxicity can indeed condense pDNA into small complexes when calcium is added. Such particles offer an interesting opportunity for repeat dosing to treat lung cancer if efficient transfection can be balanced with low cytotoxicity.

Here, a nine amino acid polylysine (K9) was complexed with pDNA and condensed with calcium chloride. This simple formulation (the K9-pDNA-Ca²⁺ complex) was explored using four different human cell lines: 1) A549 (a lung cancer cell), 2) HeLa (a cervix cancer cell), 3) MDA-MB-231 (a breast cancer cell), 4) HEK-293 (a virus-immortalized kidney cell)) and one mouse cell line, LLC (a lung cancer cell) using a luciferase reported plasmid DNA (pLUC) to assess transfection efficiency. Angiotensin II type 2 receptor (AT2R) is known to stimulate apoptosis and inhibit cell proliferation in different cell lines such as endothelial cells, cardiomyocytes, neuronal cells, prostate cancer cells and lung cancer cells^{5,16}, therefore, AT2R plasmid DNA (pAT2R) was delivered to LLC tumor-bearing mice. These K9-pAT2R complexes were administered *via* intravenous (IV) injection and/or *via* intratracheal (IT) spray to determine lung cancer attenuation in LLC tumor-bearing mice.

3.2. Materials and Methods

3.2.1. Materials

Plasmid DNA (pDNA) encoding firefly luciferase (pLUC, pGL3) was obtained from Promega (Madison, WI). Plasmid DNA (pDNA) encoding human AT2R (pAT2R, pcDNA3.1p) was obtained from the UMR cDNA Resource Center (University of Missouri, Rolla, MO). K9 peptide (KKKKKKKKK; M_w = 1170.65 Da; Purity > 95%) was purchased from Biomatik Corporation (Cambridge, Ontario, Canada). Branched polyethylenimine (PEI, 25 kDa), mouse serum albumin (MSA) and glucose were from Sigma-Aldrich (Milwaukee, WI). Calcium chloride dihydrate (CaCl₂·2H₂O) was obtained from Fisher Scientific (Pittsburgh). A549 (CCL-185), Lewis lung carcinoma (LLC; CRL-1642), and HeLa (CCL-2) cell line were obtained from American Type Culture Collection (ATCC; Rockville, Maryland). MDA-MB-231 and HEK-293 cell line were gifts from Dr. Nikki Cheng (University of Kansas Medical Center).

3.2.2. Preparation of the K9-pDNA-Ca²⁺ Complex

For the *in vitro* studies, the K9-pLUC-Ca²⁺ complex solution was prepared by adding 15 μ L K9 peptide solution (polymer nitrogen to pLUC phosphate (N/P) ratio 10) to 10 μ L pDNA (0.1 μ g/ μ L in 1 x Tris-acetate-EDTA (TAE) Buffer), followed by fast pipetting for 20 seconds. Then, 15 μ L calcium chloride solution (*e.g.*, 19, 114, and 228 mM) was added and mixed by fast pipetting. The K9-pDNA-Ca²⁺ complex solution was incubated at 4°C for 20 to 25 minutes and used for each experiment. For the intravenous (IV) administration of the K9-pAT2R-Ca²⁺ complex, 160 μ L complex solution was mixed with 40 μ L 1% mouse serum albumin (MSA) (the final volume of the complex is 200 μ l, 4 μ g pAT2R, and 53 μ g K9 peptide). For the intratracheal (IT) administration, 40 μ L the K9-pAT2R-Ca²⁺ complex solution was mixed with 10 μ L 10% glucose for the osmolality adjustment (the final volume of the complex is 50 μ l, 1 μ g pAT2R, and 13 μ g K9 peptide).

3.2.3. Preparation of the PEI-pLUC Complex

The PEI-pLUC complex solution was prepared by adding 15 μ L PEI solution (N/P ratio 10) to 10 μ L pLUC (0.1 μ g/ μ L) followed by fast pipetting for 20 seconds. The PEI-pLUC complex solution was incubated at 4°C for 20 to 25 minutes and used for each experiment. The complex solution was prepared immediately before each experiment and used as a control for all *in vitro* studies.

3.2.4. Agarose Gel Electrophoresis

The K9-pLUC-Ca²⁺ complex solution was mixed with 4 μ L TAE buffer. Then, 4 μ L SYBR Green 1 was mixed with the complex solution, followed by incubation at 4°C for 20 to 25 minutes. After adding 7 μ L of 6X DNA Loading Dye, the mixture solutions were loaded onto a 1 % agarose gel, and electrophoresed for 30 minutes at 110 V.

3.2.5. Size and Zeta Potential

The particle size (effective diameter (nm)) of the K9-pLUC complex with or without calcium chloride was determined by dynamic light scattering (Brookhaven Instruments, Holtsville, NY). The zeta potentials of the complexes were measured by Zeta PALS dynamic light scattering (Brookhaven Instrument). Particle size was measured after dispersing the complexes into nuclease-free water (NFW) or serum-free media (SFM). Zeta potential was measured after dispersing the complexes into 1 mM potassium chloride solution.

3.2.6. Cell Culture

A549 cell line were grown in F-12K Nutrient Mixture media (Mediatech, Inc., Manassas, VA) supplemented with 10% (v/v) fetal bovine serum (FBS; Hyclone, Logan, UT) and 1% (v/v) Penicillin-streptomycin (MB Biomedical, LLC, Solon, OH). HeLa, MDA-MB-231, LLC, and HEK-293 cell lines were grown in Dulbecco's Modified Eagle's Medium (DMEM; Invitrogen/Life Technologies, Grand Island, NY) supplemented with 10% FBS and 1% Penicillin/streptomycin. These cell lines were incubated at 37°C in 5% CO₂ humidified the air. Cell line was authenticated by short-tandem repeat (STR) DNA profiling. The cells were maintained in low passage (<15) for this study.

3.2.7. Transfection Efficiency of the K9-pDNA-Ca²⁺ Complexes to Cultured Cells

MDA-MB-231, LLC, and HEK-293 cell (80,000 cells/well) were cultured in 96-well plates for 24 hours prior to the transfection. The cells were washed once with SFM and 100 μL transfection solution (a mixture of 20 μL of the K9-pLUC-Ca²⁺ complex and 80 μL of SFM, 0.5 μg pLUC/well) was added to each well. After 5 hours of incubation, the transfection solution was replaced with 100 μL fresh growth medium. After 48 hour of incubation, total cellular protein was collected by using BCA Protein Assay Reagent (Thermo Fisher Scientific Inc., Waltham, MA). The efficiency

of the gene transfection by the complexes was determined by Luciferase Reporter Assay using Luciferase Assay System Freezer Pack (Promega). The Luciferase expression was measured by a microplate reader (SpectraMax; Molecular Devices Crophe, CA). The transfection efficiency was expressed as Relative Light Units (RLUs) per milligram (mg) of cellular protein.

3.2.8. Cytotoxicity of K9 peptide, PEI, and Calcium Chloride *in vitro*

Cytotoxicity of K9 peptide, PEI, and calcium chloride was determined using a CellTiter 96® Aqueous Non-Radioactive Cell Proliferation Assay (MTS) obtained from Promega. A549, HeLa, MDA-MB-231, LLC, and HEK-293 cells were cultured in a 96-well plate in growth media as described previously. Cells were treated with the samples (0-5 mg/mL as indicated in the **Figure 4**) for ~24 hours. After 24 hours of incubation, the media were replaced with a mixture of 100 μ L of fresh serum medium and 20 μ L of MTS. Then, the plate was incubated for 3 hours in the incubator. To determine cell viability, the absorbance of each well was measured by a microplate reader (SpectraMax) at 490 nm and normalized to untreated control cells.

3.2.9. Assessment of DNA Accessibility to the K9-pLUC Complex by SYBR Green Assay

The degree of pLUC accessibility in the K9- or PEI-pLUC complex was assessed by the double-stranded-DNA-binding reagent SYBR Green. Briefly, 10 μ L pLUC (0.1 mg pDNA/mL) was mixed with 15 μ L of K9 peptide (N/P ratio 10), then 15 μ L deionized water or 38 mM calcium chloride solution was added. After 30 minutes incubation at room temperature, 120 μ L PBS, and 160 μ L 10X SYBR Green solutions (Invitrogen) were added. Then, 100 μ L sample was added to one well of a 96-well cell culture plate. The fluorescence was measured using a fluorescence plate reader (SpectraMax M5; Ex., 250 nm; Em, 520 nm).

3.2.10. Animals

Six-week-old wild-type male C57BL/6 mice were obtained from Charles River Laboratories International, Inc. All mice were housed in a clean facility and held for 10 days to acclimatize. All animal experiments were carried out under strict adherence to the Institutional Animal Care and Use Committee (IACUC) protocols and the Institutional Biosafety Committee set by Kansas State University (Manhattan, KS).

3.2.11. Lung Cancer Graft in Syngeneic Mouse and Treatment with the K9-pAT2R-Ca²⁺ Complex

Seven week old C57BL/6 mice were intravenously injected with 1.2×10^6 LLC cells suspended in 200 μ L PBS *via* the tail vein using a 1 mL syringe with a 27G needle. The K9-pAT2R-Ca²⁺ complex solution was prepared immediately before injection as described above. For the intravenous (IV) administration of the K9-pAT2R-Ca²⁺ complex, 160 μ L complex solution was mixed with 40 μ L 1% mouse serum albumin (MSA). For the intratracheal (IT) administration, 40 μ L the K9-pAT2R-Ca²⁺ complex solution was mixed with 10 μ L 10% glucose for the osmolality adjustment. After 7 days of the LLC injection, the mice were injected with 200 and 50 μ L of the complexes with each composition *via* IV and IT, respectively. The PBS and K9-Ca²⁺ solutions without pAT2R were used as control. In addition, K9-pLUC-Ca²⁺ complex prepared as described above was also injected into LLC tumor-bearing mice *via* IV and IT as a non-specific gene control. Mice were sacrificed by cervical dislocation under anesthesia at 14 days after the complex treatment. The lungs were dissected, and tumor burden were analyzed.

3.2.12. Immunohistochemical Analysis for AT2R, Cell Proliferation and Apoptosis in LLC Allografts

Fixed lung tissues were sectioned at 4 μ m and stained with haematoxylin and eosin (HE) staining for histological examination. To analyze the AT2R expression and cell proliferation by Ki-67 in

LLC tumors, sections were deparaffinized and heat-induced epitope unmasking was performed in the citrate buffer followed by incubation with 3% H₂O₂/methanol for 3 minutes to block endogenous peroxidase activity. Sections were incubated with polyclonal anti-AT2R (1:100 dilution, for 18 hours at 4°C, Abcam) and polyclonal anti-Ki-67 (1:500 dilution, for 18 hours at 4°C, Abcam) antibodies. After the incubation with primary antibodies, sections were induced into reaction with a biotin-conjugated anti-rabbit IgG antibody (Vector Laboratories) at a 1:100 dilution for 1 hour at 37°C, followed by reaction with the avidin-biotin-peroxidase complex reagent (Vector Laboratories) for 40 minutes at 37°C. Reactions were developed with 3, 3'-diaminobenzidine tetrahydrochloride (Sigma) and counterstained lightly with Mayer`s hematoxylin. The cell proliferation index was assessed as the fold change of the average percentage of positive cells in three randomly selected fields in the tumor nodules. Apoptotic cells in LLC tumors were detected by a terminal deoxynucleotidyl transferase dUTP nick end labeling (TUNEL) assay by using the DeadEnd Colorimetric TUNEL System (Promega), according to the manufacturer's instructions with a slight modification ²⁹. The apoptotic index was assessed as the fold change of the average number of positive cells in three randomly selected fields in the tumor nodules.

3.2.13. Statistical Analysis

The data was analyzed by using GraphPad software. All values were expressed as the mean ± standard error of the mean. All experiments were conducted with multiple sample determinations. A statistical evaluation comparing the significance of the difference in gene expression (RLUs/mg protein) between the means of two data sets was performed using a *t* test. One-way ANOVA, Tukey post-test was used to analyze the differences when more than two data sets were compared.

3.3. Results

3.3.1. Formation of the K9-pLUC-Ca²⁺ Complex

The K9-pDNA-Ca²⁺ and PEI-pDNA complexes were prepared by mixing pLUC or pAT2R with K9 peptide at various N/P ratios as described in the materials and methods section. In order to demonstrate complex formation, agarose gel electrophoresis assay was performed using 1% agarose gel, and electrophoresed for 30 minutes. Uncomplexed pLUC (naked pLUC) was used as a control. The K9 peptide and pLUC mixture showed ability to form complexes of pLUC and K9 peptide regardless of the presence of 38 mM calcium chloride at N/P ratios 5, 10, and 30. Since the size of these complexes was significantly bigger than pLUC, the complexes stayed in the loading wells without migrating into the gel and no bands were observed in the electrophoresis (**Figure 1A**). Although lower N/P ratios (1 to 4) also showed no bands in the absence of calcium chloride, the N/P ratios lower than 0.5 showed bands (**Figure 1B**). In addition, mixing with calcium chloride and pLUC did not form stable complexes (**Figure 1C**).

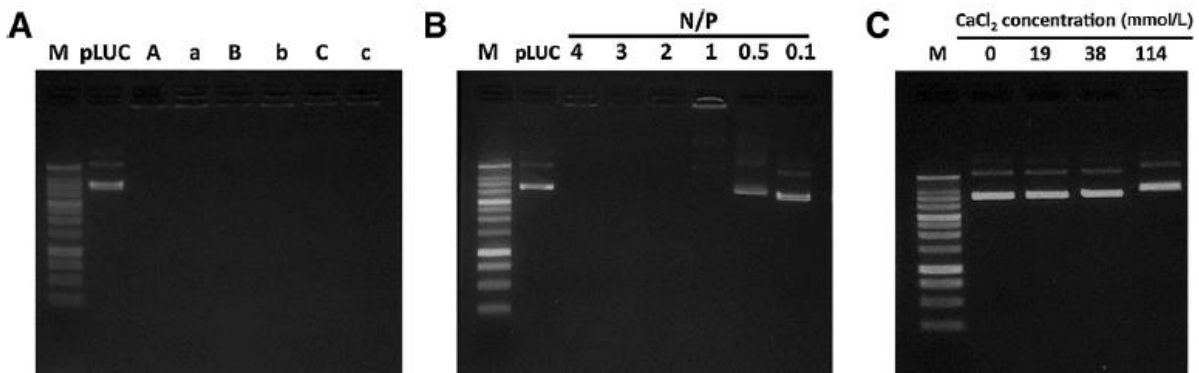


Figure 1. Agarose gel electrophoresis study of K9-pDNA-Ca²⁺ complexes at N/P ratios of 5, 10, or 30 with or without 38 mM calcium chloride (**A**), K9-pDNA complexes without calcium chloride at N/P ratios of 4, 3, 2, 1, 0.5, or 0.1 (**B**), and pLUC/calcium chloride complexes with 0, 19, 38, or 114 mM of calcium chloride (**C**). In the panel I, A, B and C refer to N/P 5, N/P 10, and N/P 30 in the presence of 38 mM calcium chloride, respectively, whereas a, b, and c refer to N/P 5, N/P 10, and N/P 30 in the absence of calcium chloride, respectively. “M” Refers to the size marker.

3.3.2. Physical Characterization of the K9-pLUC-Ca²⁺ and the PEI-pLUC Complexes

The effect of calcium chloride concentration on the surface charge and particle size of the K9-pLUC complex was investigated. As shown in **Figure 2A**, addition of calcium chloride of 37.7 and 113 mM (final concentration) significantly decreased the particle size of the K9-pLUC-Ca²⁺ complex, with relatively narrow polydispersity (~0.1), in both nuclease-free water (NFW) and in serum-free F-12 media (SFM). The zeta potential of the K9-pLUC-Ca²⁺ and PEI-pLUC complexes increased significantly with increases in the concentration of calcium chloride (**Figure 2B**).

SYBR Green assay provides a non-destructive and simple method to examine pDNA accessibility within complexes. As shown in **Figure 2C**, pLUC was accessible in the K9-pLUC complex, whereas pLUC accessibility in the PEI-pLUC complex was low compared to pLUC alone. Although pLUC accessibility in the K9-pLUC complex was significantly decreased in the presence of 38 mM calcium chloride, DNA accessibility was lower in the PEI-pLUC complex. These results suggest that the addition of calcium chloride significantly decreased the size of the K9-pLUC complex, but the pLUC in the complex was more accessible than in the PEI-pLUC complex.

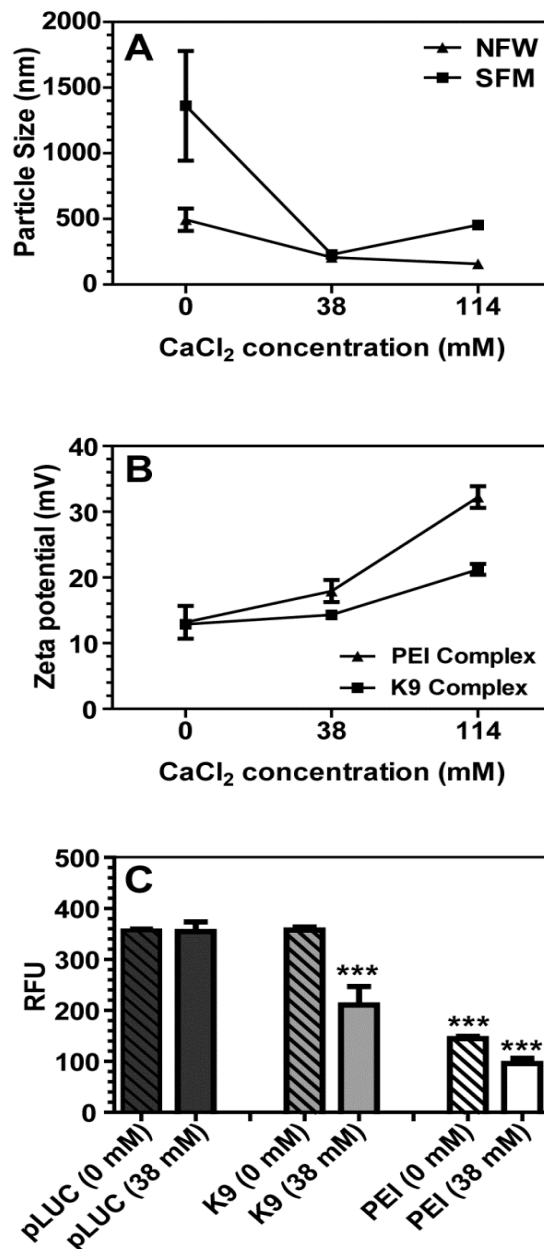


Figure 2. Evaluation of the particle sizes (effective diameters), zeta potentials, and SYBR Green assay of the K9-pLUC and PEI-pLUC complexes with or without calcium chloride. (A), the particle size of the K9-pLUC complexes (N/P ratio = 10) were determined by DLS in the presence of various concentrations of calcium chloride (0, 38, and 114 mM) in nuclease-free water (NFW), or serum-free F-12 media (SFM). (B), zeta potentials of the K9-pLUC and PEI-pLUC complexes (N/P ratio = 10) were determined by Zeta PALS dynamic light scattering in the presence of various concentrations of calcium chloride (0, 38, and 114 mM). (C), effect of calcium chloride concentration at 0 and 38 mM on pLUC accessibility in K9-pLUC and PEI-pLUC complexes at an N/P ratio of 10 was evaluated using the SYBR Green assay. The pLUC alone in the solution was used as a control. Results are presented as mean \pm SD (n = 3). ***, P < 0.0001, one-way ANOVA, Tukey post-test comparison to pDNA.

3.3.3. The K9-pLUC-Ca²⁺ Complex Caused Efficient Gene Transfection with Low Cytotoxicity *in Vitro*

The *in vitro* transfection efficiency of the K9-pLUC-Ca²⁺ and the PEI-pLUC complexes was studied using the four different human cell lines and the mouse cell line. Luciferase gene expression was evaluated 48 hours after the transfection using the K9-pLUC-Ca²⁺ and the PEI-pLUC complexes at N/P ratios 5, 10, 20, and 30, and at various calcium chloride concentrations during the complex formulation (**Figure 3A**). The K9-pLUC-Ca²⁺ complexes had a high level of gene expression at a calcium chloride concentration of 38 mM (N/P ratio 10) in A549 cells. Luciferase gene expression was decreased when calcium concentration was higher than 114 mM in all N/P ratios tested. This result was further confirmed in other cell lines: A549 cells (**Figure 3B**), HeLa cells (**Figure 3C**), MDA-MB-231 cells (**Figure 3D**), HEK-293 cells (**Figure 3E**), and LLC cells (**Figure 3F**). In all cell lines examined, the transfection efficiency of the K9-pLUC-Ca²⁺ with 38 mM calcium chloride was significantly higher than those with PEI-pLUC and the K9-pLUC-Ca²⁺ with 114 mM calcium chloride (**Figure 3**). Significance of including K9 peptide in pDNA transfection was further examined by comparing pLUC expression efficiency in the presence or absence of the peptide in various cell lines (**Figure Appendix 1**). The transfection efficiency of the pLUC-Ca²⁺ complex (without K9 peptide) was significantly lower than that of the K9-pLUC-Ca²⁺ complex at the same calcium chloride concentration.

High transfection efficiency and low cytotoxicity are vital attributes for nonviral gene vectors. To examine whether K9, PEI, and calcium chloride affected the viability of live cells, a membrane translocalization signal (MTS) cytotoxicity assay was conducted using five different cell lines. The five cell lines were individually incubated with up to 5 mg/mL K9, PEI, or calcium chloride for 24 hours and then MTS assay was performed (**Figure 4**). The K9 peptide showed no cytotoxicity to 2.5 mg/mL. Only HEK-293 cell viability was decreased at 1 mg/mL levels of K9

peptide. Calcium chloride also did not show strong cytotoxicity until 1 mg/mL. However, PEI induced significant cytotoxicity even at 10 $\mu\text{g/mL}$ in the four cell lines. Although HEK-293 cells were resistant to PEI-induced cytotoxicity, their cell viability was gradually decreased at higher concentrations. This MTS assay strongly suggested that the K9-pDNA- Ca^{2+} complex is a low cytotoxic pDNA transfection vector.

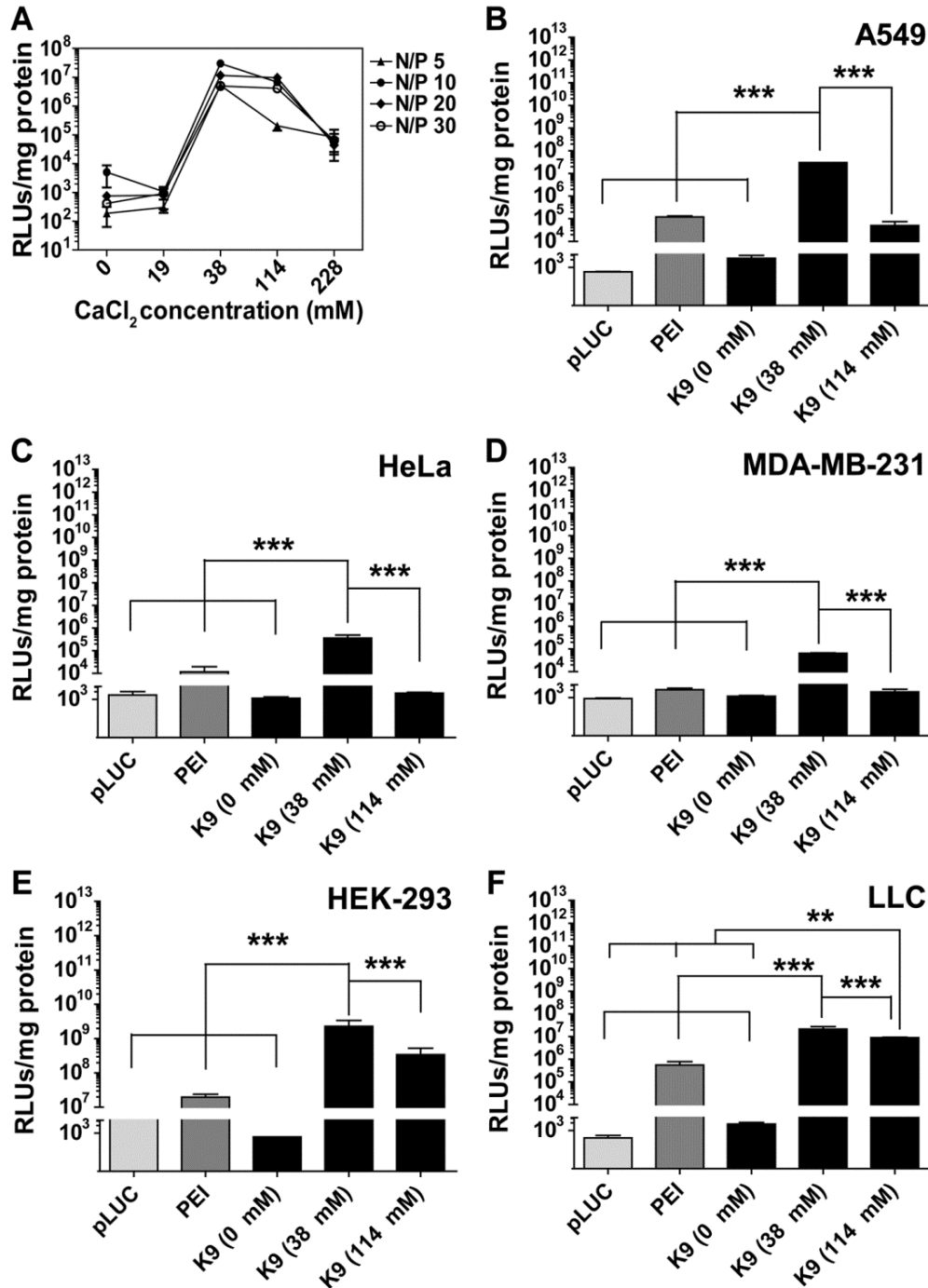


Figure 3. The transfection efficiencies of the K9-pLUC complex. (A), the transfection efficiencies in various concentrations of calcium chloride (0, 19, 38, 114, and 228 mM) in A549 cells at N/P ratios of 5, 10, 20 and 30. The transfection efficiencies of the K9-pLUC complexes with different concentrations of added calcium chloride (0, 38, and 114 mM) at an N/P ratio 10 in A549 cells (B), HeLa cells (C), MDA-MB-231 cells (D), HEK-293 cells (E) and LLC cells (F). RLU refers to relative light units. Results are presented as mean \pm SD (n = 4). ***, P < 0.0001; **, P < 0.001; one-way ANOVA; Tukey post-test.

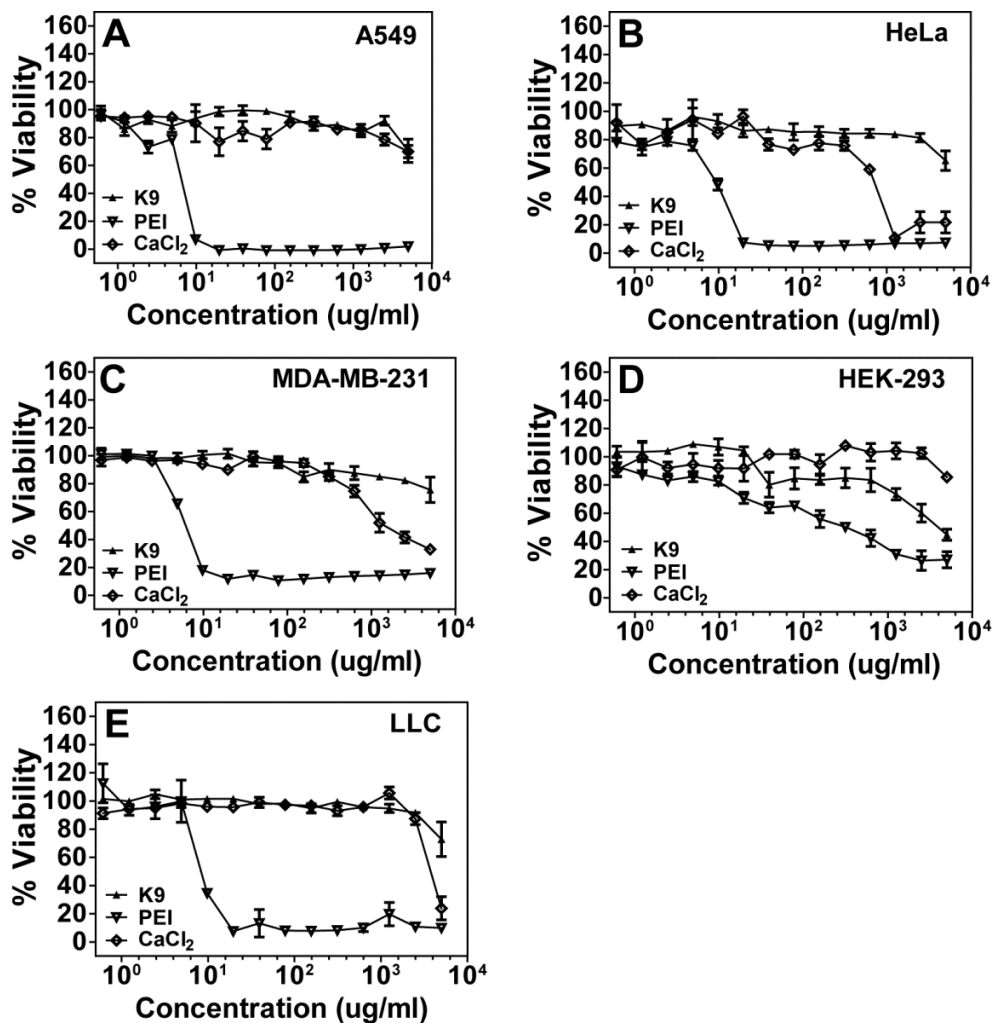


Figure 4. Cytotoxicity profiles of K9, PEI, and calcium chloride in A549 cells (A), HeLa cells (B), MDA-MB-231 cells (C), HEK-293 cells (D), and LLC cells (E). Cell viability was determined by MTS assay. Results are presented as mean \pm SD (n = 3).

3.3.4. Treatment with the K9-pAT2R-Ca²⁺ Complex *via* Intravenous Injection or Intratracheal Spray Caused Significant Growth Attenuation of Lung Tumors

The effect of the K9-pAT2R-Ca²⁺ complex delivering the endogenous apoptosis-inducer gene AT2R was examined using orthotopic LLC allografts in syngeneic C57BL/6 mice. To evaluate the effect of the complex on the lung tumor growth, LLC cells (1.2 x 10⁶) were injected *via* the tail vein. Seven days after cancer cell injection, the mice were treated with a single dose of

the K9-pAT2R-Ca²⁺ complexes containing 4 µg pAT2R intravenously (IV) or 1 µg pAT2R intratracheally (IT). The tumor growth attenuating the effect of these complexes was observed both macroscopically (**Figure 5A**) and microscopically (**Figure 5B**). Macroscopically, a large number and large size of tumor nodules were detected in PBS or K9 treated mouse lungs. The average lung weight (mg) of the K9-pAT2R-Ca²⁺ IT (190.6±48.3) and the K9-pAT2R-Ca²⁺ IV (201.6±67.0) treated groups were significantly smaller than that of the control PBS group (325.7±69.4, P<0.05, **Figure 5C** and **Table Appendix 1**). Histological examination of tumors in H&E stained lung sections also displayed only a small number and small size of LLC tumor nodules in mouse lungs treated with the K9-pAT2R-Ca²⁺ complexes (**Figure 5B**). Average numbers of tumor nodules in the lungs in the IT (6.0±4.2) and the IV (4.6±3.4) groups were significantly smaller than that of the control PBS group (17.8±6.0, P<0.01, **Figure 5D** and **Table Appendix 2**). On the other hand, treatment with K9-pLUC-Ca²⁺ complexes did not show any effect on the average lung weight (246.8±70.3 in PBS, 213.9 ±52.3 in K9-pLUC-Ca²⁺ IV, and 267.3 ±6.9 in K9-pLUC-Ca²⁺ IT) and the average numbers of tumor nodules (20.4±4.0, 20.2±11.9, and 25.7±1.5 in the same group order as the lung weights described above) in LLC tumor-bearing mouse lung (**Figure Appendix 2, Table Appendix 3** and **4**). Both local (*i.e.* pulmonary) and systemic treatment with the K9-pAT2R-Ca²⁺ complexes were equally effective in attenuating the growth of LLC lung tumor grafts in immunocompetent mice.

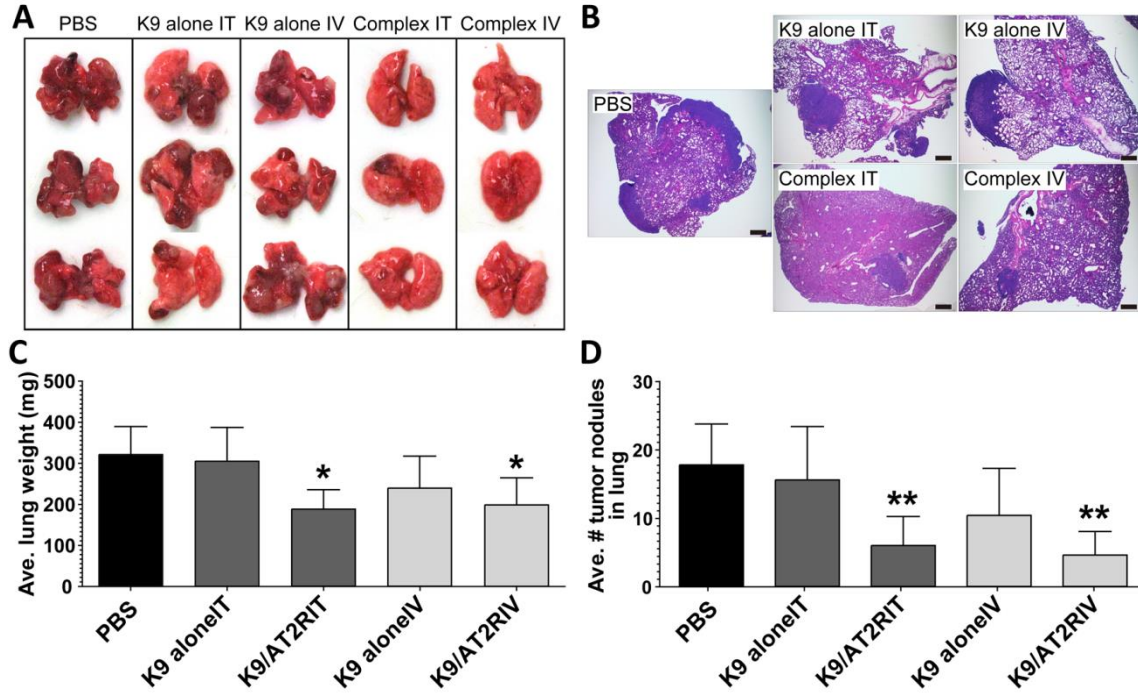


Figure 5. Macroscopic analysis of LLC tumors in C57BL/6 mouse lungs (A) and microscopic views (B) of the lung from PBS, K9-alone IT, K9-alone IV, K9-pAT2R-Ca²⁺ IT (complex IT), or K9-pAT2R-Ca²⁺ IV (complex IV)-treated mice (n=5). Average lung weight (C) and number of tumor nodules (D) in each treatment group were expressed in the bar graphs. Scale bars in panel B indicate 500µm. *, P < 0.05; **, P < 0.01 as compared with the level of PBS control. (n=5, one-way ANOVA Tukey post-test). K9, nine amino acid polylysine; IT, intratracheal; IV, intravenous.

3.3.5. Immunohistochemical Analysis of AT2R Expression, Cell Proliferation and Apoptosis in LLC Grafts

The expression of AT2R gene in the lung was determined immunohistochemically (Figure 6). As shown in Figure 6A, AT2R expression was upregulated in the tumor cells in the K9-pAT2R-Ca²⁺ IV and IT spray groups but not in other groups. These observations suggested that the K9-pAT2R-Ca²⁺ administration *via* IV and IT significantly attenuated the lung tumor growth by expressing AT2R in the tumor cells. Immunohistochemical analysis of cell proliferation in tumors using anti-Ki-67 antibody did not show many differences (Figure 6B). Although the average number of apoptotic cells detected by TUNEL assay tended to increase in the K9-pAT2R-

Ca²⁺ treatment groups (**Figure 6C**), there was no statistical significance between groups due to large variations within the samples. Since the analysis was carried out 14 days after treatment with the K9-pAT2R-Ca²⁺ complex, these results may suggest that the treatment with the K9-pAT2R-Ca²⁺ complex attenuated tumor growth during an early stage of LLC tumorigenesis. Nevertheless, these results support that both IV and IT administration of the K9-pAT2R-Ca²⁺ offer effective modalities for lung cancer targeted nonviral gene therapy.

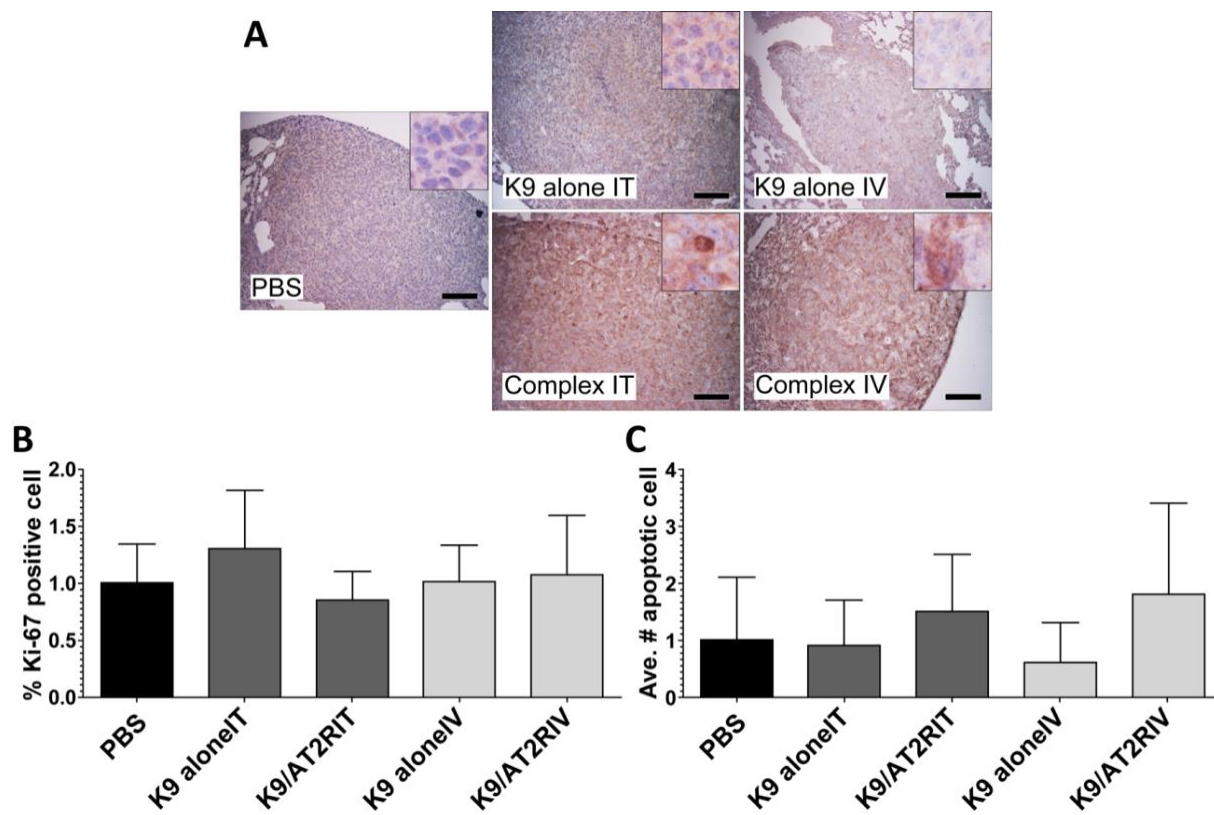


Figure 6. Immunohistochemical analysis of AT2R expression (**A**), cell proliferation (**B**) and apoptosis (**C**) in LLC graft tumors in PBS, K9-alone IT, K9-pAT2R-Ca²⁺ IT (complex IT), K9-alone IV or K9-pAT2R-Ca²⁺ IV (complex IV)-treated mice (n=5). **A**, Microscopic images of immunohistochemistry for AT2R expression (original magnification at 200x). AT2R expression was observed in the tumor cells from complex IT or complex IV-treated mice (insets). Scale bars in the panel A indicate 100 μ m. Cell proliferation index (**B**) and apoptotic index (**C**) were evaluated by Ki-67 expressions and TUNEL assay in the tumor cells, respectively. K9, nine amino acid polylysine; IT, intratracheal; IV, intravenous.

3.4. Discussion

Development in the field of gene therapy is presently hindered by the lack of robust gene delivery methods. Synthetic, nonviral gene vectors such as polycationic peptides (e.g. polylysine) are promising vectors^{10, 17, 18}. The toxicity of these CPPs may be minimized or eliminated by reducing their molecular size. However, the level of transfection efficiency mediated by smaller polypeptides is typically low compared to larger polypeptides¹⁷. CPPs have been used to deliver various anti-cancer agents (e.g., small molecules, proteins, and nucleic acids) into cells *in vivo* and have been observed to be effective in inhibiting tumor growth in preclinical tumor models^{17, 30, 31}. The main goals of this work were to examine the transfection efficiency of the K9-pDNA-Ca²⁺ complex and to determine whether pDNA (pAT2R) can be distributed to lung cancer cells, resulting in therapeutically effective gene expression.

The *in vitro* transfection efficiency of the K9-pDNA-Ca²⁺ complex was evaluated using luciferase pDNA (pLUC) in the four different human cell lines (kidney, cervix, breast, and lung) and one mouse cancer cell line (lung). Over expression of the AT2R gene in lung cancer cells³², or other type of CPP-pDNA-Ca²⁺ complex-based IT delivery of the AT2R gene was known to reduce lung cancer cell growth.¹⁶ IV injection or IT spray of the K9-pAT2R-Ca²⁺ complexes yielded robust gene expression, primarily in lung cancer cells, and significantly attenuated cancer growth. Therefore, this study presents an effective *in vitro* and *in vivo* gene delivery system using a low-molecular-weight cationic CPP (K9 peptide) for lung cancer therapy.

The formation of complexes between K9 and pDNA was observed in both the K9-pLUC-Ca²⁺ and K9-pLUC complexes as observed *via* agarose gel electrophoresis (**Figure 1**) when the N/P ratio is higher than 0.5. By itself, calcium chloride showed negligible ability to complex naked pLUC even at a high concentration (114 mM) (**Figure 1B**). However, the K9-pLUC complex

without calcium chloride exhibited very low gene expression (**Figure 3A**), and the size of this complex was inappropriately large (500 to 1500 nm) for gene delivery (**Figure 2A**). The addition of calcium chloride in the K9-pLUC complex significantly decreased the complex size in water and culture medium (**Figure 2A**) and correspondingly increased gene transfection (**Figure 3A**). Therefore, calcium chloride acted as an effective condensing agent to decrease the particle size of the K9-pLUC complex and enhance transfection efficiency. These observations are in good agreement with our previous study in which calcium chloride also decreased particle sizes of CPP-pLUC complexes with other types of CPP³³. In this regard, it is of interest to note that the PEI-pLUC complex did not show a decrease in particle sizes as calcium chloride increased¹⁷. Calcium ion-dependent increase of the total positive charge of the K9-pLUC-Ca²⁺ complex may also play an important role enhancing transfection efficiency by the stronger interaction with the negatively charged plasma membrane³⁴. In addition, accessibility of SYBER green to the pLUC in the K9-pLUC complex was significantly decreased when calcium chloride (38 mM) was added to the complex solution (**Figure 2C**), suggesting the K9-pLUC complex was effectively condensed, and calcium chloride played an essential role in condensation of the complex. The reduction in the particle size of the K9-pDNA-Ca²⁺ complexes likely led to an increase in transfection efficiency.

The effect of calcium chloride on the transfection efficiency of the K9-pDNA complex was first assessed using A549 cells. The best transfection efficiency was achieved at 38-76 mM calcium chloride (**Figure 3A**). Interestingly, no significant level of gene expression was detected without calcium chloride. Since calcium chloride appeared to be an essential component in the condensation of the K9-pLUC complex, yielding small complexes with optimal pLUC expression, the transfection efficiency of the K9-pLUC-Ca²⁺ and PEI-pLUC complexes (N/P ratio 10) was assessed across five cell lines using three different calcium chloride concentrations (0, 38, and 114

mM, **Figure 3**). This experiment confirmed that pLUC transfection by the K9-pLUC-Ca²⁺ complex was highest at 38 mM calcium chloride, and the LUC expression was significantly better than that of PEI-pLUC complex (25kDa PEI) ³⁵.

In another study, the importance of the K9 peptide in gene expression was evaluated by comparing pLUC-Ca²⁺ complex (without K9 peptide) and the K9-pLUC-Ca²⁺ complex in the same calcium concentration. The result in **Figure Appendix 1** clearly shows that pLUC expression resulting from the pLUC-Ca²⁺ complex (without K9 peptide) was significantly lower than that of the K9-pLUC-Ca²⁺ complex suggesting that K9 in the complex is indeed important to achieve the high gene expression from the K9-pLUC-Ca²⁺ complex. The PEI-pDNA complex had high transfection efficiency in the absence of calcium chloride ^{17, 18, 33}.

A successful gene vector should be able to deliver genetic material to the target cells without influencing the viability of the host cells. The present study clearly indicated negligible cytotoxicity *in vitro* up to 2.5 mg/mL for K9 peptide and 1 mg/mL for calcium chloride after 24 hours for all five cell lines, whereas PEI exhibited strong cytotoxicity at low micromolar concentrations in all cell lines except for HEK-293 cells (**Figure 4**). Additionally, the low toxicity of the K9-pAT2R-Ca²⁺ complexes was also observed in the mouse study after IV and IT applications, in which all mice receiving K9-alone or the K9-pAT2R-Ca²⁺ complex survived during the experimental period and did not show acute inflammatory reaction or any histologically detectable abnormality. Therefore, data strongly suggested that the K9-pAT2R-Ca²⁺ complex represents a safe and efficient gene transfection vector.

The robust gene expression in various cell lines with negligible cytotoxicity compelled *in vivo* gene transfection studies. An endogenous apoptosis inducer gene, AT2R, was delivered using K9-pAT2R-Ca²⁺ complexes administered to LLC tumor-bearing mice. As shown in **Figure 5**, the

treatment with the K9-pAT2R-Ca²⁺ complex *via* either IT or IV administrations significantly attenuated tumor growth macroscopically and microscopically, while the treatment with the non-specific control gene complex (K9-pLUC-Ca²⁺) did not show any tumor growth attenuation effect (**Figure Appendix 2**). Immunohistochemical analysis of AT2R protein expression in the lung indicated that the expression of this gene was detected mainly in lung cancer cells, but not in normal lung tissues, which suggests that the K9-pAT2R-Ca²⁺ complex preferentially delivered the therapeutic gene into cancer cells. It has been known that an increased expression of anionic molecules in the membrane of cancer cells, such as the phosphatidylserine, O-glycosylated mucins, sialylated gangliosides, and heparin sulfate, resulted in an increased net negative charge compared to the nonmalignant cell membrane ³⁶.

These electric characters of cancer cells support that polycationic peptide-based nanoparticles are suited for cancer-targeted gene therapy. The observed increase of apoptotic cells in the K9-pAT2R-Ca²⁺ complex treated groups (**Figure 6**) suggested AT2R expression in the tumors induced apoptosis in cancer cells. These results are consistent with earlier studies confirming that AT2R expression attenuates growth of various cancer cells including lung cancer cells ^{16, 32, 37-39}. Therefore, AT2R gene expression is a potential treatment scheme for primary as well as metastatic lung cancers. A single IV bolus injection or IT spray of K9-alone did not attenuate cancer growth significantly as compared with the PBS controls (**Figure 5**). Dosing K9 alone or K9-pLUC neither exhibited any side effects such as abnormal clinical or histological signs in the native tissue of the lung nor altered the tumor growth. These results suggest that K9 peptide is a useful and safe vector for cancer gene therapy.

In the present study, K9-pDNA-Ca²⁺ complex-based gene delivery was found to be a useful tool for *in vivo* gene delivery system for lung cancer treatment in immunocompetent mice. Since

it is obvious that both cellular and humoral immune systems in the tumor microenvironment play a significant role in the regulation of tumor growth^{36, 40}, use of immunocompetent mice for the evaluation of the newly developed treatment regimen is appropriate. Although our study has provided first proof of principle data using murine lung carcinoma cells and syngeneic immunocompetent mouse model, further evaluation of this gene therapy using multiple types of human lung cancer cells in mouse xenograft models will solidify this discovery.

A recent study has evaluated the utilize the use of polylysine dendrimers for the delivery of Polo-like kinase 1 (PLK1)-specific short interfering RNA (siRNA) for the treatment of non-small cell lung cancer *in vitro* and *in vivo*⁴¹. The apparent safety and acceptable transfection efficiency of polylysine dendrimers may support the calcium condensed polylysine complexes used for pDNA delivery in the present study. The K9-pDNA-Ca²⁺ complex is a simple approach, thus its usefulness in future translational studies appears to be very high.

3.5. Conclusions

The addition of calcium chloride to nascent complexes of polylysine CPP (K9 peptide) and pDNA (pLUC and pAT2R) produced small and stable complexes. These complexes exhibited high gene expression in various human and mouse cancer cells comparable to PEI-pDNA complexes. Single IV or IT administrations of the K9-pAT2R-Ca²⁺ complexes significantly attenuated the growth of LLC cell allografts in mouse lungs, suggesting that K9 peptide-based gene therapy is effective and that the AT2R gene is potentially useful for lung cancer gene therapy. K9 peptide showed negligible cytotoxicity in cell culture, supporting the notion that this CPP is a safe delivery vehicle for genetic materials (*e.g.*, siRNA and pDNA). Although, further studies are required to confirm the *in vivo* safety of the K9-pAT2R-Ca²⁺ complexes by formal pharmacokinetics, pharmacodynamics, and multispecies toxicity studies, these data showed that the K9-pDNA-Ca²⁺ complexes could be an effective and safe nonviral gene transfection tool.

3.6. References

1. Howlader, N.; Noone, A.; Krapcho, M. SEER Cancer Statistics Review, 1975-2009 (Vintage 2009 Populations). Bethesda, MD: National Cancer Institute; April 2012. http://seer.cancer.gov/csr/1975_2009_pops09/, based on November 2011 SEER data submission, posted to the SEER web site **April 2012**.
2. Hensing, T.; Chawla, A.; Batra, R.; Salgia, R., A personalized treatment for lung cancer: molecular pathways, targeted therapies, and genomic characterization. In *Systems Analysis of Human Multigene Disorders*, LLC., S. S. M., Ed. Springer: Philadelphia, New York, 2014; pp 85-117.
3. Cai, K.; Sham, M.; Tam, P.; Lam, W. K.; Xu, R. Lung cancer gene therapy. *Gene Ther Mol Biol* **2003**, *7*, 255-272.
4. Tsutsumi, Y.; Matsubara, H.; Masaki, H.; Kurihara, H.; Murasawa, S.; Takai, S.; Miyazaki, M.; Nozawa, Y.; Ozono, R.; Nakagawa, K. Angiotensin II type 2 receptor overexpression activates the vascular kinin system and causes vasodilation. *Journal of Clinical Investigation* **1999**, *104*, (7), 925-935.
5. Du, H.; Liang, Z.; Zhang, Y.; Jie, F.; Li, J.; Fei, Y.; Huang, Z.; Pei, N.; Wang, S.; Li, A. Effects of Angiotensin II Type 2 Receptor Overexpression on the Growth of Hepatocellular Carcinoma Cells In Vitro and In Vivo. *PloS one* **2013**, *8*, (12), e83754.
6. Benihoud, K.; Yeh, P.; Perricaudet, M. Adenovirus vectors for gene delivery. *Current Opinion in Biotechnology* **1999**, *10*, (5), 440-447.
7. Simons, M.; Beinroth, S.; Gleichmann, M.; Liston, P.; Korneluk, R.; MacKenzie, A.; Bähr, M.; Klockgether, T.; Robertson, G.; Weller, M. Adenovirus-Mediated Gene Transfer of Inhibitors

of Apoptosis Proteins Delays Apoptosis in Cerebellar Granule Neurons. *Journal of neurochemistry* **1999**, 72, (1), 292-301.

8. Karagiannis, E. D.; Alabi, C. A.; Anderson, D. G. Rationally Designed Tumor-Penetrating Nanocomplexes. *ACS nano* **2012**, 6, (10), 8484-8487.

9. Khondee, S.; Baoum, A.; Siahaan, T. J.; Berkland, C. Calcium condensed LABL-TAT complexes effectively target gene delivery to ICAM-1 expressing cells. *Molecular pharmaceutics* **2011**, 8, (3), 788-798.

10. Alhakamy, N. A.; Nigatu, A. S.; Berkland, C. J.; Ramsey, J. D. Noncovalently associated cell-penetrating peptides for gene delivery applications. *Therapeutic delivery* **2013**, 4, (6), 741-757.

11. Deng, J.; Gao, N.; Wang, Y.; Yi, H.; Fang, S.; Ma, Y.; Cai, L. Self-assembled cationic micelles based on PEG-PLL-PLLeu hybrid polypeptides as highly effective gene vectors. *Biomacromolecules* **2012**, 13, (11), 3795-3804.

12. Bennett, J. Immune response following intraocular delivery of recombinant viral vectors. *Gene therapy* **2003**, 10, (11), 977-982.

13. Liu, Q.; Muruve, D. Molecular basis of the inflammatory response to adenovirus vectors. *Gene therapy* **2003**, 10, (11), 935-940.

14. Kwoh, D. Y.; Coffin, C. C.; Lollo, C. P.; Jovenal, J.; Banaszczyk, M. G.; Mullen, P.; Phillips, A.; Amini, A.; Fabrycki, J.; Bartholomew, R. M. Stabilization of poly-L-lysine/DNA polyplexes for in vivo gene delivery to the liver. *Biochimica et Biophysica Acta (BBA)-Gene Structure and Expression* **1999**, 1444, (2), 171-190.

15. Li, S.; Huang, L. Nonviral gene therapy: promises and challenges. *Gene therapy* **2000**, 7, (1), 31-34.

16. Kawabata, A.; Baoum, A.; Ohta, N.; Jacquez, S.; Seo, G.-M.; Berkland, C.; Tamura, M. Intratracheal administration of a nanoparticle-based therapy with the angiotensin II type 2 receptor gene attenuates lung cancer growth. *Cancer research* **2012**, *72*, (8), 2057-2067.
17. Baoum, A.; Xie, S.-X.; Fakhari, A.; Berkland, C. “Soft” Calcium Crosslinks Enable Highly Efficient Gene Transfection Using TAT Peptide. *Pharmaceutical research* **2009**, *26*, (12), 2619-2629.
18. Alhakamy, N. A.; Berkland, C. J. Polyarginine molecular weight determines transfection efficiency of calcium condensed complexes. *Molecular pharmaceutics* **2013**, *10*, (5), 1940-1948.
19. Felgner, P. L.; Gadek, T. R.; Holm, M.; Roman, R.; Chan, H. W.; Wenz, M.; Northrop, J. P.; Ringold, G. M.; Danielsen, M. Lipofection: a highly efficient, lipid-mediated DNA-transfection procedure. *Proceedings of the National Academy of Sciences* **1987**, *84*, (21), 7413-7417.
20. Tang, M. X.; Redemann, C. T.; Szoka, F. C. In vitro gene delivery by degraded polyamidoamine dendrimers. *Bioconjugate chemistry* **1996**, *7*, (6), 703-714.
21. Hofland, H. E.; Nagy, D.; Liu, J.-J.; Spratt, K.; Lee, Y.-L.; Danos, O.; Sullivan, S. M. In vivo gene transfer by intravenous administration of stable cationic lipid/DNA complex. *Pharmaceutical research* **1997**, *14*, (6), 742-749.
22. Dennison, S. R.; Phoenix, A. J.; Phoenix, D. A. Effect of salt on the interaction of Hal18 with lipid membranes. *European Biophysics Journal* **2012**, *41*, (9), 769-776.
23. Koo, H.; Kang, H.; Lee, Y. Analysis of the relationship between the molecular weight and transfection efficiency/cytotoxicity of Poly-L-arginine on a mammalian cell line. *Bull. Korean Chem. Soc* **2009**, *30*, 927-930.

24. de Raad, M.; Teunissen, E. A.; Lelieveld, D.; Egan, D. A.; Mastrobattista, E. High-content screening of peptide-based non-viral gene delivery systems. *Journal of Controlled Release* **2012**, *158*, (3), 433-442.
25. Zhang, X.; Oulad-Abdelghani, M.; Zelkin, A. N.; Wang, Y.; Haïkel, Y.; Mainard, D.; Voegel, J.-C.; Caruso, F.; Benkirane-Jessel, N. Poly (L-lysine) nanostructured particles for gene delivery and hormone stimulation. *Biomaterials* **2010**, *31*, (7), 1699-1706.
26. Kim, S. W. Polylysine Copolymers for Gene Delivery. *Cold Spring Harbor Protocols* **2012**, *2012*, (4), pdb. ip068619.
27. Ward, C. M.; Read, M. L.; Seymour, L. W. Systemic circulation of poly (L-lysine)/DNA vectors is influenced by polycation molecular weight and type of DNA: differential circulation in mice and rats and the implications for human gene therapy. *Blood* **2001**, *97*, (8), 2221-2229.
28. Toncheva, V.; Wolfert, M. A.; Dash, P. R.; Oupicky, D.; Ulbrich, K.; Seymour, L. W.; Schacht, E. H. Novel vectors for gene delivery formed by self-assembly of DNA with poly (L-lysine) grafted with hydrophilic polymers. *Biochimica et Biophysica Acta (BBA)-General Subjects* **1998**, *1380*, (3), 354-368.
29. Matsuzuka, T.; Rachakatla, R. S.; Doi, C.; Maurya, D. K.; Ohta, N.; Kawabata, A.; Pyle, M. M.; Pickel, L.; Reischman, J.; Marini, F.; Troyer, D.; Tamura, M. Human umbilical cord matrix-derived stem cells expressing interferon-beta gene significantly attenuate bronchioloalveolar carcinoma xenografts in SCID mice. *Lung Cancer* **2010**, *70*, (1), 28-36.
30. Lindsay, M. A. Peptide-mediated cell delivery: application in protein target validation. *Current opinion in pharmacology* **2002**, *2*, (5), 587-594.
31. Snyder, E. L.; Dowdy, S. F. Cell penetrating peptides in drug delivery. *Pharmaceutical research* **2004**, *21*, (3), 389-393.

32. Pickel, L.; Matsuzuka, T.; Doi, C.; Ayuzawa, R.; Maurya, D. K.; Xie, S.-X.; Berkland, C.; Tamura, M. Over-expression of angiotensin II type 2 receptor gene induces cell death in lung adenocarcinoma cells. *Cancer biology & therapy* **2010**, *9*, (4), 277-285.
33. Baoum, A. A.; Berkland, C. Calcium condensation of DNA complexed with cell-penetrating peptides offers efficient, noncytotoxic gene delivery. *Journal of pharmaceutical sciences* **2011**, *100*, (5), 1637-1642.
34. Nam, H. Y.; Kim, J.; Kim, S.; Yockman, J. W.; Kim, S. W.; Bull, D. A. Cell penetrating peptide conjugated bioreducible polymer for siRNA delivery. *Biomaterials* **2011**, *32*, (22), 5213-5222.
35. Lee, W.-S.; Kim, Y.-K.; Zhang, Q.; Park, T.-E.; Kang, S.-K.; Kim, D.-W.; Cho, C.-S.; Choi, Y.-J. Polyxylytol-based gene carrier improves the efficiency of gene transfer through enhanced endosomal osmolysis. *Nanomedicine: Nanotechnology, Biology and Medicine* **2014**, *10*, (3), 525-534.
36. Schweizer, F. Cationic amphiphilic peptides with cancer-selective toxicity. *European journal of pharmacology* **2009**, *625*, (1), 190-194.
37. Stoll, M.; Steckelings, U. M.; Paul, M.; Bottari, S. P.; Metzger, R.; Unger, T. The angiotensin AT2-receptor mediates inhibition of cell proliferation in coronary endothelial cells. *Journal of Clinical Investigation* **1995**, *95*, (2), 651.
38. Yamada, T.; Horiuchi, M.; Dzau, V. J. Angiotensin II type 2 receptor mediates programmed cell death. *Proceedings of the National Academy of Sciences* **1996**, *93*, (1), 156-160.
39. Miura, S. i.; Karnik, S. S. Ligand-independent signals from angiotensin II type 2 receptor induce apoptosis. *The EMBO journal* **2000**, *19*, (15), 4026-4035.

40. Gajewski, T. F.; Schreiber, H.; Fu, Y.-X. Innate and adaptive immune cells in the tumor microenvironment. *Nature immunology* **2013**, *14*, (10), 1014-1022.
41. McCarroll, J.; Dwarte, T.; Baigude, H.; Dang, J.; Yang, L.; Erlich, R.; Kimpton, K.; Teo, J.; Sagnella, S.; Akerfeldt, M. Therapeutic targeting of polo-like kinase 1 using RNA-interfering nanoparticles (iNOPs) for the treatment of non-small cell lung cancer. *Oncotarget* **2014**.

Chapter 4

Dynamic Measurements of Membrane Insertion Potential of Synthetic Cell Penetrating Peptides

Published as:

Alhakamy, N. A.; Kaviratna, A.; Berkland, C. J.; Dhar, P. Dynamic Measurements of Membrane Insertion Potential of Synthetic Cell Penetrating Peptides. *Langmuir* 2013, 29, (49), 15336-15349. (2013)

4.1. Introduction

Recent research has seen an accelerated development of vectors that aid in the delivery and/or cellular uptake of therapeutic macromolecules (e.g. small peptides, proteins, and nucleic acids)¹⁻⁴. Cell penetrating peptides (CPPs) are one of the most efficient and promising nonviral vectors that allow transport of large, hydrophilic biomacromolecules through the seemingly impenetrable plasma membrane without cellular rupture⁵⁻⁸. CPPs normally constitute between 5-30 amino acid sequences, are cationic, can display low toxicity, and are uniquely capable of transporting even negatively charged DNA or siRNA through the cell membrane and nuclear membrane. They can generally be divided into three categories, depending on their origin: protein-derived CPPs such as HIV-TAT and penetratin; chimeric peptides like transportan and MPG; and synthetic peptides such as polylysine, polyarginine or amphipathic versions of these peptides^{8,9}. While it is now well accepted that the mechanism of penetration is not receptor-mediated and is energy-independent^{4, 10, 11}, the exact mechanisms of cellular uptake of these CPPs remains a significant unanswered piece of the puzzle^{8,12}. The absence of signs of internalization by known uptake mechanisms has led to the proposal that direct interactions with the phospholipid of plasma membrane is an important first step during the early stages of the internalization process¹³.

Since most CPPs generally have a high content of cationic amino acids such as lysine and arginine, experimental observations have predominantly stressed the role of electrostatic interaction of cationic CPPs with negatively charged phospholipid headgroups or negatively charged cell membrane proteoglycans as the primary triggers for internalization^{4, 14, 15}. A few studies have also suggested that hydrophobic interactions or membrane curvature may influence the early stages of internalization¹⁶. The nature of the CPPs (e.g. molecular weight, chemical structure of the residues, charge, and hydrophilicity) influence the internalization mechanisms⁸.

¹⁴. For example, strong experimental evidence suggests that arginine residues play an important role in membrane penetration. Consequently, studies to determine the factors that improve cellular penetration of natural and synthetic arginine-rich CPPs are an important research effort ¹⁷.

The TAT peptide (derived from the transcriptional activator of the HIV-1 virus) is one of the most extensively studied arginine-rich CPPs, and has been shown to interact strongly with model membranes^{18, 19}. As a result, synthetic arginine-rich polypeptides offer great potential for application in efficient drug delivery, particularly by altering the patterning of the amino acid sequence. For example, polyarginine peptides (e.g. R9) with high potency ^{6, 20} have been advanced by the insertion of hydrophobic residues ^{1, 21, 22}. Rydberg et al. demonstrated that the penetration efficiency increases with increased tryptophan content (a hydrophobic amino acid); additionally, the CPP activity is more efficient if the tryptophan residues are positioned as a block in the center of the CPP sequences than if they are placed as a block at the N-terminus ¹. Higher polyarginine molecular weight can promote more efficient penetration ^{23, 24}, but optimal lengths of polyarginine peptides with 7 to 9 residues ^{25, 26} have shown high penetration activity as well ^{1, 23, 27}.

Identification of the mode of penetration of CPPs is essential for the design of future CPPs and forms the main motivation of this study. Phospholipid monolayers are extensively used as a model for one leaflet of the cell membrane ²⁸⁻³¹, the charge density and packing of which can be simply adjusted by altering the phospholipid composition and/or surface pressure ²⁸. Here, the mechanisms of insertion of eight different synthetic CPPs were compared using three different phospholipid monolayers. 1-palmitoyl-2-oleoyl-sn-glycero-3-phosphatidylglycerol (POPG) (unsaturated phospholipids), 1-palmitoyl-2-oleoyl-sn-glycero-3-phosphocholine (POPC) (unsaturated phospholipids), and 1, 2-dihexadecanoyl-sn-glycero-3-phosphocholine (DPPC) monolayers (saturated phospholipids) (**Table 1**) at the air-water interface were chosen as the

phospholipids of interest. POPG was used as a model anionic monolayer, POPC and DPPC were used as model zwitterionic monolayers, and a 1:1 mixture of DPPC:POPG was used to study the effect of charge density on CPP insertion. By keeping the phospholipid monolayer area constant, changes in S.P. are recorded upon addition of CPPs to the subphase³²⁻³⁵. Even if eukaryotic plasma membranes are mostly composed of zwitterionic phospholipids in their external layer, a very small proportion of anionic phospholipids is also present. It must also be noted that the external leaflet of the plasma membrane contains a high amount of negative charges due to the presence of glycosaminoglycans such as heparan sulfate at the cell surface. It is therefore hypothesized that negatively charged lipids, although small in number, and glycosaminoglycans play a significant role in the mechanism of internalization of the positively charged CPPs, by facilitating electrostatic interactions with the cell membrane^{6, 36-38}. Therefore, in accordance with previous studies in this area, POPG was chosen as a representative negatively charged phospholipid for our studies.

Alterations in the membrane packing as well as the peptides' penetration activity at the air/phospholipid monolayer interface was studied for five hydrophilic CPPs (dTAT, R9, L9, H9, and RH9) and three amphiphilic CPPs (RA9, RL9, and RW9) (**Table 2**). Most of these CPPs share a common high density of arginine residues (6 arginine residues) except for K9 and H9. Our choice of peptides is influenced by previous research in this area. R8 and R9 are the most extensively studied arginine-rich peptides, and are inspired by the highly basic minimal transduction domain of the HIV-1 TAT protein, typically consisting of 9 amino acids (RKKRRQRRR)³⁹. Based on prior reports^{1, 37}, four of the arginine rich CPPs (RH9, RA9, RL9, and RW9) have replaced the arginine residues at positions 3, 4 and 7 with histidine, alanine, leucine, or tryptophan in order to study the effect of amino acid patterning on the penetration activity

Table 1. Name, synonyms, classification, and structure of the POPG, POPC and DPPC membrane models.

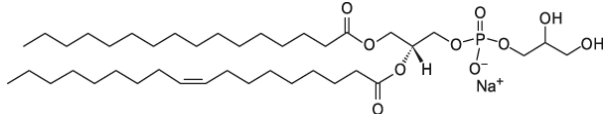
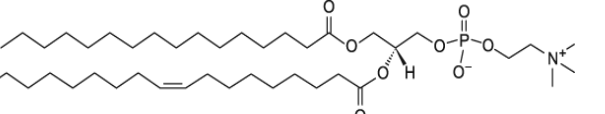
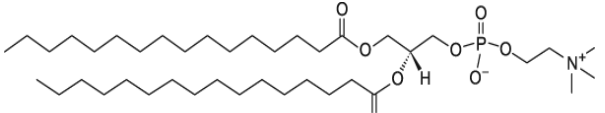
Name	Synonyms	Classification	Structure
POPG	1-hexadecanoyl-2-(9Z-octadecenoyl)-sn-glycero-3-phospho-(1'-rac-glycerol)	Anionic Phospholipid (Unsaturated)	
POPC	1-hexadecanoyl-2-(9Z-octadecenoyl)-sn-glycero-3-phosphocholine	Zwitterionic Phospholipid (Unsaturated)	
DPPC	1,2-dihexadecanoyl-sn-glycero-3-phosphocholine	Zwitterionic Phospholipid (Saturated)	

Table 2. Identification of the eight CPPs and their properties (peptide sequence, number of residues, classification, molecular weight, and sequence composition).

Name	Interpreted Sequence	Number of Residues	Classification	Molecular Weight (g/mol)	Sequence Composition (in percentage) *		
					Hydrophobic	Basic	Neutral
dTAT	R K K R R Q R R R H R R K K R	15	Hydrophilic	2200.75	0	93.33	6.67
H9	H H H H H H H H H	9	Hydrophilic	1251.38	0	100	0
K9	K K K K K K K K K	9	Hydrophilic	1170.65	0	100	0
R9	R R R R R R R R R	9	Hydrophilic	1422.74	0	100	0
RH9	R R H H R R H R R	9	Hydrophilic	1365.62	0	100	0
RA9	R R A A R R A R R	9	Amphiphilic	1167.41	33.33	66.67	0
RL9	R R L L R R L R R	9	Amphiphilic	1293.68	33.33	66.67	0
RW9	R R W W R R W R R	9	Amphiphilic	1512.83	33.33	66.67	0

* Hydrophobic/ Neutral/ Basic amino acid % = $(N_x/N)*100$, N_x : Number of hydrophobic/ neutral/ basic amino acid residues present in the input sequence. N : Input sequence length (net charge at neutral pH).

4.2. Materials and Methods

4.2.1. Materials

dTAT (RKKRRQRRRHRRKKR; $M_w = 2201.7$ Da) peptide, H9 (HHHHHHHHH; $M_w = 1251.38$ Da) peptide, K9 (KKKKKKKKK; $M_w = 1170.65$ Da) peptide, R9 (RRRRRRRRR; $M_w = 1422.74$ Da) peptide, RH9 (RRHRRRHRR; $M_w = 1365.62$ Da) peptide, RA9 (RRA ARRARR; $M_w = 1167.41$ Da) peptide, RL9 (RLLRRLRR; $M_w = 1293.68$ Da) peptide, and RW9 (RRWWRRWRR; $M_w = 1512.83$ Da) peptide were purchased from Biomatik Corporation (Cambridge, Ontario, Canada) (Purity > 95%). 1-palmitoyl-2-oleoyl-sn-glycero-3-phospho-(1'-rac-glycerol) (sodium salt) (POPG), 1-hexadecanoyl-2-(9Z-octadecenoyl)-sn-glycero-3-phosphocholine (sodium salt) (POPC), and 1,2-dipalmitoyl-sn-glycero-3-phosphocholine (DPPC) were purchased from Avanti Polar Lipids, Alabaster, AL, as organic mixtures in chloroform at a final concentration of 5 mg/mL. Texas Red ® 1,2-dihexadecanoyl-sn-glycero-3-phosphoethanolamine, triethylammonium salt, (TXR-DHPE) lipid dye was purchased in the dried form from Life Technologies (Invitrogen Corp., Carlsbad, CA, USA). All organic solvents used for this work was purchased from Fisher Scientific. Dulbecco's phosphate-buffered saline (PBS) (pH 7.4) were purchased from Fisher Scientific Inc. in powder form and made into solution using a Millipore Gradient System (Billerica, MA). Petri dishes (Falcon 1008, Becton-Dickinson Labware, Franklin Lakes, NJ) were purchased from Fisher Scientific. All samples and lipid mixtures were stored at -20 °C when not in use.

4.2.2. Methods

4.2.2.1. Langmuir Trough Experiments

The insertion potential of the different synthetic CPPs was measured using model phospholipid monolayers containing different amounts of a negatively charged phospholipid (POPG, POPC, DPPC, and POPG/DPPC (1:1)) at the air-PBS buffer interface. Surface pressure changes were recorded by a Wilhelmy plate sensor, which is part of the KSV-NIMA Langmuir trough purchased from Biolin Scientific, while petri dishes (volume 4 ml, 35 x 10) were used as “mini-troughs” for the experiments that did not involve fluorescence imaging. Penetration of the CPPs into preformed monolayers was recorded in the presence of the phospholipid monolayers. A wet calibrated filter paper flag was dipped into this buffer solution and used as a probe to monitor changes in the surface pressure due to adsorption of surface active material. The phospholipid monolayers were spread from chloroformic solutions, on PBS subphase, pH 7.4, using a Hamilton microsyringe (Hamilton Co., Reno, NV). The spreading phospholipid solvents were allowed to evaporate for 20 minutes prior to compression and adding the CPPs. The CPPs aqueous solutions were injected underneath the surface of phospholipid monolayers, and the changes in surface pressure with respect to time were measured immediately. The final concentration of the CPPs in the subphase was maintained at 10 μM (using dTAT, RW9, and RL9, this concentration was found to be beyond a so-called “saturation concentration”). The peptide-to-lipid (P/L) molar ratio at an initial surface pressure of 20 and 30 mN/m is ≈ 0.5 (at peptide concentration 1 μM)⁵. Precaution was taken to ensure that the injection did not disrupt the phospholipid monolayer. Adsorption to a bare air-buffer interface was recorded for all the CPPs studied here to ensure that the changes in the surface pressure of the monolayers were due to interaction of the CPPs. Each experiment was run for 30 minutes at 22 ± 2 °C.

4.2.2.2. Fluorescence Microscopy

Fluorescence microscopy was used concurrently with penetration experiments to monitor the morphology of the phospholipid monolayers on insertion of CPPs. These measurements were performed using a Teflon trough (volume 40 ml, area 174 X 50 mm) adapted for microscopy (Biolin Scientific). The Langmuir trough was mounted on a Leica DM fluorescence microscope with a custom designed stage equipped with a 10x or 40x long working distance objective designed for fluorescent light. A dichoric mirror/barrier filter assembly directed the excitation light onto the monolayer films at a normal angle of incidence and filtered the emitted light. An 89 North PhotoFluor II 200 W Metal Halide lamp was used for excitation of the probe. Alterations in the surface morphology of the phospholipid monolayers due to the CPPs were visualized with a fast camera (Andor Luca S). Short image sequences (5 frames) were recorded for a period of 30 minutes and stored for further analysis using the Andor capture software. The image processing and analysis were performed offline by using the software, ImageJ 1.47 (NIH) for Windows.

It must be noted that unsaturated phospholipid films such as POPG and POPC do not display any lipid domains, when viewed using the fluorescence microscopy technique. Therefore, a 1:1 mixture of DPPC:POPG was used for all imaging experiments. To initiate each experiment, the trough was cleaned with methanol, ethanol, isopropanol and chloroform and thoroughly rinsed with Mili-Q water prior to each experiment. A mixed DPPC/POPG monolayer with 1% TXR-DHPE dye was formed by spreading an organic mixture of this lipid composition dropwise onto 38 mL of a PBS buffer subphase (at pH=7.4), using a Hamilton airtight glass syringe. The solvent was allowed to evaporate completely, by waiting 30 minutes before starting a measurement. Changes in surface pressures with time were recorded by a Wilhelmy plate sensor. The concentration of the CPPs used was such that the final concentration in the subphase is 10 μ M.

Images from at least two different monolayers for each sample were taken, and the lens frequently translocated to different areas of the trough to ensure uniformity and reproducibility of the data.

4.2.2.3. Statistical Analysis

Data were analyzed by using GraphPad software. Statistical evaluation between the means of the data was performed using an unpaired *t* test. One-way ANOVA, Tukey post-test was used to analyze the differences when more than two data sets were compared. Each monolayer penetration experiment was repeated at least three times ($n = 3$).

4.3. Results and Discussion

A Langmuir monolayer approach coupled with fluorescence microscopy was used to determine the differences in ability of the synthetic CPPs to penetrate into cell membranes. Phospholipid monolayers with varying composition and headgroup charges representing one leaflet of a cell membrane were used as model membranes. Penetration to a phospholipid membrane is typically recorded by one of two methods, a constant area method or constant surface pressure method. In the constant area method used here, the surface pressure of the phospholipid monolayer is fixed at a particular surface pressure (here 20 mN/m and 30 mN/m). Membrane insertion of injected peptide is accompanied by an increase in the surface pressure, since the area of the trough surface is kept constant. Using a fluorescence microscope, we also directly visualize the changes in packing of lipid domains due to peptide insertion. Insertion of the peptides is expected to alter the monolayer packing. Since contrast in the images is due to the selective segregation of the lipid dye into more fluid regions, disruptions in monolayers manifest themselves as an increase in bright regions when compared with a well-packed film.

4.3.1. Penetration of CPPs into POPG Phospholipid Monolayers

In order to establish a correlation between the chemical structure of the CPPs and their penetration activity, we recorded their affinity to insert into phospholipid monolayers with different compositions of an anionic phospholipid. We used POPG as the phospholipid of choice, since the penetration of TAT to this phospholipid monolayer has previously been reported. It was reported that TAT demonstrated an inability to penetrate the monolayer at bilayer equivalent surface pressures⁵. Therefore, as a first step, increasing amounts of CPPs (dTAT, R9, and RW9) were injected into PBS subphase and alterations in the surface pressure recorded.

Figure 1, shows changes in surface pressure as a function of peptide concentration (1, 5, 10 and 20 μM) for dTAT (**Figure 1A**), R9 (**Figure 1B**), and RW9 (**Figure 1C**), keeping the initial pressure of POPG to be 20 mN/m. The saturation surface pressure attained in each case as a function of concentration of the CPPs is summarized in **Figure 1D**. Our results illustrate that the surface pressure increased in each case, reaching a saturation plateau after about 10 to 30 minutes after injection for all penetration experiments which indicates quick migration of the CPPs to the phospholipid monolayers. However, the time taken to reach a saturation value also depended on the bulk concentration of protein. Further, **Figure 1D** indicates that a statistically significant difference was observed in the penetration ability of the three peptides. RW9 (maximum change in surface pressure of 11.26 mN/m,) interacted more strongly with the monolayer, when compared with dTAT (the gold standard) and R9 (an arginine rich sequence expected to have high potency in cell penetration). We believe that this increased penetration in case of RW9 may be due to the hydrophobicity or the aromatic ring of tryptophan amino acids, which also increased the amphiphilicity of the peptide. Further, our data show a saturation in the total change in surface pressure for all three cases, beyond a concentration of 10 μM , which appears to be a “critical

concentration.” Therefore, this concentration was chosen for all other studies described in this paper⁵.

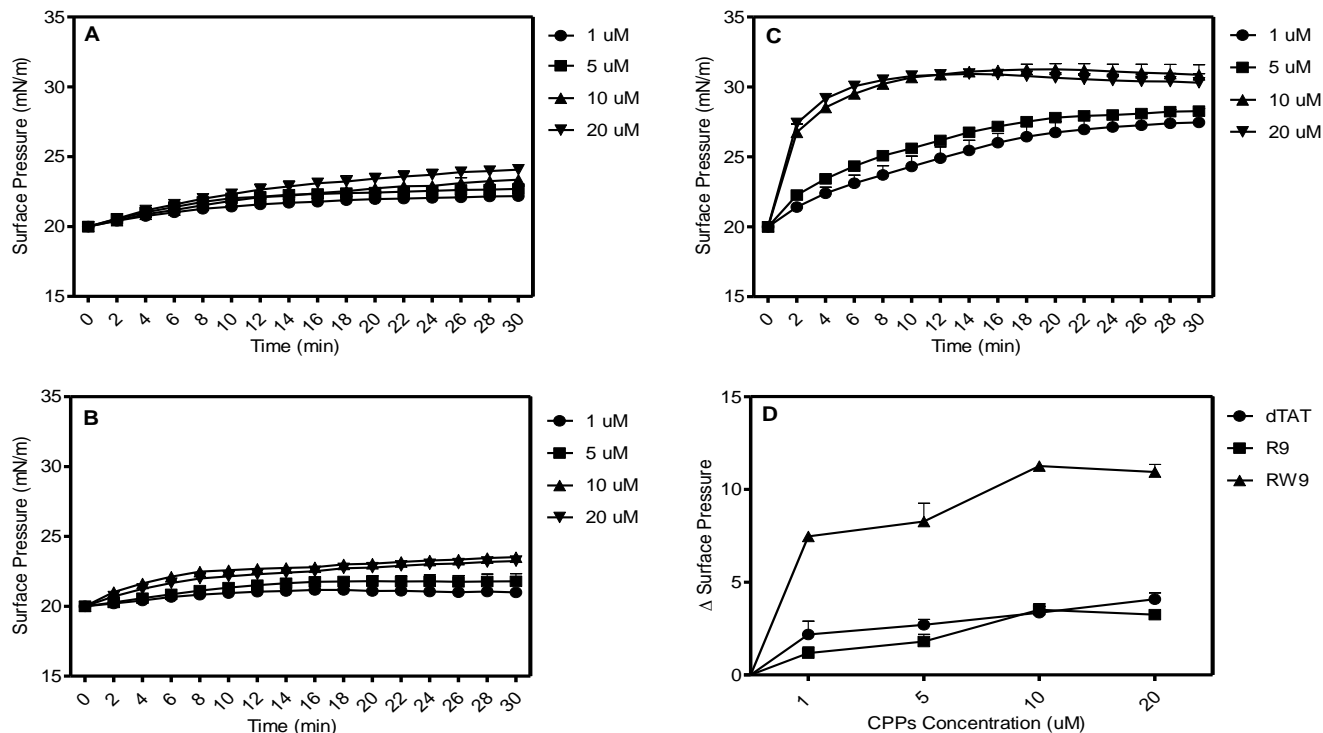


Figure 1. Changes in surface pressure recorded after adsorption of 1, 5, 10, and 20 μM of (A) dTAT, (B) R9, and (C) RW9 to a POPG phospholipid monolayer spread at an initial surface pressure of 20 mN/m. (D) The maximum change in surface pressure (plateau values) recorded at concentrations of 1, 5, 10 and 20 μM of the three CPPs. dTAT, R9, and RW9 were found to rapidly adsorb to the phospholipid monolayer. The results are presented as mean \pm SD ($n = 3$).

In order to better understand the impact of phospholipid packing on peptide insertion, the kinetics of surface pressure changes as a function of time, following dTAT injection into the subphase, were studied at different initial surface pressures (0, 15, 20, 30, and 40 mN/m) as shown in **Figure 2A**. The total change in surface pressure in the presence of dTAT resulted in increased maximum surface pressure values (**Figure 2B**) at the initial surface pressures (15, 20, and 30 mN/m) due to the fact that packing of the phospholipids is not so dense (low phospholipid densities) to facilitate dTAT peptides to attach and penetrate. On the other hand, penetration

decreased when the phospholipid packing density increased (the initial surface pressure 40 mN/m). At a high initial surface pressure (40 mN/m), there is a limited incorporation of the CPP into the phospholipid monolayer, and the process is much slower. From the figures, we conclude that the maximum surface pressure value is at the initial surface pressure 20 mN/m. Therefore, in addition to the bilayer equivalent pressure of 30 mN/m, we also report the insertion of our peptides at an initial surface pressure of 20 mN/m.

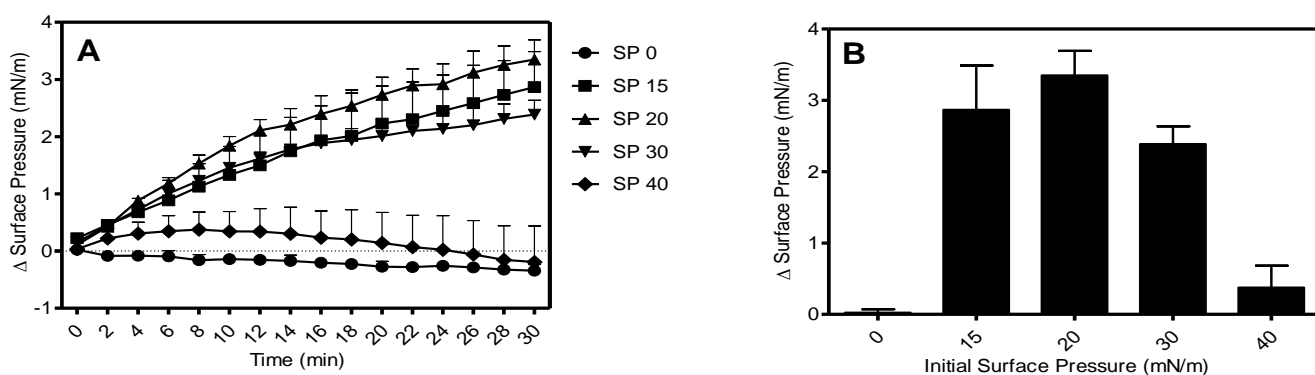


Figure 2. (A) Time course for surface pressure changes following adsorption of dTAT peptides at a bulk concentration of 10 μ M to a POPG monolayer spread at initial surface pressures of 0, 15, 20, 30 and 40 mN/m. (B) The maximum surface pressure (plateau values) reached due to peptide adsorption to the phospholipid monolayer, showing that the penetration of the CPPs is the maximum for phospholipid films held at a surface pressure of 20 mN/m. Results are presented as mean \pm SD (n = 3).

Figure 3 illustrates the changes in the surface pressure of the POPG monolayers as a function of time, following interactions with eight CPPs (10 μ M) at initial surface pressures of 20 mN/m (**Figure 3A**) and 30 mN/m (**Figure 3B**). It is clear from the figures that the kinetics of insertion of RW9 and RL9 are dramatically faster than the other CPPs. **Figures 3C** and **3D** present the maximum change in surface pressure for each of the eight peptides, when injected below a POPG monolayer held at an initial surface pressure of 20 mN/m (**Figure 3C**) or 30 mN/m (**Figure 3D**). From these figures, it is clear that for both surface pressures, the change in surface pressure

with time is significantly higher for RW9 and RL9 compared to other CPPs ($p > 0.0001$). It must also be noted that the hydrophilic CPPs (dTAT, H9, K9, R9, and RH9) and RA9 do exhibit moderate surface activities (as indicated by an increase in the total surface pressure).

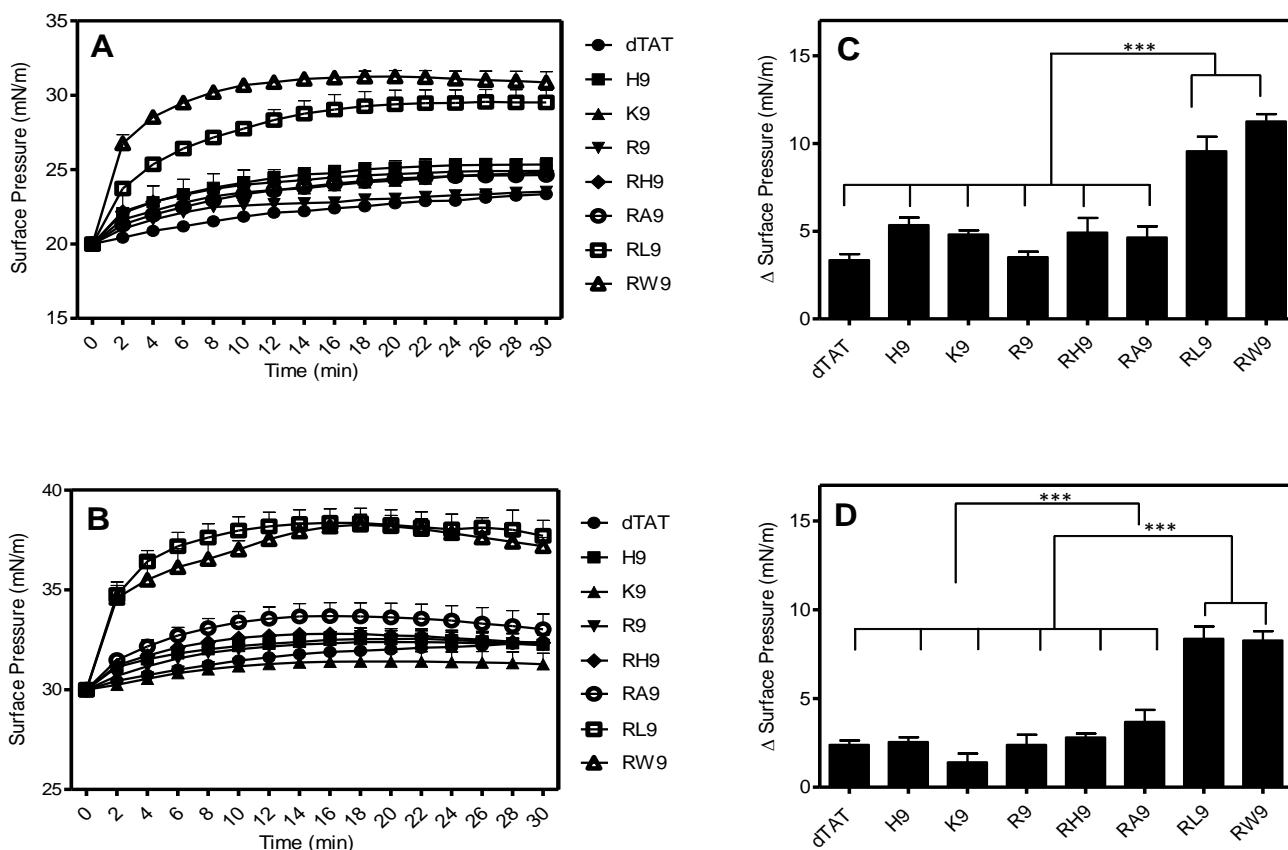


Figure 3. Changes in surface pressure as a function of time following injection of the eight CPPs below POPG monolayers held at an initial surface pressure of (A) 20 mN/m and (B) 30 mN/m. The corresponding maximum surface pressures (plateau values) recorded for the eight CPPs (peptide concentration = 10 μ M) for initial phospholipid pressures of (C) 20 mN/m and (D) 30 mN/m. The p of different peptides were compared with each CPP. Results are presented as mean \pm SD ($n = 3$), (***) = $p < 0.0001$, one-way ANOVA, Tukey post-test).

Phospholipid monolayers are used as model systems to study insertion of biomolecules and/or other particles into biological membranes. Such studies have been exhaustively used to study interaction of antimicrobial peptides with membranes^{30, 40}. Since CPPs share some commonalities with antimicrobial peptides, in this study, we have used these model membranes to

gain insight into the biophysical mechanisms of interaction in case of synthetic CPPs. In general, it is now accepted that particles that interact only with the head groups of phospholipid monolayers typically induce slight changes in surface pressure. On the other hand, insertion into the hydrophobic "tail" region (the fatty acyl core) of the phospholipid monolayer can cause a significant increase in surface pressure ⁴⁰. Although numerous studies were interested in the "arginine magic," i.e. the ability of arginine rich peptide sequences to penetrate the cell membrane, only a limited number of studies dealt with model systems (e.g. dTAT and R9) to explain the binding mechanism of polyarginine peptides to phospholipid membranes ¹⁷. It has been shown that physical characteristics (e.g. the hydrophobicity/hydrophilicity and the surface charge) of CPPs can influence their binding with phospholipid monolayers ³². However, to the best of our knowledge, the influence of introducing other amino acids into an arginine sequence has not been extensively studied in model phospholipid systems, such as those described here ¹. Our results suggest that the introduction of tryptophan and leucine residues into polyarginine 9 improve the penetration activity significantly.

Additionally, numerous studies have mentioned the importance of peptide structural conformational changes upon phospholipid interactions to facilitate membrane translocation⁴¹⁻⁴³. It was found that the different penetration properties of the cationic CPPs and amphiphilic CPPs may arise from the insertion mechanism into phospholipid monolayers ³⁷. Walrant et al. indicated that while RW9 and RL9 have an affinity for anionic phospholipids, the affinity is just a little higher for RW9 than RL9. The interactions are mostly ruled by hydrophobic assistances in both CPPs ^{6,37}. Additionally, they found that a flip of the CPP occurs where the arginine residues aid as a hinge, letting the hydrophobic amino acids insert deeper in the plasma membrane ³⁷. Although alanine is a hydrophobic amino acid, RA9 demonstrates only a moderate surface activity when

compared to RW9 and RL9. This behavior is possibly due to the chemical structure of the hydrophobic residues; alanine has a very small side chain when compared with the more bulky tryptophan. Before studying the incorporation of the CPPs with the phospholipid monolayers, we examined the behavior of the eight CPPs at a bare air/water interface by using the Langmuir technique described above in the absence of the phospholipids (**Figure Appendix 3**). All eight CPPs showed no or little surface activity for the 30 minutes duration, which is in agreement with the nature of the five hydrophilic CPPs (dTAT, H9, K9, and RH9) and weak amphiphilic characters of the three CPPs (RA9, RL9, and RW). These results indicate that the change in surface pressure recorded in **Figure 3** is clearly due to interactions with the anionic phospholipid films.

4.3.2. Penetration of the CPPs in DPPC and POPC Phospholipid Monolayers

In order to test the effect of electrostatic interactions versus hydrophobic interactions on the insertion potential of these synthetic peptides into model membranes, we compare the insertion potential of the eight CPPs into zwitterionic monolayers (POPC [unsaturated] and DPPC [saturated]) compared with the POPG monolayer. **Figure 4A** shows the change in surface pressure as a function of time, for the POPC film initially held at a surface pressure of 20 mN/m. As seen in the figure, low penetration activity was observed for the synthetic peptides, except for RW9 and RL9. In fact, the penetration activity of RW9 and RL9 is found to be significantly higher than the other CPPs. **Figure 4B** shows the change in surface pressure versus time for an initial surface pressure of 30 mN/m. The maximum surface pressures reached in each case is summarized in bar graphs in **Figure 4C** and **4D**. As seen, both RW9 and RL9 have significant surface activity compared to other CPPs ($p > 0.0001$) as shown by the maximum values of 5.9 and 4.3 mN/m respectively (at the initial surface pressure of 20 mN/m) and 3.7 and 1.9 mN/m respectively (at the initial surface pressure of 30 mN/m). In contrast, even though RA9 is an amphiphilic peptide, it

does not display significant insertion into the POPC films. **Figure 5** presents a summary of the comparison of the maximum surface pressure values that were recorded at a concentration of 10 μM (the initial surface pressures 20 mN/m [**Figure A**] and 30 mN/m [**Figure B**]) for the eight CPPs, for an anionic phospholipid film (POPG) and a zwitterionic phospholipid film (POPC). This graph clearly indicates that anionic phospholipid head groups play an important role for interactions with the eight CPPs. However, for two of the three arginine-rich peptides modified by hydrophobic residues, the membrane penetration potential is significantly enhanced.

Figure 6A shows the change in surface pressure as a function of time, for the DPPC (more tightly packed monolayer) film initially held at a surface pressure of 20 mN/m. As seen in the figure, no penetration activity was observed for the synthetic peptides, except for RW9 and RL9. In fact, the penetration activity of RW9 and RL9 is found to be significantly higher than the other CPPs. **Figure 6B** shows the change in surface pressure versus time for an initial surface pressure of 30 mN/m. For clarity, we only show the change in surface pressure for RW9 and RL9. The maximum surface pressures reached in each case is summarized in bar graphs in **Figure 6C** and **6D**. As seen, both RW9 and RL9 have significant surface activity compared to other CPPs ($p > 0.0001$) as showed by the maximum values of 4.0 and 1.7 mN/m respectively (at the initial surface pressure of 20 mN/m) and 4.5 and 0.6 mN/m respectively (at the initial surface pressure of 30 mN/m). The smaller penetration activity for zwitterionic DPPC monolayers (saturated phospholipids) in some CPPs when compared to anionic POPG and POPC (both unsaturated phospholipids) monolayers indicate weak interactions between the CPPs and DPPC. The reduced insertion of all but RW9 into the DPPC phospholipid monolayer may also be the result of a well-packed monolayer preventing CPPs insertion.

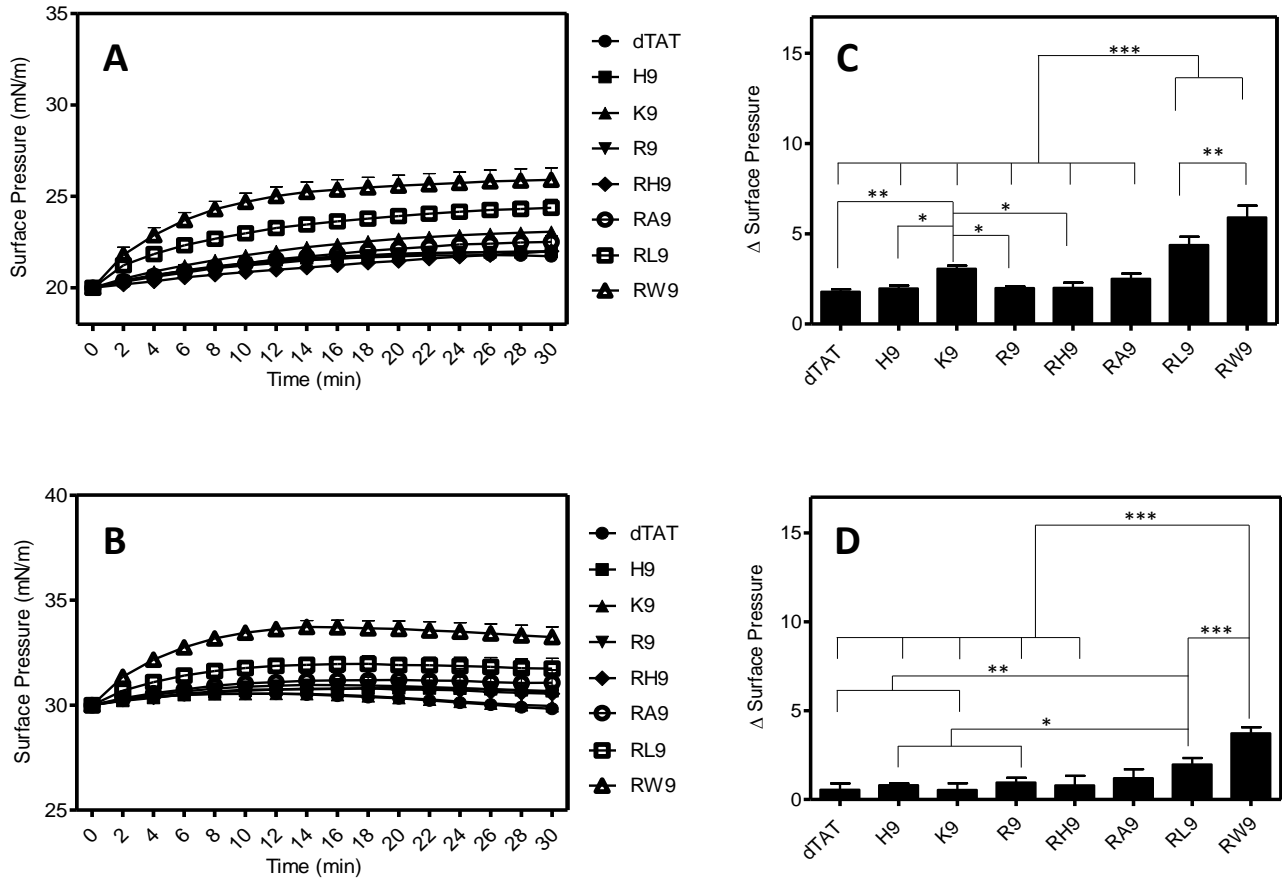


Figure 4. Changes in surface pressure as a function of time following injection of the eight CPPs below POPC monolayers held at an initial surface pressure of (A) 20 mN/m and (B) 30 mN/m. The corresponding maximum surface pressures (plateau values) recorded for the eight CPPs (peptide concentration = 10 μ M) for initial phospholipid pressures of (C) 20 mN/m and (D) 30 mN/m. The p of different peptides were compared with each CPP. Results are presented as mean \pm SD ($n = 3$), (***) = $p < 0.0001$, (**) = $p < 0.001$ and (*) = $p < 0.05$, one-way ANOVA, Tukey post-test).

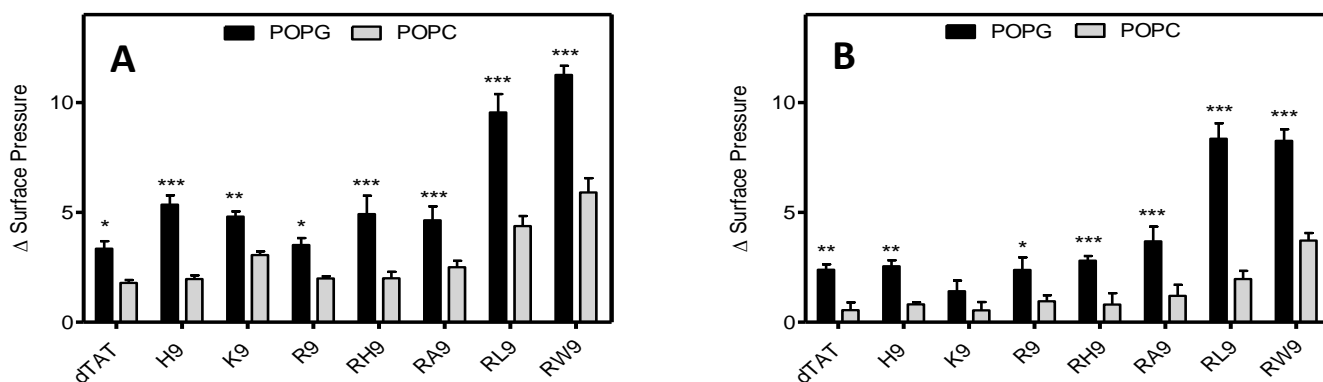


Figure 5. The maximum change in surface pressure of the phospholipid monolayers (POPG and POPC) initially held at surface pressures of 20 mN/m (A) and 30 mN/m (B) for the eight CPPs. Results are presented as mean \pm SD ($n = 3$), (***) = $p < 0.0001$, (**) = $p < 0.001$, and (*) = $p < 0.05$ unpaired t test). The p of different peptides were compared for an initial surface pressure of POPG phospholipid monolayers with POPC phospholipid monolayers for each CPPs.

Figure 6 also shows that the penetration activity of RW9 is significantly higher than RL9 or RA9 in both initial surface pressures, even though all three of these arginine-rich peptides were modified by hydrophobic moieties. It was found that the addition of one tryptophan residue to a polyarginine 7 peptide (R7) increased its penetration efficiency⁴⁴. Clearly, tryptophan residue has a key role in cell penetration, possibly due to the bulky side chains^{1, 37, 45, 46}. In summary, our results show that in addition to electrostatic effects, hydrophobic interactions as well as the chemical nature of the amino acids do influence the differences in membrane penetration potential of the CPPs.

4.3.3. Penetration of the CPPs in Mixed (POPG:DPPC) Phospholipid Monolayers

The mixing properties of a mixed monolayer of DPPC and POPG was used as a model to understand the role of different composition of the anionic phospholipid headgroup on peptide insertion in order to simultaneously image the insertion and possible alterations in monolayer packing. We have chosen this mixture to be consistent with the fluorescent microscopy experiments

(section 3.4.). The mixture of saturated PC (DPPC) phospholipids and fluid unsaturated PG (POPG) phospholipids have been used so that lipid domains can be observed.

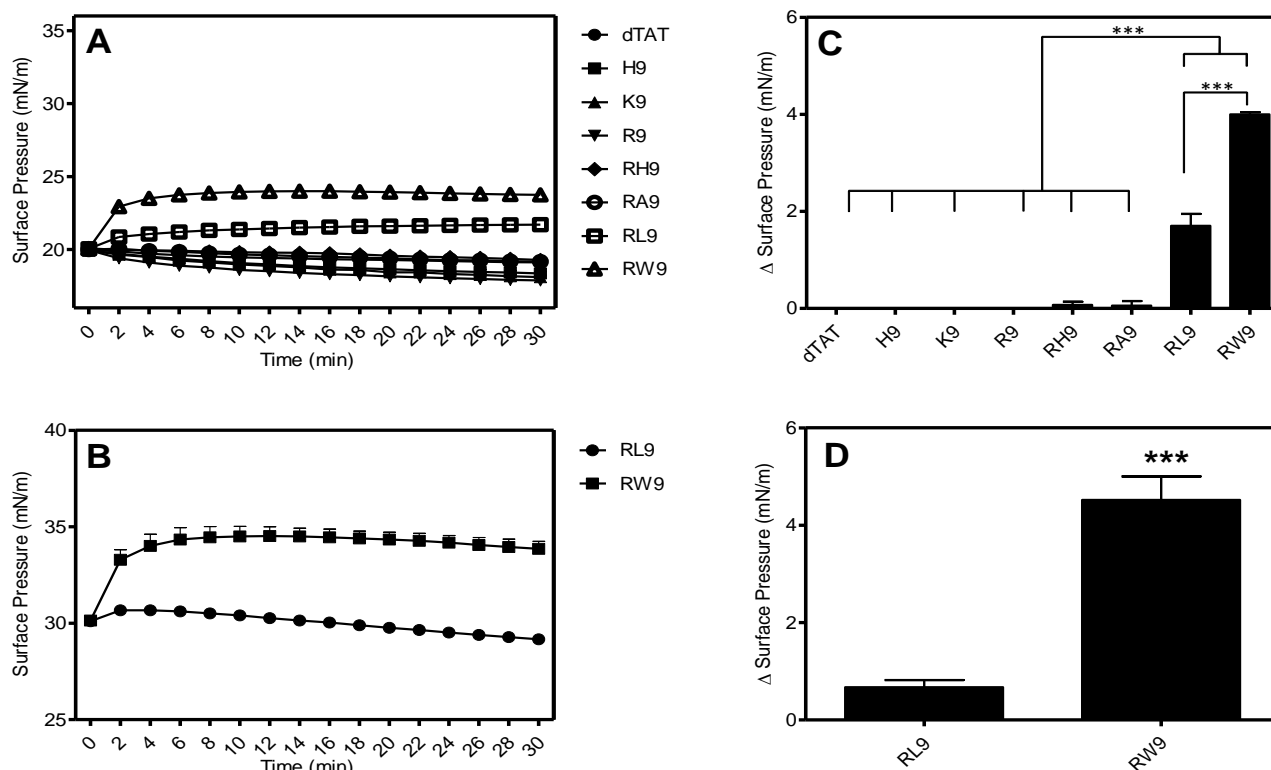


Figure 6. Surface pressure change as a function of time for a DPPC monolayer (A) at an initial surface pressure of 20 mN/m following interaction with eight CPPs (10 μ M) (B) at an initial surface pressure of 30 mN/m following injection of RL9 and RW9. The maximum change in surface pressure (plateau values) recorded for the eight CPPs at initial phospholipid surface pressure of (C) 20 mN/m for the 8 peptides and (D) 30 mN/m for RL9 and RW9. The p of different peptides were compared with each CPP. Results are presented as mean \pm SD ($n = 3$), (***) = $p < 0.0001$, one-way ANOVA, Tukey post-test).

Figure 7 shows change in surface pressure of a mixed phospholipid film as a function of time, for the eight CPPs (10 μ M) at the initial surface pressure 20 (**Figure 7A**) and 30 mN/m (**Figure 7B**). Our results indicated that reducing the surface charge density of the phospholipid monolayers by using mixed phospholipids (POPG/DPPC) caused a decrease in the surface pressure. **Figure 7C** and **7D** summarize the maximum change in surface pressure for the eight

CPPs. Our results show that the hydrophilic CPPs (dTAT, H9, K9, R9, and RH9) and RA9 have moderate surface activity when the maximum surface pressure values are between 1.5 and 3.0 mN/m (the initial surface pressure 20 mN/m) and between 1.2 and 2.6 mN/m (the initial surface pressure 30 mN/m). Conversely, RW9 and RL9 have large surface pressure increases as shown by the maximum values of 8.0 and 9.4 mN/m, respectively, (the initial surface pressure 20 mN/m) and 5.6 and 4.9 mN/m respectively (the initial surface pressure 30 mN/m). **Figure 8** presents the summary of the maximum surface pressure values that were recorded at a concentration of 10 μ M (the initial surface pressures 20 and 30 mN/m) for the eight CPPs, for all four phospholipid films (POPG, POPC, DPPC and, POPG:DPPC). This summary clearly indicates that while anionic phospholipid headgroups play the most important role for interactions with the hydrophilic CPPs (dTAT, H9, K9, R9, and RH9), the insertion of the arginine peptides is also significantly influenced by the presence of tryptophan residues.

To further our understanding of the role of the 3D peptide structure on the insertion potential of the CPPs, we used circular dichroism spectroscopy (CD) to determine the helicity of the eight CPPs in PBS solution (**Figure Appendix 4**). Our data confirmed that the free CPPs had random coil conformations, suggesting that the initial steps in peptide insertion are not influenced by the 3-D structure. However, NMR, CD and molecular dynamics simulation studies by other groups have shown that insertion into the lipid bilayers can induce different degrees of structural re-orientation depending on the amino acid sequence^{6, 47, 37, 48}. This may also explain the differences in a peptide's ability to translocate through the membrane. Therefore, we conclude that while the 3D structure in solution does not seem to influence the surface activity of the 8 CPPs, the penetration and translocation through cell membranes may be influenced by a lipid bilayer induced alteration in the protein structure. This suggests that while the surface pressure changes in

a Langmuir trough may be a good screening test to determine the penetration potential of synthetic peptides into cell membranes, the ultimate translocation potential of the peptide may be dictated by their 3-D structure upon membrane penetration.

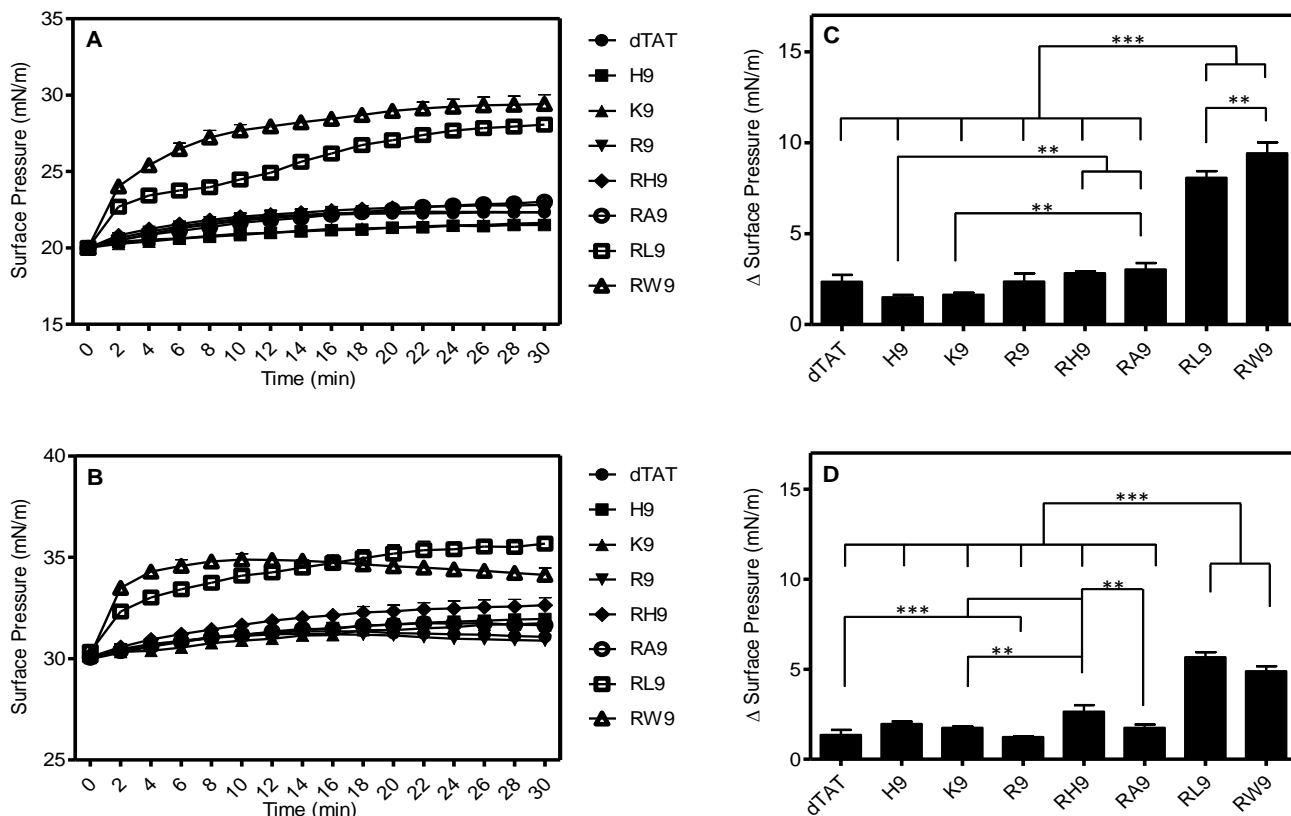


Figure 7. Changes in surface pressure as a function of time for the mixed phospholipids (POPG/DPPC at a ratio of 1:1) held at an initial surface pressure of (A) 20 mN/m and (B) 30 mN/m, following injection of the eight CPPs into the subphase. The maximum change in surface pressure (plateau values) recorded for the phospholipids held at an initial surface pressure of (C) 20 mN/m and (D) 30 mN/m. The p of different peptides were compared with each peptide. Results are presented as mean \pm SD ($n = 3$), (** = $p < 0.001$, and *** = $p < 0.0001$, one-way ANOVA, Tukey post-test).

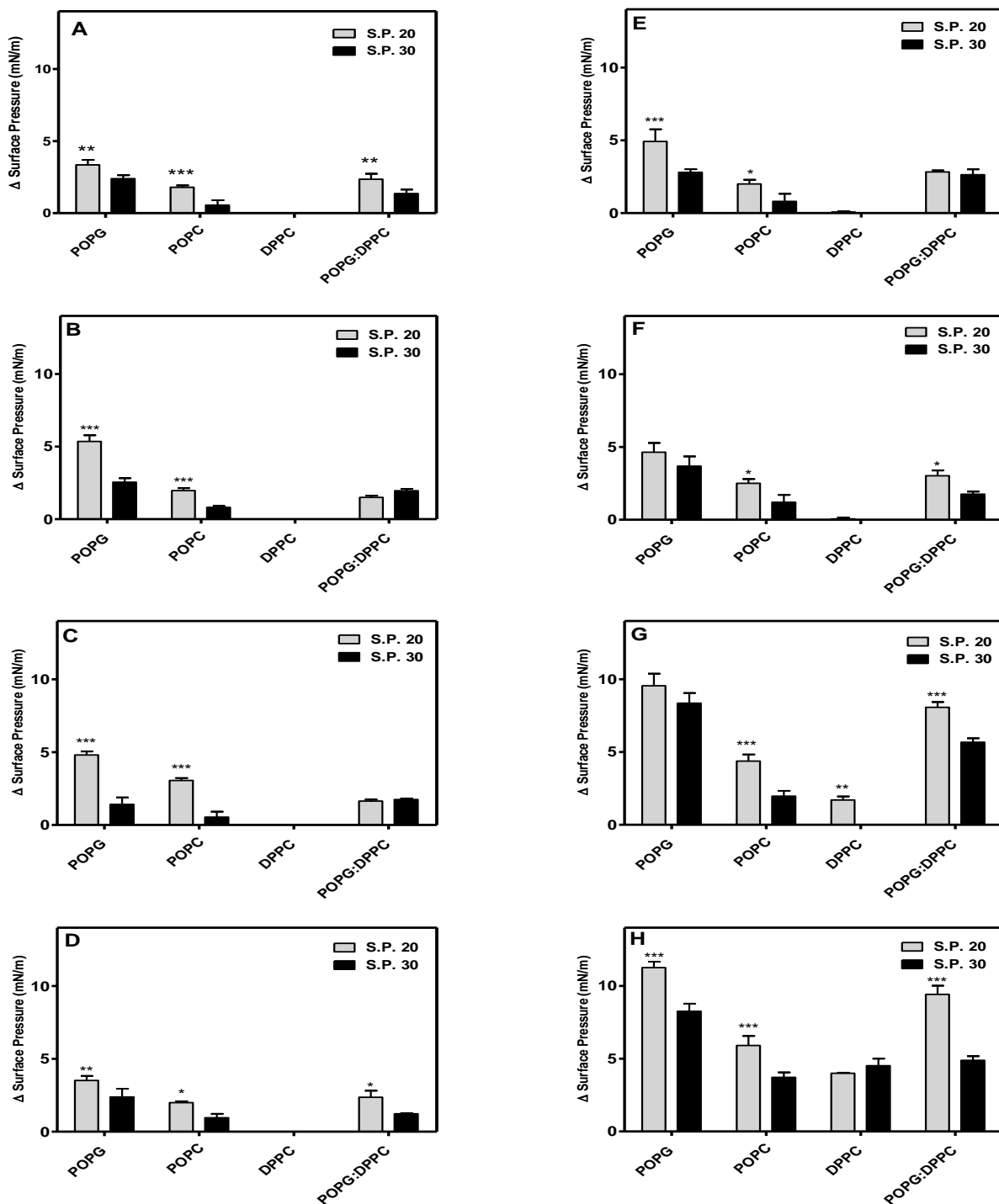


Figure 8. Summary of results showing the maximum change in surface pressure of the phospholipid monolayers (POPG, POPC, DPPC, and POPG:DPPC) initially held at surface pressures of 20 and 30 mN/m for the eight CPPs: (A) dTAT, (B) H9, (C) K9, (D) R9, (E) RH9, (F) RA9, (G) RL9, and (H) RW9. Results are presented as mean \pm SD ($n = 3$), (***) = $p < 0.0001$, (**) = $p < 0.001$, and (*) = $p < 0.05$ unpaired t test). The p of different peptides were compared for an initial surface pressure of 20 mN/m with 30 mN/m for each CPPs.

It is expected that analysis of the kinetics and thermodynamics of the 8 CPPs will provide a more complete understanding of the nature of the CPP partitioning into the phospholipid monolayers. Using Langmuir models of protein insertion into phospholipid monolayers⁴⁹⁻⁵⁵, we can calculate the kinetics of protein partitioning into different monolayer systems. Such analysis will form the topic for a future manuscript currently under preparation.

4.3.4. Fluorescence Microscopy

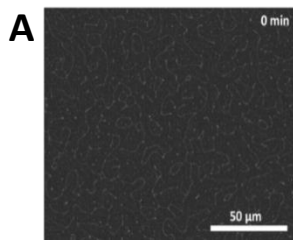
Using fluorescence imaging of the monolayer surface, it is possible to gain insight into the structure of the phospholipid monolayers. Fluorescence microscopy helps us to understand alterations in organization of phospholipid monolayers after injection of the CPPs in the subphase. Furthermore, it is an appropriate effective technique to study the structural phase separation and disruption induced by CPP interactions with phospholipid monolayers^{30, 56}. **Figure 9A** demonstrates the morphology of the POPG/DPPC (1:1) phospholipid monolayer domains (at the surface pressure 30 mN/m) before injection of the CPPs. It shows characteristic stripe patterns with dark regions (the bright regions in the dark domains looked like veins on a leaf). Contrast in these images is due to selective segregation of the lipid dye molecules into the liquid expanded regions, while the closely packed liquid condensed domains exclude the bulky dye molecules. The domains were magnified as compression proceeded, and the view field becomes almost dark⁵⁷ at the bilayer equivalent pressures studied here. The images were obtained at 1, 5, 10, 20, and 30 minutes, respectively after injection of the CPPs into the subphase.

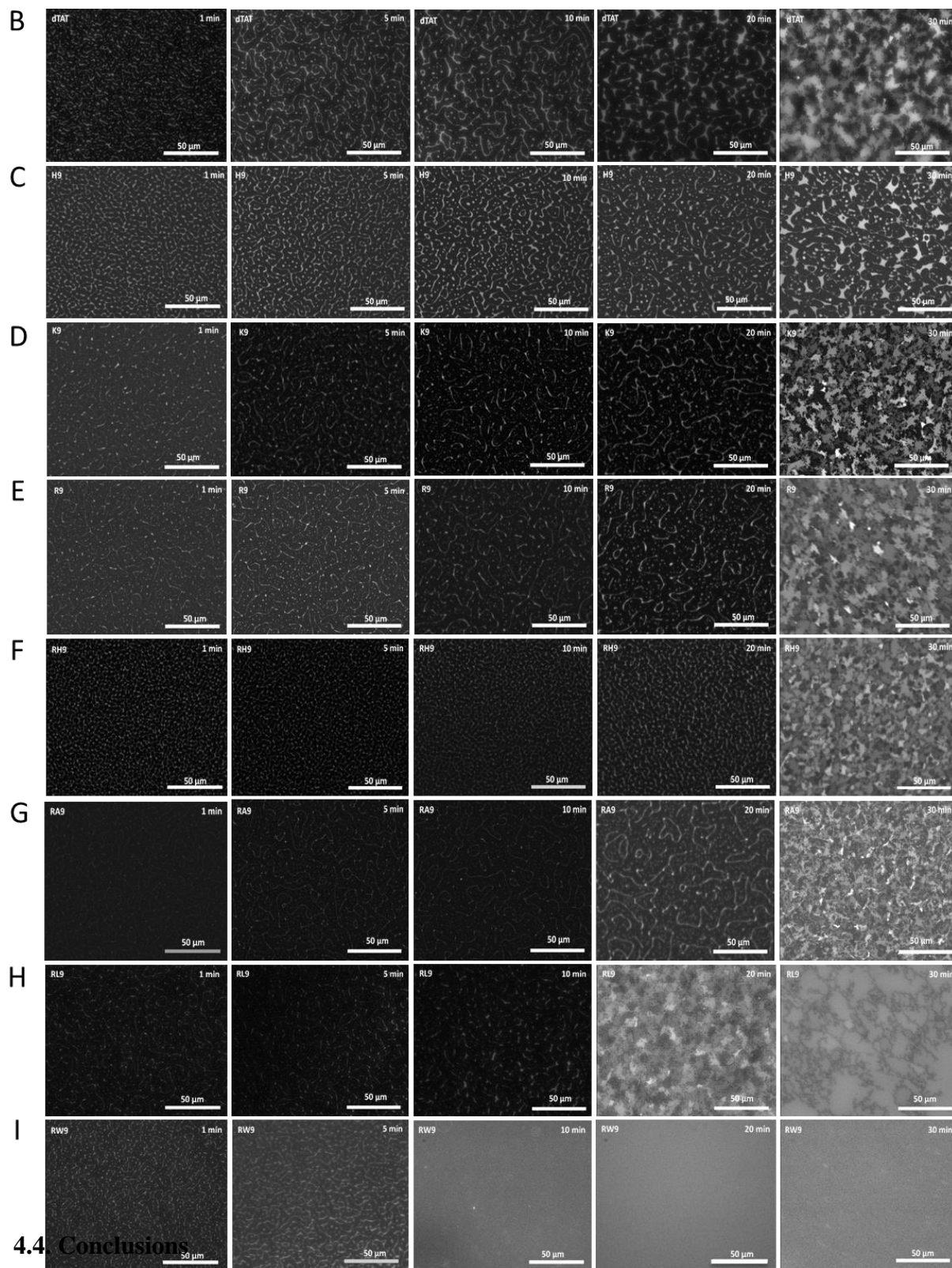
Remarkably, the domain morphology altered significantly depending on the nature of the CPP. The images display that CPPs induce different morphologies even at the first minutes after injection. In the case of dTAT, H9, K9, R9, RH9, and RA9 (**Figure 9B, C, D, E, F, and G**, respectively), the overall change in the domain morphology is limited (a very slight increase in the

gray regions) for the first 10 minutes (after the CPP was injected) except for RW9. In case of RW9 (**Figure 9I**), within 10 minutes of CPP injection, the dark domains completely disappeared (no domains could be observed) after approximately 5 minutes of the injection. Interestingly, after 20 minutes the morphologies of the domains were vividly different for all CPPs. In the case of RL9 (**Figure 9H**), blurred gray patches began to appear, while all other CPPs showed an increase in the brightness and width of the stripe pattern. At 30 minutes all of the peptides (except H9) showed either blurred gray patches, or more disrupted monolayers like RL9 and RW9. Our results also show that H9 shows the minimum perturbation of the phospholipid packing among all the CPPs studied, even after 30 minutes (darker domains are still visible). Moreover, the arginine-rich peptides all induce significantly higher changes in the phospholipid packing compared to dTAT. Peptide RW9 demonstrates the maximum disruption of monolayer packing, followed by RL9 and RA9. R9 and RH9 seem to induce very similar membrane perturbation.

In general, our results reinforce the role of not only electrostatics and hydrophobic interactions, but also the chemical nature of amino acids on the membrane penetration potential of CPPs. While all CPPs show the maximum membrane penetration in the presence of anionic headgroups, amphiphilic CPPs with tryptophan residues show a significant membrane insertion potential for all model lipid monolayers. Moreover, we present direct evidence of destabilization of phospholipid packing induced by amphiphilic arginine-rich CPPs, which is also most pronounced by the presence of tryptophan residues.

Figure 9. Fluorescent micrographs of a POPG/DPPC (1:1) monolayer at a surface pressure of 30 mN/m on PBS buffer: (A) before injection of peptides (0 minutes), after injection of (B) dTAT (10 μ M) into the sub-phase, (C) H9 (10 μ M) in the sub-phase, (D) K9 (10 μ M) in the sub-phase, (E) R9 (10 μ M) in the sub-phase, (F) RH9 (10 μ M) in the sub-phase, (G) RA9 (10 μ M) in the sub-phase, (H) RL9 (10 μ M) in the sub-phase, and (I) RW9 (10 μ M) in the sub-phase. The relative increase in the bright area from 1 to 30 minutes corresponds to the increase in the disordered fluid phase caused by peptides insertion. The scale bar in the lower right represents 50 μ m. The shape of the phospholipid monolayer domains change depending on the nature of the CPP.





4.4. Conclusions

Understanding the interactions of synthetic CPPs with phospholipid membranes is an important step when designing future synthetic CPPs capable of intracellular drug delivery. In this study, phospholipid monolayers with different composition of anionic headgroups (POPG, POPC, DPPC, or POPG/DPPC) have been used to study the penetration, and/or interaction with eight synthetic peptides including hydrophilic CPPs (dTAT, H9, K9, R9, and RH9) and the amphiphilic CPPs (RA9, RL9, and RW9). Insertion of the CPPs into the phospholipid monolayers were followed using Langmuir monolayer techniques and fluorescence microscopy. As expected, the incorporation of the cationic CPPs into the anionic phospholipids (POPG) was much higher when compared with the zwitterionic phospholipids (POPC and DPPC).

In addition to electrostatic interactions, hydrophobic interactions as well as the chemical nature of the amino acid residues influenced the membrane insertion potential. The presence of tryptophan residues induced maximum perturbation of the phospholipid packing. All CPPs interacted with anionic phospholipids, but the interactions of RW9 and RL9 with membrane monolayers was significantly different when compared with the other peptides. RW9 and RL9 strongly penetrated the model cell membranes and also induced the maximum alterations in phospholipid packing. The five hydrophilic CPPs (dTAT, R9, L9, H9, and RH9) and RA9 peptides also showed penetration into the model membranes, but did not appear to cause significant membrane disruption. The different mechanisms of the eight CPPs compel additional investigations using these CPPs for delivery of macromolecules in cellular systems. Further elucidating performance in light of these mechanistic findings will aid the design of the next generation of CPPs.

4.6. References

1. Rydberg, H. A.; Matson, M.; Åmand, H. L.; Esbjörner, E. K.; Nordén, B. Effects of tryptophan content and backbone spacing on the uptake efficiency of cell-penetrating peptides. *Biochemistry* **2012**, *51*, (27), 5531-5539.
2. Ziello, J. E.; Huang, Y.; Jovin, I. S. Cellular endocytosis and gene delivery. *Molecular Medicine* **2010**, *16*, (5-6), 222.
3. Guo, J.; Bourre, L.; Soden, D. M.; O'Sullivan, G. C.; O'Driscoll, C. Can non-viral technologies knockdown the barriers to siRNA delivery and achieve the next generation of cancer therapeutics? *Biotechnology advances* **2011**, *29*, (4), 402-417.
4. Deshayes, S.; Morris, M. C.; Divita, G.; Heitz, F. Interactions of amphipathic CPPs with model membranes. *Biochimica et Biophysica Acta (BBA)-Biomembranes* **2006**, *1758*, (3), 328-335.
5. Dennison, S. R.; Baker, R. D.; Nicholl, I. D.; Phoenix, D. A. Interactions of cell penetrating peptide Tat with model membranes: a biophysical study. *Biochemical and biophysical research communications* **2007**, *363*, (1), 178-182.
6. Walrant, A.; Correia, I.; Jiao, C.-Y.; Lequin, O.; Bent, E. H.; Goasdoué, N.; Lacombe, C.; Chassaing, G.; Sagan, S.; Alves, I. D. Different membrane behaviour and cellular uptake of three basic arginine-rich peptides. *Biochimica et Biophysica Acta (BBA)-Biomembranes* **2011**, *1808*, (1), 382-393.
7. Fonseca, S. B.; Pereira, M. P.; Kelley, S. O. Recent advances in the use of cell-penetrating peptides for medical and biological applications. *Advanced drug delivery reviews* **2009**, *61*, (11), 953-964.

8. Alhakamy, N. A.; Nigatu, A. S.; Berkland, C. J.; Ramsey, J. D. Noncovalently associated cell-penetrating peptides for gene delivery applications. *Therapeutic delivery* **2013**, *4*, (6), 741-757.
9. Lindgren, M.; Langel, Ü., Classes and prediction of cell-penetrating peptides. In *Cell-Penetrating Peptides*, Springer: 2011; pp 3-19.
10. Wender, P. A.; Mitchell, D. J.; Pattabiraman, K.; Pelkey, E. T.; Steinman, L.; Rothbard, J. B. The design, synthesis, and evaluation of molecules that enable or enhance cellular uptake: peptoid molecular transporters. *Proceedings of the National Academy of Sciences* **2000**, *97*, (24), 13003-13008.
11. Derossi, D.; Calvet, S.; Trembleau, A.; Brunissen, A.; Chassaing, G.; Prochiantz, A. Cell internalization of the third helix of the Antennapedia homeodomain is receptor-independent. *Journal of Biological Chemistry* **1996**, *271*, (30), 18188-18193.
12. Hassane, F. S.; Saleh, A.; Abes, R.; Gait, M.; Lebleu, B. Cell penetrating peptides: overview and applications to the delivery of oligonucleotides. *Cellular and molecular life sciences* **2010**, *67*, (5), 715-726.
13. Thorén, P. E.; Persson, D.; Lincoln, P.; Nordén, B. Membrane destabilizing properties of cell-penetrating peptides. *Biophysical chemistry* **2005**, *114*, (2), 169-179.
14. Silhol, M.; Tyagi, M.; Giacca, M.; Lebleu, B.; Vivès, E. Different mechanisms for cellular internalization of the HIV-1 Tat-derived cell penetrating peptide and recombinant proteins fused to Tat. *European Journal of Biochemistry* **2002**, *269*, (2), 494-501.
15. Magzoub, M.; Kilk, K.; Eriksson, L.; Langel, Ü.; Gräslund, A. Interaction and structure induction of cell-penetrating peptides in the presence of phospholipid vesicles. *Biochimica et Biophysica Acta (BBA)-Biomembranes* **2001**, *1512*, (1), 77-89.

16. Schmidt, N.; Mishra, A.; Lai, G. H.; Wong, G. C. Arginine-rich cell-penetrating peptides. *FEBS Lett* **2010**, *584*, (9), 1806-13.
17. Schwieger, C.; Blume, A. Interaction of poly (l-arginine) with negatively charged DPPG membranes: calorimetric and monolayer studies. *Biomacromolecules* **2009**, *10*, (8), 2152-2161.
18. Gonçalves, E.; Kitas, E.; Seelig, J. Binding of oligoarginine to membrane lipids and heparan sulfate: structural and thermodynamic characterization of a cell-penetrating peptide. *Biochemistry* **2005**, *44*, (7), 2692-2702.
19. Vivès, E.; Brodin, P.; Lebleu, B. A truncated HIV-1 Tat protein basic domain rapidly translocates through the plasma membrane and accumulates in the cell nucleus. *Journal of Biological Chemistry* **1997**, *272*, (25), 16010-16017.
20. Mitchell, D.; Steinman, L.; Kim, D.; Fathman, C.; Rothbard, J. Polyarginine enters cells more efficiently than other polycationic homopolymers. *The Journal of Peptide Research* **2000**, *56*, (5), 318-325.
21. Thorén, P. E.; Persson, D.; Isakson, P.; Goksör, M.; Önfelt, A.; Nordén, B. Uptake of analogs of penetratin, Tat (48–60) and oligoarginine in live cells. *Biochemical and biophysical research communications* **2003**, *307*, (1), 100-107.
22. Thorén, P. E.; Persson, D.; Esbjörner, E. K.; Goksör, M.; Lincoln, P.; Nordén, B. Membrane binding and translocation of cell-penetrating peptides. *Biochemistry* **2004**, *43*, (12), 3471-3489.
23. Rothbard, J. B.; Kreider, E.; VanDeusen, C. L.; Wright, L.; Wylie, B. L.; Wender, P. A. Arginine-rich molecular transporters for drug delivery: role of backbone spacing in cellular uptake. *Journal of medicinal chemistry* **2002**, *45*, (17), 3612-3618.

24. Takechi, Y.; Yoshii, H.; Tanaka, M.; Kawakami, T.; Aimoto, S.; Saito, H. Physicochemical mechanism for the enhanced ability of lipid membrane penetration of polyarginine. *Langmuir* **2011**, *27*, (11), 7099-7107.
25. Futaki, S.; Goto, S.; Sugiura, Y. Membrane permeability commonly shared among arginine-rich peptides. *Journal of Molecular Recognition* **2003**, *16*, (5), 260-264.
26. Futaki, S.; Nakase, I.; Tadokoro, A.; Takeuchi, T.; Jones, A. Arginine-rich peptides and their internalization mechanisms. *Biochemical Society Transactions* **2007**, *35*, (4), 784.
27. Wender, P. A.; Galliher, W. C.; Goun, E. A.; Jones, L. R.; Pillow, T. H. The design of guanidinium-rich transporters and their internalization mechanisms. *Advanced drug delivery reviews* **2008**, *60*, (4), 452-472.
28. Barzyk, W.; Campagna, S.; Więclaw, K.; Korchowiec, B.; Rogalska, E. The affinity of two antimicrobial peptides derived from bovine milk proteins for model lipid membranes. *Colloids and Surfaces A: Physicochemical and Engineering Aspects* **2009**, *343*, (1), 104-110.
29. Brockman, H. Lipid monolayers: why use half a membrane to characterize protein-membrane interactions? *Current opinion in structural biology* **1999**, *9*, (4), 438-443.
30. Volinsky, R.; Kolusheva, S.; Berman, A.; Jelinek, R. Investigations of antimicrobial peptides in planar film systems. *Biochimica et Biophysica Acta (BBA)-Biomembranes* **2006**, *1758*, (9), 1393-1407.
31. Brezesinski, G.; Möhwald, H. Langmuir monolayers to study interactions at model membrane surfaces. *Advances in colloid and interface science* **2003**, *100*, 563-584.
32. Peetla, C.; Stine, A.; Labhasetwar, V. Biophysical interactions with model lipid membranes: applications in drug discovery and drug delivery. *Molecular pharmaceutics* **2009**, *6*, (5), 1264-1276.

33. Preetha, A.; Huilgol, N.; Banerjee, R. Comparison of paclitaxel penetration in normal and cancerous cervical model monolayer membranes. *Colloids and Surfaces B: Biointerfaces* **2006**, *53*, (2), 179-186.
34. Demel, R.; Geurts van Kessel, W.; Zwaal, R.; Roelofsen, B.; Van Deenen, L. Relation between various phospholipase actions on human red cell membranes and the interfacial phospholipid pressure in monolayers. *Biochimica et Biophysica Acta (BBA)-Biomembranes* **1975**, *406*, (1), 97-107.
35. Blume, A. A comparative study of the phase transitions of phospholipid bilayers and monolayers. *Biochimica et Biophysica Acta (BBA)-Biomembranes* **1979**, *557*, (1), 32-44.
36. Joanne, P.; Galanth, C.; Goasdoué, N.; Nicolas, P.; Sagan, S.; Lavielle, S.; Chassaing, G.; El Amri, C.; Alves, I. D. Lipid reorganization induced by membrane-active peptides probed using differential scanning calorimetry. *Biochimica et Biophysica Acta (BBA)-Biomembranes* **2009**, *1788*, (9), 1772-1781.
37. Witte, K.; Olausson, B. E.; Walrant, A.; Alves, I. D.; Vogel, A. Structure and dynamics of the two amphipathic arginine-rich peptides RW9 and RL9 in a lipid environment investigated by solid-state NMR and MD simulations. *Biochimica et Biophysica Acta (BBA)-Biomembranes* **2012**.
38. Jiao, C.-Y.; Delaroche, D.; Burlina, F.; Alves, I. D.; Chassaing, G.; Sagan, S. Translocation and endocytosis for cell-penetrating peptide internalization. *Journal of Biological Chemistry* **2009**, *284*, (49), 33957-33965.
39. Deshayes, S.; Morris, M.; Divita, G.; Heitz, F. Cell-penetrating peptides: tools for intracellular delivery of therapeutics. *Cellular and Molecular Life Sciences CMLS* **2005**, *62*, (16), 1839-1849.

40. Zhang, L.; Rozek, A.; Hancock, R. E. Interaction of cationic antimicrobial peptides with model membranes. *Journal of Biological Chemistry* **2001**, *276*, (38), 35714-35722.
41. Sakai, N.; Futaki, S.; Matile, S. Anion hopping of (and on) functional oligoarginines: from chloroform to cells. *Soft Matter* **2006**, *2*, (8), 636-641.
42. Lins, L.; Decaffmeyer, M.; Thomas, A.; Brasseur, R. Relationships between the orientation and the structural properties of peptides and their membrane interactions. *Biochimica et Biophysica Acta (BBA)-Biomembranes* **2008**, *1778*, (7), 1537-1544.
43. Eiríksdóttir, E.; Konate, K.; Langel, Ü.; Divita, G.; Deshayes, S. Secondary structure of cell-penetrating peptides controls membrane interaction and insertion. *Biochimica et Biophysica Acta (BBA)-Biomembranes* **2010**, *1798*, (6), 1119-1128.
44. Maiolo, J. R.; Ferrer, M.; Ottinger, E. A. Effects of cargo molecules on the cellular uptake of arginine-rich cell-penetrating peptides. *Biochimica et Biophysica Acta (BBA)-Biomembranes* **2005**, *1712*, (2), 161-172.
45. Yau, W.-M.; Wimley, W. C.; Gawrisch, K.; White, S. H. The preference of tryptophan for membrane interfaces. *Biochemistry* **1998**, *37*, (42), 14713-14718.
46. Landolt-Marticorena, C.; Williams, K. A.; Deber, C. M.; Reithmeier, R. A. Non-random distribution of amino acids in the transmembrane segments of human type I single span membrane proteins. *Journal of molecular biology* **1993**, *229*, (3), 602-608.
47. Futaki, S.; Suzuki, T.; Ohashi, W.; Yagami, T.; Tanaka, S.; Ueda, K.; Sugiura, Y. Arginine-rich peptides An abundant source of membrane-permeable peptides having potential as carriers for intracellular protein delivery. *Journal of Biological Chemistry* **2001**, *276*, (8), 5836-5840.

48. Bechara, C.; Pallerla, M.; Zaltsman, Y.; Burlina, F.; Alves, I. D.; Lequin, O.; Sagan, S. Tryptophan within basic peptide sequences triggers glycosaminoglycan-dependent endocytosis. *The FASEB Journal* **2013**, *27*, (2), 738-749.
49. Sánchez-Martín, M. J. s.; Haro, I.; Alsina, M. A.; Busquets, M. A.; Pujol, M. A Langmuir Monolayer Study of the Interaction of E1 (145– 162) Hepatitis G Virus Peptide with Phospholipid Membranes. *The Journal of Physical Chemistry B* **2009**, *114*, (1), 448-456.
50. Varas, M.; Sánchez-Borzzone, M.; Sánchez, J. M.; Barioglio, S. R. d.; Perillo, M. a. A. Surface Behavior and Peptide– Lipid Interactions of the Cyclic Neuropeptide Melanin Concentrating Hormone. *The Journal of Physical Chemistry B* **2008**, *112*, (24), 7330-7337.
51. Eeman, M.; Berquand, A.; Dufrene, Y.; Paquot, M.; Dufour, S.; Deleu, M. Penetration of surfactin into phospholipid monolayers: nanoscale interfacial organization. *Langmuir* **2006**, *22*, (26), 11337-11345.
52. Jiang, D.; Dinh, K. L.; Ruthenburg, T. C.; Zhang, Y.; Su, L.; Land, D. P.; Zhou, F. A kinetic model for β -amyloid adsorption at the air/solution interface and its implication to the β -amyloid aggregation process. *The Journal of Physical Chemistry B* **2009**, *113*, (10), 3160-3168.
53. Sospedra, P.; Haro, I.; Alsina, M.; Reig, F.; Mestres, C. Viral synthetic peptide interactions with membranes: A monolayer study. *Langmuir* **1999**, *15*, (16), 5303-5308.
54. Ambroggio, E. E.; Separovic, F.; Bowie, J.; Fidelio, G. D. Surface behaviour and peptide– lipid interactions of the antibiotic peptides, Maculatin and Citropin. *Biochimica et Biophysica Acta (BBA)-Biomembranes* **2004**, *1664*, (1), 31-37.
55. Marczewski, A. W. Analysis of kinetic Langmuir model. Part I: integrated kinetic Langmuir equation (IKL): a new complete analytical solution of the Langmuir rate equation. *Langmuir* **2010**, *26*, (19), 15229-15238.

56. Peggion, E.; Mammi, S.; Schievano, E. Conformation and interactions of bioactive peptides from insect venoms: The bombolitins. *Peptide Science* **1997**, *43*, (6), 419-431.
57. Fujita, K.; Kimura, S.; Imanishi, Y.; Rump, E.; Ringsdorf, H. Two-dimensional assembly formation of hydrophobic helical peptides at the air/water interface: fluorescence microscopic study. *Langmuir* **1995**, *11*, (1), 253-258.

Chapter 5

Effect of Lipid Headgroup Charge and pH on the Stability and Membrane Insertion Potential of Calcium Condensed Gene Complexes

Published as:

Alhakamy, N. A.; Elandalousi, I.; Ghazvini, S.; Berkland, C. J.; Dhar, P. Effect of Lipid Headgroup Charge and pH on the Stability and Membrane Insertion Potential of Calcium Condensed Gene Complexes. *Langmuir* 2015, 31, (14), 4232-4245. (2015)

5.1. Introduction

Efficient intracellular delivery of genetic material (DNA and RNAi) suffers from several bottlenecks. Unlike micromolecules that can enter the cell by passive diffusion or through specific channels, the larger size and anionic nature of the macromolecules prevent them from penetrating through the plasma membrane. As a result, most macromolecules enter the cell through the endocytosis mechanism^{1,2}. However, this process suffers from bottlenecks of its own, including effective cellular uptake as well as timely escape from the endosomal pathway to prevent enzymatic degradation of the nucleic acids in lysosomes³⁻⁶. The plasma membranes as well as the membranes in the intracellular compartment serve as barriers that prevent penetration or escape of macromolecules and are the principal deterrents to efficient intracellular delivery^{7, 8}. Subsequently, tremendous efforts have been made to develop gene vectors (both viral and nonviral) that can easily penetrate the plasma membrane as well as effectively avail of the cell's intracellular transport mechanism to enable intracellular delivery of genetic material. Vector unpacking at the intracellular site is also a necessary step in this process⁹. Viral vectors are highly efficient in this process, but safety concerns (e.g., immunogenicity) still persist¹⁰⁻¹². Nonviral vectors, on the other hand, offer several advantages over viral vectors, such as ease of synthesis, low cost, and low degree of immunogenicity¹²⁻¹⁴. Therefore, efficient design of nonviral vectors for intracellular gene delivery necessitates an understanding of the mechanisms through which the nonviral vectors can effectively trigger cellular uptake, as well as escape from late endosomes to deliver their payload.

The main structural component of the plasma membrane, as well as the various compartments in the intracellular trafficking pathway, is phospholipids. While the zwitterionic phosphatidylcholine (PC) headgroups make up the major phospholipid content of all eukaryotic

cell membranes, anionic phospholipids such as phosphatidylserine (PS) are present in the inner leaflet of the plasma membrane, as well as the lipid membranes that make the endosomes^{7,15}. Cell membranes also contain very small amounts of anionic phosphatidylglycerol (PG), while late endosomes are unique in their composition of Bis (Monoacylglycero) Phosphate (BMP), which is a structural isomer of PG. In fact, compared to the outer leaflet of the cell membrane, the endosomes are significantly enriched in anionic lipids such as PS and BMP¹⁶. In addition to the change in the lipid headgroup moieties, the intracellular pH also decreases along the endocytic pathway, from the early endosome to the lysosomes¹⁵. Therefore, understanding the mechanisms of nonviral gene delivery vectors requires an understanding of their interactions with these biological barriers.

Noncovalent complexation of genetic material (e.g., DNA and siRNA) using polycations is being considered as a potential nonviral gene vector that can deliver larger genetic payloads at the required delivery site¹². Unfortunately, the most efficient polycations, such as polyethylenimine (PEI), are also the most toxic. Further, while high-molecular-weight polycations are often essential to condense larger genetic material such as plasmid DNA (pDNA) into small particles, the increase in molecular weight often increases cytotoxicity as well¹⁷. We and others have shown that the use of synthetic cell penetrating peptides (CPPs) is a potentially interesting method for condensation of genetic material as well as their delivery across the cell membrane^{6, 11, 12, 18-20}. CPPs consist of low-molecular-weight cationic or amphiphilic sequences of about 30 residues^{12, 17, 18, 21}. Since their discovery in the early 1990s, they have attracted a lot of attention as potential candidates for delivery of biomolecules to cells^{12, 22, 23}. In general, CPPs can be classified into three types, depending on their origin: natural CPPs (protein-derived) (e.g., TAT peptide); synthetic CPPs (e.g., polyarginine); and chimeric CPPs (e.g., transportan)¹². Simple

polyarginine or polylysine molecules influenced by a highly basic minimal transduction domain of the protein-derived TAT protein, typically consisting of nine amino acids (RKKRRQRRR) were shown to cross the plasma membrane even more readily than the TAT peptide^{2,24}. Due to the faith in “arginine’s magic” several groups, including us have previously reported on the ability of using these polypeptides as CPPs²⁵⁻²⁷. It has also been shown that the membrane insertion potential of synthetic peptides is dependent on the positive charge on the CPPs interacting with anionic phospholipids within the membrane.²⁸ Particularly, synthetic CPPs with 7-9 amino acids have demonstrated the best cell penetration efficiency, and this efficiency has been found to go down as the residue sequence length is either increased or decreased^{17,29,30}. Further, we and others have shown that the presence of hydrophobic moieties, such as tryptophan can also enhance phospholipid penetration^{2,31}. Particularly, the properties of the guanidyl group were extremely efficient in increasing the membrane penetration behavior of arginine polypeptides²⁵.

Numerous studies have also demonstrated that adding calcium chloride (CaCl₂) to CPP-siRNA or pDNA complexes produced stable and small nanoparticles that improved the transfection efficiency of these gene complexes *in vitro* and *in vivo*^{6,11,14,20,32}. It was also found that adding 100 mM CaCl₂ to the CPP-pDNA samples yielded the highest gene expression compared to 50, 150, and 300 mM¹⁷, possibly by enhancing their endosomal release before degradation by lysosomes^{33,34}. However, how does complexing CPPs with genetic material in the presence of CaCl₂ impacts their cell insertion potential has not been previously reported. While the calcium condensed CPP-pDNA complex uptake may be aided by endocytosis or cell penetration, which in turn involves interactions with specific cell membrane lipids or possibly interactions with membrane associated proteoglycans, the desirable goal of endosomal escape is typically destabilization of the endosomal membrane to allow timely escape of genetic material²².

³⁵⁻³⁷. Therefore, understanding the mechanism of cell penetration (or cellular uptake) of these CPP induced condensed complexes as well as the mechanisms of escape of these nonviral gene vectors from endosomal compartments is essential for designing efficient CPP-pDNA vectors ^{2, 38, 39}.

In order to better understand the stability of gene complexes and their interactions with phospholipid membranes in the endocytic pathway (plasma, endosome, and lysosome membranes), the mechanisms of interactions between the condensed gene complexes with phospholipid membranes form the focus of this study. In particular, we report on the interactions of seven different gene complexes with model PC, PS and PG phospholipid monolayers at two pHs (7.4 and 4.4). Based on previous studies, our choice of CPPs consists of four hydrophilic CPPs (i.e., dTAT, K9, R9, and RH9) and three amphiphilic arginine-rich peptides (RW9, RL9, RA9) (**Table 1**). Positively charged synthetic polypeptides (polyarginine R9 and polylysine K9) were used to study the effect of specific amino acids on gene complex formation and interaction with the plasma membrane. Arginine-rich CPPs where the arginine residues at positions 3, 4, and 7 are replaced with tryptophan, leucine, alanine, and histidine (RW9, RL9, RA9, and RH9) were used to study the effect of a combination of positively charged and hydrophobic residues on the insertion efficiency of the CPP-gene complexes ². dTAT (double-TAT) is a natural HIV protein derived CPP that was used as a control. In our studies, unsaturated fatty acids with mixed alkyl chains were used as simple models of the phospholipid barriers. POPC monolayers were used as model zwitterionic monolayers, while POPS and POPG phospholipids were used as model anionic monolayers (**Table 2**) to study the effect of lipid headgroup charge density on the phospholipid insertion potential of gene complexes. One of the advantages of using model membranes is that their packing can be easily controlled and varied. Additionally, model membranes have previously been used to study the individual interactions of DNA as well as CPPs, to better understand their

mechanisms of interaction. The two pHs represent the extreme limits in the acidic nature of the environment in the endocytic pathway. Finally, since several previous *in vitro* and *in vivo* studies have shown that calcium improves the transfection efficiency of gene complexes^{6, 11, 14, 17, 20, 32, 40, 41}, here we also present the effect of the addition of calcium on the stability and membrane insertion potential of our gene complexes.

Table 1. Identification of the seven CPPs and their properties (peptide sequence, number of residues, classification, net charge at pH 7 and molecular weight).

Name	Interpreted Sequence	Number of Residues	Classification	Charge		Molecular Weight (g/mol)
				pH 7.4	pH 4.4	
dTAT	RKKRRQRRRHRRK KR	15	Hydrophilic	+13	+14	2200.75
K9	KKKKKKKKK	9	Hydrophilic	+9	+9	1170.65
R9	RRRRRRRRR	9	Hydrophilic	+9	+9	1422.74
RH9	RRHHRRHRR	9	Hydrophilic	+6	+9	1365.62
RA9	RRAARRARR	9	Amphiphilic	+6	+6	1167.41
RL9	RRLLRRLRR	9	Amphiphilic	+6	+6	1293.68
RW9	RRWWRRWRR	9	Amphiphilic	+6	+6	1512.83

Table 2. Name, synonyms, classification, and structure of the POPC, POPS and POPG membrane models.

Name	Synonyms	Classification	Relative Charge *		pKa *	Structure
			pH 7.4	pH 4.4		
POPC	1-hexadecanoyl-2-(9Z-octadecenoyl)-sn-glycero-3-phosphocholine	Zwitterionic Phospholipid (Unsaturated)	0	0	pKa ~ 1	
POPS	1-palmitoyl-2-oleoyl-sn-glycero-3-phospho-L-serine (sodium salt)	Anionic Phospholipid (Unsaturated)	~ - 1.0	~ - 1.0	pKa ~ 5.5 pKa ~ 2.6 pKa ~ 11.55	
POPG	1-hexadecanoyl-2-(9Z-octadecenoyl)-sn-glycero-3-phospho-(1'-rac-glycerol)	Anionic Phospholipid (Unsaturated)	~ - 0.9	~ - 0.9	pKa ~ 3.5	

* Marsh, D. CRC handbook of lipid bilayers. 1990.

5.2. Materials and Methods

5.2.1. Materials

Plasmid DNA (pDNA) encoding firefly luciferase (pGL3, 4818 bp) was obtained from Promega (Madison, Wisconsin). The pDNA purity level was determined by UV-Spectroscopy and agarose gel electrophoresis. dTAT (RKKRRQRRRHRRKKR; $M_w = 2201.7$ Da) peptide, K9 (KKKKKKKKK; $M_w = 1170.65$ Da) peptide, R9 (RRRRRRRRR; $M_w = 1422.74$ Da) peptide, RH9 (RRHRRHRR; $M_w = 1365.62$ Da) peptide, RA9 (RRA ARRARR; $M_w = 1167.41$ Da) peptide, RL9 (RLLRRLRR; $M_w = 1293.68$ Da) peptide, and RW9 (RRWWRRWRR; $M_w = 1512.83$ Da) peptide were purchased from Biomatik Corporation (Cambridge, Ontario, Canada) (Purity > 95%). 1-hexadecanoyl-2-(9Z-octadecenoyl)-sn-glycero-3 phosphocholine (sodium salt)

(POPC), 1-palmitoyl-2-oleoyl-sn-glycero-3-phospho-L-serine (sodium salt) (POPS), and 1-palmitoyl-2-oleoyl-sn-glycero-3-phospho-(1'-rac-glycerol) (sodium salt) (POPG) were purchased from Avanti Polar Lipids, Alabaster, AL, as organic mixtures in chloroform. Agarose (Medium-EEO/Protein Electrophoresis Grade) was purchased from Fisher Scientific. Bench Top DNA Ladder was purchased from Promega (Madison, WI). SYBR Green I Nucleic Acid Gel Stain was obtained from Invitrogen (Carlsbad, CA). Calcium chloride dehydrate ($\text{CaCl}_2 \cdot 2\text{H}_2\text{O}$) was purchased from Fisher Scientific. Other organic chemicals used for this work was purchased from Fisher Scientific. Petri dishes (Falcon 1008, Becton-Dickinson Labware, Franklin Lakes, NJ) were purchased from Fisher Scientific. All samples and lipid mixtures were stored at -20°C when not in use.

5.2.2. Methods

5.2.2.1. Preparation of CPP-pDNA- Ca^{2+} Complexes

CPP-pDNA complexes were prepared by adding 15 μL of CPPs solution (0.28 $\mu\text{g}/\mu\text{L}$) to 10 μL (0.1 $\mu\text{g}/\mu\text{L}$) of pDNA (TAE Buffer (1x) was used as a solution for DNA storage), followed by fast pipetting for 20 seconds. At that point, 15 μL of CaCl_2 of desired molarity (100 mM in most cases) was added and mixed by fast pipetting for a further 20 seconds. This process resulted in the formation of condensed complexes containing pDNA and the CPP. After preparing the gene complexes, they were stored at 4°C for 15 to 20 minutes and then used for further analysis. The peptide-to-lipid (P/L) molar ratio at an initial S.P. of 20 and 30 mN/m was 0.25.

5.2.2.2. Agarose Gel Electrophoresis

4 μL (1 x) of Tris-acetate-EDTA (TAE) buffer was added to the solution containing the gene complexes of interest. EDTA interacts with the divalent metal ions in solution and thus inhibits metal-dependent nucleases. 4 μL of SYBR Green 1 (a highly sensitive DNA gel stain used for

visualization of DNA in agarose or acrylamide gels) was mixed with the gene complexes. The mixture was well-mixed and stored at 4°C for 15 to 20 minutes. After the storage, 7 µL of 6X DNA Loading Dye (dye used to prepare DNA markers and samples for loading on agarose gels) was added to allow visual tracking of DNA migration during electrophoresis. A one kb DNA ladder was used. The presence of glycerol ensures that the DNA in the ladder and sample forms a layer at the bottom of the well. The approximate mass of DNA in each of the bands is provided for approximating the mass of DNA in comparatively concentrated samples of similar size. The mixture solutions were loaded onto a 1 % agarose gel, and electrophoresed for 30 minutes at 110 V.

5.2.2.3. Particle Size

The particle size (effective diameter (nm)) of CPP-pDNA complexes with calcium chloride was determined by dynamic light scattering (Brookhaven Instruments, Holtsville, NY). All samples intended for particle size measurements were prepared using PBS at pH 7.4 and 4.4.

5.2.2.4. Zeta Potential

The zeta potentials of the complexes were measured by Zeta PALS dynamic light scattering (Brookhaven Instrument, Holtsville, NY). All samples intended for particle size measurements were prepared using PBS, nuclease free water (NFW), and serum-free media (SFM). All samples intended for zeta potential measurements were prepared using PBS at pH 7.4 and pH 4.4.

5.2.2.5. Langmuir Trough Experiments

The insertion potential of the different synthetic complexes and CPPs was measured using model phospholipid monolayers (PMs) containing different amounts of a zwitterionic (POPC) or negatively charged phospholipid (POPS, and POPG) at the air-PBS buffer interface. S.P. changes were recorded by a Wilhelmy plate sensor, which is part of the KSV-NIMA Langmuir trough purchased from Biolin Scientific, while petri dishes (volume 4 ml, 35 x 10) were used as “mini-

troughs” for the experiments. Insertion of the gene complexes and CPPs into preformed monoayers was recorded in the presence of phospholipid membranes. A wet calibrated filter paper flag was dipped into this buffer solution and used as a probe to monitor changes in the surface pressure due to adsorption of surface active material. The phospholipid membranes were spread from chloroform solutions, on PBS subphase, at pH 7.4 and 4.4, using a Hamilton microsyringe (Hamilton Co., Reno, NV). The spreading phospholipid solvents were allowed to evaporate for 20 minutes prior to adding of the gene complexes (or free CPPs). The gene complexes (and free CPPs) aqueous solutions were injected underneath the surface of lipid membranes, and the changes in surface pressure with respect to time were measured immediately. Precaution was taken to ensure that the injection did not disrupt the phospholipid monolayer. Adsorption to a bare air/buffer interface was recorded for all the gene complexes (and free CPPs) studied here to ensure that the changes in the S.P. of the monolayers were due to interaction of the gene complexes (or free CPPs) with the cell membrane. Each experiment was run for 60 minutes at 22 ± 2 °C. All figures were normalized by subtraction of the control (the phospholipids [POPC, POPS, and POPG] without complexes or free CPPs) at pH 7.4 and 4.4 to ensure that the differences in the S.P. of the monolayers were due to interaction of complexes and peptides.

5.2.2.6. Statistical Analysis

Data were analyzed by using the GraphPad software. Statistical evaluation between the means of the data was performed using an unpaired *t* test. One-way ANOVA, Tukey post-test was used to analyze the differences when more than two data sets were compared. Each experiment was repeated three times ($n = 3$).

5.3. Results and Discussion

5.3.1. Physical Characterization of the CPP-pDNA-Ca²⁺ Complexes

Two important characteristics of CPP-pDNA-Ca²⁺ complexes are their particle size and overall charge. **Figure 1A** illustrates the particle size of the seven CPP (dTAT, K9, R9, RH9, RA9, RL9, and RW9)-pDNA-Ca²⁺ complexes in PBS (ionic strength, 185 mM) at pH 7.4 and 4.4. Overall, the particle size of the complexes was around 250 nm at pH 7.4 (with relatively narrow polydispersity (<0.2)), irrespective of the CPP used, suggesting that the choice of CPP has little effect on the particle size at normal pH. Further, an increase in particle size was noted at low pH (4.4), compared to the physiological pH (7.4), suggesting that an acidic environment reverses the condensing effect of Ca²⁺. Moreover, a reduction in the photon counting rate (kilo-counts per second; Kcps), at the more acidic pH also supports the argument that these gene complexes may be partially dissociated or are no longer condensed at pHs that are relevant to the late endosomal or lysosomal environment. Such acidic pH induced dissociation has previously been reported for DNA-calcium complexes^{17, 42}. **Figure 1B** presents the zeta potential of these gene complexes at normal and acidic pHs. We find that at the neutral pH, the zeta potential values are positive, although there are small differences in the individual values. This is possibly due to the charge on the CPPs making up the condensed gene complexes. The net positive zeta potential of our condensed complexes verifies the cationic nature of the complexes, and confirms that while there is a core of pDNA, the CPP, being in excess form the shell of these gene complexes. **Figure 1B** also shows that the net charge on the particles is switched when the pH is lowered, and the gene complexes become anionic or neutral. These observations confirm that a lowering of the environmental pH destabilized the noncovalently condensed pDNA complexes, allowing the pDNA to be exposed or released from the complex.

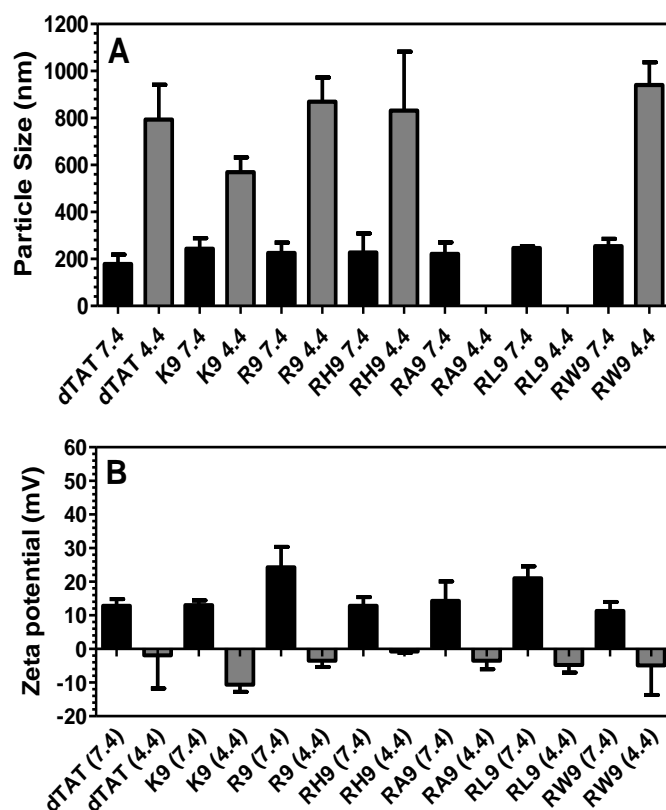


Figure 1. (A) Particle size of the seven CPPs (dTAT, K9, R9, RH9, RA9, RL9, and RW9)-pDNA- Ca^{2+} complexes, which was measured in phosphate buffer saline and at pH 7.4 and 4.4. For missing data points, diameter was undetectable. (B) Zeta potentials of CPPs (dTAT, K9, R9, RH9, RA9, RL9, and RW9)-pDNA- Ca^{2+} complexes in phosphate buffer saline and at pH 7.4 and 4.4. Results are presented as mean \pm SD ($n = 3$).

To further prove that at pH ~ 7.4 , the pDNA is immobilized with the CPP to form complexes, we ran agarose gel electrophoresis assay for these complexes. **Figure 2** illustrates the results of this assay for these complexes. Free pDNA was used as a control, while the leftmost column shows the molecular weight marker. When an electric field is applied across the cells, the appearance of different bands along the column corresponds to the migration of any free DNA. Our results show that most of the gene complexes completely immobilized the pDNA (no bands were observed during electrophoresis), except RA9 containing complexes, which looked slightly unstable.

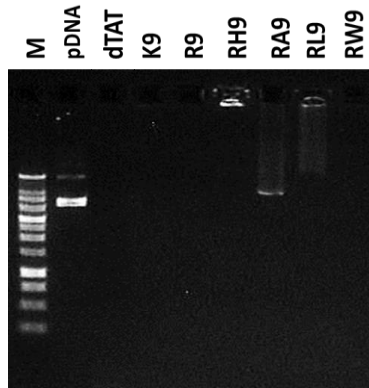


Figure 2. Agarose gel electrophoresis study of the seven CPPs (dTAT, K9, R9, RH9, RA9, RL9, and RW9)-pDNA- Ca^{2+} complexes. “M” Refers to the size marker.

5.3.2. Insertion of the CPP/pDNA- Ca^{2+} Complexes into Model Membranes

As cell membranes are complex systems, many model membranes have become commonly used for studying the membrane activity of various natural and synthetic compounds (e.g., peptides, drugs, and surfactants). Lipid monolayers are the most common biomimetic systems used to study the insertion of biomolecules into cell membranes. These monolayers can be considered as models for one leaflet of the cell membrane. These two-dimensional models show many advantages compared to other models (e.g., lipid vesicles). Some parameters (e.g., the composition of the subphase [pH and ionic strength], temperature, and the packing of the molecules) can be easily varied in a controlled manner allowing several biophysical studies of the phospholipid-gene complex interactions. However, one of the limitations of the monolayer system is that they represent only one leaflet of the cell membranes without any other components such as membrane proteins. Therefore, they do not reflect the complexity of cell structures^{2, 43}. Yet, these simple models are often used to understand the biophysical interactions governing molecular interactions in phospholipid membranes. For example, it is well known that if the area of the monolayer is kept constant (constant area assay), adsorption followed by insertion of molecules into the hydrophobic

region of phospholipid monolayers (tails) can cause a significant increase in the surface pressure. On the other hand, particles that interact with the hydrophilic region (head groups) typically induce only slight changes in surface pressure ^{2, 44}. In order to understand the physical mechanisms of interactions of calcium condensed gene complexes with cell membranes in the endosomal environment, the membrane insertion potential of seven different complexes was recorded using two model phospholipid monolayers. Zwitterionic phospholipid (POPC) and anionic phospholipids (POPS and POPG) were used as simple mimics of the cell membranes. PC is the most common phospholipid in the cell membrane of eukaryotic cells ⁴⁵, whereas anionic PS is normally found in the inner leaflet of the plasma membrane as well as endosomal membranes ^{7, 46, 47}. Even though PG headgroups are present at 1 to 2% in the plasma membrane, they have often been used as model anionic lipids to study the function of CPP ^{7, 46}. More relevant to this study, BMP, an isomer of PG with the same headgroup charge ^{48, 49}, but differences in the position of the glycerol units on the phosphate moiety, is a unique anionic lipid found in significant fractions in the late endosomes ^{7, 49, 50}. Since BMP was not stable as a monolayer in our experimental set-up because of its high solubility and tendency to form vesicles ⁵¹⁻⁵³, we chose to use PG headgroups as model lipid system that remains anionic at the pHs relevant to this study, in order to understand the interactions of the CPPs with anionic headgroups that are enriched in the late endosomes ⁴⁸⁻⁵⁰.

The effect of hydrophobic interactions versus electrostatic interactions on the phospholipid membrane insertion potential of gene complexes was monitored using gene complexes that contained both hydrophilic and amphiphilic peptides. Additionally, we have studied the effect of pH of the cytoplasm/early endosome versus late endosome/lysosome on this insertion process by monitoring the changes in the surface pressures at two different pHs, 7.4 and 4.4. Therefore, by studying the insertion potential of these different cationic gene complexes into phospholipids at

different pHs, we expect to develop a mechanistic understanding of interactions of the gene complexes with phospholipids in the endosomal pathway. While the insertion potential of the gene complexes was initially measured for different monolayer surface pressures (20-40 mN/m), our previous ² and current work indicate that the maximum difference in the results between the samples was monitored at a surface pressure of 20 mN/m (**Figure Appendix 5**). Therefore, in this work, we report the insertion of our gene complexes into monolayers held at an initial surface pressure of 20 mN/m.

Figure 3 shows the changes in surface pressure of the three phospholipid monolayers as a function of time, following interactions with the seven complexes at pH 7.4. **Figure 3A** presents the change in surface pressure with time while **Figure 3D** presents the maximum change in surface pressure (Δ surface pressure, the maximum absolute value of the surface pressure recorded during the 60 minutes period) for each of the seven complexes, when injected below the POPC monolayer. The change in surface pressure with time is significantly higher for gene complexes condensed using the CPPs and calcium when compared with the control (pDNA alone), indicating that the gene complexes have significantly higher insertion efficiency into the model zwitterionic phospholipid monolayer, when compared with an equal amount of free pDNA. However, no significant difference in the surface pressure was observed between the different cationic gene complexes. Since the size of these condensed complexes are comparable, our results suggest that at physiological pH, the gene complexes do not show significant insertion into the zwitterionic phospholipids. However, the significant difference in the insertion potential of the complexes when compared to the change in surface pressure of the PC monolayer in the presence of free pDNA suggest that condensing the complex with CPPs enabled increased interactions of the genetic material with the plasma membrane. Further, this observation also confirms that the

increased interactions in the presence of gene complexes cannot be associated with pDNA phospholipid monolayer interactions that occur in lipoplexes⁵⁴. To further verify that the increase in surface pressure was not due to the presence of cations, we also performed control experiments in the presence of 100 mM calcium chloride without any complexes, even though we do not expect such a high concentration of free ions (the calcium is added during the complexation process and is expected to associate with the pDNA-CPP complex). As shown in **Figure 3**, the increase in surface pressure in the presence of gene complexes was highly significant, when compared with calcium chloride alone, verifying that the change in the surface pressure is due to phospholipid-gene complex interactions, and not due to the presence of calcium ions.

Figure 3B and **3E** show the recorded changes in the surface pressure for the seven complexes, when injected below the anionic POPS monolayer. Similarly, changes in the surface pressure with time and the maximum change in surface pressure, of a POPG monolayer, due to insertion of the seven complexes, are shown in **Figure 3C** and **3F**. Our results demonstrated that for both anionic lipids studied here, the increase in surface pressure with time was significantly higher for all the complexes, when compared with the free pDNA. Moreover, the amphiphilic RL9 and RW9 containing complexes demonstrated a significant increase in the surface pressure of the anionic phospholipid monolayer, when compared with the hydrophilic complexes. Therefore, **Figure 3** provides conclusive evidence that gene complexes containing amphiphilic RL9 and RW9 peptides show enhanced insertion into anionic lipid monolayers at neutral pH.

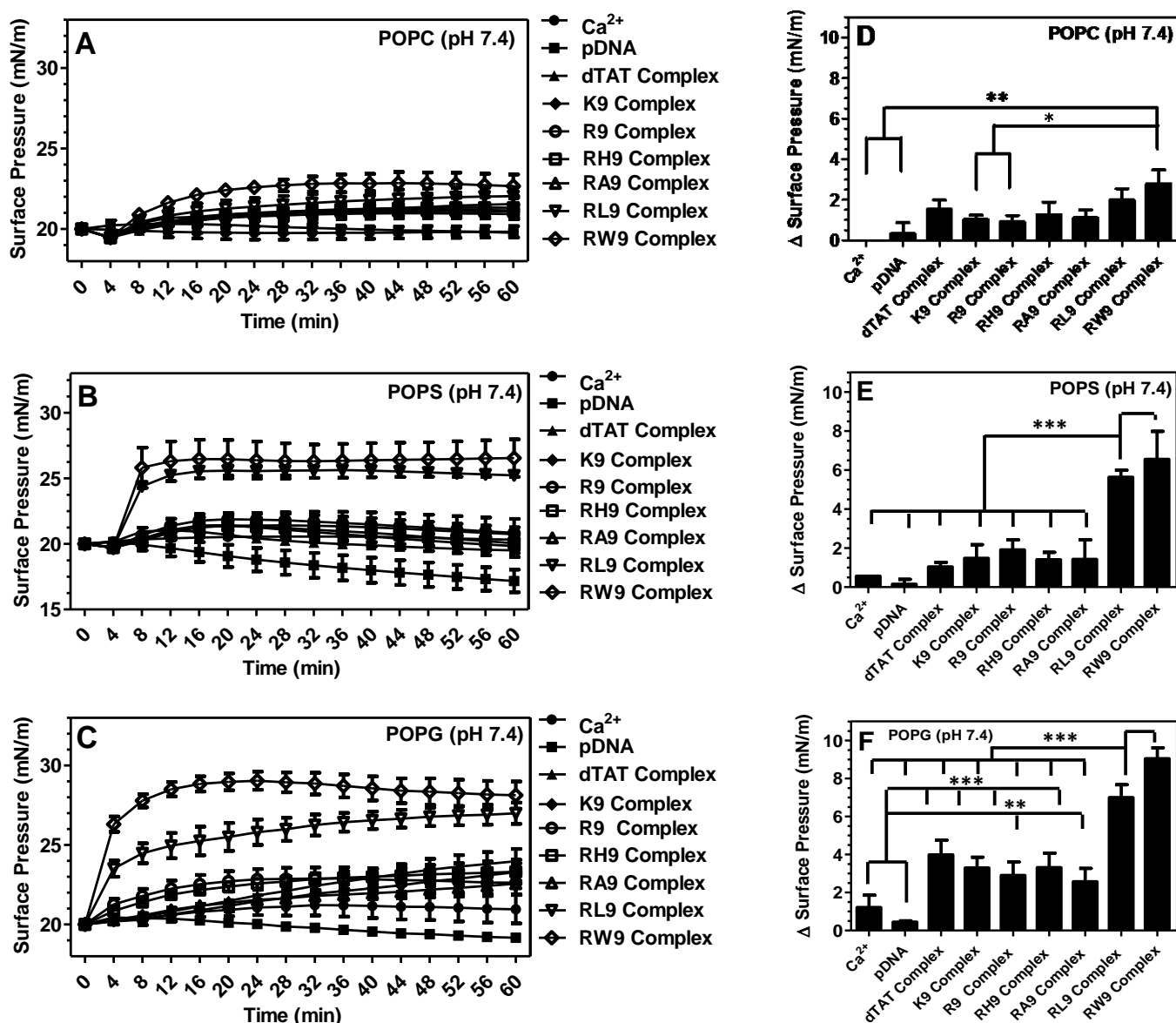


Figure 3. Changes in surface pressure as a function of time following injection of the seven CPPs (dTAT, K9, R9, RH9, RA9, RL9, and RW9)-pDNA-Ca²⁺ complexes below POPC (A), POPS (B), and POPG (C) monolayers held at an initial surface pressure of 20 mN/m and at pH 7.4. The maximum change in surface pressure (plateau values) of the seven complexes when inserted below (D) POPC, (E) POPS, (F) POPG monolayers. Results are presented as mean SD (n = 3), (***) = p < 0.0001, ** = p < 0.001, and * = p < 0.05, one-way ANOVA, Tukey post-test).

We and others have previously shown that electrostatic interactions between CPP and phospholipids are enhanced by hydrophobic interactions, if the peptide is also able to penetrate the phospholipid membrane^{2,55}. To elucidate if this cooperative interaction is also true for our gene

complexes, **Figure 4** presents a comparison of the maximum change in surface pressure of each of the seven complexes with the three monolayers (POPC, POPS and POPG) at pH 7.4. The hydrophilic, positively charged dTAT, K9, R9 and RH9 containing gene complexes as well as the amphiphilic RA9 complex showed a slight increase in the maximum surface pressure change in case of POPS monolayers, when compared to the POPC monolayers. However, unlike the gene complexes containing hydrophilic CPPs, the complexes composed of amphiphilic RW9 and RL9 peptides demonstrated a significantly higher increase in surface pressure, when they were injected below a POPS monolayer, compared to a POPC monolayer. Further, POPG showed the maximum increase in surface pressure for all the gene complexes. The overall increase in the insertion potential of gene complexes into anionic POPS and POPG phospholipids can be attributed to electrostatic interactions between the anionic phospholipid monolayers and the cationic gene complexes. However, the significant increase in surface pressure for anionic lipid monolayers, in the presence of gene complexes containing RL9 and RW9 support the idea that addition of hydrophobic amino acids potentially enhances the insertion potential of these complexes. Based on our results, we conclude that for the cationic gene complexes studied here, the initial surface activity of the complexes in the presence of anionic lipids is probably driven by electrostatic interactions between the charged amino acids and the anionic lipid headgroups, while the insertion is controlled by the hydrophobic nature of the tryptophan and leucine residues. Complexes containing RW9, presents the highest insertion into the anionic lipids, possibly because of the strong hydrophobicity or the aromatic ring of tryptophan amino acids in RW9. Complexes with amphiphilic RA9 peptides do not follow this trend, possibly because of the weak hydrophobicity, and small size of the alanine amino acid, which prevents the complexes from penetrating deeper into the monolayer. Therefore, we conclude that calcium condensed gene complexes containing

hydrophilic cationic peptides do not disrupt the phospholipid monolayers, but the presence of large hydrophobic amino acid moieties can increase the insertion potential of condensed gene complexes.

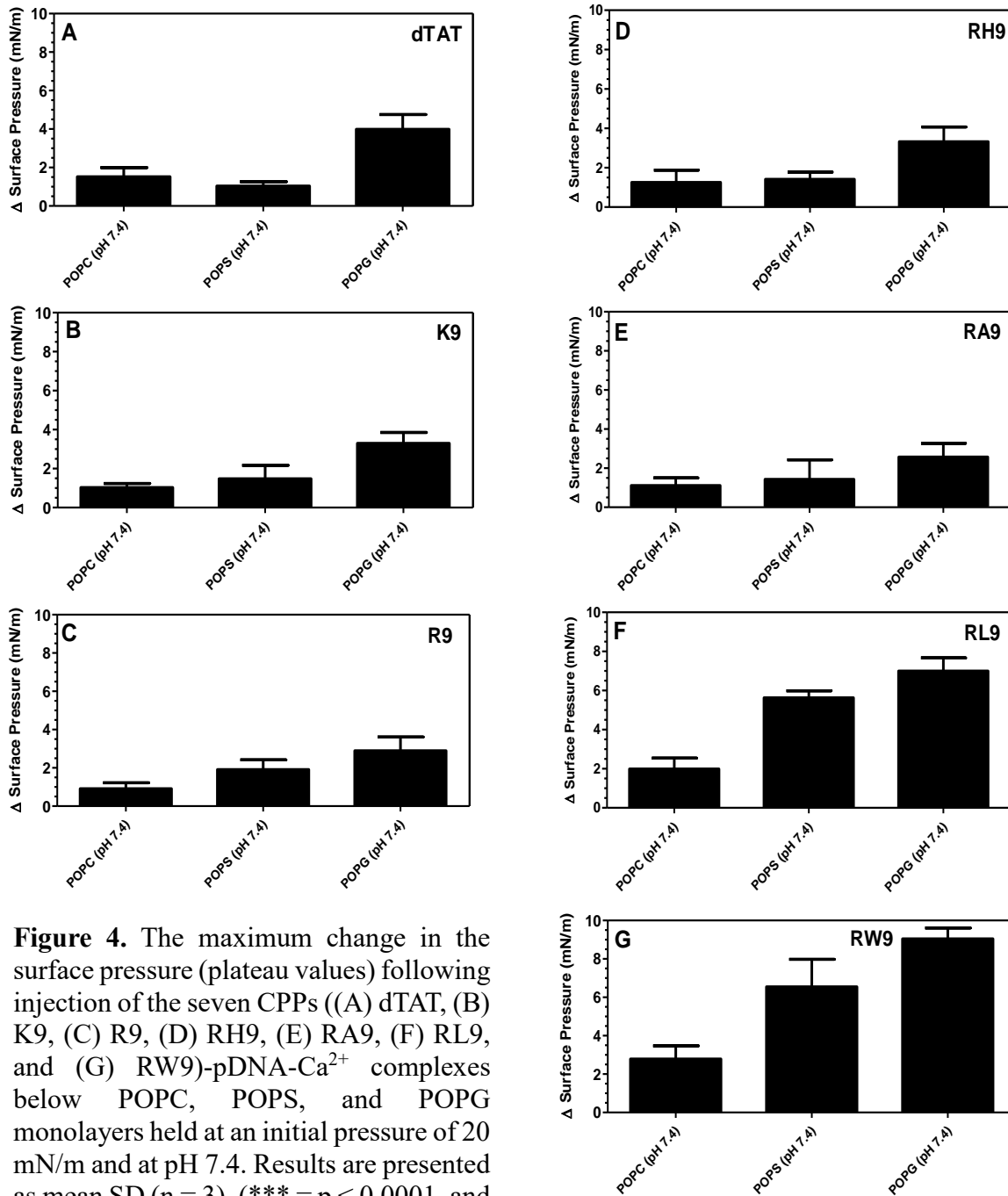


Figure 4. The maximum change in the surface pressure (plateau values) following injection of the seven CPPs ((A) dTAT, (B) K9, (C) R9, (D) RH9, (E) RA9, (F) RL9, and (G) RW9)-pDNA- Ca^{2+} complexes below POPC, POPS, and POPG monolayers held at an initial pressure of 20 mN/m and at pH 7.4. Results are presented as mean SD ($n = 3$), (***) = $p < 0.0001$, and ** = $p < 0.001$, one-way ANOVA, Tukey post test).

However, the difference in the maximum surface pressure of the anionic POPS and POPG lipids in the presence of the gene complexes cannot be explained by electrostatic or hydrophobic interactions. To understand the difference in the insertion into POPS and POPG monolayers, differences in the organization of the phospholipid headgroups should also be considered. Even though both POPS and POPG are anionic phospholipids, the dipole moment P^-N^+ for the PS and PG headgroups are different. The polar PS headgroup has both a positive charge due to the NH_3^+ , and a negative charge due to the presence of COO^- groups. As a result, the cationic gene complexes can interact with the phospholipid headgroup without significant insertion into the membrane. On the other hand, the polar PG headgroup is itself uncharged. The negative charge on PG is due to the phosphate moiety that binds the polar headgroup with the glycerol backbone. This implies that the gene complexes would have to insert deeper into the PG membranes to interact with the negatively charged phosphate moiety, which was indeed found to be the case.

5.3.3. Insertion of the CPP-pDNA- Ca^{2+} Complexes into POPC, POPS, and POPG PMs at Acidic pH

Cytoplasmic delivery of genetic material to subcellular targets can be achieved by initiating endosomal escape of the macromolecules and thus preventing their enzymatic degradation in the lysosome⁵⁶. One possible route of endosomal escape is *via* disruption of the endosomal membranes, which would result in leakage of the genetic payload^{12, 25}. Since the transmembrane pH has been proposed to play a significant role in endosomal escape of peptides, we hypothesized that changes in the subphase pH (from a neutral pH in the plasma membrane to an acidic pH in endosomes) can also effect the interactions of our gene complexes with model phospholipid membranes²⁵. Since the pH decreases along the endocytic pathway from the early endosome (pH

6) *via* the late endosome (pH 5.0) to the lysosome (pH 4.5), we have chosen to study the effect of the most acidic pH on the penetration potential and stability of our CPP-pDNA complexes ¹⁵.

Figure 5 shows the changes in surface pressure of a phospholipid monolayer as a function of time, following interactions with the seven complexes at a subphase pH of 4.4. **Figure 5A** represents the measured change in surface pressure with time while **Figure 5D** shows the maximum change in surface pressure that was measured for each of the complexes, when injected below a POPC monolayer. We found that there was no statistically significant difference in the insertion potential of the gene complexes compared with pDNA. On the other hand, **Figure 5B** and **5E** show that both the measured change in surface pressure with time and the maximum change in surface pressure is significantly higher for the gene complexes containing arginine based CPPs compared to the free pDNA, when injected below the POPS monolayers. The other complexes also exhibit higher surface activities compared to the free pDNA. Similarly, **Figure 5C** and **5F** show that both the measured change in surface pressure with time and the maximum change in surface pressure of POPG monolayers is significantly higher for the gene complexes compared to the free pDNA, although, the change is lower than for the POPS monolayers. In order to explore the role of electrostatics on the insertion potential of each gene complex into different phospholipid membranes at acidic sub-phase pH, **Figure 6** presents a comparison of the maximum change in surface pressure of each of the seven complexes, when injected below POPC, POPS, or POPG monolayers at a sub-phase pH of 4.4. Further, **Figure 7** presents a comparison of the maximum change in surface pressure of the seven complexes, when injected below POPC, POPS or POPG monolayers at the two pHs, to develop a fundamental understanding of the effect of pH on the change in the surface pressure of different phospholipid monolayers. Complexes containing hydrophilic peptides show an increase in membrane insertion in a more acidic pH, compared to

neutral pH. However, as seen in **Figure 7C**, the gene complexes showed a reduced tendency to change the surface pressure when injected below POPG monolayers at a sub-phase pH of 4.4.

To interpret the differences in the pH induced changes in the membrane insertion potential of our condensed CPP-pDNA complexes, we first discuss the effects of pH on the phospholipid headgroup charge. While the zwitterionic PC headgroups are stable at both pHs, the acidic environment can lower the relative charge on the anionic lipids. The POPS phospholipid has three pKas ~ 11.55, 5.5, and 2.6 (R-NH₃, R-COOH, and R-H₂PO respectively), whereas the POPG phospholipid has one pKa ~3.5 (R₂-HPO₄) at an ionic strength of 0.1 M (NaCl)⁵⁷. Therefore, both PS and PG lipids undergo a decrease in the relative headgroup charge at lower pHs, although this effect is more pronounced for the PS monolayers. For the PS and PC monolayers, the net headgroup charge is zero (i.e. the lipid headgroups are zwitterionic) at a pH of 4.4, while the PG headgroup has a negative relative charge. Since the charge on the zwitterionic PC headgroup remains unaltered by a drop in the subphase pH, the increase in phospholipid insertion potential of the complexes at pH 4.4 is unclear at this time. It can be attributed to the physical characteristics of the gene complexes at pH 4.4. Particle size analysis shows that the gene complexes become larger at the lower pH, while zeta potential measurements demonstrate that the particles become neutral or anionic. Previous results with gold nanoparticles show that positively charged nanoparticles penetrate into a zwitterionic bilayer at a neutral pH, while negatively charged particles do not⁵⁸. Applying this knowledge to our system would imply that the gene complexes demonstrate a lowering of the surface pressure change, contrary to results presented here. Therefore, we conclude that the increase in the environmental acidity helps the ability of the gene complexes to penetrate the zwitterionic phospholipid monolayer by increasing the size of the complex. In the case of the PS phospholipid, a pure electrostatic interaction based argument would

imply a decrease in the maximum surface pressure in the acidic pH, which is contrary to the observed results. Therefore, based on our results, we conclude, that even for the PS lipids, the increased size of the gene complexes helps with their insertion potential. In fact, even for complexes that seem to dissociate at lower pHs (RA9 and RL9), a significant increase in the insertion was noted, further validating our conclusion that for phospholipid with a net neutral headgroup charge, unstable complexes or complexes with large size increase the insertion potential of the complex into phospholipids, when compared with condensed complexes. However, the behavior of the complexes when interacting with the POPG lipids is possibly controlled by the electrostatic repulsion between the anionic gene complexes and the anionic lipid headgroup, which results in a decrease in the insertion potential into the POPG monolayers. It must be noted that while PG headgroups are not common in the late endosome membranes, late endosomes are characterized by an increase in the composition of anionic lipids including BMP, which is a structural isomer of PG. Our results imply that for the calcium condensed gene complexes studied here, the enrichment of anionic lipids in the late endosome would prevent the insertion and escape of the genetic payload, but early endosomes rich in anionic lipids can enable endosomal escape and delivery of the genetic material in the cytosol.

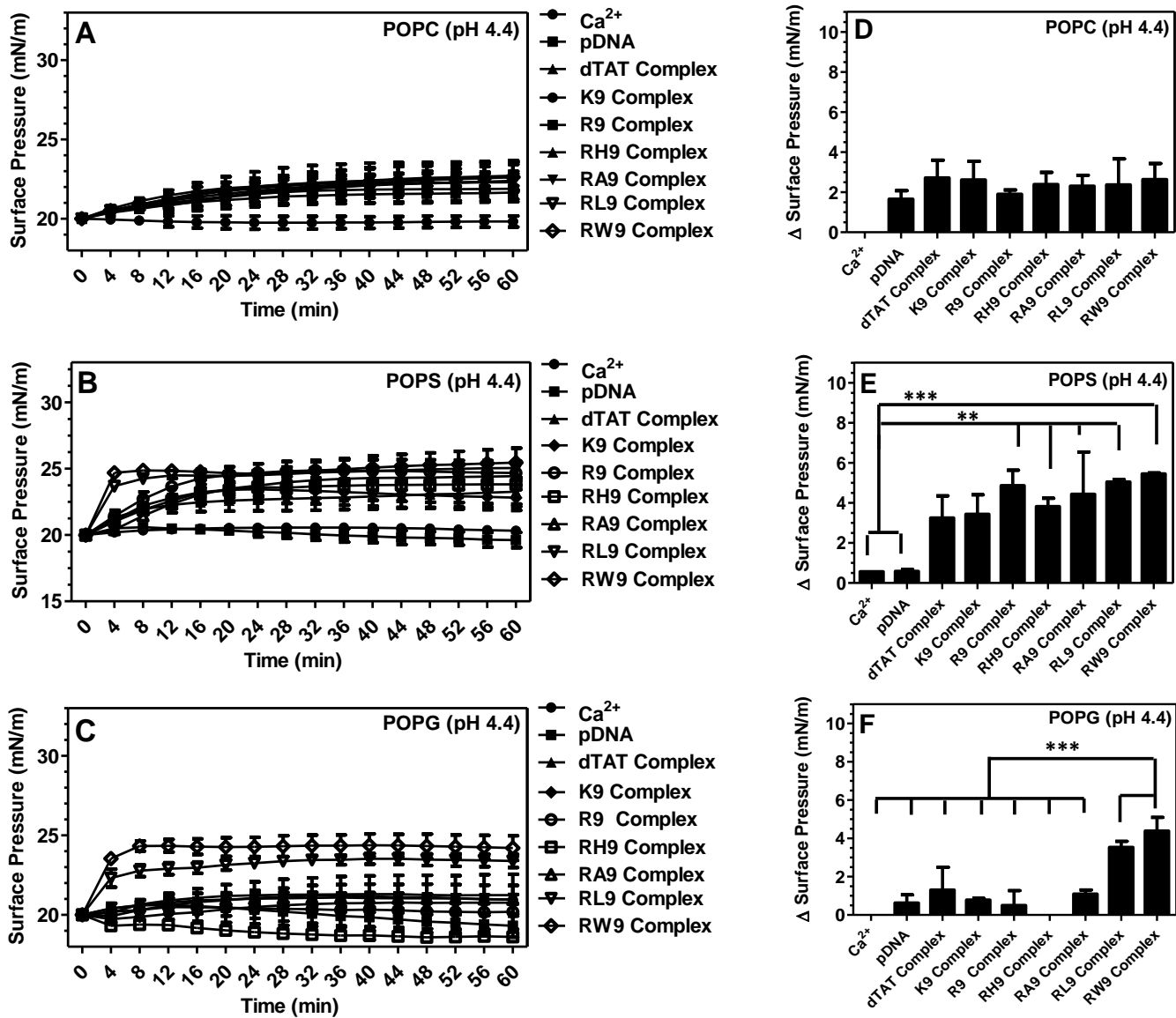


Figure 5. Changes in the surface pressure as a function of time following injection of the seven CPPs (dTAT, K9, R9, RH9, RA9, RL9, and RW9)-pDNA- Ca^{2+} complexes below POPC (A), POPS (B), and POPG (C) monolayers held at an initial surface pressure of 20 mN/m and at pH 4.4. The maximum change in the surface pressure (plateau values) of the seven complexes upon interaction with (D) POPC, (E) POPS, (F) POPG monolayers. Results are presented as mean SD ($n = 3$), (***) = $p < 0.0001$, (**) = $p < 0.001$, and (*) = $p < 0.05$, one-way ANOVA, Tukey post-test).

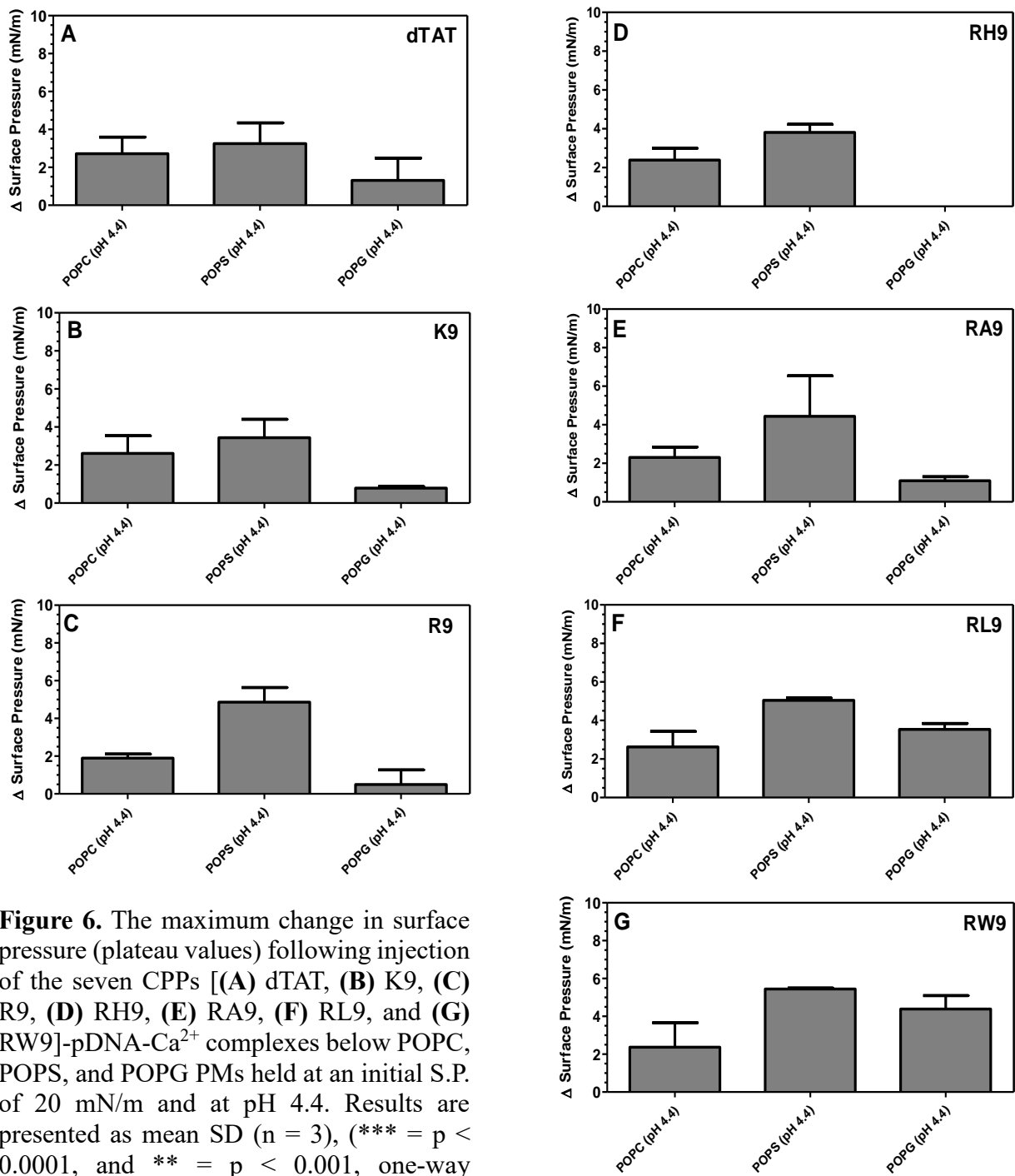


Figure 6. The maximum change in surface pressure (plateau values) following injection of the seven CPPs [(A) dTAT, (B) K9, (C) R9, (D) RH9, (E) RA9, (F) RL9, and (G) RW9]-pDNA-Ca²⁺ complexes below POPC, POPS, and POPG PMs held at an initial S.P. of 20 mN/m and at pH 4.4. Results are presented as mean SD (n = 3), (***) = p < 0.0001, and (**) = p < 0.001, one-way ANOVA, Tukey post-test).

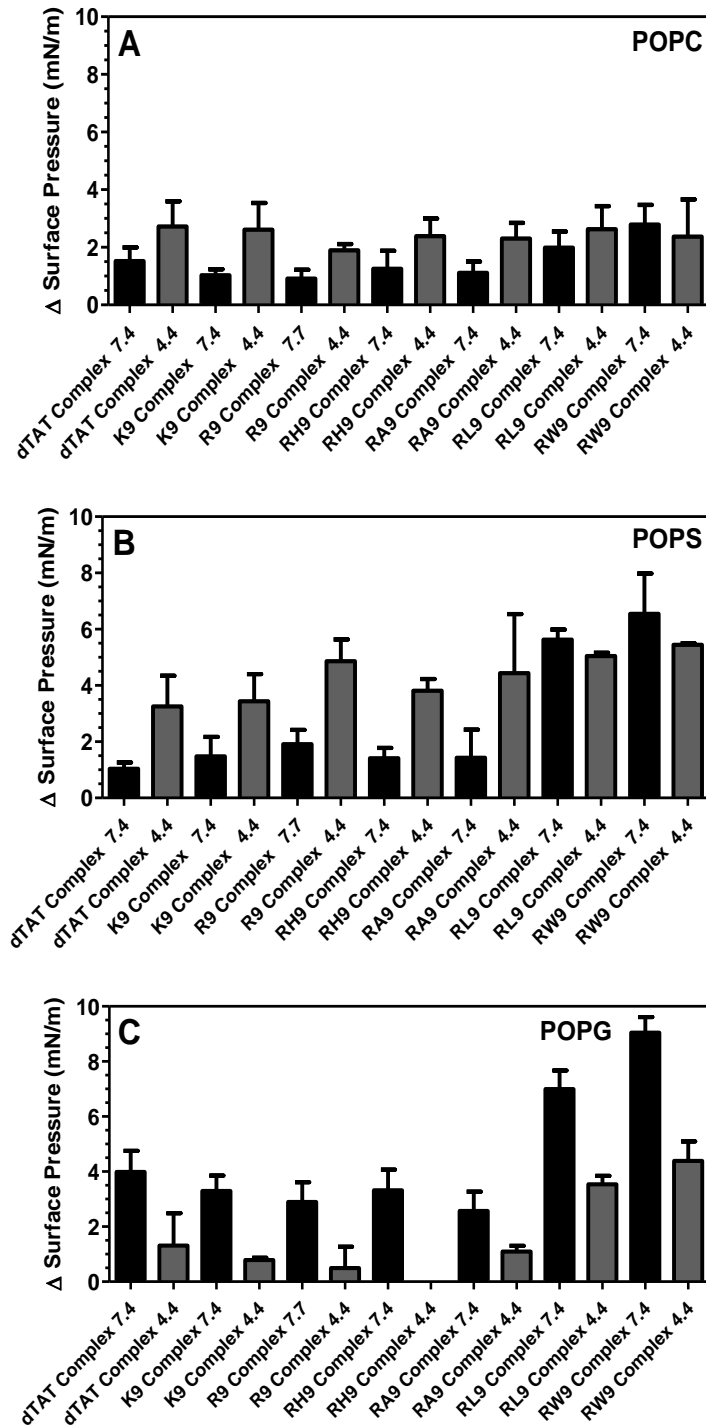


Figure 7. The maximum change in surface pressure (plateau values) of (A) POPC, (B) POPS, and (C) POPG held at an initial S.P. of 20 mN/m and at pH 7.4 and 4.4. in the presence of the seven CPPs (dTAT, K9, R9, RH9, RA9, RL9, and RW9)-pDNA-Ca²⁺ complexes. Results are presented as mean SD (n = 3).

To further understand if the insertion is due to the pDNA, the CPPs or both, we have also measured the changes in the surface pressure of the seven CPPs alone at pH 7.4 and 4.4, when injected below the POPC, POPS, and POPG monolayers (**Figure Appendix 6 and 7**). Our results are summarized in **Figure 8**, which presents a comparison of the maximum change in the S.P. of the seven complexes and the seven CPPs at pH 7.4 and 4.4. Generally, the maximum change in surface pressure of the phospholipids was found to be higher for the gene complexes compared to the free CPPs when they were injected below the anionic phospholipids (i.e., POPS and POPG) (**Figure 8B, C, E, and F**), particularly for the complexes containing amphiphilic peptides RW9 and RL9. On the other hand, no difference was noted when the different complexes were injected below the zwitterionic lipid (POPC) (**Figure 8A and D**). Since the total CPP concentration was kept constant in both the experiments (free CPPs versus condensed complexes), and we expect most of the CPP to exist as a condensed complex with the pDNA, the increase in the surface pressure of the phospholipids in the presence of gene complexes can be attributed to the presence of CPPs on the complexes.

Therefore, our results suggest that the mechanisms of interactions of gene complexes with phospholipid membranes during cellular uptake and intracellular delivery are determined by both the changes in the physical characteristics of the gene complexes as well as the phospholipid headgroup charge. Further, our results also confirm that among all the polypeptides used as CPPs, condensed complexes of pDNA with amphiphilic CPPs show the maximum membrane insertions into anionic phospholipids at normal pH. However, no difference is noted in the insertion potential of the seven peptides into zwitterionic POPC monolayers. A schematic of our proposed mechanism of gene complex action is shown in **Figure 9**. Based on our results, we propose that the CPP-pDNA complexes initially interact with the zwitterionic PC headgroups and trigger

cellular uptake, regardless of the composition of the CPP. Once endocytosed, the complexes undergo a pH induced partial disassembly of the complex. This uncondensed gene complex induces changes in the membranes, possibly by interacting with the CPP, allowing the pDNA to escape into the cytosol. Surprisingly, we found that at the more acidic pH, the insertion potential of the gene complexes did not depend on the composition of the CPPs. Analysis of kinetics of adsorption of the complexes into different phospholipid systems will provide additional understanding of the nature of the adsorption and insertion of the complexes into different monolayer systems at neutral and acidic pHs and is the topic for a future publication. The findings described here make the noncovalently condensed gene complexes interesting candidates as nonviral gene delivery vectors. Future studies will focus on *in vitro* and *in vivo* performance of these gene delivery vectors.

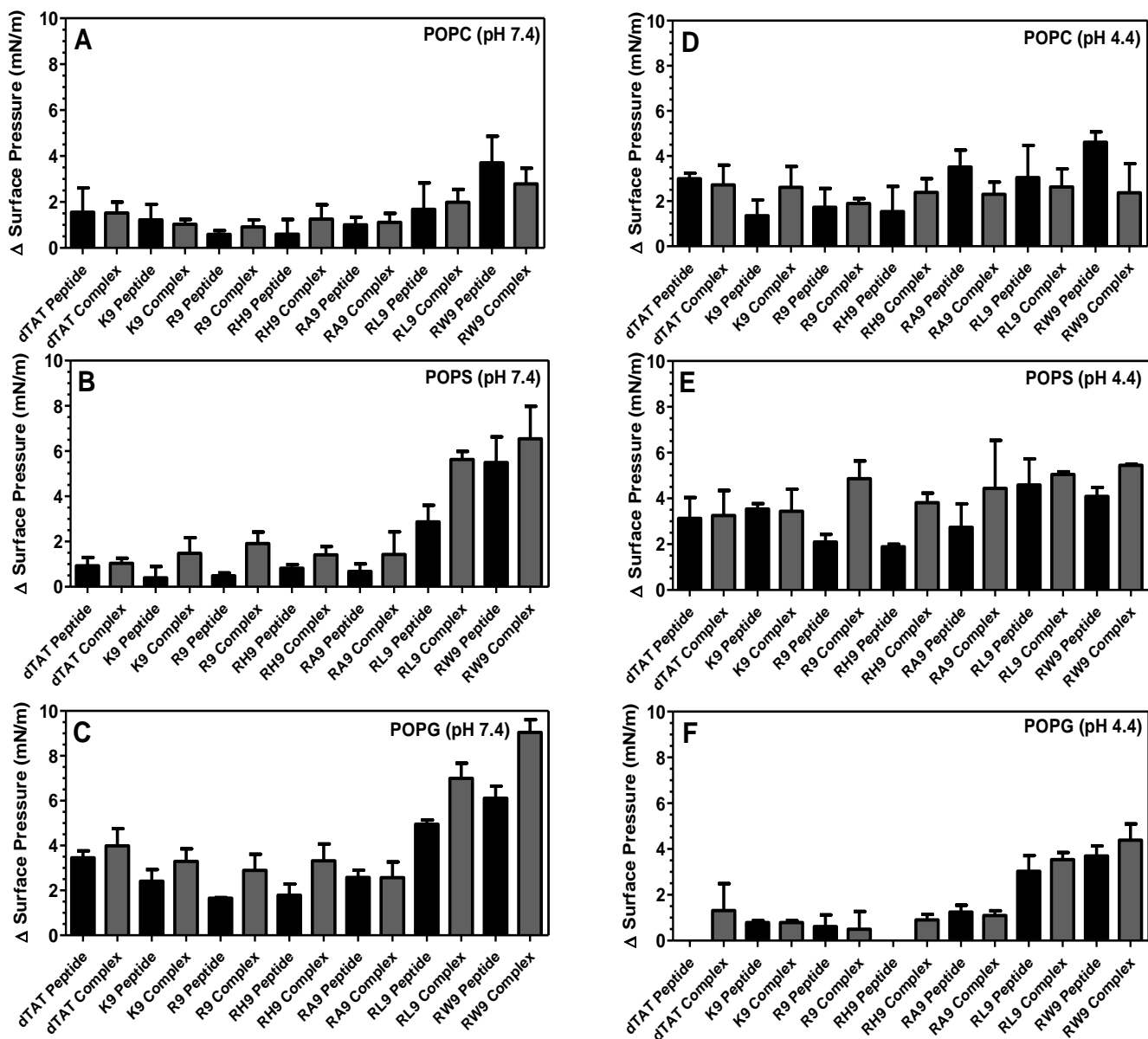


Figure 8. The maximum change in surface pressure (plateau values) of (A) POPC at pH 7.4, (B) POPS at pH 7.4, (C) POPG at pH 7.4, (D) POPC at pH 4.4, (E) POPS at pH 4.4, and (F) POPG at pH 4.4 due to interactions with the seven CPPs (dTAT, K9, R9, RH9, RA9, RL9, and RW9) and the seven CPPs (dTAT, K9, R9, RH9, RA9, RL9, and RW9)-pDNA-Ca²⁺ complexes. The initial surface pressure of the monolayers was 20 mN/m. Results are presented as mean SD (n = 3).

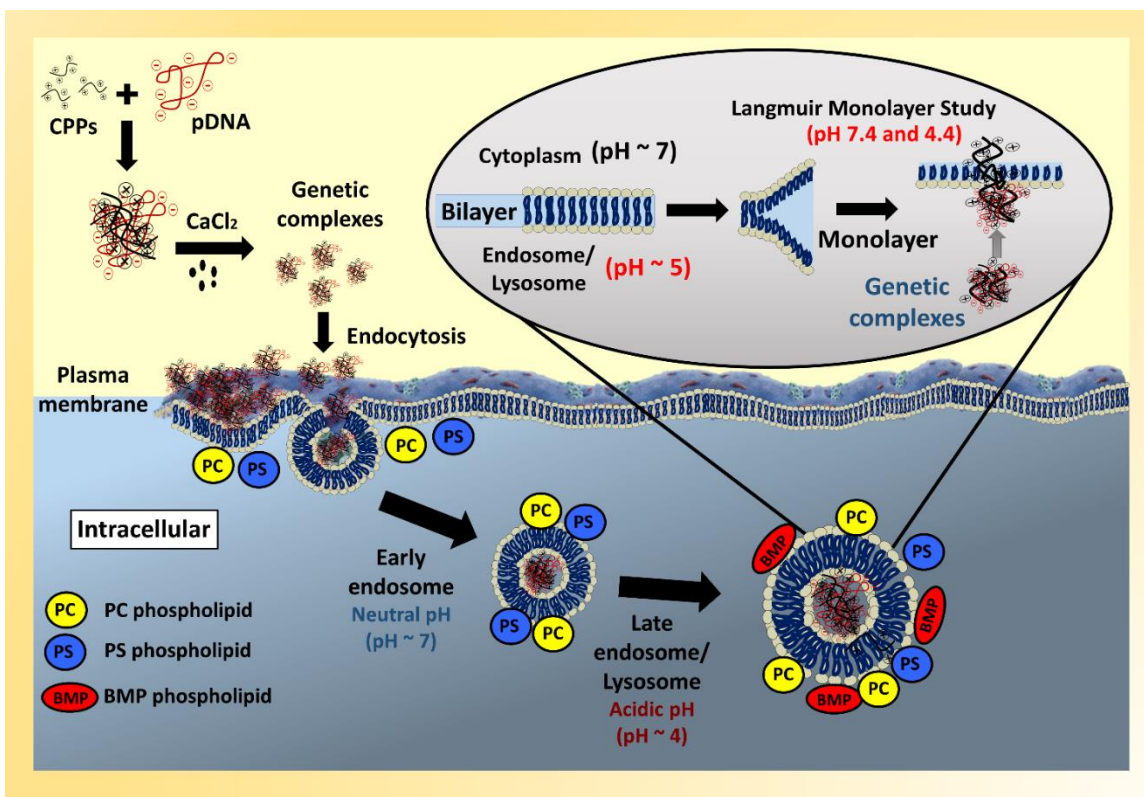


Figure 9. A schematic of our proposed mechanism of gene complex action at neutral pH (cytoplasm) and acidic pH (late endosome and lysosome).

5.4. Conclusions

Understanding the interactions of gene complexes with phospholipid membranes can be an important first step in predicting the membrane insertion efficiency of calcium condensed gene complexes containing CPPs and efficiently delivering genetic material to the cytosolic environment. In this study, phospholipid membranes POPC, POPS, and POPG have been used to study the membrane insertion of the seven CPP-pDNA-Ca²⁺ complexes, containing hydrophilic (i.e., dTAT, K9, R9, and RH9) and amphiphilic (i.e., RA9, RL9, and RW9) CPPs, at different pHs (pH 7.4 and 4.4). Our results showed that using CPPs with differences in the net charge and hydrophobicity did not alter their ability to form complexes with pDNA. In fact, the complexes had the same size at neutral pH. Further, the complexes were found to be cationic, due to an excess of the CPP during the synthesis process. However, an increase in the acidity of the environment did cause a decrease in the particle size, possibly because of partial dissociation of the gene complex, which also caused a decrease in the surface charge on the particles. Using Langmuir monolayers as our model phospholipid membranes, we also showed that there was no difference in the insertion potential of gene complexes of different composition, when interacting with a zwitterionic phospholipid at a neutral pH. However, when interacting with anionic phospholipid membranes, all complexes showed an increase in their insertion potential, although there was a significant difference in the membrane insertion potential of complexes containing amphiphilic CPPs. This suggests that while the initial interactions of our calcium condensed gene complexes with phospholipid membranes are facilitated by electrostatic interactions, the hydrophobic amino acids further facilitated membrane insertion. However, in more acidic environments such as those in the intracellular vesicles (endosomes/lysosomes) all gene complexes show a greater insertion into the POPC and POPS membranes, irrespective of the composition. Since both POPC and POPS

are zwitterionic at the acidic pH, we conclude that the acidic pH induced an increase in the size of the gene complexes possibly due to a reversal of the condensing effect of Ca^{2+} . This increase in the complex size may trigger the disturbance and even disruption of endosomal membranes, leading to escape of the genetic payload into the cytosol. In conclusion, the Langmuir monolayer technique can help to determine the type and degree of interaction of gene complexes with membrane systems. We believe that measuring the insertion potential of gene complexes into model membranes will serve as a screening method to test the potential insertion ability of gene complexes, before they are tested in cells or in more involved therapeutic situations. Our results also suggest that overall, designing gene complexes with amphiphilic peptides may not necessarily demonstrate more transfection efficiency, because of the differences in the insertion potential of the amphiphilic peptides at neutral and acidic pH, even though the amphiphilic peptides have the potential to disrupt anionic membranes at neutral pH. However, additional experiments with *in vitro* cell assays are essential to obtain a complete understanding on the mechanism of action of the full transfection mechanism. Ultimately, our results will aid in the design of the next generation of CPP based nonviral gene complexes and is a first step in our overall goal of using short synthetic CPPs for efficient intracellular delivery of nucleic acids. Further, our results also propose the potential of synthetic CPPs with hydrophobic amino acid sequences for use in designing anti-bacterial membranes, where the CPPs will interact with anionic PG headgroups and may enable membrane disruptions.

5.5. References

1. Doherty, G. J.; McMahon, H. T. Mechanisms of endocytosis. *Annual review of biochemistry* **2009**, *78*, 857-902.
2. Alhakamy, N. A.; Kaviratna, A.; Berkland, C. J.; Dhar, P. Dynamic Measurements of Membrane Insertion Potential of Synthetic Cell Penetrating Peptides. *Langmuir* **2013**, *29*, (49), 15336-15349.
3. Figueiredo, I. R.; Freire, J. M.; Flores, L.; Veiga, A. S.; Castanho, M. A. Cell-penetrating peptides: A tool for effective delivery in gene-targeted therapies. *IUBMB life* **2014**, *66*, (3), 182-194.
4. Margus, H.; Padari, K.; Pooga, M. Cell-penetrating peptides as versatile vehicles for oligonucleotide delivery. *Molecular Therapy* **2012**, *20*, (3), 525-533.
5. Nakamura, Y.; Kogure, K.; Futaki, S.; Harashima, H. Octaarginine-modified multifunctional envelope-type nano device for siRNA. *Journal of controlled release* **2007**, *119*, (3), 360-367.
6. Baoum, A. A.; Berkland, C. Calcium condensation of DNA complexed with cell-penetrating peptides offers efficient, noncytotoxic gene delivery. *Journal of pharmaceutical sciences* **2011**, *100*, (5), 1637-1642.
7. Yang, S.-T.; Zaitseva, E.; Chernomordik, L. V.; Melikov, K. Cell-penetrating peptide induces leaky fusion of liposomes containing late endosome-specific anionic lipid. *Biophysical journal* **2010**, *99*, (8), 2525-2533.
8. Belting, M.; Wittrup, A. Macromolecular drug delivery: basic principles and therapeutic applications. *Molecular biotechnology* **2009**, *43*, (1), 89-94.

9. Chen, H. H.; Ho, Y.-P.; Jiang, X.; Mao, H.-Q.; Wang, T.-H.; Leong, K. W. Quantitative comparison of intracellular unpacking kinetics of polyplexes by a model constructed from quantum dot-FRET. *Molecular Therapy* **2008**, *16*, (2), 324-332.
10. Karagiannis, E. D.; Alabi, C. A.; Anderson, D. G. Rationally Designed Tumor-Penetrating Nanocomplexes. *ACS nano* **2012**, *6*, (10), 8484-8487.
11. Khondee, S.; Baoum, A.; Siahaan, T. J.; Berkland, C. Calcium condensed LABL-TAT complexes effectively target gene delivery to ICAM-1 expressing cells. *Molecular pharmaceutics* **2011**, *8*, (3), 788-798.
12. Alhakamy, N. A.; Nigatu, A. S.; Berkland, C. J.; Ramsey, J. D. Noncovalently associated cell-penetrating peptides for gene delivery applications. *Therapeutic delivery* **2013**, *4*, (6), 741-757.
13. Chen, S.; Han, K.; Yang, J.; Lei, Q.; Zhuo, R.-X.; Zhang, X.-Z. Bioreducible Polypeptide Containing Cell-Penetrating Sequence for Efficient Gene Delivery. *Pharmaceutical research* **2013**, *30*, (8), 1968-1978.
14. Baoum, A.; Xie, S.-X.; Fakhari, A.; Berkland, C. “Soft” Calcium Crosslinks Enable Highly Efficient Gene Transfection Using TAT Peptide. *Pharmaceutical research* **2009**, *26*, (12), 2619-2629.
15. Hullin-Matsuda, F.; Taguchi, T.; Greimel, P.; Kobayashi, T. In *Lipid compartmentalization in the endosome system*, Seminars in cell & developmental biology, 2014; Elsevier.
16. Zaitseva, E.; Yang, S.-T.; Melikov, K.; Pourmal, S.; Chernomordik, L. V. Dengue virus ensures its fusion in late endosomes using compartment-specific lipids. *PLoS pathogens* **2010**, *6*, (10), e1001131.

17. Alhakamy, N. A.; Berkland, C. J. Polyarginine molecular weight determines transfection efficiency of calcium condensed complexes. *Molecular pharmaceutics* **2013**, *10*, (5), 1940-1948.
18. Ziegler, A.; Li Blatter, X.; Seelig, A.; Seelig, J. Protein transduction domains of HIV-1 and SIV TAT interact with charged lipid vesicles. Binding mechanism and thermodynamic analysis. *Biochemistry* **2003**, *42*, (30), 9185-9194.
19. Lindgren, M.; Hällbrink, M.; Prochiantz, A.; Langel, Ü. Cell-penetrating peptides. *Trends in pharmacological sciences* **2000**, *21*, (3), 99-103.
20. Baoum, A.; Ovcharenko, D.; Berkland, C. Calcium condensed cell penetrating peptide complexes offer highly efficient, low toxicity gene silencing. *International journal of pharmaceutics* **2012**, *427*, (1), 134-142.
21. Wagstaff, K. M.; Jans, D. A. Protein transduction: cell penetrating peptides and their therapeutic applications. *Current medicinal chemistry* **2006**, *13*, (12), 1371-1387.
22. Witte, K.; Olausson, B. E.; Walrant, A.; Alves, I. D.; Vogel, A. Structure and dynamics of the two amphipathic arginine-rich peptides RW9 and RL9 in a lipid environment investigated by solid-state NMR and MD simulations. *Biochimica et Biophysica Acta (BBA)-Biomembranes* **2012**.
23. Järver, P.; Langel, Ü. Cell-penetrating peptides—a brief introduction. *Biochimica et Biophysica Acta (BBA)-Biomembranes* **2006**, *1758*, (3), 260-263.
24. Deshayes, S.; Morris, M.; Divita, G.; Heitz, F. Cell-penetrating peptides: tools for intracellular delivery of therapeutics. *Cellular and Molecular Life Sciences CMLS* **2005**, *62*, (16), 1839-1849.
25. Schwieger, C.; Blume, A. Interaction of poly (l-arginine) with negatively charged DPPG membranes: calorimetric and monolayer studies. *Biomacromolecules* **2009**, *10*, (8), 2152-2161.

26. Rothbard, J. B.; Jessop, T. C.; Lewis, R. S.; Murray, B. A.; Wender, P. A. Role of membrane potential and hydrogen bonding in the mechanism of translocation of guanidinium-rich peptides into cells. *Journal of the American Chemical Society* **2004**, *126*, (31), 9506-9507.
27. Futaki, S. Oligoarginine vectors for intracellular delivery: Design and cellular-uptake mechanisms. *Peptide Science* **2006**, *84*, (3), 241-249.
28. Dennison, S. R.; Phoenix, A. J.; Phoenix, D. A. Effect of salt on the interaction of Hal18 with lipid membranes. *European Biophysics Journal* **2012**, *41*, (9), 769-776.
29. Futaki, S.; Goto, S.; Sugiura, Y. Membrane permeability commonly shared among arginine-rich peptides. *Journal of Molecular Recognition* **2003**, *16*, (5), 260-264.
30. Futaki, S.; Nakase, I.; Tadokoro, A.; Takeuchi, T.; Jones, A. Arginine-rich peptides and their internalization mechanisms. *Biochemical Society Transactions* **2007**, *35*, (4), 784.
31. Witte, K.; Olausson, B. E.; Walrant, A.; Alves, I. D.; Vogel, A. Structure and dynamics of the two amphipathic arginine-rich peptides RW9 and RL9 in a lipid environment investigated by solid-state NMR and MD simulations. *Biochimica et Biophysica Acta (BBA)-Biomembranes* **2013**, *1828*, (2), 824-833.
32. Kawabata, A.; Baoum, A.; Ohta, N.; Jacquez, S.; Seo, G.-M.; Berkland, C.; Tamura, M. Intratracheal administration of a nanoparticle-based therapy with the angiotensin II type 2 receptor gene attenuates lung cancer growth. *Cancer research* **2012**, *72*, (8), 2057-2067.
33. Zaitsev, S.; Haberland, A.; Otto, A.; Vorob'ev, V.; Haller, H.; Böttger, M. H1 and HMG17 extracted from calf thymus nuclei are efficient DNA carriers in gene transfer. *Gene therapy* **1997**, *4*, (6).

34. Khosravi-Darani, K.; Mozafari, M. R.; Rashidi, L.; Mohammadi, M. Calcium based non-viral gene delivery: an overview of methodology and applications. *Acta Med. Iran* **2010**, *48*, (3), 133-141.
35. Jiao, C.-Y.; Delaroche, D.; Burlina, F.; Alves, I. D.; Chassaing, G.; Sagan, S. Translocation and endocytosis for cell-penetrating peptide internalization. *Journal of Biological Chemistry* **2009**, *284*, (49), 33957-33965.
36. Blume, A. A comparative study of the phase transitions of phospholipid bilayers and monolayers. *Biochimica et Biophysica Acta (BBA)-Biomembranes* **1979**, *557*, (1), 32-44.
37. Joanne, P.; Galanth, C.; Goasdoué, N.; Nicolas, P.; Sagan, S.; Lavielle, S.; Chassaing, G.; El Amri, C.; Alves, I. D. Lipid reorganization induced by membrane-active peptides probed using differential scanning calorimetry. *Biochimica et Biophysica Acta (BBA)-Biomembranes* **2009**, *1788*, (9), 1772-1781.
38. Bally, M. B.; Harvie, P.; Wong, F. M.; Kong, S.; Wasan, E. K.; Reimer, D. L. Biological barriers to cellular delivery of lipid-based DNA carriers. *Advanced drug delivery reviews* **1999**, *38*, (3), 291-315.
39. Peetla, C.; Jin, S.; Weimer, J.; Elegbede, A.; Labhasetwar, V. Biomechanics and Thermodynamics of Nanoparticle Interactions with Plasma and Endosomal Membrane Lipids in Cellular Uptake and Endosomal Escape. *Langmuir* **2014**, *30*, (25), 7522-7532.
40. Loyter, A.; Scangos, G. A.; Ruddle, F. H. Mechanisms of DNA uptake by mammalian cells: fate of exogenously added DNA monitored by the use of fluorescent dyes. *Proceedings of the National Academy of Sciences* **1982**, *79*, (2), 422-426.

41. Haberland, A.; Knaus, T.; Zaitsev, S. V.; Stahn, R.; Mistry, A. R.; Coutelle, C.; Haller, H.; Böttger, M. Calcium ions as efficient cofactor of polycation-mediated gene transfer. *Biochimica et Biophysica Acta (BBA)-Gene Structure and Expression* **1999**, *1445*, (1), 21-30.
42. Bisht, S.; Bhakta, G.; Mitra, S.; Maitra, A. pDNA loaded calcium phosphate nanoparticles: highly efficient non-viral vector for gene delivery. *International journal of pharmaceutics* **2005**, *288*, (1), 157-168.
43. Eeman, M.; Deleu, M. From biological membranes to biomimetic model membranes. *Base* **2010**, *14*, 719-736.
44. Zhang, L.; Rozek, A.; Hancock, R. E. Interaction of cationic antimicrobial peptides with model membranes. *Journal of Biological Chemistry* **2001**, *276*, (38), 35714-35722.
45. Song, C.; Nerdal, W. Olanzapine interaction with dipalmitoyl phosphatidylcholine (DPPC) and 1-palmitoyl-2-oleoyl phosphatidylserine (POPS) bilayer: A ¹³C and ³¹P solid-state NMR study. *Biophysical chemistry* **2008**, *134*, (1), 47-55.
46. Van Meer, G.; Voelker, D. R.; Feigenson, G. W. Membrane lipids: where they are and how they behave. *Nature reviews molecular cell biology* **2008**, *9*, (2), 112-124.
47. Leventis, P. A.; Grinstein, S. The distribution and function of phosphatidylserine in cellular membranes. *Annual review of biophysics* **2010**, *39*, 407-427.
48. Bouvier, J.; Berry, K. A. Z.; Hullin-Matsuda, F.; Makino, A.; Michaud, S.; Geloën, A.; Murphy, R. C.; Kobayashi, T.; Lagarde, M.; Delton-Vandenbroucke, I. Selective decrease of bis (monoacylglycero) phosphate content in macrophages by high supplementation with docosahexaenoic acid. *Journal of lipid research* **2009**, *50*, (2), 243-255.

49. Meikle, P.; Duplock, S.; Blacklock, D.; Whitfield, P.; Macintosh, G.; Hopwood, J.; Fuller, M. Effect of lysosomal storage on bis (monoacylglycero) phosphate. *Biochem. J* **2008**, *411*, 71-78.
50. Hullin-Matsuda, F.; Kawasaki, K.; Delton-Vandenbroucke, I.; Xu, Y.; Nishijima, M.; Lagarde, M.; Schlame, M.; Kobayashi, T. De novo biosynthesis of the late endosome lipid, bis (monoacylglycero) phosphate. *Journal of lipid research* **2007**, *48*, (9), 1997-2008.
51. Frederick, T. E.; Goff, P. C.; Mair, C. E.; Farver, R. S.; Long, J. R.; Fanucci, G. E. Effects of the endosomal lipid bis (monoacylglycero) phosphate on the thermotropic properties of DPPC: A 2H NMR and spin label EPR study. *Chemistry and physics of lipids* **2010**, *163*, (7), 703-711.
52. Frederick, T. E.; Chebukati, J. N.; Mair, C. E.; Goff, P. C.; Fanucci, G. E. Bis (monoacylglycero) phosphate Forms Stable Small Lamellar Vesicle Structures: Insights into Vesicular Body Formation in Endosomes. *Biophysical Journal* **2009**, *96*, (5), 1847.
53. Urbina, P.; Flores-Díaz, M.; Alape-Girón, A.; Alonso, A.; Goñi, F. M. Effects of bilayer composition and physical properties on the phospholipase C and sphingomyelinase activities of *Clostridium perfringens* α -toxin. *Biochimica et Biophysica Acta (BBA)-Biomembranes* **2011**, *1808*, (1), 279-286.
54. Gromelski, S.; Brezesinski, G. DNA condensation and interaction with zwitterionic phospholipids mediated by divalent cations. *Langmuir* **2006**, *22*, (14), 6293-6301.
55. Travkova, O. G.; Brezesinski, G. Adsorption of the antimicrobial peptide arenicin and its linear derivative to model membranes—A maximum insertion pressure study. *Chemistry and physics of lipids* **2013**, *167*, 43-50.

56. Zhang, S.; Nelson, A.; Coldrick, Z.; Chen, R. The effects of substituent grafting on the interaction of pH-responsive polymers with phospholipid monolayers. *Langmuir* **2011**, *27*, (13), 8530-8539.
57. Marsh, D. CRC handbook of lipid bilayers. *CRC Press: Boca Raton, FL* **1990**.
58. Tatur, S.; Maccarini, M.; Barker, R.; Nelson, A.; Fragneto, G. Effect of functionalized gold nanoparticles on floating lipid bilayers. *Langmuir* **2013**, *29*, (22), 6606-6614.

Chapter 6

Charge Type, Charge Spacing, and Hydrophobicity of Arginine-Rich Cell-Penetrating Peptides Dictate Gene Transfection

Published as:

Alhakamy, N. A.; Dhar, P.; Berkland, C. J. Charge Type, Charge Spacing, and Hydrophobicity of Arginine-Rich Cell Penetrating Peptides Dictate Gene Transfection. Molecular pharmaceuticals 2016. (2016)

6.1. Introduction

Gene therapy has become an auspicious strategy for the treatment of several diseases (e.g., hemophilia and cancer) that are considered incurable¹. The poor permeability of nucleic acids (e.g., pDNA and RNAi) as well as their sensitivity to enzymatic degradation considerably complicates the development of most gene therapies. The success of gene therapy largely depends on the design of safe and efficient gene vectors²⁻⁶. Viral vectors have dominated clinical applications, but nonviral vectors offer advantages such as the potential for biological safety, ease of synthesis, relatively unrestricted nucleic acid size for packing, low-cost, and potential low degrees of immunogenicity compared to viruses^{1,5-9}. Unfortunately, the use of nonviral vectors is still hindered by their lower transfection levels compared to viral vectors¹. Numerous methods have been studied to overcome this problem. Among them, cell penetrating peptides (CPPs), which consist of cationic or amphiphilic sequences of about 30 or fewer amino acids, seem particularly promising^{8,10,11}.

Several colloid properties such as molecular weight, charge, and colloidal stability can affect the efficiency of gene delivery systems. In the case of polyelectrolyte nanoparticles, these properties are influenced by polycations. High-molecular-weight polycations often condense a large mass of genetic material (pDNA) into small and stable nanoparticles with high transfection efficiency. Unfortunately, these polycations have been plagued with cytotoxicity¹². On the other hand, low-molecular-weight polycations often produce large and unstable complexes with poor transfection efficiency, but with low cytotoxicity¹³⁻¹⁶. Furthermore, the structure of the protonated group and charge spacing can influence the ability of CPPs to protect and complex with nucleic acids^{17,18}. Two main approaches have indicated the efficient use of CPPs to deliver nucleic acids. The first approach uses linkers to covalently bind CPPs to their cargo, and the second approach

depends on electrostatic interactions (ionic interactions) to form complexes between CPPs and their cargo⁸. The risk of reducing the activity of the CPPs may limit the benefit of the covalent approach^{8,19}.

Polyarginine peptide is one of the widest cationic peptides used for gene delivery¹². Many studies have suggested that CPPs with 7 to 9 amino acids have optimal cell penetration efficiency^{20,21}. We have established that low-molecular-weight polyarginine peptides (e.g., polyarginine R9) are efficient for gene delivery and can condense pDNA into small nanoparticles (~150 nm) when calcium chloride (CaCl₂) is added^{5, 9, 22-26}. Calcium condensation of polyplexes is reversible, allowing the release of low-molecular-weight CPPs such as polyarginine R9 at low pH, which may increase membrane permeability within the cell^{5, 12, 25, 27}. Although the role of calcium in the transfection mechanism is ambiguous, these studies encouraged exploration of calcium with complexes formed from a diverse panel of hydrophilic and amphiphilic CPPs.

In this study, the transfection efficiency of pDNA polyelectrolyte complex nanoparticles made using five different arginine-rich CPPs was investigated. CPPs included the well-known hydrophilic polyarginine R9 peptide (RRRRRRRRR), a hydrophilic RH9 peptide (RRHRRHRR), and three amphiphilic peptides with similar charge distributions; RA9 (RRAARRARR), RL9 (RRLRLRLR), and RW9 (RRWRRWR) (**Table 1**). The RL9 and RW9 peptides originate from RL16 peptide (RRLRLLRLLRRLR) and RW16 peptide (RRWRRWRRWRRWRR) respectively. RL9 and RW9 peptides were originally designed from a structure/function study of penetratin²⁸. The five arginine-rich CPPs (R9, RH9, RA9, RL9, and RW9) share a common high density of arginine residues providing nine positive charges to R9 and six positive charges to RH9, RA9, RL9, and RW9 at neutral pH. It has also been established that the penetration efficiency of CPPs increases with increased tryptophan content. Additionally,

the CPP activity is more efficient if the tryptophan residues are located in the center of the CPP sequences than if they are placed at the N-terminus ^{12, 16, 18}. Many studies also reported that RW9 is efficiently internalized into cells ^{16, 29}.

Our previous studies have shown that RL9 and RW9 peptides and RL9-pDNA-Ca²⁺ or RW9-pDNA-Ca²⁺ complexes strongly penetrated model cell membranes and also induced the maximum changes in phospholipid packing compared to R9, RA9, and RH9 peptides or complexes made using these peptides ^{16, 18}. Here, we determined how these changes in CPP charge type, charge spacing, and hydrophobicity affected the transfection efficiency of the five CPP-pDNA-Ca²⁺ complexes. The five CPPs were complexed with pDNA and condensed with CaCl₂ to form small complexes. This simple formulation was explored using two human cell lines: 1) HEK-293 kidney and 2) A549 lung cancer cells using a luciferase reporter plasmid (pGL3) to assess the relationship between CPP structure and transfection efficiency.

Table 1. Identification of the Five CPPs and Their Properties: Peptide Sequence, the Number of Residues, Classification, Molecular Weight, Net Charge at pH 7, and Sequence Composition.

Name	Interpreted Sequence	Number of Residues	Classification	Molecular Weight (g/mol)	Net Charge at pH 7	Sequence Composition (in percentage) *	
						Hydrophobic	Basic
R9	RRRRRRRRR	9	Hydrophilic	1422.74	9	0	100
RH9	RRHRRHRR	9	Hydrophilic	1365.62	6.3	0	100
RA9	RRAARRARR	9	Amphiphilic	1167.41	6	33.33	66.67
RL9	RLLRRLRR	9	Amphiphilic	1293.68	6	33.33	66.67
RW9	RRWRRWRR	9	Amphiphilic	1512.83	6	33.33	66.67

* Hydrophobic/ Neutral amino acid % = (Nx/N)*100, Nx: Number of hydrophobic/ neutral amino acid residues present in the input sequence. N: Input sequence length (net charge at neutral pH).

6.2. Materials and Methods

6.2.1. Materials

Plasmid DNA (pDNA) encoding firefly luciferase (pGL3, 4818 bp) was purchased from Promega (Madison, Wisconsin). The pDNA purity level was determined by UV-spectroscopy and agarose gel electrophoresis. R9 peptide (RRRRRRRRR; $M_w = 1422.74$ Da), RH9 peptide (RRHHRRHRR; $M_w = 1365.62$ Da), RA9 peptide (RRA ARRARR; $M_w = 1167.41$ Da), RL9 peptide (RLLRRLRR; $M_w = 1293.68$ Da), and RW9 peptide (RRWWRRWRR; $M_w = 1512.83$ Da) (the C-terminal of the five peptides is synthesized as an amide) were obtained from Biomatik Corporation (Cambridge, Ontario, Canada) (Purity > 95%). Branched polyethylenimine (PEI, 25 kDa) was purchased from Sigma-Aldrich (Milwaukee, Wisconsin). A549 cell line (carcinogenic human alveolar basal epithelial) was purchased from American Type Culture Collection (ATCC; Rockville, Maryland). HEK-293 (human embryonic kidney) cell line was a gift from Dr. Cheng Lab (Nikki Cheng, Ph.D, University of Kansas Medical Center, Department of Pathology and Laboratory Medicine (obtained from American Type Culture Collection [ATCC; Rockville, Maryland])). F-12K Nutrient Mixture, Kaighn's modified with L-glutamine was purchased through Cellgro (Mediatech, Inc., Manassas, VA). Dulbecco's Modified Eagle's Medium (DMEM) was obtained from Invitrogen/Life Technologies (Gibco®) (Grand Island, NY 14072, USA). Fetal bovine serum (FBS) was purchased from Hyclone (Logan, UT). Penicillin-streptomycin was obtained from MB Biomedical, LLC (Solon, OH). Trypsin-EDTA was purchased from Invitrogen (Carlsbad, CA). Luciferase Assay System Freezer Pack and CellTiter 96® AQueous one solution cell proliferation assay (MTS) were purchased from Promega (Madison, Wisconsin). BCA Protein Assay Reagent (bicinchoninic acid) was purchased from Thermo Fisher Scientific Inc. Tris-acetate-EDTA (TAE) Buffer (10 x) was purchased from Promega (Madison, Wisconsin). Sterile

water (DNase, RNase-free) was purchased from Fisher Scientific. Calcium chloride dihydrate ($\text{CaCl}_2 \cdot 2\text{H}_2\text{O}$) was purchased from Fisher Scientific. Agarose (Medium-EEO/protein electrophoresis grade) was obtained from Fisher Scientific. BenchTop DNA Ladder was obtained from Promega (Madison, WI). SYBR Green I Nucleic Acid Gel Stain was obtained from Invitrogen (Carlsbad, CA). Dextran Sulfate Sodium Salt was purchased from Fisher Scientific. Other organic chemicals used for this work were obtained from Fisher Scientific. Gelatin solution (Type B, 2% in H_2O , tissue culture grade, sterile, BioReagent, suitable for cell culture) was purchased from Sigma-Aldrich (Milwaukee, Wisconsin). 1-Hexadecanoyl-2-(9Z-octadecenoyl)-sn-glycero-3 phosphocholine (sodium salt) (POPC), 1-palmitoyl-2-oleoyl-sn-glycero-3-phospho-L-serine (sodium salt) (POPS), and 1-palmitoyl-2-oleoyl-sn-glycero-3-phospho-(1'-rac-glycerol) (sodium salt) (POPG) were purchased from Avanti Polar Lipids (Alabaster, AL) as organic mixtures in chloroform. Agarose (medium-EEO/protein electrophoresis grade) was purchased from Fisher Scientific.

6.2.2. Methods

6.2.2.1. Nanoparticle Formation

CPP-pDNA- Ca^{2+} nanoparticles were prepared by adding 15 μL of the CPP solution (N/P ratios: 5, 10, 20, and 30 represent different polymer nitrogen to pDNA phosphate (N/P), molar ratios) to 10 μL (0.1 $\mu\text{g}/\mu\text{L}$) of pDNA (TAE Buffer (1x) was used as a solution for DNA storage), followed by repeated pipetting for 20 to 25 seconds. At that point, 15 μL of CaCl_2 (0, 50, 100, or 300 mM) was added and mixed by pipetting. After formulating the complexes, they were stored at 4°C for ~20 minutes. PEI-pDNA complexes were prepared by adding 15 μL of PEI solution (N/P ratio 10) to 10 μL (0.1 $\mu\text{g}/\mu\text{L}$) of pDNA followed by fast pipetting for 20 to 25 seconds. After preparing the

complexes, they were stored at 4°C for ~20 minutes. All complexes were prepared immediately before each experiment.

6.2.2.2. Agarose Gel Electrophoresis

Complexes were prepared as defined previously and subsequently, 4 µL of Tris-acetate-EDTA (TAE) buffer were added. Then, 4 µL of SYBR Green 1 was mixed with the complexes. Afterward, the mixture was stored at 4°C for 20 to 25 minutes. Then, 7 µL of 6X DNA Loading dye were added. A one kb DNA ladder was used. The mixture solutions were loaded onto a 1% agarose gel, and electrophoresed for 30 minutes at 110V.

6.2.2.3. Size and Zeta Potential

The particle size (effective diameter (nm)) of CPP-pDNA complexes with or without CaCl₂ was determined by dynamic light scattering (DLS, Brookhaven Instruments, Holtsville, NY). The zeta potentials of the complexes were measured by Zeta PALS dynamic light scattering (Brookhaven Instrument, Holtsville, NY). All samples intended for particle size measurements were prepared using phosphate buffered saline (PBS), serum-free media (SFM) and nuclease free water (NFW). All samples intended for zeta potential measurements were prepared using KCl (1 mM).

6.2.2.4. Cell Culture

HEK-293 and A549 cell lines were grown in F-12K Nutrient Mixture media (Kaighn's modified with L-glutamine, for A549) and Dulbecco's Modified Eagle's Medium (DMEM, for HEK-293) with 1% (v/v) Penicillin-streptomycin and 10% (v/v) fetal bovine serum (FBS) at 37°C in 5% CO₂ humidified air.

6.2.2.5. Transfection Studies

HEK-293 and A549 cell lines were cultured in 96-well plates for 24 hours prior to transfection. The concentration of the cells in every well was approximately 800,000 cells/mL. The wells were washed once with serum-free media (SFM) and later a 100 µL sample (which consisted of 20 µL

of the complexes and 80 μ L of SFM) was added to each well. Then, a 96-well plate was incubated for 5 hours in an incubator. After the incubation, the sample was replaced with 100 μ L of fresh serum medium and then incubated again for approximately 48 hours. Our previous studies indicated that serum did not significantly inhibit the transfection mediated by CPPs (e.g. R9)-Ca-pDNA complexes (a slight decrease in transfection efficiency was observed)^{9,24}.

To determine the gene expression of the complexes, the Luciferase Reporter Assay from Promega was used. The results of the transfections were expressed as relative light units (RLU) per milligram (mg) of cellular protein, and PEI-pDNA was used as a control. BCA Protein Assay Reagent (bicinchoninic acid) was used to measure total cellular protein concentration in the cell extracts. The Luciferase Assay and BCA were measured by a microplate reader (SpectraMax; Molecular Devices Croyce, CA). HEK-293 cells are semiadherent, and can easily lift from the growth surface during the transfection assays that required multiple washes. Gelatin solution was used to coat the 96-well plate for the culture of HEK-293 cells. The wells were washed once with sterile water and later 300 μ L of 2% (w/v) gelatin solution was added to each well. Then, the plate was incubated for 1 hour in an incubator (37°C). The wells were washed two times with sterile water. After washing, the plate was left to dry in TC hood (LABCONCO Purifier Class II Biosafety Cabinet) for 30 to 60 minutes before use.

6.2.2.6. Cytotoxicity Assay

Cytotoxicity of CPPs, PEI, and CaCl₂ was determined using a CellTiter 96® Aqueous Non-Radioactive Cell Proliferation Assay (MTS) obtained from Promega (Madison, Wisconsin). HEK-293 and A549 cells were cultured in a 96-well plate as described previously. Cells were treated with the samples for ~24 hours. After the incubation, the media were replaced with a mixture of 100 μ L of fresh serum medium and 20 μ L of MTS. Then, the plate was incubated for 3 to 4 hours

in the incubator. To determine cell viability, the absorbance of each well was measured by a microplate reader (SpectraMax; Molecular Devices Crope, CA) at 490 nm and normalized to untreated control cells.

6.2.2.7. SYBR Green Assay

The degree of pDNA accessibility following complexation with the five CPPs or PEI was assessed by the double-stranded-DNA-binding reagent SYBR Green (Invitrogen). Briefly, 10 μL (0.1 mg/mL) of pDNA was mixed with 15 μL of CPPs or PEI solution, then 15 μL of deionized water or CaCl_2 solution were added. The complexes were allowed to form for 30 minutes at room temperature prior to use. After incubation, 120 μL of PBS and 160 μL of 10X SYBR Green solutions were added. Then, 100 μL of the sample were added to one well of a 96-well cell culture plate. The fluorescence was measured using a fluorescence plate reader (SpectraMax M5; Ex., 250 nm; Em, 520 nm).

6.2.2.8. The Effect of Dextran Sulfate on the Stability of CPPs and PEI Nanoparticles

The effect of dextran sulfate on the stability of complexes was evaluated by means of the change in fluorescence intensity obtained with the fluorescent probe SYBR Green. R9, RH9, RA9, RL9, RW9, and PEI complexes were prepared with or without CaCl_2 (300 mM) as described above. Dextran sulfate solution (120 μL) was added to complexes suspensions to yield final concentrations up to 50 $\mu\text{g}/\mu\text{L}$, then incubated for 30 minutes at room temperature before 160 μL 10X SYBR Green were added. Three samples (80 μL) of each sample of each test article were added to a 96-well plate and the fluorescence was measured (SpectraMax M5; Ex., 250 nm; Em, 520 nm) to determine the accessibility of pDNA.

6.2.2.9. Langmuir Trough Experiments

The surface pressure (Langmuir trough) experiments were described in detail previously^{16, 18}. The surface pressure changes were recorded by a Wilhelmy plate sensor, which is part of the KSV-NIMA Langmuir trough purchased from Biolin Scientific, and petri dishes (volume 4 ml, 35 x 10) were used as “mini-troughs” for the experiments. A Langmuir monolayer approach was used to determine the differences in the ability of the CPPs and complexes to penetrate into cell membranes. Phospholipid monolayers with varying composition and headgroup charges, representing one leaflet of a cell membrane, were used as model membranes. Penetration to a phospholipid membrane is typically recorded by a constant area method. In this method, the surface pressure (millinewton per meter (mN/m)) of the phospholipid monolayer is fixed. Membrane penetration of injected CPPs or complexes is accompanied by an increase in the surface pressure, because the area of the trough surface is kept constant. The penetration of the CPPs or complexes is expected to alter the monolayer packing. Here, the penetration potential of the different CPPs and complexes was measured using model phospholipid monolayers containing different amounts of a zwitterionic (1-palmitoyl-2-oleoyl-sn-glycero-3-phosphocholine [POPC]) or negatively charged phospholipids (1-palmitoyl-2-oleoyl-sn-glycero-3-phospho-L-serine [POPS], and 1-palmitoyl-2-oleoyl-sn-glycero-3-phosphatidylglycerol [POPG]) at the air-PBS buffer interface.

6.2.2.10. Statistical Analysis

Data were analyzed by using GraphPad software. A statistical evaluation comparing the significance of the difference in gene expression (RLUs/mg protein) between the means of two data sets was performed using a *t* test. One-way ANOVA, Tukey post-test was used to analyze the

differences when more than two data sets were compared. The Pearson's correlation coefficient was calculated with one-tailed probability.

6.3. Results and Discussion

Five arginine-rich CPPs were studied for their ability to complex pDNA (**Table 1**). Nanoparticles were formulated at various N/P ratios (different polymer nitrogen [positive charge] to pDNA phosphate [negative charge] ratios) and then CaCl₂ was added to decrease the particle size. Agarose gel electrophoresis studies showed that some of the nanoparticles were robust enough to immobilize pDNA when complexed with the arginine-rich CPPs (**Figure 1**). Uncomplexed pDNA (free pDNA, pGL3) was used as a control. PEI complexes (without CaCl₂) and R9, RH9, and RW9 complexes (with 100 mM CaCl₂) at N/P ratio 10 immobilized pDNA (**Figure 1A**). On the other hand, RA9 and RL9 complexes exhibited some free pDNA. Additionally, CaCl₂ alone showed negligible ability to complex pDNA (without CPPs) even at a high concentration (600 mM) (**Figure 1B**). **Figures 1C to H** show the five CPP-pDNA complexes across a range of N/P ratios 1 to 5 (without CaCl₂). R9 complexes were able to immobilize pDNA completely at minimum N/P ratio 4 (**Figure 1D**). PEI and RW9 were able to immobilize pDNA completely at all N/P ratios (**Figure 1C and 1H**). RH9 complexes were able to immobilize pDNA completely at minimum N/P ratio 9 (**Figure Appendix 8A**). Clearly, RA9 and RL9 did not complex pDNA (all bands were observed during electrophoresis) at all N/P ratios (**Figure 1A, 1F, and 1G**). However, RA9 and RL9 complexes were able to immobilize pDNA completely at minimum N/P ratios 13 and 11 respectively (**Figure Appendix 8B and 8C**).

R9 and RW9 formed stable complexes with pDNA at low N/P ratios (N/P ratio 1 to 5). In addition, RH9, RA9, and RL9 (the six positive charges (amphiphilic CPP)) did not form stable

complexes at the low N/P ratios, probably due to the nine positive charges of the R9 at neutral pH compared to six positive charges for the other peptides. On the other hand, RW9 (amphiphilic with six positive charges) was able to complex pDNA. This is may be due to the aromatic ring of tryptophan interacted with pDNA or perhaps stabilized the nanoparticles *via* self-associations³⁰.

The particle size and zeta potential are important characteristics of the five CPP-pDNA- Ca^{2+} complexes. The effect of CaCl_2 concentration (0, 100, and 300 mM) on particle size was determined in nuclease free water (NFW) (**Figure 2A**), and in serum-free F-12 media (SFM) (**Figure 2B**). The CPP-pDNA- Ca^{2+} complexes generally showed a decrease in particle size as CaCl_2 concentration increased (with relatively narrow polydispersity, < 0.15) in both NFW and SFM. In comparison, PEI-pDNA complexes showed an increase in particle size as the calcium concentration increased⁹. The net positive charge of the complexes also plays a significant role in transfection efficiency that can increase the attractive force to the negative charge of the cell⁸. **Figure 2C** indicates that the zeta potential of the complexes is generally increased with higher concentration of CaCl_2 (100 and 300 mM). The net positive charge of the complexes confirms the cationic nature of the complexes and verifies that the CPPs, being in excess, form the shell of the complexes. Interestingly, PEI and R9 complexed with pDNA (without CaCl_2) at an N/P ratio of 1 had higher positive charges (~ 6 to ~ 10 mV) compared to the other complexes (RH9, RA9, RL9, and RW9), which had net negative charges (-3 to -10 mV) (**Figure 2D**). Interestingly, replacing three residues of R9 peptide with a hydrophilic (histidine) or hydrophobic residues (alanine, leucine, or tryptophan) showed the zeta potential was reduced to half.

Table 1. Identification of the five CPPs and their properties (peptide sequence, the number of residues, classification, molecular weight, net charge at pH 7, and sequence composition).

Name	Interpreted Sequence	Number of Residues	Classification	Molecular Weight (g/mol)	Net Charge at pH 7	Sequence Composition (in percentage) *	
						Hydrophobic	Basic
R9	RRRRRRRRR	9	Hydrophilic	1422.74	9	0	100
RH9	RRHHRRHRR	9	Hydrophilic	1365.62	6.3	0	100
RA9	RRAARRARR	9	Amphiphilic	1167.41	6	33.33	66.67
RL9	RRLRLRLRR	9	Amphiphilic	1293.68	6	33.33	66.67
RW9	RRWWRRWRR	9	Amphiphilic	1512.83	6	33.33	66.67

* Hydrophobic/ Neutral amino acid % = $(N_x/N) \times 100$, N_x : Number of hydrophobic/ neutral amino acid residues present in the input sequence. N: Input sequence length (net charge at neutral pH).

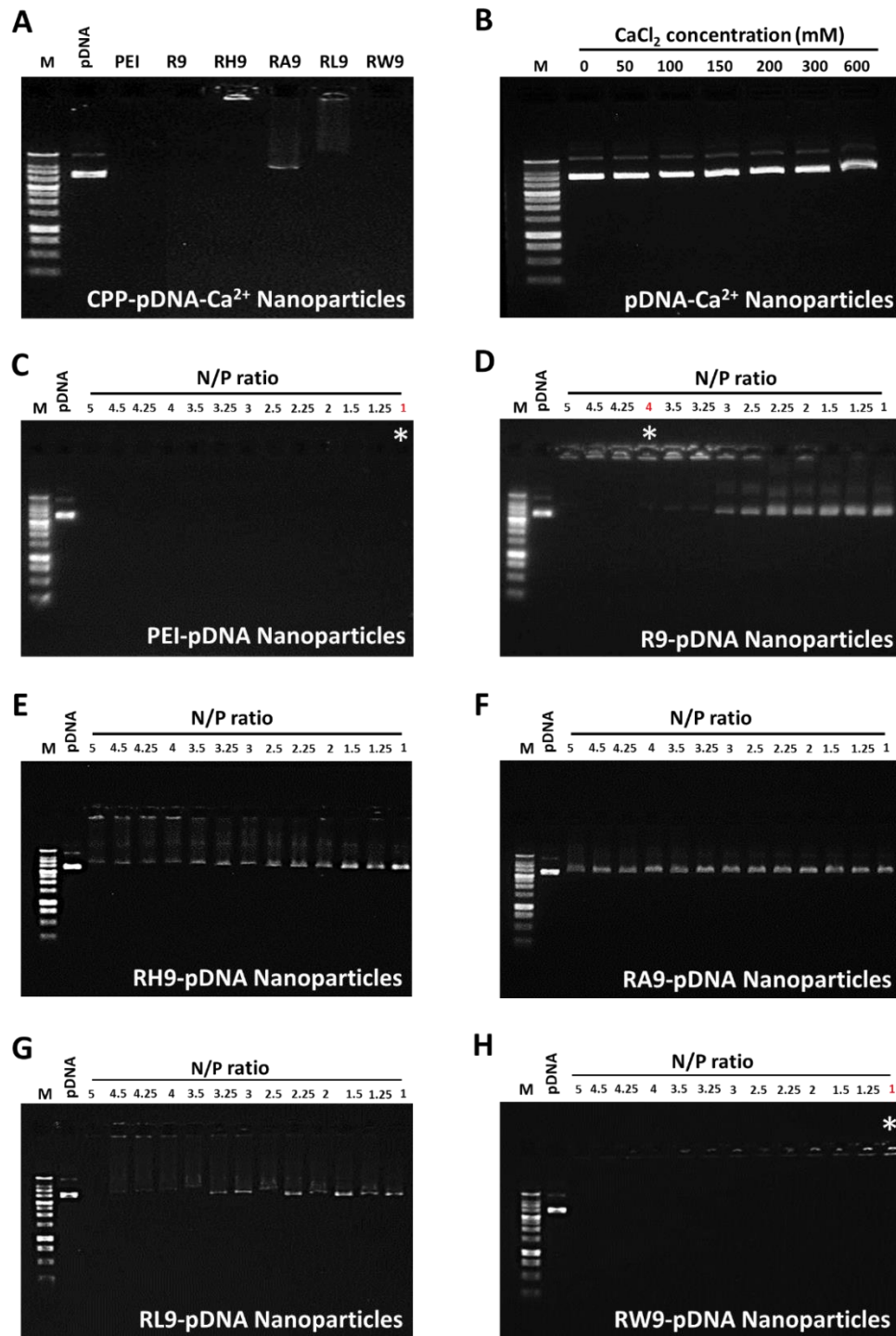


Figure 1. Agarose gel electrophoresis study of gene complexes at N/P ratios 10, 5, 4.5, 4.25, 4, 3.5, 3.25, 3, 2.5, 2.25, 2, 1.5, 1.25, and 1. **(A)** PEI, R9, RH9, RA9, RL9, and RW9-pDNA- Ca^{2+} complexes (N/P ratio 10 and 100 mM CaCl_2). **(B)** CaCl_2 -pDNA complexes; 0, 50, 100, 150, 200, 300, and 600 mM of CaCl_2 . **(C)** PEI-pDNA complexes. **(D)** R9-pDNA complexes. **(E)** RH9-pDNA complexes. **(F)** RA9-pDNA complexes. **(G)** RL9-pDNA complexes. **(H)** RW9-pDNA complexes. “Star” (*) refers to the minimum N/P ratio whereas CPPs were able to immobilize pDNA completely. “M” Refers to the size marker.

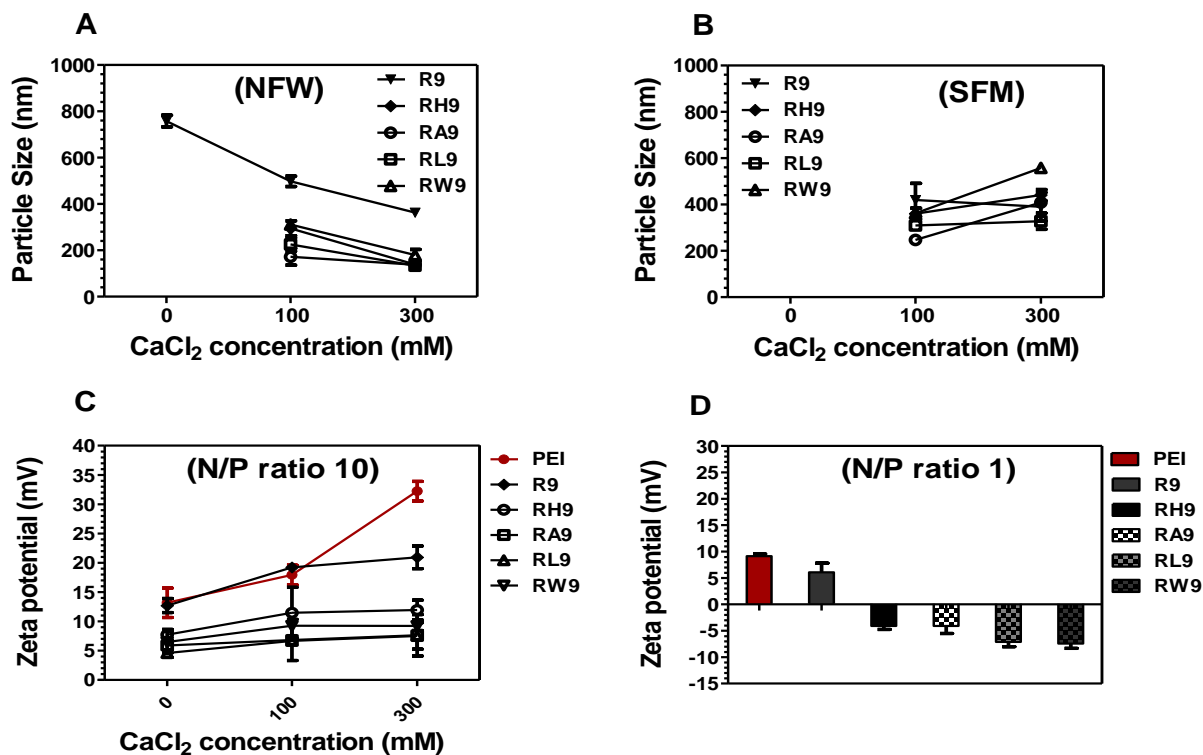


Figure 2: Particle size (effective diameter) and zeta potential of R9-, RH9-, RA9-, RL9-, or RW9-pDNA complexes at N/P ratio 10 with and without CaCl₂. The particle size of complexes with CaCl₂ concentration (100, 200, and 300 mM) were determined (A) in nuclease free water (NFW), and (B) in serum-free F-12 media (SFM). For missing data points, the diameter was > 1 μ m. The zeta potential of the five CPPs and PEI complexes: (C) CaCl₂ concentration: 0, 100, and 300 mM and N/P ratio 10. (D) CaCl₂ concentration 0 mM and N/P ratio 1. Results are presented as mean \pm SD (n = 3).

The SYBR green assay provides a simple, nondestructive, and high-throughput technique for examining DNA accessibility within the complexes. **Figure 3** shows the effect of CaCl₂ concentration (0 and 100 mM) on the five CPP-pDNA and PEI-pDNA complexes by using the SYBR Green assay to assess pDNA accessibility. Overall, PEI, R9, RL9, and RW9 complexes showed weak fluorescence intensity, which suggests that these CPPs condensed pDNA. However, the other complexes (RH9 and RA9 complexes) showed strong fluorescence intensity (high RFU value). The addition of CaCl₂ (100 mM) increased the condensation of all complexes as

demonstrated by the reduced fluorescence, indicating reduced accessibility of SYBR Green to pDNA.

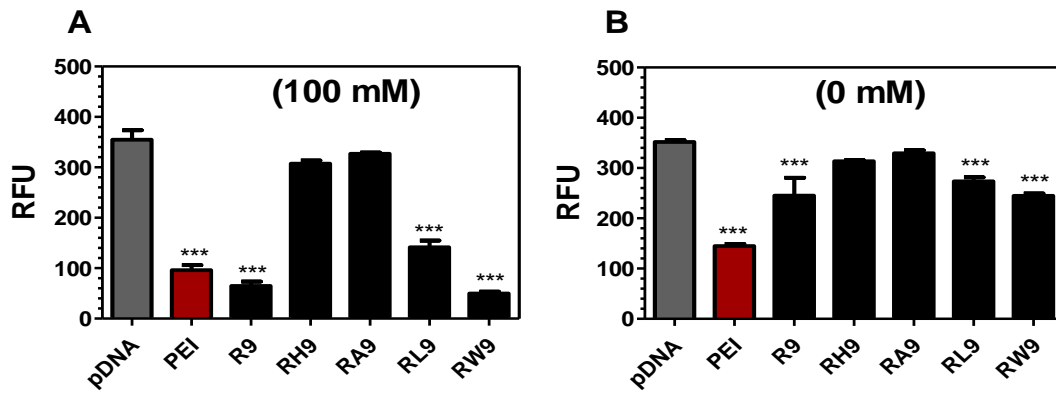


Figure 3. Effect of CaCl₂ concentration (**A**) 100 mM and (**B**) 0 mM on PEI-pDNA complexes and R9-, RH9-, RA9-, RL9-, or RW9-pDNA complexes (N/P ratio 10) by using the SYBR Green assay to assess pDNA accessibility. Results are presented as mean \pm SD (n = 3) (***) = P < 0.0001, one-way ANOVA, Tukey post-test comparison to pDNA).

Next, the stability of the five CPP-pDNA and PEI-pDNA complexes when exposed to dextran sulfate was studied by determining changes in the SYBR Green fluorescence. Exposing the complexes to dextran sulfate increased the fluorescence signal, suggesting exposure or complete release of the plasmid DNA from the complexes as the dextran sulfate concentration increased (0.001 to 100 mg/mL) and at different N/P ratios (1, 2, 3, 4, and 10) (**Figure Appendix 9**). **Figure 4** shows the fluorescence of the five CPP-pDNA and PEI-pDNA complexes by dextran sulfate (0.01 mg/mL) displacement of pDNA (without CaCl₂) across a range of N/P ratios (1-3). Overall, PEI, R9, and RW9 limited pDNA accessibility within the complexes (weak fluorescence intensity), which suggests that these CPPs strongly complexed pDNA when compared to RH9, RA9, and RL9 at the different N/P ratios.

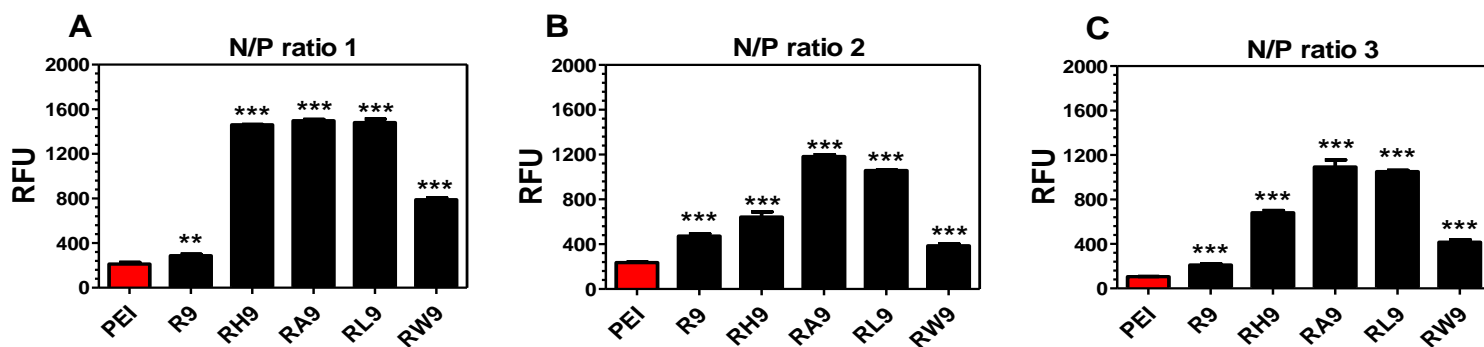


Figure 4. SYBR Green fluorescence of R9-, RH9-, RA9-, RL9-, or RW9-pDNA and PEI-pDNA complexes by dextran (0.01 mg/mL) displacement of pDNA. (A) N/P ratio 1, (B) N/P ratio 2, and (C) N/P ratio 3. Results are presented as mean \pm SD ($n = 3$) (***) = $P < 0.0005$, ** = $P < 0.001$, comparison to PEI, t test).

Next, the five CPPs were complexed with pDNA, and the transfection of A549 cells was studied as a function of N/P ratio (5, 10, 20, and 30) and CaCl_2 concentration (0, 50, 100, 200, and 300 mM) (**Figure 5A-D**). In general, the five nanoparticles had the maximum-gene expression levels at CaCl_2 concentrations of 100 and 200 mM. Additionally, it seemed that there was no significant difference in the transfection efficiency across a range of N/P ratios (5-30). Some of the CPP-pDNA complexes showed higher levels of gene expression at 100 mM of added calcium when compared to PEI (**Figure 5E and 5F**), which had high transfection efficiency in the absence of CaCl_2 . The transfection efficiency of PEI-pDNA complexes and the five CPP-pDNA- Ca^{2+} (0, 100, and 300 mM) at N/P ratio 10 was assessed in A549 cells (**Figure 5E**) and HEK-293 cells (**Figure 5F**).

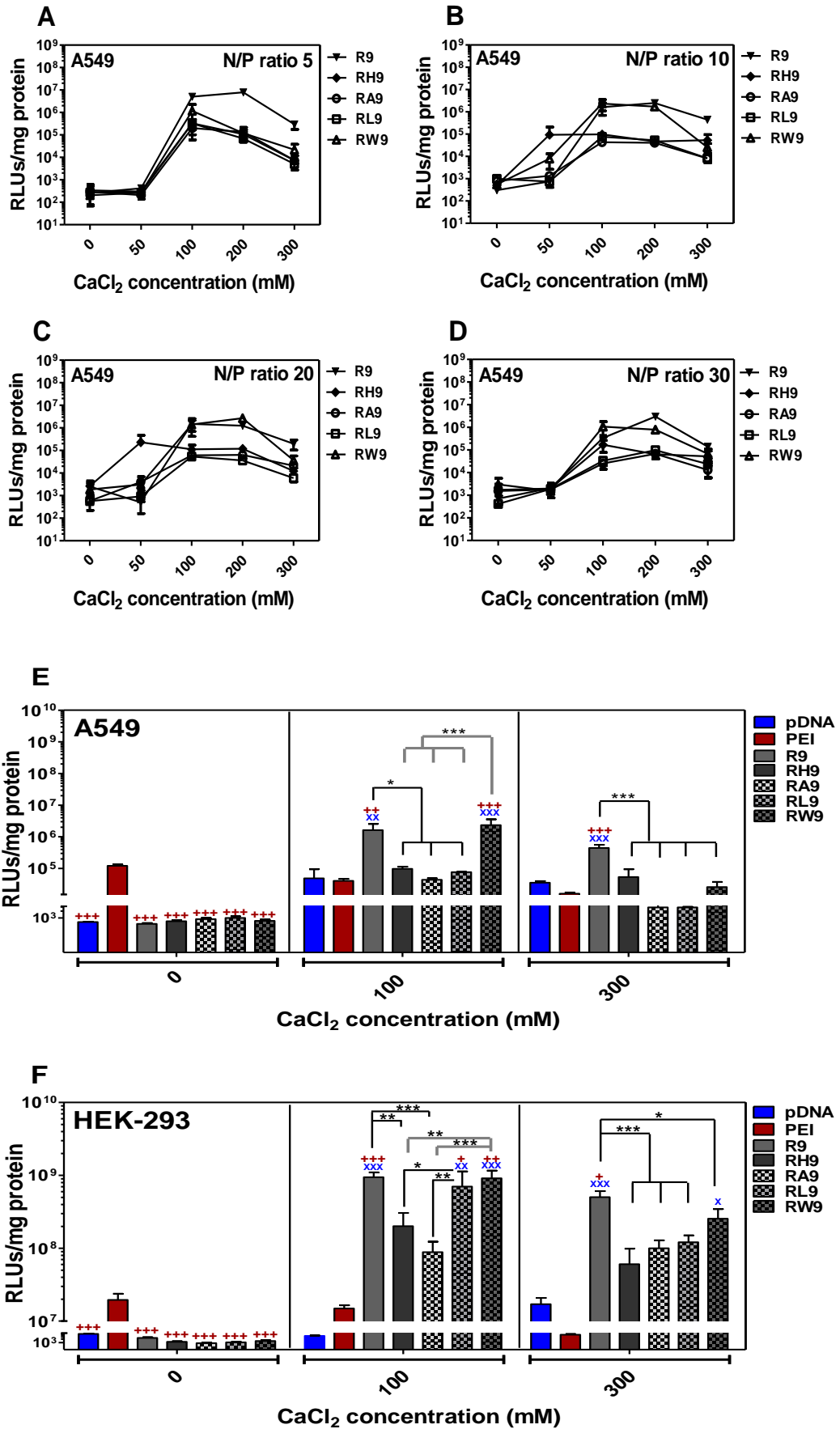


Figure 5. Transfection efficiency R9-, RH9-, RA9-, RL9-, or RW9-pDNA and PEI-pDNA with different concentrations of added CaCl₂ (0, 50, 100, 200, and 300 mM) in A549 cells at an N/P ratio of (A) 5, (B) 10, (C) 20, and (D) 30. The transfection efficiency of pDNA-Ca²⁺, the five CPPspDNA, and PEI-pDNA complexes with different concentrations of added CaCl₂ (0, 100, and 300 mM) at N/P ratio 10, (E) in A549 cells, (F) in HEK-293 cells. PEI-pDNA complex (N/P ratio 10) was used as a standard. RLU refers to relative light units. Results are presented as mean ± SD (n = 4) (xxx = < 0.0001, xx = P < 0.001, x = P < 0.05, comparison to pDNA) (+++ = < 0.0001, ++ = P < 0.001, + = P < 0.05, comparison to PEI) (** = P < 0.0001, * = P < 0.001, * = P < 0.05, one-way ANOVA, Tukey post-test).

Remarkably, there was no notable gene expression observed for the five CPP-pDNA complexes without CaCl₂ in both of the cell lines. Data from the A549 cell line showed RH9, RA9, and RL9 complexes had low-gene expression even when adding CaCl₂ to condense the complexes; however, R9 and RW9 complexes yielded high-gene expression values. The HEK-293 cell line showed that all five CPP-pDNA-Ca²⁺ complexes had a high-gene expression with CaCl₂ (100 and 300 mM) compared to PEI. Clearly, R9 and RW9 complexes yielded the maximum-gene expression values. Generally, RH9, RA9, and RL9 complexes appeared significantly less effective than R9 and RW9 complexes for transfection in both of the cell lines. As mentioned earlier, the electrophoretic mobility of RH9, RA9, and RL9 complexes exhibited free pDNA at low N/P ratios (1 to 5). On the other hand, R9 and RW9 complexes were able to immobilize pDNA. These findings support the notion that the low gene expression values of these complexes were due to poor DNA packaging or instability of the complexes.

The guanidine headgroups of polyarginine peptides are a critical structural component responsible for biological activity³¹. This is in part due to the ability of the guanidine group to form a very stable bidentate hydrogen bond with anions (e.g., phosphate or sulfate)³¹. Our previous studies^{16, 18} established that the interaction of CPPs or CPP-pDNA complexes with three phospholipid monolayers (POPG, POPS, and POPC) was not different when comparing CPPs used

here (**Table 2, Figure Appendix 10**). POPG, POPS, and POPC are extensively used as a model for one leaflet of the cell membrane. In the previous reports, RW9 and RL9 peptides or complexes strongly penetrated model cell membranes and induced the maximum alterations in phospholipid packing (high Δ surface pressure (mN/m))¹⁶. Conversely, the other CPPs or complexes (R9, RH9, and RA9) also showed penetration into the model membranes but did not appear to cause significant membrane disruption (low Δ surface pressure). This suggests that although the initial interaction of the complexes with cell membranes is facilitated by ionic interactions, the hydrophobic residues (tryptophan and leucine) further facilitate membrane penetration. Yet, RW9 complexes appeared significantly more effective than RL9 complexes for transfection, suggesting that the high membrane penetration efficiency of RL9 and RW9 complexes did not explain increased levels of gene expression compared to R9 complexes. The difference in the transfection efficiency between R9, RH9, and RA9 complexes was also probably not due to the penetration efficiency of these peptides or complexes¹⁸.

Table 2. Maximum Change in Surface Pressure, Plateau Values, of the Five Complexes When Inserted below POPG, POPS, POPC Monolayers. Results are presented as mean \pm SD (n = 3).

Complexes	Maximum change in surface pressure (Δ surface pressure (mN/m))		
	POPG	POPS	POPC
	phospholipid monolayer	phospholipid monolayer	phospholipid monolayer
R9	2.9 \pm 0.71	1.9 \pm 0.50	0.9 \pm 0.31
RH9	3.3 \pm 0.75	1.4 \pm 0.37	1.2 \pm 0.62
RA9	2.5 \pm 0.70	1.4 \pm 0.99	1.1 \pm 0.38
RL9	7 \pm 0.67	5.4 \pm 0.35	1.9 \pm 0.56
RW9	9 \pm 0.56	6.5 \pm 1.4	2.8 \pm 0.67

CaCl₂ was an essential component to condense the complexes, yielding small nanoparticles with the ability to release nucleic acids and CPPs as pH drops. Only combinations of CPPs and CaCl₂ effectively boosted gene transfection, because the transfection efficiency of pDNA-Ca²⁺ complexes without R9 and RW9 peptides was significantly lower than that of the complexes with R9 and RW9 peptides at the same CaCl₂ concentration (**Figure 5E and 5F**).

An efficient gene delivery method should be able to transport nucleic acids to the target cells without negatively affecting the viability of the host cell. To examine whether the five CPPs, PEI, and CaCl₂ affected the viability of the four cell lines, an MTS cytotoxicity assay of the five CPPs, PEI, and CaCl₂ was conducted. The cytotoxicity profiles of the five CPPs, PEI, and CaCl₂ was determined in A549 cells (**Figure 6A**) and HEK-293 cells (**Figure 6B**). Generally, the data indicated that CaCl₂ and R9, RH9, RA9, and RL9 peptides revealed no evidence of cytotoxicity at low or medium concentrations, and cells maintained high viability, whereas some of the peptides showed moderate cytotoxicity at very high concentrations in both of the cell lines. Clearly, PEI induced significant cytotoxicity in both of the cell lines.

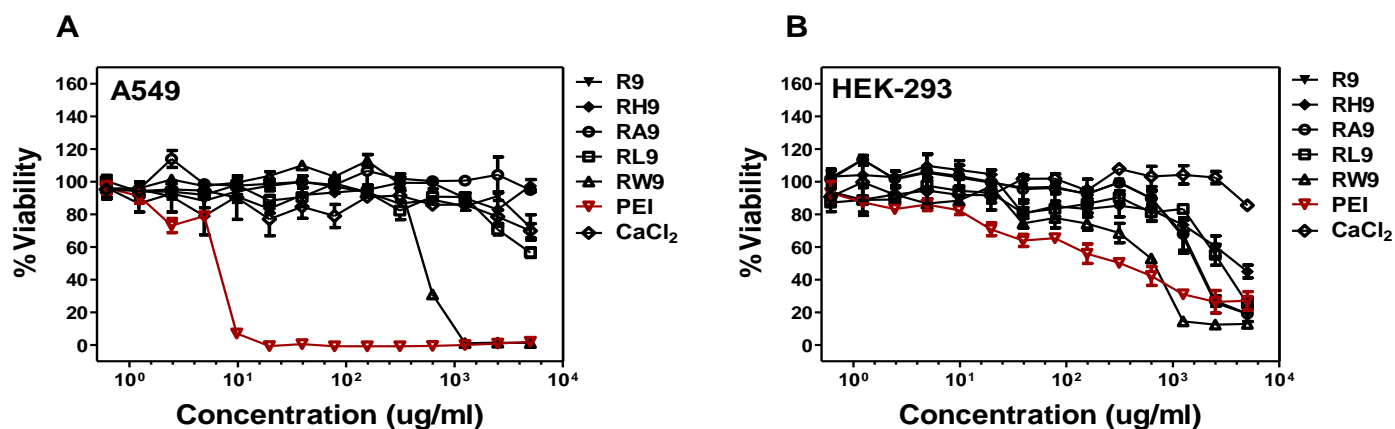


Figure 6. Cytotoxicity profiles of R9, RH9, RA9, RL9, RW9, PEI, and CaCl₂ (A) in A549 cells and (B) in HEK-293 cells. Viability is expressed as a function of the CPPs, PEI, and CaCl₂ concentration. Results are presented as mean \pm SD (n = 3).

One possible mechanism of the enhanced transfection efficiency could be the disintegration of the complexes as pH decreases (late endosome/lysosome)^{8, 18}. **Figure Appendix 11** shows the particle size of the nanoparticles in PBS at different pH values (7.4, 6.4, 5.4, 4.4, and 3.4). Particle size increased as pH value decreased, suggesting complexes dissociated at these conditions. The decrease photon counting rate (kilo-counts per second; Kcps) at low pH suggested complexes dissociated, which is also supported by our previous studies^{8, 12}. Furthermore, earlier reports of calcium and DNA precipitates were reported to dissociate when exposed to similar conditions³². In contrast, PEI-pDNA complexes showed no significant change in particle size. Additionally, **Figure Appendix 12** shows the zeta potential of the five complexes at neutral (7.4) and acidic (4.4) pH values. In general, the total charge of the complexes is positive at pH 7.4, which may be due to charge on the CPPs making up the complexes, whereas, the net charge of the complexes become neutral or anionic when the pH was lowered. The drop in pH appeared to destabilize the complexes, allowing the pDNA to be exposed.

Since transfection efficiency did not correlate to the membrane activity of CPPs, other mechanisms were explored. RW9 and R9 complexes were able to immobilize pDNA completely at low N/P ratios, 1 and 4, respectively (**Figure 1**). As mentioned before RW9 and R9 complexes displayed weak fluorescence intensity (RFU), which indicated that these complexes bound strongly to pDNA (**Figures 3 and 4**). **Figure 7** shows the correlation coefficient between RLUs/mg protein (**Figure 5E and 5F**) and the change in the maximum surface pressure (**Table 2**) of the five CPP complexes. **Figures 7A to 7F** indicate that there was no significant correlation between the transfection efficiency (in A549 and HEK-293 cell lines) and the CPP membrane penetration efficiency (below POPG, POPS, and POPC phospholipid monolayers). On the other hand, **Figure 8** indicates a significant correlation between the transfection efficiency of the five CPP complexes and the ability of CPPs to immobilize pDNA completely by using agarose gel electrophoresis experiments (N/P ratios 1 to 15, integer numbers) (excluding PEI complexes, **Figure 1 and Figure Appendix 8**). Furthermore, **Figure 9** shows the correlation coefficient between the transfection efficiency and unpackaging of the complexes by dextran sulfate displacement of pDNA across a range of N/P ratios 1-3 in A549 cells (**Figures 9A-C**) and HEK-293 cells (**Figures 9D-E**). In general, there was a significant correlation between the transfection efficiency and the unpackaging. Thus, the high transfection efficiency of R9 and RW9 complexes may be driven by the strong interaction between CPPs and pDNA, rather than differences in the membrane penetration efficiency of the complexes. R9 complexes had high transfection efficiency when compared with RH9, RA9, and RL9 complexes, which may be due to the larger number of positively charged arginine residues. RW9 complexes also had high transfection efficiency when compared with RH9, RA9, and RL9 complexes. This behavior is possibly due to the chemical structure of tryptophan residues (the aromatic ring), which may facilitate peptide binding with

nucleic acids even though the peptide charge is significantly lower than R9¹⁶. On the basis of these results, we concluded that the structure of the CPPs dictated the ability of CPPs to protect and deliver nucleic acids independent of their ability to penetrate membranes.

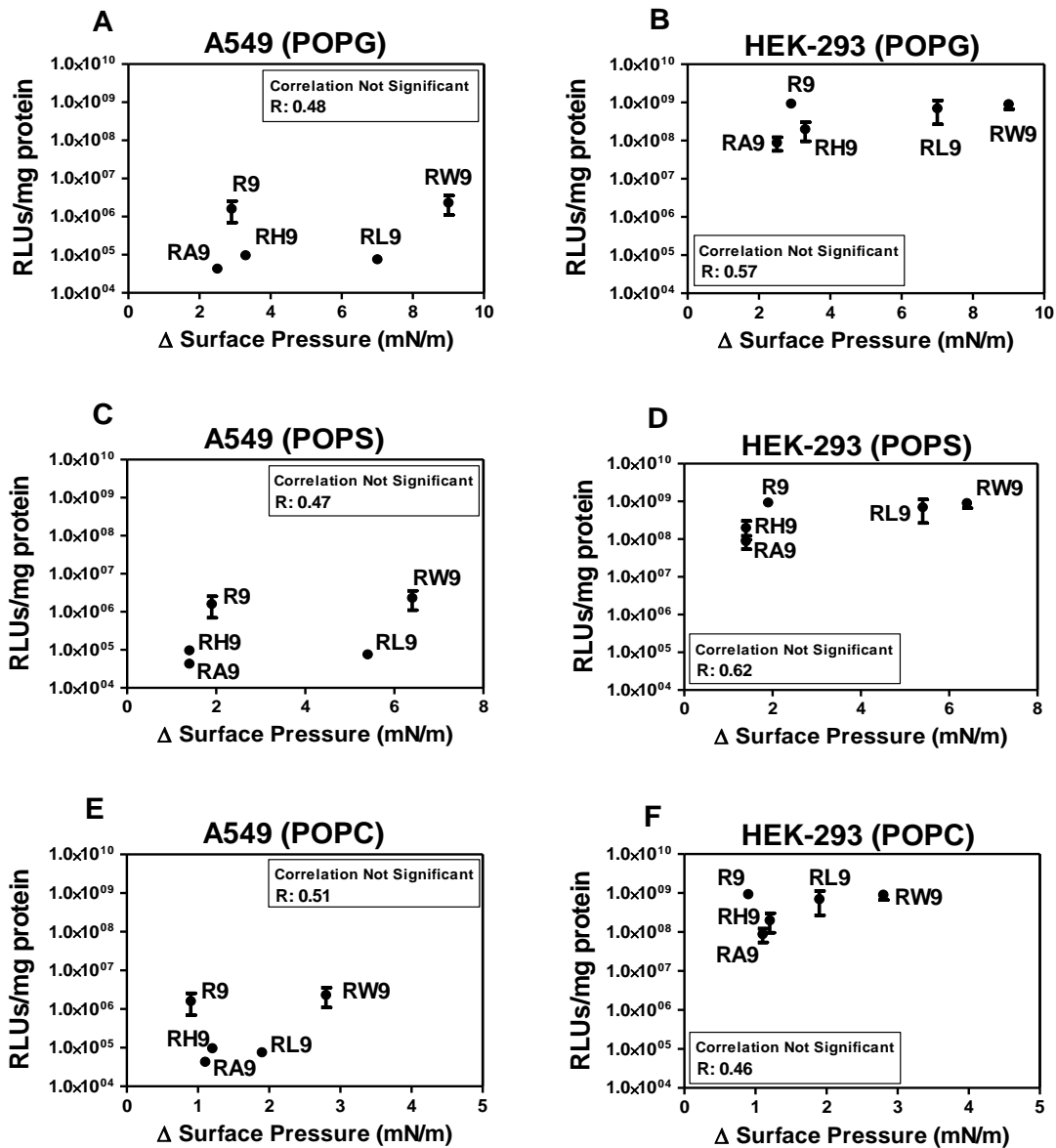


Figure 7. No correlation was observed between the transfection efficiency (in A549 and HEK-293 cell lines, 100 mM CaCl₂ concentration and at N/P ratio 10) and the changes in surface pressure as following injection of R9-, RH9-, RA9-, RL9-, or RW9-pDNA complexes into model phospholipid monolayers (POPG, POPS, or POPC). **(A)** A549 cell line and POPG phospholipid monolayer. **(B)** HEK-293 cell line and POPG phospholipid monolayer. **(C)** A549 cell line and POPS phospholipid monolayer. **(D)** HEK-293 cell line and POPG phospholipid monolayer. **(E)** A549 cell line and POPC phospholipid monolayer. **(F)** HEK-293 cell line and POPC phospholipid monolayer. The Pearson correlation coefficient was calculated with one-tailed probability.

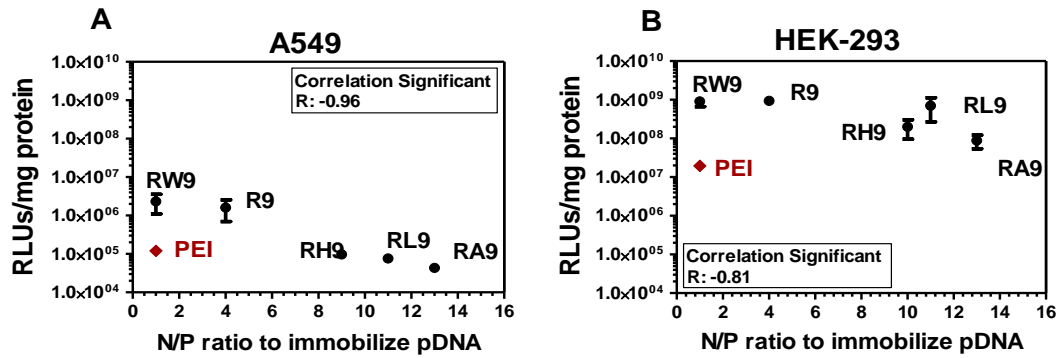


Figure 8. Correlation was found between the transfection efficiency and the minimum N/P ratio where PEI and CPPs were able to immobilize pDNA completely (Agarose gel electrophoresis) for R9-, RH9-, RA9-, RL9-, or RW9-pDNA complexes (100 mM CaCl₂ concentration and at N/P ratio 10). **(A)** A549 cells. **(B)** HEK-293 cells. The Pearson's correlation coefficient was calculated with one-tailed probability (excluding PEI complexes).

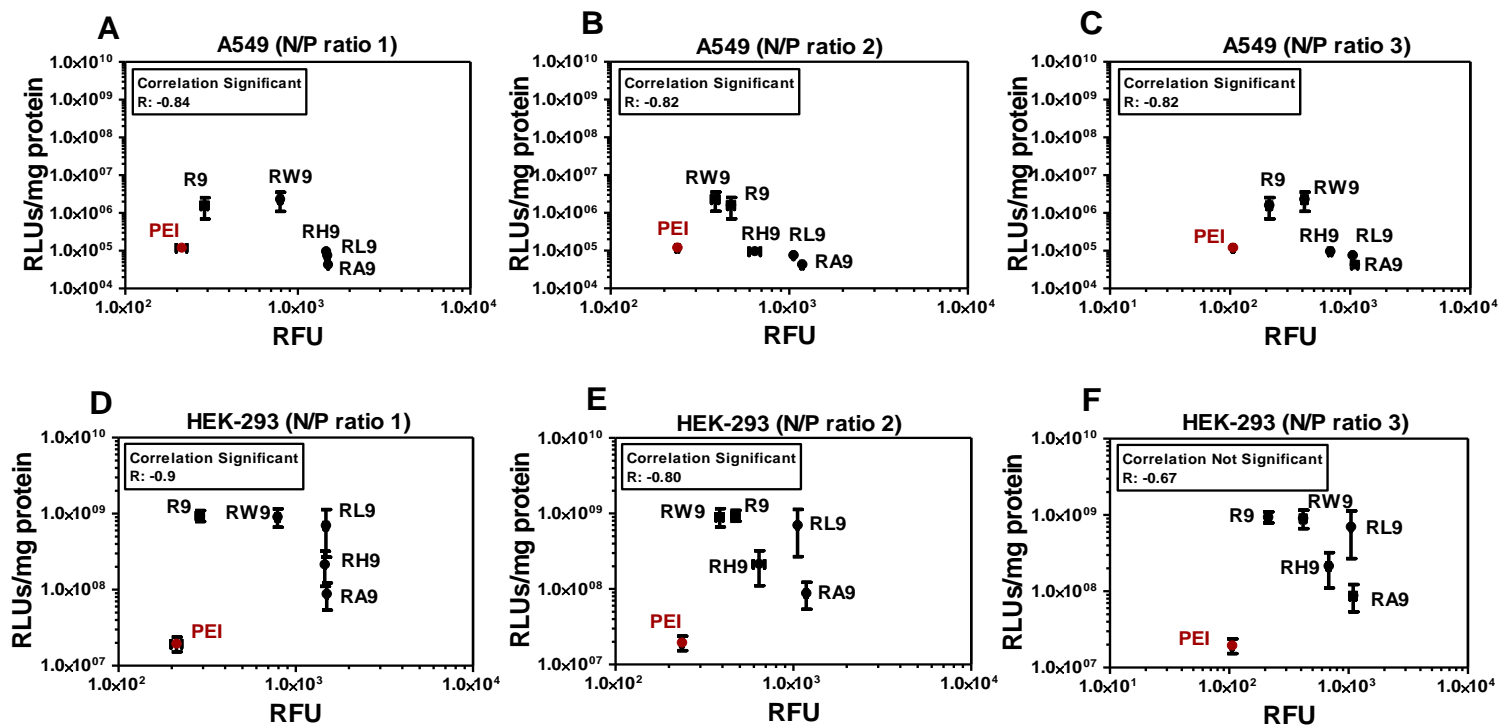


Figure 9. Correlation was found between the transfection efficiency and unpackaging of R9-, RH9-, RA9-, RL9-, RW9-, or -PEI pDNA complexes by dextran sulfate displacement of pDNA at N/P ratios 1, 2, 3, and 4 in A549 or HEK-293 cells. (A) A549 N/P ratio 1, (B) A549 N/P ratio 2, (C) A549 N/P ratio 3, (D) HEK-293 N/P ratio 1, (E) HEK-293 N/P ratio 2, and (F) HEK-293 N/P ratio 3. The Pearson's correlation coefficient was calculated with one-tailed probability (excluding PEI complexes).

6.4. Conclusions

The addition of CaCl_2 to low-molecular-weight hydrophilic CPPs (R9 and RH9) and amphiphilic CPPs (RA9, RL9, and RW9) complexed with pDNA, produced small nanoparticles, leading to gene expression levels higher than detected for PEI complexes in a normal cell line (HEK-293) and a cancer cell line (A549). Clearly, replacing three residues of the R9 peptide with a hydrophilic residue (histidine) or hydrophobic residues (alanine, leucine, and tryptophan) at positions 3, 4, and 7 did not enhance the transfection efficiency compared to R9 complexes. R9 and RW9 complexes appeared especially effective compared to other CPP complexes, whereas RH9, RA9, and RL9 complexes seemed to have moderate- to low-gene expression. Initially, this suggested CPPs with better membrane penetration yielded higher gene expression. After further exploration, we discovered the charge spacing of CPPs affected the ability of CPPs to complex with nucleic acids and this property correlated to gene expression levels.

6.6. References

1. Aldawsari, H.; Edrada-Ebel, R.; Blatchford, D. R.; Tate, R. J.; Tetley, L.; Dufès, C. Enhanced gene expression in tumors after intravenous administration of arginine-, lysine-and leucine-bearing polypropylenimine polyplex. *Biomaterials* **2011**, *32*, (25), 5889-5899.
2. Margus, H.; Padari, K.; Pooga, M. Cell-penetrating peptides as versatile vehicles for oligonucleotide delivery. *Molecular Therapy* **2012**, *20*, (3), 525-533.
3. Zuhorn, I. S.; Engberts, J. B.; Hoekstra, D. Gene delivery by cationic lipid vectors: overcoming cellular barriers. *European Biophysics Journal* **2007**, *36*, (4-5), 349-362.
4. Nakamura, Y.; Kogure, K.; Futaki, S.; Harashima, H. Octaarginine-modified multifunctional envelope-type nano device for siRNA. *Journal of controlled release* **2007**, *119*, (3), 360-367.
5. Khondee, S.; Baoum, A.; Siahaan, T. J.; Berkland, C. Calcium condensed LABL-TAT complexes effectively target gene delivery to ICAM-1 expressing cells. *Molecular pharmaceutics* **2011**, *8*, (3), 788-798.
6. Chen, S.; Han, K.; Yang, J.; Lei, Q.; Zhuo, R.-X.; Zhang, X.-Z. Bioreducible Polypeptide Containing Cell-Penetrating Sequence for Efficient Gene Delivery. *Pharmaceutical research* **2013**, *30*, (8), 1968-1978.
7. Karagiannis, E. D.; Alabi, C. A.; Anderson, D. G. Rationally Designed Tumor-Penetrating Nanocomplexes. *ACS nano* **2012**, *6*, (10), 8484-8487.
8. Alhakamy, N. A.; Nigatu, A. S.; Berkland, C. J.; Ramsey, J. D. Noncovalently associated cell-penetrating peptides for gene delivery applications. *Therapeutic delivery* **2013**, *4*, (6), 741-757.

9. Baoum, A.; Xie, S.-X.; Fakhari, A.; Berkland, C. “Soft” Calcium Crosslinks Enable Highly Efficient Gene Transfection Using TAT Peptide. *Pharmaceutical research* **2009**, *26*, (12), 2619-2629.
10. van Asbeck, A. H.; Beyerle, A.; McNeill, H.; Bovee-Geurts, P. H.; Lindberg, S.; Verdurmen, W. P.; Hällbrink, M.; Langel, U. I.; Heidenreich, O.; Brock, R. Molecular Parameters of siRNA–cell penetrating peptide nanocomplexes for efficient cellular delivery. *ACS nano* **2013**, *7*, (5), 3797-3807.
11. Wagstaff, K. M.; Jans, D. A. Protein transduction: cell penetrating peptides and their therapeutic applications. *Current medicinal chemistry* **2006**, *13*, (12), 1371-1387.
12. Alhakamy, N. A.; Berkland, C. J. Polyarginine molecular weight determines transfection efficiency of calcium condensed complexes. *Molecular pharmaceutics* **2013**, *10*, (5), 1940-1948.
13. Pack, D. W.; Hoffman, A. S.; Pun, S.; Stayton, P. S. Design and development of polymers for gene delivery. *Nature Reviews Drug Discovery* **2005**, *4*, (7), 581-593.
14. de Raad, M.; Teunissen, E. A.; Lelieveld, D.; Egan, D. A.; Mastrobattista, E. High-content screening of peptide-based non-viral gene delivery systems. *Journal of Controlled Release* **2012**, *158*, (3), 433-442.
15. Koo, H.; Kang, H.; Lee, Y. Analysis of the relationship between the molecular weight and transfection efficiency/cytotoxicity of Poly-L-arginine on a mammalian cell line. *Notes* **2009**, *30*, (4), 927.
16. Alhakamy, N. A.; Kaviratna, A.; Berkland, C. J.; Dhar, P. Dynamic Measurements of Membrane Insertion Potential of Synthetic Cell Penetrating Peptides. *Langmuir* **2013**, *29*, (49), 15336-15349.

17. Trabulo, S.; Cardoso, A. L.; Cardoso, A. M.; Düzgünes, N.; Jurado, A. S.; Pedroso de Lima, M. C. Cell-penetrating peptide-based systems for nucleic acid delivery: a biological and biophysical approach. *Methods Enzymol* **2012**, *509*, 277-300.
18. Alhakamy, N. A.; Elandaloussi, I.; Ghazvini, S.; Berkland, C. J.; Dhar, P. Effect of Lipid Headgroup Charge and pH on the Stability and Membrane Insertion Potential of Calcium Condensed Gene Complexes. *Langmuir* **2015**, *31*, (14), 4232-4245.
19. Heitz, F.; Morris, M. C.; Divita, G. Twenty years of cell-penetrating peptides: from molecular mechanisms to therapeutics. *British journal of pharmacology* **2009**, *157*, (2), 195-206.
20. Futaki, S.; Goto, S.; Sugiura, Y. Membrane permeability commonly shared among arginine-rich peptides. *Journal of Molecular Recognition* **2003**, *16*, (5), 260-264.
21. Futaki, S.; Nakase, I.; Tadokoro, A.; Takeuchi, T.; Jones, A. Arginine-rich peptides and their internalization mechanisms. *Biochemical Society Transactions* **2007**, *35*, (4), 784.
22. Zaitsev, S.; Haberland, A.; Otto, A.; Vorob'ev, V.; Haller, H.; Böttger, M. H1 and HMG17 extracted from calf thymus nuclei are efficient DNA carriers in gene transfer. *Gene therapy* **1997**, *4*, (6), 586-592.
23. Khosravi-Darani, K.; Mozafari, M. R.; Rashidi, L.; Mohammadi, M. Calcium based non-viral gene delivery: an overview of methodology and applications. *Acta Med. Iran* **2010**, *48*, (3), 133-141.
24. Baoum, A. A.; Berkland, C. Calcium condensation of DNA complexed with cell-penetrating peptides offers efficient, noncytotoxic gene delivery. *Journal of pharmaceutical sciences* **2011**, *100*, (5), 1637-1642.

25. Kawabata, A.; Baoum, A.; Ohta, N.; Jacquez, S.; Seo, G.-M.; Berkland, C.; Tamura, M. Intratracheal administration of a nanoparticle-based therapy with the angiotensin II type 2 receptor gene attenuates lung cancer growth. *Cancer research* **2012**, *72*, (8), 2057-2067.
26. Doherty, G. J.; McMahon, H. T. Mechanisms of endocytosis. *Annual review of biochemistry* **2009**, *78*, 857-902.
27. Baoum, A. A.; Middaugh, C. R.; Berkland, C. DNA complexed with TAT peptide and condensed using calcium possesses unique structural features compared to PEI polyplexes. *International journal of pharmaceutics* **2014**, *465*, (1), 11-17.
28. Witte, K.; Olausson, B. E.; Walrant, A.; Alves, I. D.; Vogel, A. Structure and dynamics of the two amphipathic arginine-rich peptides RW9 and RL9 in a lipid environment investigated by solid-state NMR and MD simulations. *Biochimica et Biophysica Acta (BBA)-Biomembranes* **2013**, *1828*, (2), 824-833.
29. Walrant, A.; Correia, I.; Jiao, C.-Y.; Lequin, O.; Bent, E. H.; Goasdoué, N.; Lacombe, C.; Chassaing, G.; Sagan, S.; Alves, I. D. Different membrane behaviour and cellular uptake of three basic arginine-rich peptides. *Biochimica et Biophysica Acta (BBA)-Biomembranes* **2011**, *1808*, (1), 382-393.
30. Rajeswari, M. R.; Montenay-Garestier, T.; Helene, C. Does tryptophan intercalate in DNA? A comparative study of peptide binding to alternating and non-alternating A. cntdot. T sequences. *Biochemistry* **1987**, *26*, (21), 6825-6831.
31. Mitchell, D.; Steinman, L.; Kim, D.; Fathman, C.; Rothbard, J. Polyarginine enters cells more efficiently than other polycationic homopolymers. *The Journal of Peptide Research* **2000**, *56*, (5), 318-325.

32. Bisht, S.; Bhakta, G.; Mitra, S.; Maitra, A. pDNA loaded calcium phosphate nanoparticles: highly efficient non-viral vector for gene delivery. *International journal of pharmaceutics* **2005**, 288, (1), 157-168.

Chapter 7

Conclusion and Future Directions

7.1. Conclusion

Gene therapy utilizes the delivery of genetic material into target cells to correct a genetic defect or alter protein expression to address disease. Notwithstanding advances in the field, the delivery of genetic material (e.g., pDNA and siRNA) to target cells or tissues is still challenging. There are many hindrances to overcome in developing effective gene therapy including toxicity, immunogenicity, tissue and cellular transport barriers, enzymatic degradation, endosomal escape, and rapid clearance after administration.

Successful transfer of genetic material into target cells usually relies on the use of efficient carriers. Notable efforts are being made to develop viral and nonviral vectors that can cross the plasma membrane and deliver pDNA or siRNA into target cells. Viral vectors (e.g., retroviruses and adenoviruses) can be highly efficient and are currently used in the majority of ongoing clinical trials. Unfortunately viral vectors are deficient in several areas such as the induction of host immune response and challenging, expensive scale-up. Consequently, nonviral vectors are being pursued as flexible, easy, and potentially safer alternatives, yet, they continue to lack the necessary efficiency required for clinical application. Cationic lipids, polymers, and peptides are the most commonly employed nonviral carriers.

The objective of this thesis has been to design high transfection efficiency and less toxic vectors for gene delivery. Cell penetrating peptides (CPPs) were considered as potential polycations to complex and deliver genetic material. Calcium was found to compact CPP complexes through “soft” crosslinks that could be competitively disrupted in order to increase transfection efficiency. Polyarginines have been successfully used as cell penetrating peptides for delivering large cargo such as genetic material. Polyarginine-pDNA complexes condensed with calcium chloride possessed excellent transfection efficiency compared to PEI complexes in A549

lung epithelial cells. Furthermore, the low-molecular-weight polyarginine peptides (5, 7, 9 and 11) showed negligible cytotoxicity up to 5 mg/mL and maintained the expected cell proliferation rates. Polyarginine 7 appeared especially effective compared to the other polyarginines. Polyarginine 5 was ineffective compared to the other polyarginines, suggesting the minimum size should be > 5 amino acids.

K9-(pAT2R or pLUC)-Ca²⁺ complexes produced small and stable complexes. These complexes exhibited high *in vitro* gene expression in various human and mouse cancer cells comparable to PEI-pDNA complexes. Also, single IV or IT administrations of the K9-pAT2R-Ca²⁺ complexes significantly attenuated the growth of LLC cell allografts in mouse lungs, suggesting that K9 peptide-based gene therapy is effective and that the AT2R gene is potentially useful for lung cancer gene therapy. K9 peptide showed negligible cytotoxicity in cell culture, supporting the notion that this CPP is a safe delivery vehicle for genetic materials. The incorporation of CPPs into polyelectrolyte complexes using this strategy potentially offers a safe and effective approach (*in vitro* and *in vivo*) to gene delivery.

Since CPPs interact with the plasma membranes, understanding the interactions of synthetic CPPs with phospholipid membranes is an important step when designing future synthetic CPPs capable of intracellular drug delivery. Insertion of the hydrophilic CPPs (dTAT, H9, K9, R9, and RH9) and the amphiphilic CPPs (RA9, RL9, and RW9) into the phospholipid monolayers (POPG, POPC, DPPC, or POPG/DPPC) were followed using Langmuir monolayer techniques and fluorescence microscopy. In addition to electrostatic interactions, hydrophobic interactions, as well as the chemical nature of the amino acid residues, influenced the membrane insertion potential. The presence of tryptophan residues induced maximum perturbation of the phospholipid packing. All CPPs interacted with anionic phospholipids, but the interactions of RW9 and RL9

with membrane monolayers was significantly different when compared with the other peptides. RW9 and RL9 strongly penetrated the model cell membranes and also induced the maximum alterations in phospholipid packing.

Furthermore, zwitterionic phospholipid membranes (POPC) and anionic phospholipid membranes (POPS and POPG) have been used to study the membrane insertion of the seven CPP-pDNA-Ca²⁺ complexes, containing hydrophilic (i.e., dTAT, K9, R9, and RH9) and amphiphilic (i.e., RA9, RL9, and RW9) CPPs, at different pHs (pH 7.4 and 4.4). Our data showed that there was no difference in the insertion potential of gene complexes of different composition, when interacting with a zwitterionic phospholipid at a neutral pH. However, when interacting with anionic phospholipid membranes, all complexes showed an increase in their insertion potential, although there was a significant difference in the membrane insertion potential of complexes containing amphiphilic CPPs. This suggests that while the initial interactions of the complexes with phospholipid membranes are facilitated by electrostatic interactions, the hydrophobic amino acids further facilitated membrane insertion. However, in more acidic environments such as those in the intracellular vesicles (endosomes/lysosomes) all gene complexes show a greater insertion into the membranes, irrespective of the composition. In conclusion, our results also suggest that overall, designing gene complexes with amphiphilic peptides may not necessarily demonstrate more transfection efficiency, because of the differences in the insertion potential of the amphiphilic peptides at neutral and acidic pH, even though the amphiphilic peptides have the potential to disrupt anionic membranes at neutral pH.

Finally, replacing three residues of the R9 peptide with a hydrophilic residue (histidine) or hydrophobic residues (alanine, leucine, and tryptophan) at positions 3, 4, and 7 did not enhance the transfection efficiency compared to R9 complexes. R9 and RW9 complexes appeared

especially effective compared to other CPP complexes, whereas RH9, RA9, and RL9 complexes seemed to have moderate to low-gene expression. Initially, this suggested CPPs with better membrane penetration yielded higher gene expression. After further exploration, we discovered the charge spacing of CPPs affected the ability of CPPs to complex with nucleic acids and this property correlated to gene expression levels.

7.2. Future Directions

Gene therapy has incredible potential to revolutionize the way we treat human diseases and other medical conditions. Improved gene delivery, however, remains a major obstacle that must be overcome before gene therapy can advance beyond the clinical setting and into the doctor's office. Major strides are being made currently in terms of developing improved vectors to transport genes from the laboratory bench top to the diseased tissue within a patient and ultimately to the cell nucleus. CPPs are opening possibilities for addressing other drawbacks that are currently associated with nonviral vectors. While improving viral gene delivery vectors will probably have the most immediate impact, the long-term goal for many of us in the field is to develop completely synthetic nonviral vectors that perfectly mimic the efficiency of a virus with none of the drawbacks. CPPs are having immediate impacts on moving us one step closer to this goal. Nonviral vectors complexed with CPPs are being delivered directly to the cell cytosol across the cell membrane, escaping endosomal vesicles with greater efficiencies, and being transported to the cell nucleus in ways that are traditionally only associated with viruses. CPPs have been studied for more than 20 years, but their impact on the field of gene delivery has been limited predominantly to the last several years. While they have improved significantly existing vectors, further design and development of simpler and more effective CPPs will undoubtedly continue to greatly benefit

the development of nonviral gene delivery vectors as the field continues to advance. Future work with CPP gene delivery systems should further explore the mechanism of a positive effect of calcium on the gene delivery when incorporated in the nonviral gene vectors. Further emphasis on immunohistochemical and imaging studies of CPP-pDNA- Ca^{2+} complexes would provide more information on the exact mechanism of enhanced transfection. The internalization and trafficking should be investigated since it cannot be excluded from the effect of calcium on gene transfer when using CPP complexes. Moreover, further studies are required to confirm the *in vivo* safety of the CPP-pDNA- Ca^{2+} complexes by formal pharmacokinetics, pharmacodynamics, and multispecies toxicity studies.

Appendices

Table Appendix 1. Lung weight in LLC tumor-bearing mice

	Mouse #					Ave.	S.D.
	1	2	3	4	5		
PBS	402.7	258.7	353.8	228.7	384.5	325.7	69.4
K9 alone IT	313.4	181.0	442.2	325.6	284.5	309.3	83.7
K9/AT2R IT	209.1	153.8	185.3	271.9	133.0	190.6	48.3
K9 alone IV	218.9	153.0	378.4	186.2	277.2	242.7	79.3
K9/AT2R IV	260.3	163.9	154.2	128.2	301.2	201.6	67.0

Table Appendix 2. Number of tumor nodules in LLC tumor-bearing mice

	Mouse #					Ave.	S.D.
	1	2	3	4	5		
PBS	24	21	16	7	21	17.8	6.0
K9 alone IT	13	5	20	12	28	15.6	7.8
K9/AT2R IT	12	3	0	6	9	6.0	4.2
K9 alone IV	8	2	9	23	10	10.4	6.9
K9/AT2R IV	4	2	9	0	8	4.6	3.4

Table Appendix 3. Lung weight in LLC tumor-bearing mice treated with K9-pLUC-Ca²⁺ complexes

	Mouse #					Ave.	S.D.
	1	2	3	4	5		
PBS	296.4	321.7	237.2	139.3	239.6	246.8	70.3
K9/pLUC IV	280.8	216.2	151.8	174.5	246.4	213.9	52.3
K9/pLUC IT	266.7	274.4	260.7			267.3	6.9

Table Appendix 4. Number of tumor nodules in LLC tumor-bearing mice treated with K9-pLUC-Ca²⁺ complexes

	Mouse #					Ave.	S.D.
	1	2	3	4	5		
PBS	25	21	18	15	23	20.4	4.0
K9/pLUC IV	41	13	15	19	13	20.2	11.9
K9/pLUC IT	26	27	24			25.7	1.5

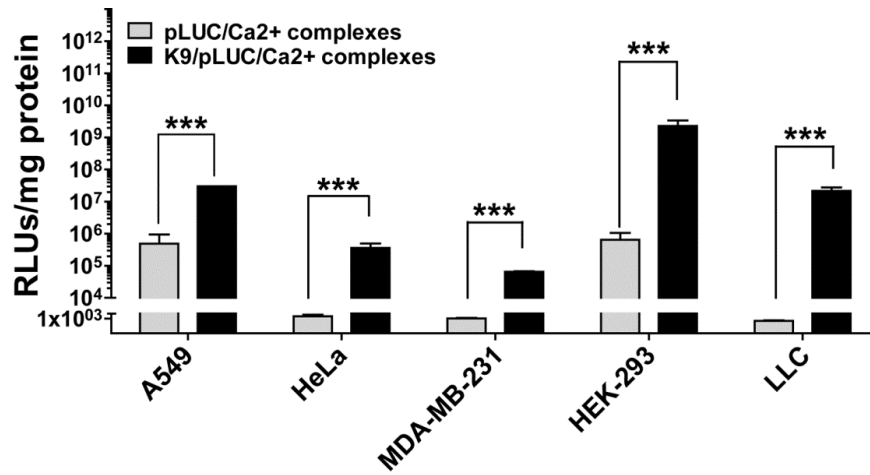


Figure Appendix 1. The transfection efficiencies of the pLUC-Ca²⁺ and the K9-pLUC-Ca²⁺ complexes in various cell lines designated in the figure were determined in the presence of 38 mM calcium chloride at an N/P ratio 10. RLUs refers to relative light units. Results are presented as mean \pm SD (n = 4). ***, P < 0.0005 determined by Student *t* test.

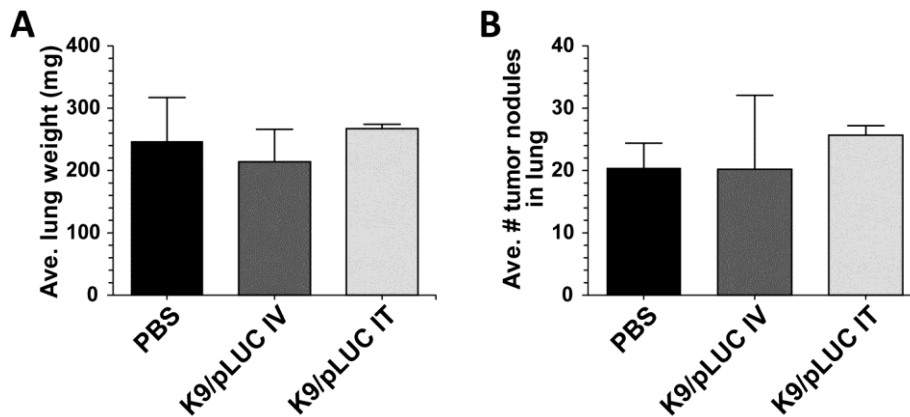


Figure Appendix 2. Bar graphs show average lung weight (**A**) and number of lung tumor nodules (**B**) in LLC tumor-bearing C57BL/6 mice treated with PBS (n=5), K9-pLUC-Ca²⁺ IV (K9-pLUC IV; n=5), or K9-pLUC-Ca²⁺ IT (K9-pLUC IT; n=5). K9, nine amino acid polylysine; IT, intratracheal; IV, intravenous.

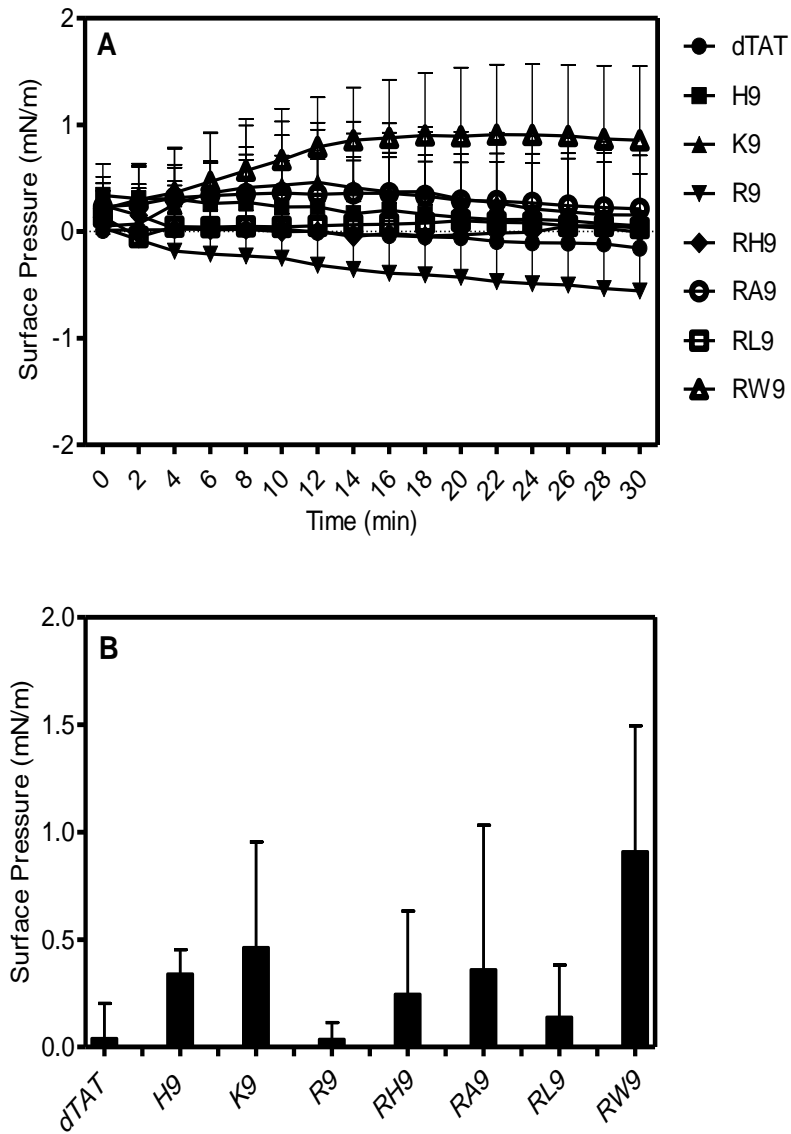


Figure Appendix 3. (A) Changes in the surface pressure versus time following adsorption of the eight CPPs into a phospholipid-free interface. The peptides are at a final concentration of 10 μ M **(B)** Maximum change in surface pressure (plateau values) recorded for the eight CPPs. The results are presented as mean \pm SD ($n = 3$).

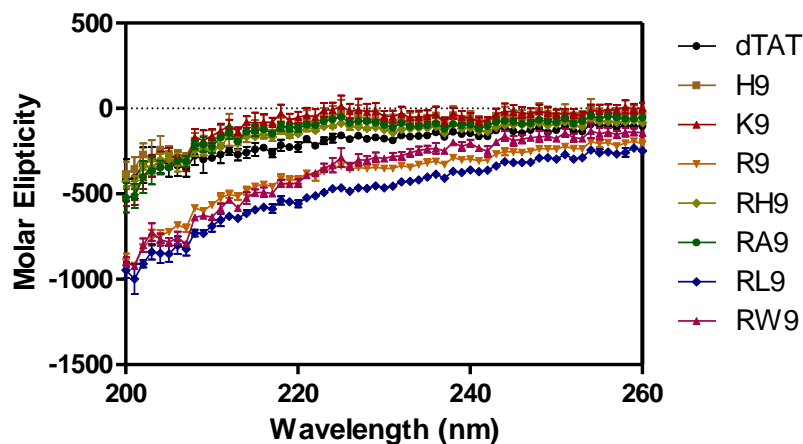


Figure Appendix 4. CD analysis of the eight CPPs. The peptide concentration used was 10 μM using a 0.1 cm path length quartz cuvette was used with a total volume of 200 μL (in PBS). Full CD spectra were collected at 22 $^{\circ}\text{C}$ for wavelengths ranging from 260 to 200 nm. CD spectra analysis of the eight CPPs showed that the eight CPPs in the PBS solution contain random-coil conformations. The results are presented as mean \pm SD ($n = 3$). CD spectra were recorded using a Chirascan (Applied Photophysics) instrument.

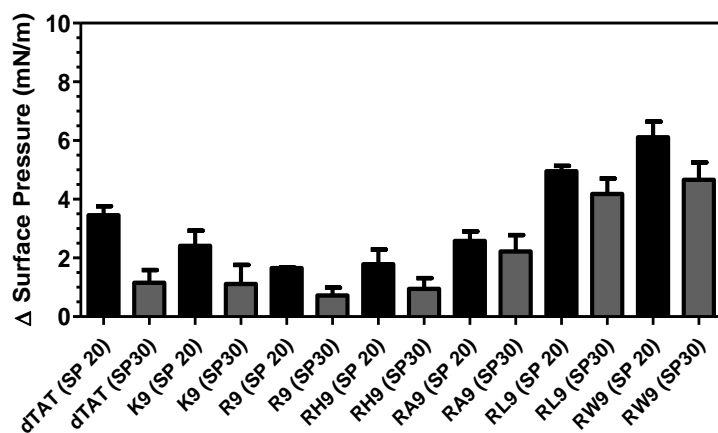


Figure Appendix 5. The maximum change in surface pressure of the seven CPPs (dTAT, K9, R9, RH9, RA9, RL9, and RW9) below POPG phospholipid monolayers held at an initial surface pressure of 20 mN/m and at pH 7.4. Results are presented as mean SD (n = 3).

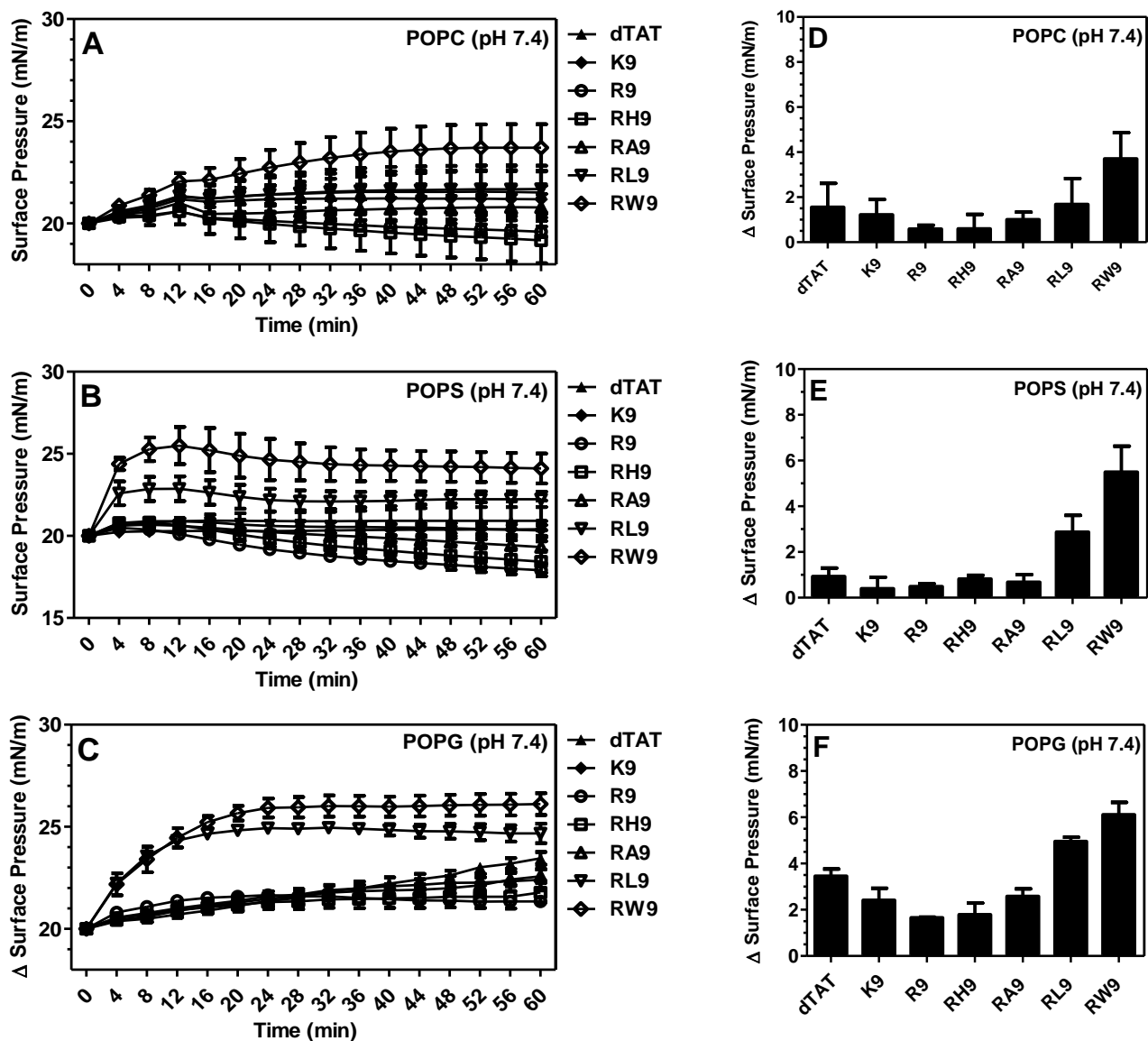


Figure Appendix 6. Changes in surface pressure as a function of time following injection of the seven CPPs (dTAT, K9, R9, RH9, RA9, RL9, and RW9) below (A) POPC, (B) POPS, and (C) POPG phospholipid monolayers held at an initial surface pressure of 20 mN/m and at pH 7.4. The maximum change in surface pressure (plateau values) of the (D) POPC, (E) POPS, (F) POPG due to adsorption of seven CPPs. Results are presented as mean SD (n = 3).

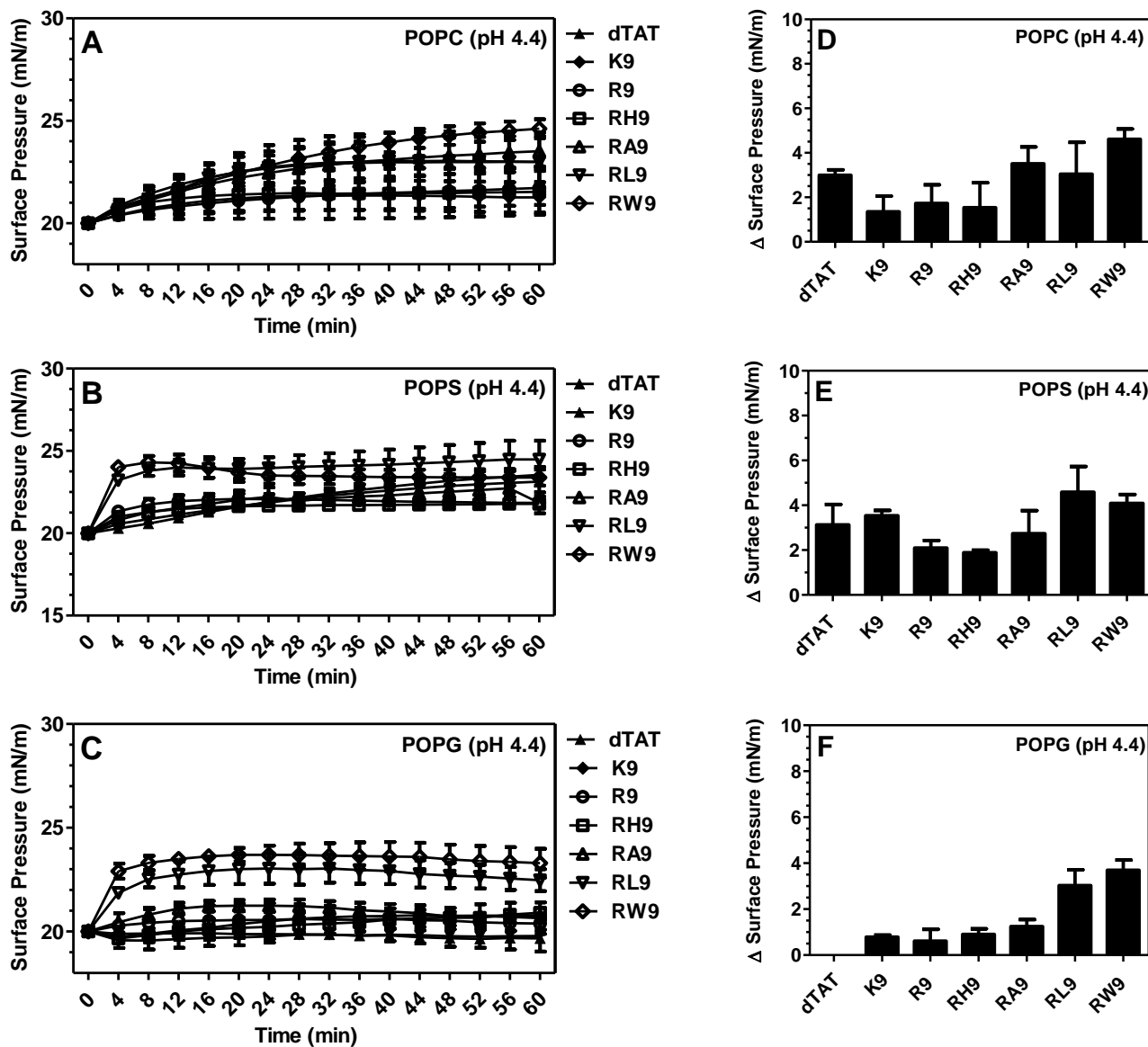


Figure Appendix 7. Changes in surface pressure as a function of time following injection of the seven CPPs (dTAT, K9, R9, RH9, RA9, RL9, and RW9) below (A) POPC, (B) POPS, and (C) POPG phospholipid monolayers held at an initial surface pressure of 20 mN/m and at pH 4.4. The maximum change in surface pressure (plateau values) of the (D) POPC, (E) POPS, (F) POPG due to adsorption of seven CPPs. Results are presented as mean SD (n = 3).

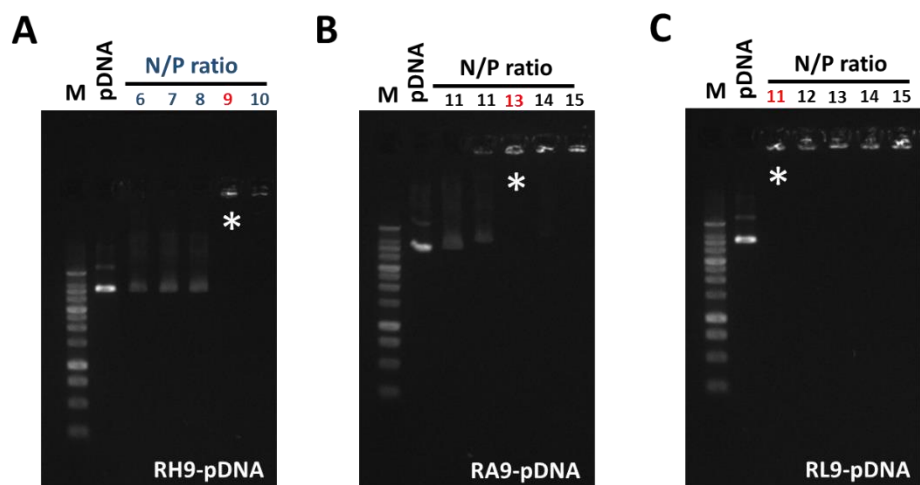


Figure Appendix 8. Agarose gel electrophoresis study of RH9-, RA9-, and RL9-pDNA complexes. **(A)** RH9-pDNA complexes at N/P ratios 6, 7, 8, 9, and 10. **(B)** RA9-pDNA complexes at N/P ratios 11, 12, 13, 14, and 15. **(C)** RL9-pDNA complexes at N/P ratios 11, 12, 13, 14, and 15. "Star *" refers to the minimum N/P ratio whereas CPPs were able to immobilize pDNA completely. "M" Refers to the size marker.

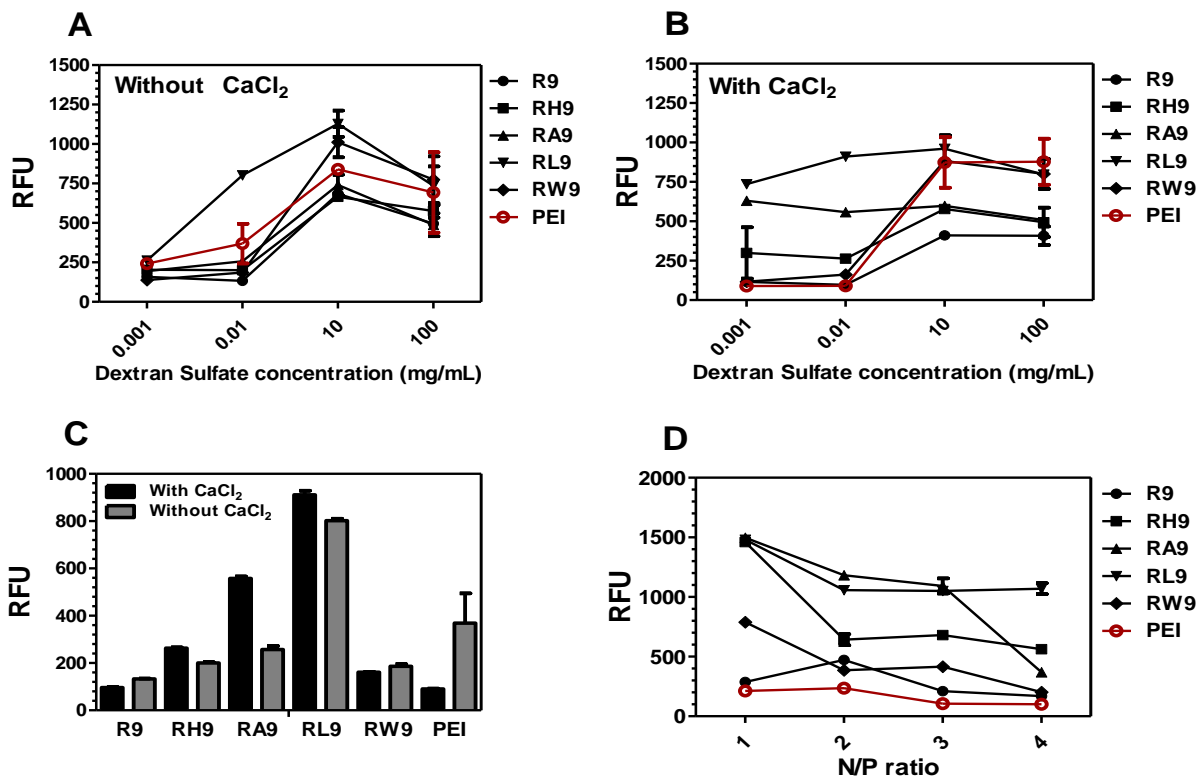


Figure Appendix 9. SYBR Green fluorescence of R9-, RH9-, RA9-, RL9-, RW9-, and PEI-pDNA complexes by dextran sulfate displacement of pDNA at different N/P ratios (1, 2, 3, 4, and 10) and with or without CaCl₂ (300 mM). **(A)** At different dextran sulfate concentrations without CaCl₂, **(B)** at different dextran sulfate concentrations with CaCl₂, **(C)** with/without CaCl₂ at dextran sulfate concentration of 0.01 mg/mL and N/P ratio 10, and **(D)** without CaCl₂ at dextran sulfate concentration of 0.01 mg/mL and N/P ratios 1, 2, 3, and 4. Results are presented as mean ± SD (n = 3)

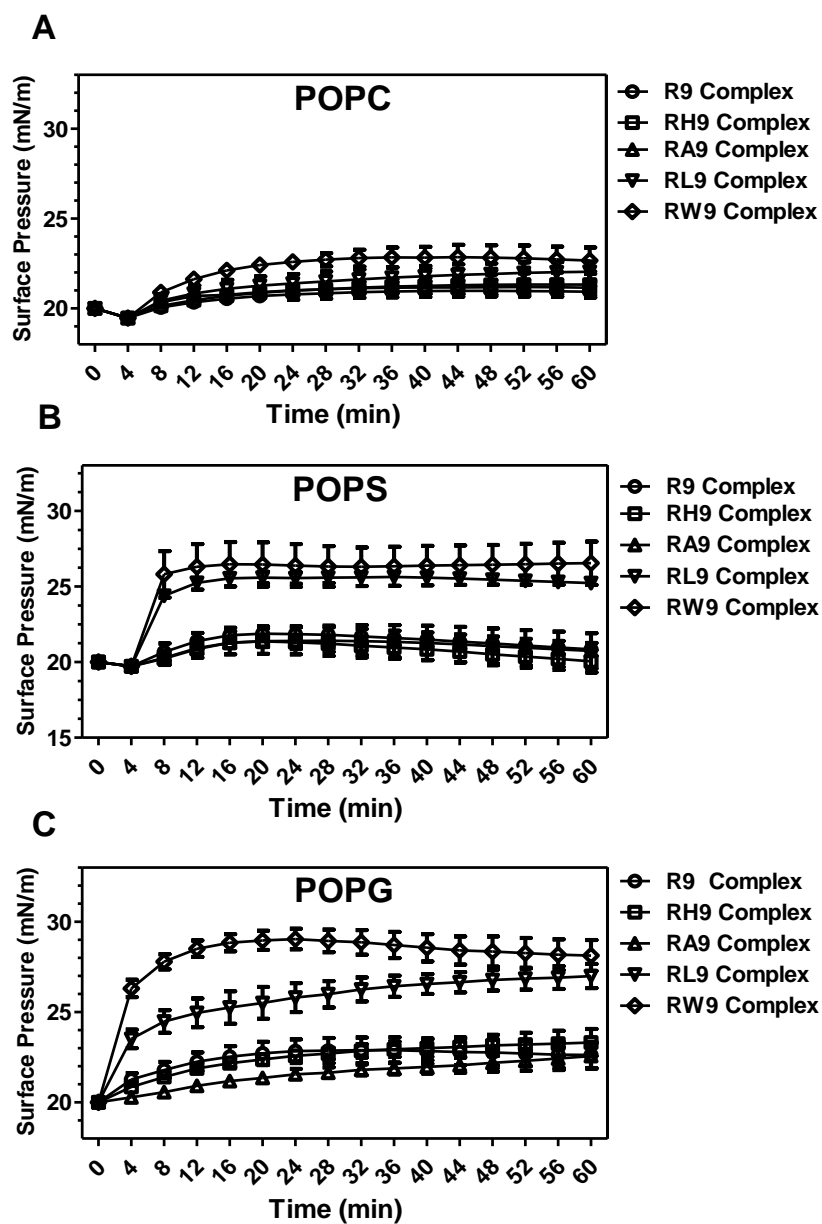


Figure Appendix 10. Changes in surface pressure as a function of time following injection of R9, RH9, RA9, RL9, or RW9-pDNA-Ca²⁺ complexes into model phospholipid monolayers: **(A)** POPC, **(B)** POPS, and **(C)** POPG held at an initial surface pressure of 20 mN/m and at pH 7.4. Results are presented as mean SD (n = 3).

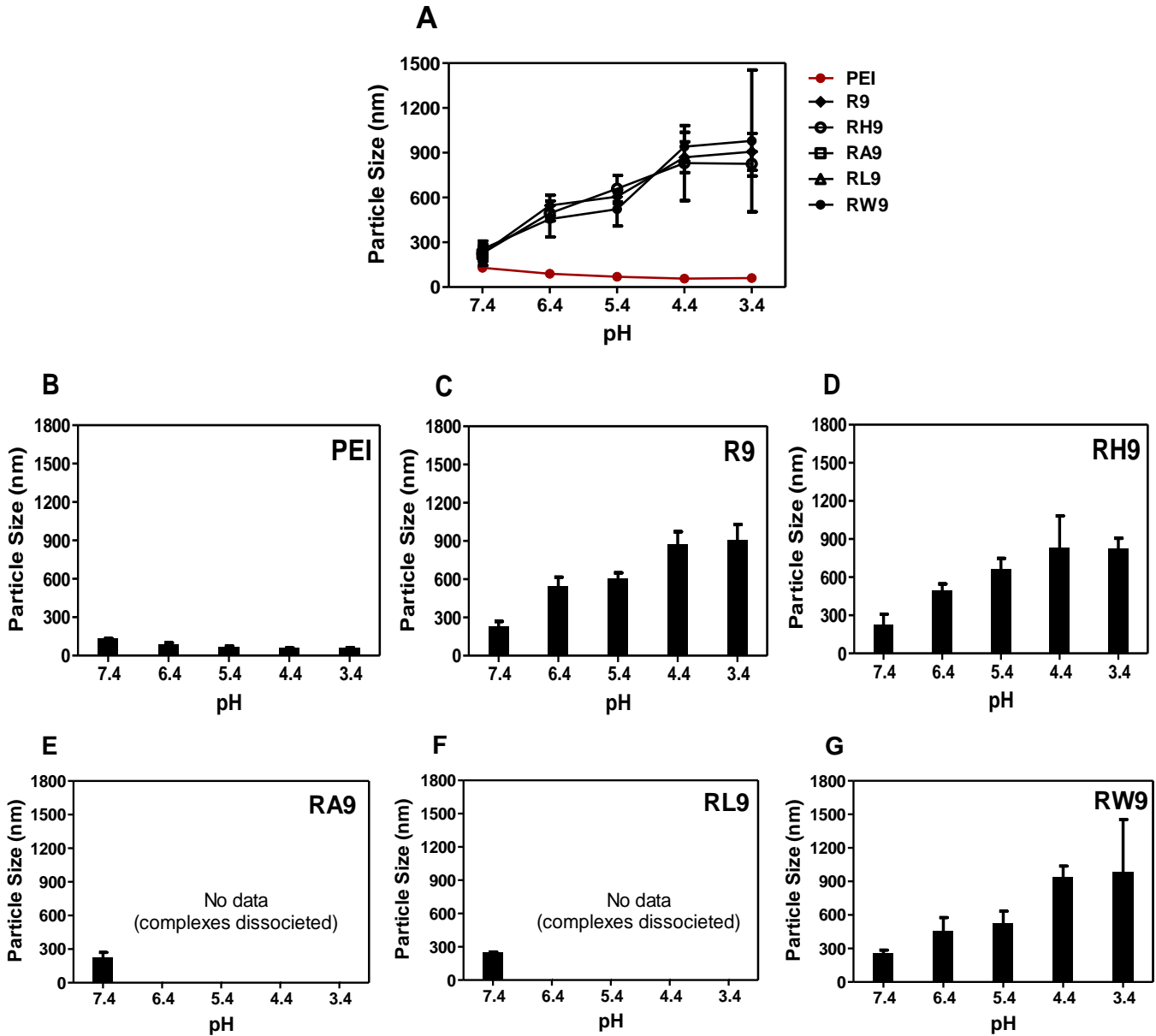


Figure Appendix 11. Particle size (effective diameter) of the five CPP-pDNA complexes with CaCl_2 concentration (100 mM) at an N/P ratio 10, at different pH 7.4, 6.4, 5.4, 4.4 and 3.4. Results are presented as mean \pm SD ($n = 3$). (A) All complexes, (B) PEI, (C) R9, (D) RH9, (E) RA9, (F) RL9, and (G) RW9. For missing data points, the diameter was undetectable. Results are presented as mean \pm SD ($n = 3$).

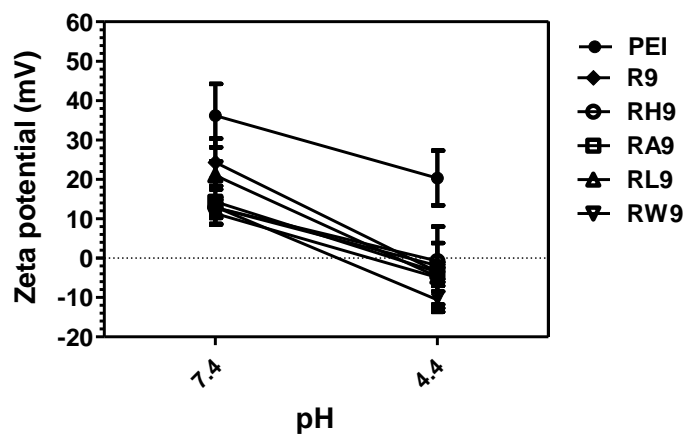


Figure Appendix 12. Zeta potentials of PEI-pDNA complexes and of CPPs (R9, RH9, RA9, RL9, and RW9)-pDNA complexes (100 mM CaCl₂ and an N/P ratio: 10) at different pH values (i.e. 7.4 and 4.4). Results are presented as mean ± SD (n = 3).